Structural aspects and chemical species involved in the hemeperoxidases catalytic oxidation of hydrogen sulfide by hydrogen peroxide and oxygen

by

Bessie B. Ríos González

A dissertation submitted in partial fulfillment of the requirements for the degree of

DOCTOR OF PHILOSOPHY
in
Applied Chemistry
(Biophysics)

UNIVERSITY OF PUERTO RICO
MAYAGÜEZ CAMPUS
2018

Approved by:

_____	_____
Juan López-Garriga, Ph.D. President, Graduate Committee	Date
_____	_____
Samuel P. Hernández Rivera, Ph.D. Member, Graduate Committee	Date
_____	_____
Carmen L. Cadilla Vázquez, Ph.D. Member, Graduate Committee	Date
_____	_____
Carmen A. Vega Olivencia, Ph.D. Member, Graduate Committee	Date
_____	_____
Abner Rodríguez, Ph.D. Representative, Graduate Studies	Date
_____	_____
Enrique Meléndez, Ph.D. Chairperson, Chemistry Department	Date

ABSTRACT

Hydrogen sulfide (H_2S) has gained attention since it is implied in human physiological functions with potential therapeutically effects. Furthermore, H_2S interacts with physiologically important hemeproteins such as myoglobin, hemoglobin, catalase, lactoperoxidase (LPO) and myeloperoxidase (MPO). LPO in the presence of hydrogen peroxide (H_2O_2) and H_2S forms a sulfheme derivative, called sulflactoperoxidase (sulfLPO), as do other proteins like hemoglobin, myoglobin, and catalase. Despite many studies, there still a need to further comprehend the species involved in the reaction of hemeperoxidases, LPO, MPO and horseradish peroxidase (HRP), with molecular oxygen or H_2O_2 in the presence of H_2S. Studies introducing mutations to the sulfide reactive, hemoglobin I (HbI) from *Lucina pectinata,* found that histidine (His) is involved in the sulfheme formation. New mutations were inserted in positions 64 and 68 of the HbI heme pocket, demonstrating that the His residue in the adequate position and orientation is crucial in the sulfheme derivative formation in heme proteins. This work presents data to further understand the LPO sulfheme development. Our results show that under strict anaerobic conditions, the addition of H_2S to LPO reduces the protein instead of inducing the formation of sulfLPO. Further experiments data indicate that the presence of O_2 or H_2O_2 is an absolute requirement for the formation of the sulfheme derivatives characterized by distinctive bands at 638 nm and 727 nm in the electronic spectrum. Interestingly, in the presence of oxidizing agents and H_2S continuous turnover of sulfLPO to regenerate the native protein occurs, indicating LPO catalyzed oxidation of sulfide by peroxide. The turnover of the sulfLPO to the native protein does not lead to any new H_2S generation or irreversible inhibition mechanisms. Pilot product analysis suggest sulfate ($SO_4^{=}$) and/or inorganic polysulfides as products in the turnover process. These results indicate that H_2S is a non-classical LPO substrate, because the porphyrin ring of the heme group is reversibly

modified during turnover via intermediate formation of sulfheme derivatives. Furthermore, EPR data suggest that during sulfheme turnover, H_2S can act as a scavenger of H_2O_2 in the presence of LPO without detectable formation of any carbon-centered radical species on the globin chain, suggesting that H_2S might be capable of protecting the enzyme from radical-mediated damage in the presence of H_2O_2. Sulfheme formation was shown to be slower in the reaction between oxyLPO and H_2S compared to the LPO catalyzed oxidation of sulfide by H_2O_2. The available literature and our results suggest that the rate determining step of sulfheme formation in the presence O_2 is the formation of compound III, while with H_2O_2 it is the formation of heme compound 0. On the other hand, experimental data show that in contrast to hemoglobin, myoglobin, catalase or LPO, MPO and HRP's main pathway in the oxidative interactions with H_2S is not the generation of the sulfheme derivative. Although all these hemeproteins have His in the active site, structural changes near the heme group causes in MPO and HRP to prefer compound III as central intermediary in the enzyme turnover by H_2S. Nevertheless, the results indicated that H_2S does not bind to the ferric LPO, MPO and HRP due the unique features of the His and arginine residues in the active site of these hemeperoxidases.

RESUMEN

El H_2S ha ganado atención ya que está implicado en funciones fisiológicas humanas con potenciales efectos terapéuticos. Además, el H_2S interactúa con hemoproteínas fisiológicamente importantes como mioglobina, hemoglobina, catalasa, lactoperoxidasa (LPO) y mieloperoxidasa (MPO). LPO en presencia de peróxido de hidrógeno (H_2O_2) y H_2S forma un derivado sulfhemo, llamado sulflactoperoxidasa (sulfLPO), así como otras proteínas como la hemoglobina, la mioglobina y la catalasa. A pesar de muchos estudios, todavía hay una necesidad de comprender mejor las especies implicadas en la reacción de las hemoperoxidasas, LPO, MPO y peroxidasa de rábano picante (HRP), con oxígeno molecular y/o H_2O_2 en presencia de H_2S. Estudios que introducen mutaciones de residuos a la hemoglobina I (HbI) de *Lucina pectinata*, que enlaza y transporta H_2S, encontraron que la histidina (His) está involucrada en la formación de derivados sulfhemo. Se insertaron nuevas mutaciones en las posiciones 64 y 68 en el sitio activo de la HbI, demostrando que el amino ácido His en la posición y orientación adecuada es crucial en la formación del sulfhemoderivado en las hemoproteínas. Este trabajo presenta datos para comprender mejor el desarrollo de sulfhemo en LPO. Nuestros resultados muestran que bajo estrictas condiciones anaeróbicas, la adición de H_2S a LPO reduce la proteína en lugar de inducir la formación de sulfLPO. Otros datos indican que la presencia de O_2 o H_2O_2 es un requisito indispensable para la formación de los derivados sulfhemo que se caracterizan por bandas distintivas a 638 nm y 727 nm en el espectro electrónico. Curiosamente, en presencia de agentes oxidantes y H_2S LPO muestra una renovación continua de sulfLPO para regenerar la proteína nativa, lo que indica que LPO cataliza la oxidación de sulfuro por peróxido. La renovación del sulfLPO a la proteína nativa no conduce a ninguna generación nueva de H_2S o mecanismos de inhibición irreversibles. Análisis preliminares sugiere que sulfato ($SO_4^{=}$) y/o polisulfuros

inorgánicos son generados como productos en el proceso de renovación. Estos resultados indican que el H_2S es un sustrato de LPO no clásico, porque el anillo de porfirina del grupo hemo se modifica de forma reversible durante la renovación mediante la formación intermedia de derivados sulfhemo. Además, los datos de RPE sugieren que durante la renovación de sulfhemo, el H_2S puede actuar como eliminador de H_2O_2 en presencia de LPO sin formación detectable de cualquier especie radical centrada en carbono en la cadena de globina, sugiriendo que H_2S podría proteger la enzima de daños inducidos por radicales en presencia de H_2O_2. Se demostró que la formación de sulfhemo era más lenta en la reacción entre oxyLPO y H_2S en comparación con la oxidación de H_2S catalizada por LPO por H_2O_2. Estudios en la literatura y nuestros resultados sugieren que la etapa determinante de la velocidad de formación de sulfhemo en presencia de O_2 es la formación del compuesto III, mientras que con H_2O_2 es la formación del compuesto 0. Por otro lado, los datos experimentales muestran que a contrario de la hemoglobina, mioglobina, catalasa o LPO, en MPO y HRP la principal vía de las interacciones oxidativas con H_2S no es la generación del sulfhemo derivado. Aunque todas estas hemoproteínas tienen His en el sitio activo, los cambios estructurales cercanos al grupo hemo provocan que MPO y HRP prefieran el compuesto III como intermediario central en la renovación enzimática por H_2S. Sin embargo, los resultados indicaron que el H_2S no se enlaza a la LPO, MPO y HRP férrica debido a la característica única de poseer los residuos His y arginina en el sitio activo de estas hemoperoxidasas.

Dedication

To my amazing husband and son

for walking alongside me in this endeavor,

belief in me and never letting me give up.

To my parents, grandparents and sister

for their love, support and motivation to pursue higher goals.

Acknowledgement

I thank God for giving me the strength and peace of mind in order to finish this research. I thank profusely my husband and son, Henry "Bebito" and Dariem, for their unceasing encouragement, patience, and unconditional love and support. I would like to acknowledge the support, motivation and love of my family, my parents, Hipólito and Aida, my sister, Arisbelis, and my grandparents, María and Benito. My friends for their encouragement, helping me develop my ideas and moral support which made many graduate years more enjoyable.

I would like to express my sincere appreciation to my mentor, Dr. Juan López Garriga, expert guidance and encouragement. I thank the distinguished members of my committee, Dr. Samuel Hernández, Dr. Carmen L. Cadilla, Dr. Mayra E. Cadiz and Dr. Carmen A. Vega, for their guidance and contributions which were extremely valuable for my thesis. I am deeply grateful to Dr. Carmen L. Cadilla and her research group for letting me use their facilities and for imparting their knowledge and expertise in this study. I would also like to thank to Dr. Gary J. Gerfen contributions in the EPR measurements, support and expertise. I wish to express my sincere thanks to Dr. Ruth Pietri for her respected expertise, guidance, dedication and advise. I thank Dr. Syun-Ru Yeh for the use of the stopped-flow instrument and Dr. Ariel Lewis for his assistance. I also express my gratitude to Dr. Péter Nagy and Dr. Paul G. Furtmüller for collaborations and suggestions and to the Department of Chemistry at UPR Mayagüez Campus and lab colleagues for their support. I thank the undergraduate students for their assistance and for letting me guide them.

This work would not have been possible without the financial support of NIH-RISE (Grant R25GM088023), the National Science Foundation (Grant 0843608) and Alfred P. Sloan (NACME Grant). It is an honor for me to thank all the people who supported me in this marvelous and sacrificed venture, and made this work possible.

List of tables

List of figures

List of symbols and abbreviations

H_2S	hydrogen sulfide
pK_a	negative base-10 logarithm of the acid dissociation constant
^oC	Celsius
HS^-	hydrosulfide anion
S^{2-}	sulfide anion
~	approximately
%	per cent
ppm	parts per million
NO	nitrogen monoxide
CO	carbon monoxide
CBS	cystathionine β-synthase
CSE	cystathionine γ-lyase
MST	3-mercaptopyruvate sulfurtransferase
DAO	D-amino acid oxidase
PLP	pyridoxal-phosphate cofactor
Mb	myoglobin
Hb	human hemoglobin
HbI	hemoglobin I
LPO	lactoperoxidase
MPO	myeloperoxidase
O_2	oxygen
H_2O_2	hydrogen peroxide

sulfHb	sulfhemoglobin
sulfMb	sulfmyoglobin
His	histidine
Val	valine
Leu	leucine
Phe	phenylalanine
g	grams
dL	deciliter
µM	micromolar
nm	nanometer
NMR	nuclear magnetic resonance
M	Molarity
s	second
HbII	hemoblobin II
HbIII	hemoglobin III
cDNA	complementary deoxyribonucleic acid
Gln	glutamine
Fe^{IV}=O Por$\bullet^{+}$	π-cation radical; compound I
Fe^{IV}=O Por	compound II
Asn	asparagine
cm^{-1}	wavenumber
•SH	sulfide radical or thiol radical
Kcal	kilocalorie

CN^-	cyanide
$NaBH_4$	sodium borohydride
NaN_3	sodium azide
$SO_4^=$	sulfate
kDa	kilodalton
Tyr	tyrosine
H_2O	water
HClO	hypochlorous acid
SCN^-	thiocyanate
$OSCN^-$	hypothiocyanite
Arg	arginine
$Fe^{III}OOH$ Por	compound 0
AH_2	reducing substrate; organic substrate
$Por•^+$	porphyrin cation radical
•AH	substrate radical
X^-	halides
HOX	hypohalous acids
Met	methionine
Glu	glutamate
Asp	aspartate
$Fe^{II}O_2$ Por / $Fe^{III}O_2^{\bullet}$ Por	compound III
MMI	methylmercaptoimidazole
sulfLPO	sulflactoperoxidase

EPR	electron paramagnetic resonance
HRP	horseradish peroxidase
bp	base pairs
DNA	deoxyribonucleic acid
LB	Luria Broth
rpm	revolutions per minute
µL	microliter
TB	Terrific Broth
IPTG	isopropyl β-D-1-thiogalactopyranoside
KH_2PO_4	potassium phosphate monobasic
K_2HPO_4	potassium phosphate dibasic
NBB	binding buffer
mM	millimolar
NaH_2PO_4	sodium phosphate monobasic
Na_2HPO_4	sodium phosphate dibasic
NaCl	sodium chloride
mL	milliliter
CV	column volume
MES	morpholinoethanesulfonic acid
EDTA	ethylenediaminetetraacetic acid
SDS-PAGE	sodium dodecyl sulphate-polyacrylamide gel electrophoresis
SDS	sodium dodecyl sulphate
TEMED	tetramethylethylenediamine

V	volt
$Na_2S \cdot 9H_2O$	sodium sulfide nonahydrate
DT	sodium dithionite
K	Kelvin
Ghz	gigahertz
mW	milliwatt
N_2	nitrogen
Ec DOS-PAS Met95His	phosphodiesterase His mutant
CHARMM	Chemistry at Harvard Molecular Mechanics (molecular simulation program)
COPD	chronic obstructive pulmonary disease
ROS	reactive oxygen species
oxy	oxygen bound to ferrous iron

Table of Contents

Chapter 1: Introduction

CHAPTER 1: INTRODUCTION

1.1 Hydrogen sulfide

Hydrogen sulfide (H_2S) is a molecule whose origin dates back 3.5 billion years when the Earth was hot and inhabitable. In those years, one of the oldest living organisms, sulfate reducing bacteria was capable of producing H_2S [1]. Approximately 600 million years ago the increase of oxygen diminished the use of H_2S as an energy source [2] making possible animal and plant life. Nowadays H_2S is found in natural sources as swamps, sulfur springs, salt marshes, bogs, natural gas, petroleum deposits and volcanoes [3–6]. H_2S is produced, used and generated by human activity in facilities such as petroleum refineries, natural gas plants, petrochemical plants, coke oven plants, kraft paper mills, viscose rayon manufacturing plants, sulfur production plants, iron smelters, food processing plants, manure treatment facilities, landfills, textile plants, waste water treatment facilities and tanneries [7–11]. Some plants, bacteria, fungi, actinomycetes and invertebrates release H_2S [1,12–15].

H_2S is a weak acid in aqueous solutions with a pK_a of 6.76 at 37 ^oC. It equilibrates with its anions, hydrosulfide anion (HS^-) and sulfide anion (S^{2-}) in aqueous solutions (Scheme 1.1). Considering a pK_{a1} value of ~ 7 and a pK_{a2} >17, under physiological conditions there is essentially no S^{2-} formed but there is ~ 20 % of H_2S and 80 % of HS^- in extracellular fluid and plasma [16,17]. Hence, the bioactive form, has not been determined. The term "H_2S" is used for the undissociated species and the hydrosulfide anion. H_2S is highly lipophilic and hence could penetrate cells by simple diffusion [18].

$$H_2S_{(g)} \leftrightarrow H_2S_{(aq)} \leftrightarrow HS^- + H^- \leftrightarrow S^{2-} + 2H^+ \qquad \text{Scheme 1.1}$$

During many years H_2S has been known to be a toxic gas with a characteristic odor of "rotten egg". H_2S primary route to the body is through inhalation. The toxic effect of H_2S will depended of the concentration and time of exposure [17]. Acute exposure to 50-100 ppm leads to sore throat, dizziness, nausea, insomnia, weight loss and respiratory effects attributed to airway irritation. At 100 ppm to 500 ppm concentration it causes convulsions, unconsciousness, inability to breathe, coma, and death. H_2S at concentration higher than 500 ppm leads to rapid unconsciousness and respiratory arrest.

H_2S was recognized for its toxic nature neglecting for many years its beneficial roles. It has been found that H_2S is produced endogenously in mammalian tissues considering it the third gasotransmitter after nitrogen monoxide (NO) and carbon monoxide (CO) [19]. H_2S is produced in mammalian cells via both non-enzymatic and enzymatic pathways. A small portion of H_2S is produced via non-enzymatic pathways, but these processes are less well understood. H_2S is produced in human erythrocytes in the presence of elemental sulfur or inorganic polysulfides [20]. Other non-enzymatic pathways for the production of H_2S are via thiosulfate and persulfide and in a thiol-dependent manner from garlic and garlic-derived organic polysulfides [17]. Most of the production of H_2S in mammalian tissues is via the enzymatic pathway. H_2S is enzymatically generated in the vasculature, heart, liver, kidney, brain, nervous system, lung, airway tissues, upper and lower gastrointestinal tract, reproductive organs, skeletal muscle, pancreas, synovial joints, connective tissues, cochlear and adipose tissues [21]. The endogenous production in human body is due to four enzymes: cystathionine β-synthase (CBS), cystathionine γ-lyase (CSE), 3-mercaptopyruvate sulfurtransferase (MST), and D-amino acid oxidase (DAO) [19,22,23]. The crystal structures of CBS, CSE, MST and DAO are shown in Figure 1-1 [24–26]. CBS and CSE

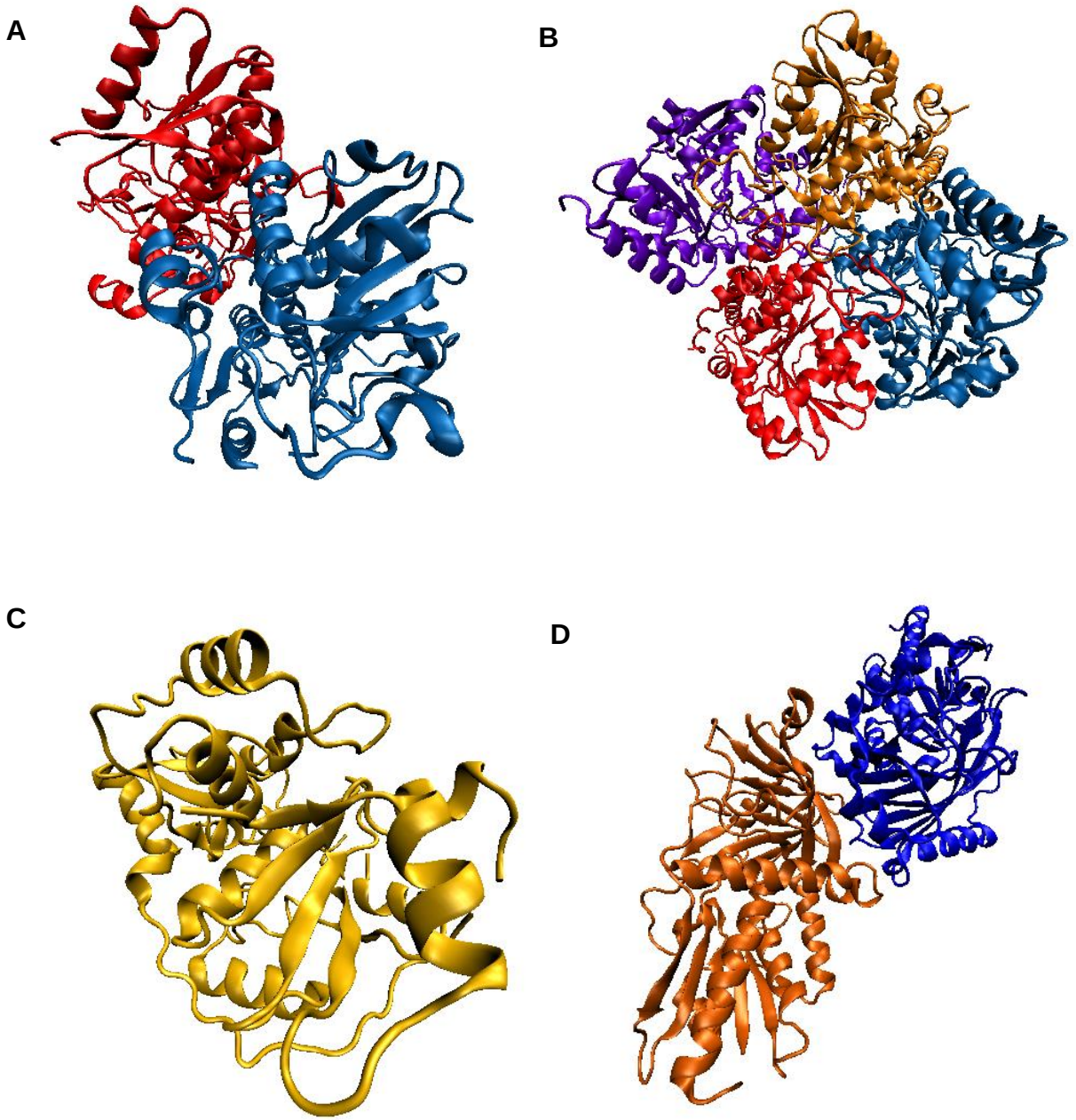

Figure 1-1. Structure of the four enzymes that produce H_2S in mammalian cells: (A) human CBS (PDB: 1JBQ) [24], (B) human CSE (PDB:2NMP) [25], (C) human MST (Image by Karlberg et. al, August 2010. PDB:3OLH) and (D) DAO (PDB: 2DU8) [26].

belong to the PLP family that uses the cofactor pyridoxal-phosphate (PLP), which is the active form of vitamin B_6. At low concentrations, H_2S is implicated in potential therapeutic effects, such as neuromodulation [27], neuroprotection [28], vasodilation [29,30], insulin release [31], inflammation [32], angiogenesis [33,34] and cytoprotection [16,35,36]. It can cause a positive or negative effect depending on the concentration and target protein.

H_2S has as target important hemeproteins, like myoglobin (Mb) [37–40], human hemoglobin (Hb) [41], and hemoglobin I (HbI) and mutants from *Lucina pectinata* [42–47] as well as catalase [38,48,49], lactoperoxidase (LPO) [50], and myeloperoxidase (MPO) [51]. These proteins have a porphyrin iron complex, called heme, as the prosthetic group. The heme consists of a protoporphyrin ring and a central iron atom shown in Figure 1-2. The iron atom has six coordination bonds, four to nitrogen atoms porphyrin rings and two perpendicular to the porphyrin. One of the two bonds perpendicular to the porphyrin is occupied by a histidine residue, called proximal histidine. The other bond is known as the distal position and is occupied by a ligand, for example water, oxygen (O_2) or hydrogen peroxide (H_2O_2).

1.2 Interaction of H_2S with Mb and Hb

The biologically important Hb and Mb are globular hemeproteins that transport and store O_2 throughout the human body, respectively (Figure 1-3). Both, Hb and Mb, bind O_2 directly to the ferrous iron of the heme prostethic group. Hb is a tetrameric protein responsible of transporting O_2 in a cooperative manner. However, myoglobin is a monomeric protein found mainly in muscle tissue where it serves as an intracellular storage site for O_2 [52]. These hemeproteins are capable of binding H_2S to the ferric iron but with low affinity. Figure 1-3C shows the distal active site were

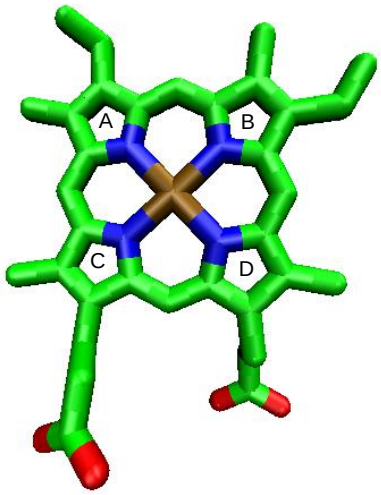

Figure 1-2. Protoporphyrin IX or heme group. The different atoms are represented by the following colors: iron (ochre), nitrogen (blue), carbon (green) and oxygen (red).

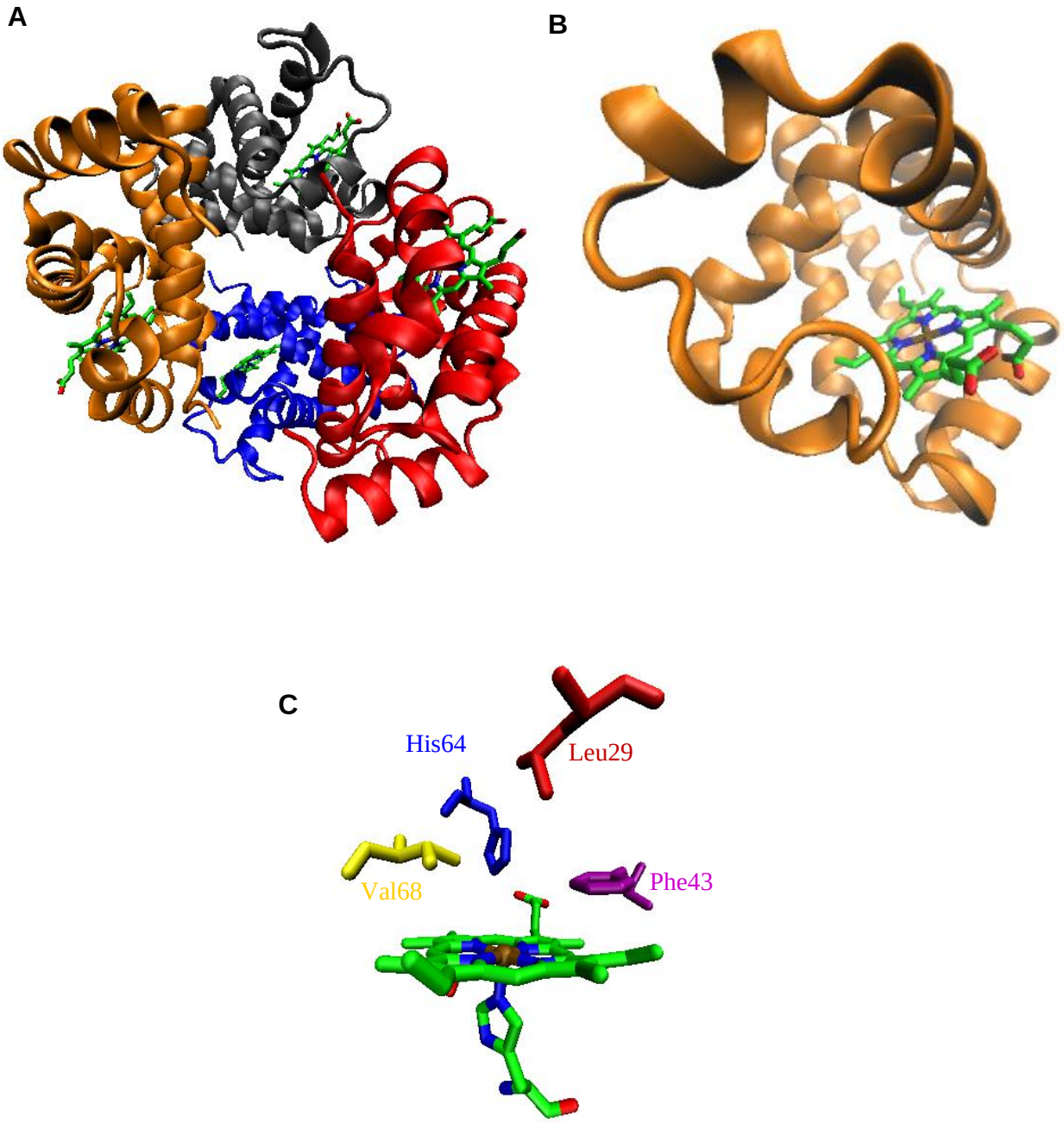

Figure 1-3. Structure of (A) human hemoglobin (PDB: 1A3N) [53] and (B) sperm whale myoglobin (PDB:1EBC) [54] and (C) active distal site of Hb and Mb. The numbers represent the position of the amino acid in the polypeptide chain.

the ligand binds to the iron including important amino acid residues for the function of the protein. Furthermore, Hb and Mb in the presence of O_2 or H_2O_2 and H_2S generate sulfhemoglobin (sulfHb) and sulfmyoglobin (sulfMb), respectively (Figure 1-4). The green sulfHb derivative was observed for the first time by Felix Hoppe-Seyler [55]. Michel et al. [37] showed the formation of an analogous compound upon interaction of oxyMb with H_2S and named the derivative sulfmyoglobin [37,38,56]. SulfHb is constantly present in the human body with normal levels in blood of below 0.037 g/dL (5.7 µM) [57]. Increases of physiological concentration of sulfheme derivatives is triggered when humans are exposed to high concentrations of H_2S, ingestion of detergents, paint or to high levels of a wide range of drugs like acetanilide, metoclopramide, phenacetin, dapsone, sulfanilamide-containing drugs, and drug overdose [21,58,59]. High levels of sulfHb and sulfMb can be poisonous, since they alter protein O_2 transport or storage functionalities, causing a condition known as sulfhemoglobinemia [60,61]. Apparently, in humans, the threshold between both scenarios is equivalent to a relative change in sulfheme concentration from 5 µM to near 100 µM [44,57]. Patients with sulfhemoglobinemia suffer a cyanosis that often leads to death. The levels of sulfHb of 0.5 g/dL (78 µM) is sufficient to detect if the patience suffer cyanosis [57]. The detection of sulfHb is very difficult, it could be found in newborns as well as in adults [62,63]. The most used clinical methods to prevent sulfhemoglobinemia are blood transfusions, exposure to high oxygen concentrations, gastric lavages, and methyl blue treatments [58,59,63]. These methods, in most cases, do not prevent organ failure.

Studies using radioactive sulfide species demonstrated that a single sulfur atom is incorporated into the heme structure per mole of Mb to form sulfMb [64]. The insertion resulted in a heme modification by the specific incorporation of the sulfur atom across the β-β double bond of heme pyrrole B [47,65]. The sulfheme derivative shows a characteristic optical band around

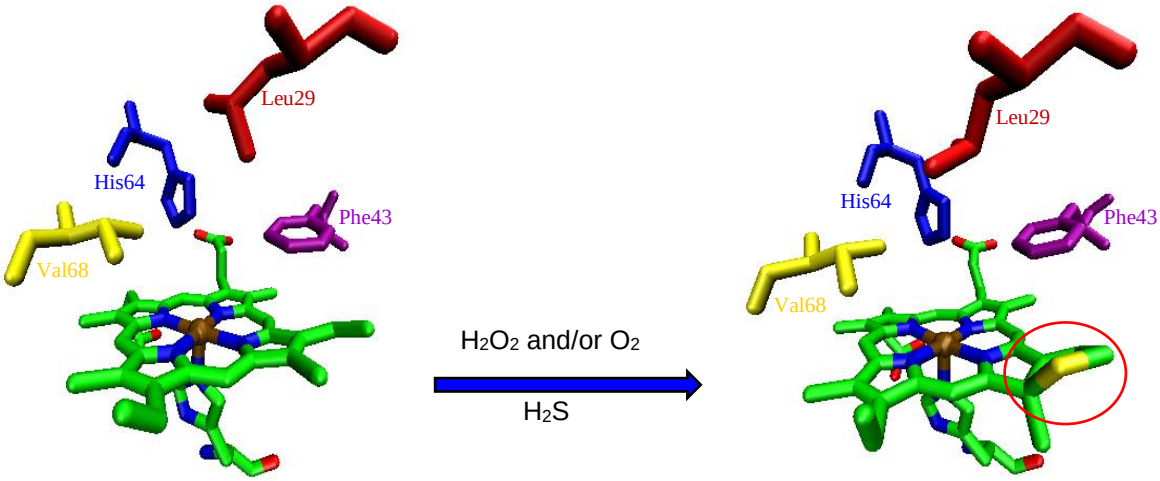

Figure 1-4. SulfMb (PDB: 1YMC) [66] formation of the interaction of Mb with H_2S in the presence of O_2 and/or H_2O_2.

620 nm and 717 nm, for the ferrous and ferric sulfMb, respectively. The band displacement depends on the type of the sulfheme isomer and, the heme-Fe oxidation and ligation states [39,65,67–69]. Proton NMR studies with sulfMbCN demonstrated the formation of three sulfheme isomeric forms named sulfMbA, sulfMbB and sulfMbC [70,71]. The sulfMbA structure has an episulfide across the β-β bond, while sulfMbB is a ring open episulfide [72]. SulfMbC is characterized by a five membered ring described as a thiochlorin structure [72]. These isomers have different chemical properties due to their stability and reactivity and were observed at different pH, protein concentration and temperature conditions [72]. The sulfMbA isomer is the precursor of sulMbB and sulfMbC since it can convert to both but conversion of sulfMbA from sulMbB and sulfMbC has not been observed [65,69]. SulfMbC is the most stable isomeric form [70,71] and appears to predominate at physiological conditions.

Efforts have been made to elucidate the species involved in the sulfheme formation and provided a reasonable mechanism of formation [37,38,44,45,47,56,64,71,73]. The sulfheme derivative can be generated with O_2 as well in the presence of H_2O_2 [37,38]. The relatively fast formation of sulfMb in the presence of H_2O_2 ($2.5\pm0.1x10^6$ $M^{-1}s^{-1}$) [73] compared to the reaction between just H_2S and myoglobin ($1.6\pm0.3x10^4$ $M^{-1}s^{-1}$) and hemoglobin ($3.2\ x10^3$ $M^{-1}s^{-1}$) [40] indicates an important role for the peroxide species to increase the reaction rate of sulfheme formation. Additionally, the inverse relationship between an increase in the rate of formation of sulfMb derivatives and the decrease in pH [37,40,73] suggests that the participation of HS^- in the sulfheme formation is very limited or it does not participate at all. Thus, this indicates that H_2S rather than HS^- is the reactive sulfur species in the sulfheme reaction mechanism [44]. As discussed later in detail, the histidine in the active site and the oxo-ferryl intermediates play an important role in sulfheme formation [38,44,45,47].

1.3 Interaction of H_2S with hemoglobin I from Lucina pectinata

Interactions of H_2S with hemeproteins have been studied in marine invertebrate organisms that live in sulfide-rich environments [74,75]. These organisms have evolved strategies to avoid sulfide toxicity, as has the clam *Lucina pectinata*. *Lucina pectinata* is a bivalve mollusk that remains unaffected in the presence of H_2O_2 and/or O_2 and H_2S [43]. It inhabits in sulfide-rich mangroves in the southwest coast of Puerto Rico and it hosts symbiotic sulfide-oxidizing bacteria that need to be supplied with O_2 and H_2S. This clam has three different hemoglobins, the sulfide-reactive hemoglobin I (HbI), and the O_2 transporting hemoglobins II and III (HbII and HbIII), all of which bind and transport their respective ligands in their heme active sites [42,43]. HbI is responsible of delivering H_2S to the bacteria. This hemoglobin is probably one of the few hemeproteins that physiologically bind H_2S in the ferric state to maintain the symbiotic relationship with the bacteria. The affinity of H_2S for ferric HbI is exceptionally high and is believed to be achieved through fast association (k_{on} = 2.3 x 10^5 $M^{-1}s^{-1}$) and very slow dissociation processes (k_{off} = 0.22 x 10^{-3} s^{-1}). The cDNA sequence and X-ray crystallographic studies of HbI show the amino acid residues present in the heme pocket [76,77]. The X-ray crystal structure of metaquo HbI in Figure 1-5 [78] depicted the peculiar amino acid composition of the HbI distal ligand binding site. HbI has a glutamine (Gln) residue at the distal 64 position instead of the typical histidine (His) found in mammalian Mb and Hb [78]. Also, in addition to Gln64, HbI has the unusual and unique Phe29 and the Phe68 residues that generate what is known as the "Phe-Cage". This peculiar arrangement of phenylalanyl residues has been suggested to be responsible for the high H_2S affinity.

The oxo-ferryl species are essential intermediaries in physiological chemical reactions produced by the reaction of hemeprotein with O_2 and/or H_2O_2 [79,80]. The oxo-ferryl heme-

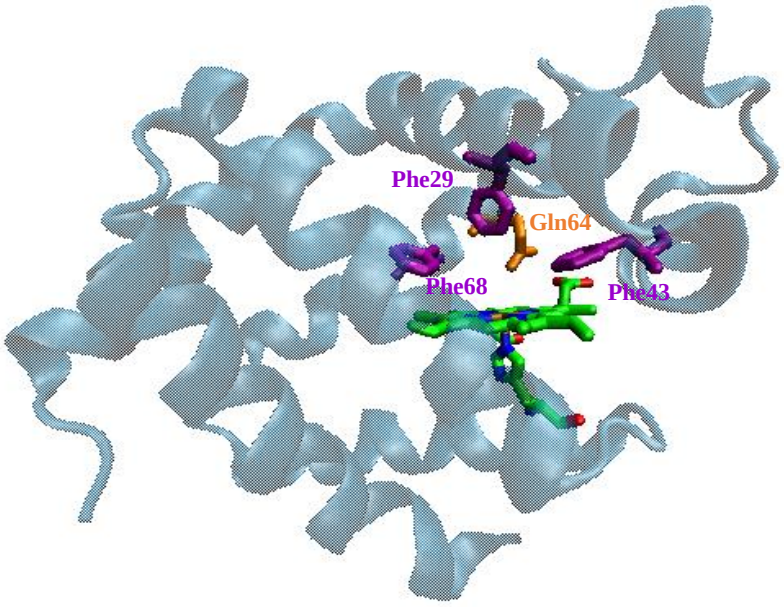

Figure 1-5. Active site of HbI (PDB: 1MOH) [78] from *Lucina pectinata*.

compound I is a π-cation radical (Fe^{IV}=O Por$^{\bullet+}$) complex while ferryl species heme-compound II is a Fe^{IV}=O Por complex [80]. HbI from *Lucina pectinata* shows the ability to stabilize the ferryl compound I a thousand times more than Mb [79]. The reaction of H_2O_2 with Mb forms compound I, which decays to compound II [80–82]. The stabilization of the Mb compound I is related to the distal His64, since it makes Mb more resistant to the H_2O_2 [80]. HbI Gln and Phe residues in the heme pocket help stabilize compound I [79]. The Phe cage creates high multipole interactions, which stabilize the incoming ligand and contribute to the ferryl precursor formation.

Studies with HbI mutants show that when the Gln64 was mutated to histidine (His64), an optical band at 624 nm characteristic of sulfheme formation was observed (Figure 1-6) [45]. None of the other HbI mutants, Gln64Asn HbI, Phe68His HbI, Phe29Leu HbI, and Phe68Val HbI, produce the characteristic sulfheme band [45,46]. Resonance Raman shows the formation of satellite bands (1353 cm^{-1} and 1390 cm^{-1}) around the oxidation state marker ν_4, for Mb and the Gln64HisHbI mutant upon reaction with H_2O_2 and H_2S which is not present in the wild hemeproteins, indicating the presence of a distorted sulfheme chromophore. Also, these native proteins show two vinyl normal modes at 1620 cm^{-1} and 1626 cm^{-1}, however, upon formation of the sulfMb and sulfGln64His HbI mutant, the 1626 cm^{-1} vinyl band is absent. These results support the unique and crucial role that histidine in the distal site plays in the mechanism of sulfheme formation [44,45]. Given these experimental observations, the function of the 64 His distal site in the reaction with H_2O_2 and H_2S to form met-aquosulfheme was explored by hybrid quantum mechanical/molecular mechanical methods. The calculations showed the reaction proceeds through the compound II oxo-ferryl intermediate interacting with a sulfide radical (•SH) with the concomitant formation of met-aquosulfheme derivatives with very favorable energy drop of 140 Kcal/mol [47], which stabilized the product. Under these circumstances, the formation of sulfheme

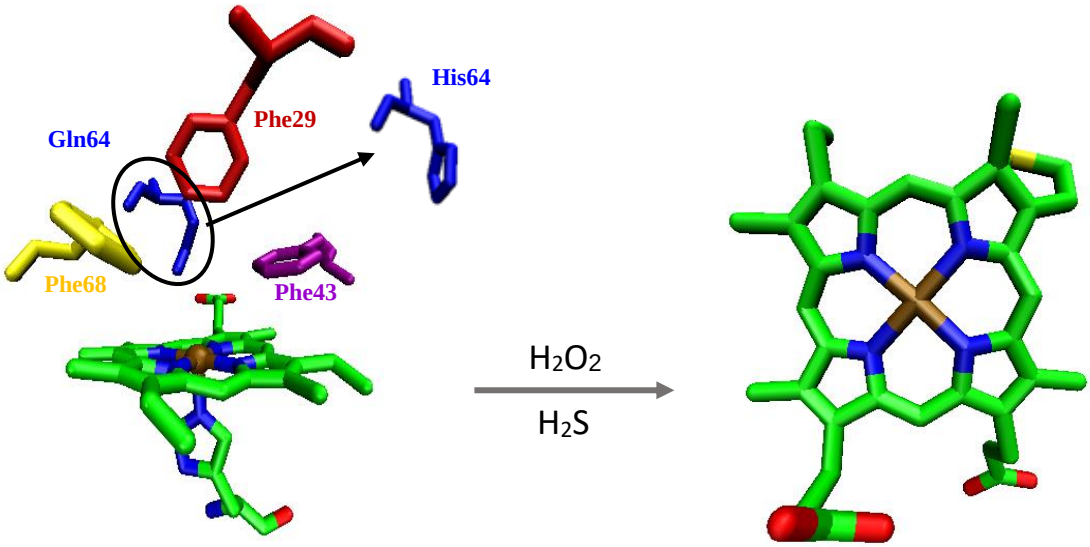

Figure 1-6. Formation of the sulfheme derivative from the Gln64His HbI mutant in the presence of H_2O_2 and H_2S.

is both kinetically and thermodynamically favorable. Attempts have also been made to understand the reverse reaction of the sulheme derivatives to the native functional proteins, since apparently significant activation energy may be required to release the bound sulfur from the sulfheme ring [38,39,64,83]. However, experiments show that photo-excitation of carboxysulfmyoglobin induced reconversion to MbCO, suggesting that the presence of an excited state may reduce the activation energy needed for the back reaction [39]. Chemically, the reconversion of sulfMb to native Mb has been observed upon reaction of these sulfheme derivatives with H_2O_2, O_2, cyanide (CN^-), sodium dithionite and excess of H_2S, $NaBH_4$, NaN_3, or strong alkaline solutions [38,64,83]. Also, radioactive sulfide data demonstrated that sulfheme decomposes to protohemin, following first order kinetics, and sulfate ($SO_4^=$) as the major product [64].

1.4 Interaction of H_2S with enzymes

Enzymes are found in bacteria, fungi, plants and animals and their function is to serve as biological catalysts. They accelerate reactions that are necessary to sustain life but some inhibitors decrease the reaction rate and turnover of enzymes. Similar to human Hb and Mb, there is a set of enzymes, like LPO and catalase that react with H_2S, forming analogous sulfheme derivatives. Nonetheless, published information about the interaction of H_2S with these enzymes is limited [38,50]. In this section we discuss the current knowledge about the interaction of H_2S with catalase and some hemeperoxidases.

1.4.1 Catalase

Catalase is a heme-containing enzyme found in many bacteria and almost all plants and animals. The protein is a tetramer and each monomer of 60 kDa contains a heme group (Figure 1-7) [84–86]. Instead of a histidine residue in the proximal site found in Mb, catalase has a tyrosine

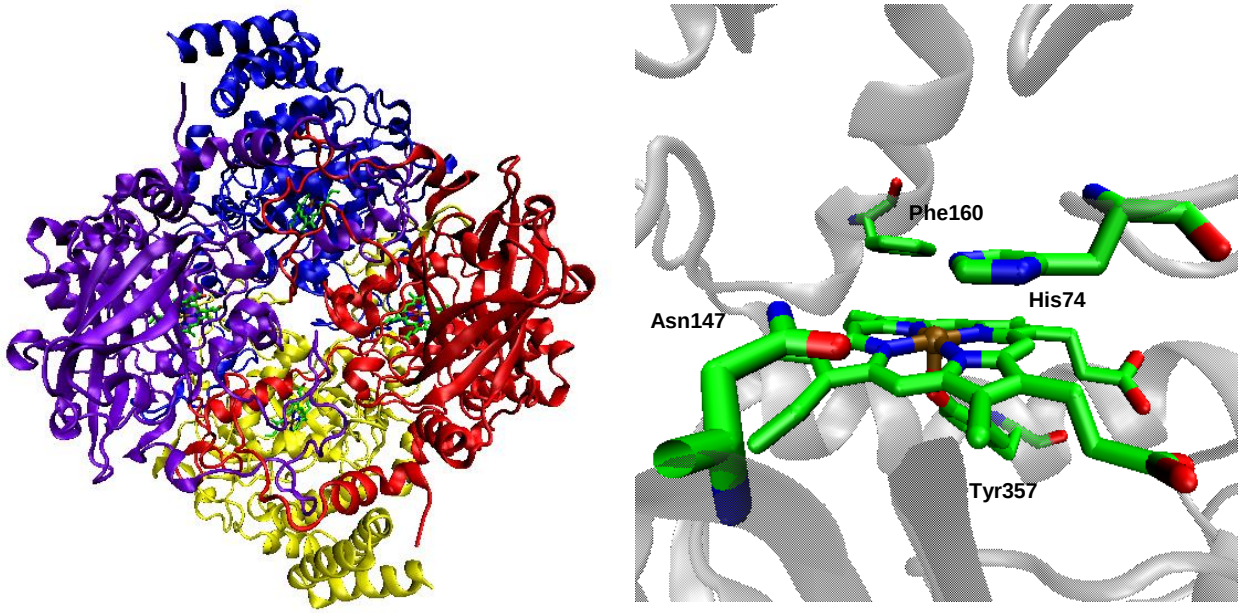

Figure 1-7. Structure and active site of catalase. Structure of (A) catalase (PDB:3RGP) [87] and active site of (B) catalase.

residue. As Scheme 1.2 shows, the enzyme protects the cells by converting H_2O_2 into water and O_2 [88]. The proposed mechanism occurs in two steps and involves the oxo-ferryl intermediates [87]. In the first step the enzyme reacts with H_2O_2 to form compound I. In the second step, compound I reacts with another molecule of H_2O_2 and the enzyme returns to the resting state. Two electrons are transferred to one molecule of H_2O_2 and then two electrons are accepted from a second H_2O_2. Catalase does not form compound II as part of the normal catalytic cycle but at low concentration of H_2O_2 and in the presence of one electron donor, generation of compound II has been observed. The efficiency of the catalytic reactions is improved by the interaction of the active site His and Asn residues (His and Asn in the positions 74 and 147, respectively) with the oxo-ferryl intermediates.

$$2H_2O_2 \rightarrow 2H_2O + O_2 \qquad \text{Scheme 1.2}$$

Step 1. $[Fe^{III}Por] + H_2O_2 \rightarrow [Fe^{IV}=O\ Por^{\bullet +}] + H_2O$

Step 2. $\left[Fe^{IV}=O\ Por^{\bullet +}\right] + H_2O_2 \rightarrow \left[\ Fe^{III}Por\right] + \ H_2O + O_2$

Catalase is inhibited by ligands like cyanide, azide, 3-amino-1,2,4-triazol and nitric oxide [89–92]. Also, as Beers and Sizer proposed, H_2S could inhibit catalase in two ways: it may form an inactive compound with the primary catalase peroxide complex and that it may react directly with either the protein moiety or with the heme group [93]. Nicholls then proposed that the interaction of H_2S with catalase was similar to that of Mb in which H_2S reacts with the oxo-ferryl compound II intermediates and modifies the heme porphyrin system to produce the analogous sulfheme derivatives [38,48]. The product of the reaction of catalase with H_2S and H_2O_2 yielded an optical spectrum with a characteristic band at 635 nm and was therefore ascribed to ferrous sulfcatalase. Ferric sulfcatalase was also observed with absorption bands at 585 nm and 710 nm.

Based on this, Bersofsky suggested that the structure of sulfcatalase should be similar to sulfMb and sulfHb [56,64,94,95]. Therefore, these observations support the notion that the sulfheme product is generated in presence of O_2 and/or H_2O_2 and that the distal His residue near the iron regulates sulfheme formation. Interestingly, catalase can be regenerated from sulfcatalase by oxidizing agents like oxygen and ethyl hydroperoxide and by small molecules like cyanide and azide, and sodium dithionite [38].

1.4.2 Hemeperoxidase (Lactoperoxidase, Myeloperoxidase and Horseradish)

Hemeperoxidases are enzymes that catalyze the oxidation of a number of inorganic and organic compounds using H_2O_2 as the primary substrate. These enzymes turn reactive oxygen species like H_2O_2, which damage cell structure, to harmless product by adding hydrogen from a donor molecule. This is achieved by a reduction-oxidation reaction in which the H_2O_2 is reduced to form water and another molecule, an electron donor, is oxidized. LPO and MPO are two important heme-containing peroxidases involved in the immune defense system [96–99]. As mammalian peroxidases, these enzymes, form part of a group of heme-containing oxidoreductases known as the peroxidase-cyclooxygenase superfamily [98,100]. LPO is found in mammary, salivary, lachrymal and bronchial submucosal glands, and human airways [96,101], whereas MPO is found in large amounts in azurophilic granules of polymorphonuclear leukocytes [102]. Both defend the system from invading microorganism by the bactericidal activities of the oxidized substrates [96,103]. For example, MPO catalyzes the formation of hypochlorous acid (HClO) from chloride species and H_2O_2, which has antimicrobial activity and kills other pathogens in humans [103]. On the other hand LPO catalyzes the oxidation of thiocyanate (SCN^-) by H_2O_2 in the lungs to produce the antimicrobial hypothiocyanite ($OSCN^-$) [104]. This enzyme is the primary

scavenger of H_2O_2 to prevent its toxic effects in events of airway inflammation in patients with asthma [105].

LPO has a molecular weight of approximately 70 kDa, while MPO has molecular weight of 144 kDa and consists of two identical subunits linked by a disulfide bridge [97]. In resting form, the heme groups of LPO and MPO are penta-coordinated with the iron in the high spin ferric state. These enzymes with the methyl groups on pyrrole rings A and C of the heme group form two ester linkages with the carboxyl groups of glutamate and aspartate residues, respectively (Figure 1-8 A and B) [97,106]. In addition to the two ester linkages MPO makes with the β-carbon of the vinyl pyrrole ring A, it forms a sulfonium ion linkage with the methionine. [97,106]. These linkages perturb the symmetry and planarity of the prosthetic group, therefore are responsible of the optical properties in these enzymes [106,107]. In the case of MPO these linkages may contribute to the efficient manner it oxidizes chloride to HClO [108].

As shown in Figure 1-8C and D, the distal sites of both enzymes have His and arginine (Arg), [97,106,107] which are important in their catalytic activities, specifically in the formation and stabilization of oxo-ferryl intermediates [100]. Figure 1-9A presents that the ferric hydroperoxo intermediate compound 0 (Fe^{III}OOH Por), the oxo-ferryl intermediates compound I (Fe^{IV}=O Por$^{\bullet+}$), and compound II (Fe^{IV}=O Por) are produced from the interaction of H_2O_2 with hemeperoxidases by a multistep mechanism [100,109–112]. At first, H_2O_2 binds to oxidize the ferric heme to produce compound I and a molecule of water. Then, a reducing substrate (AH_2) delivers one electron to the porphyrin cation radical (Por$^{\bullet+}$) to form compound II and a substrate radical (•AH). The enzyme returns to the resting state when compound II is reduced by a second substrate molecule, giving a second radical substrate and a second molecule of water. Additionally, to organic substrates (AH_2), inorganic compounds such as halides (X^-) act as electron donors which

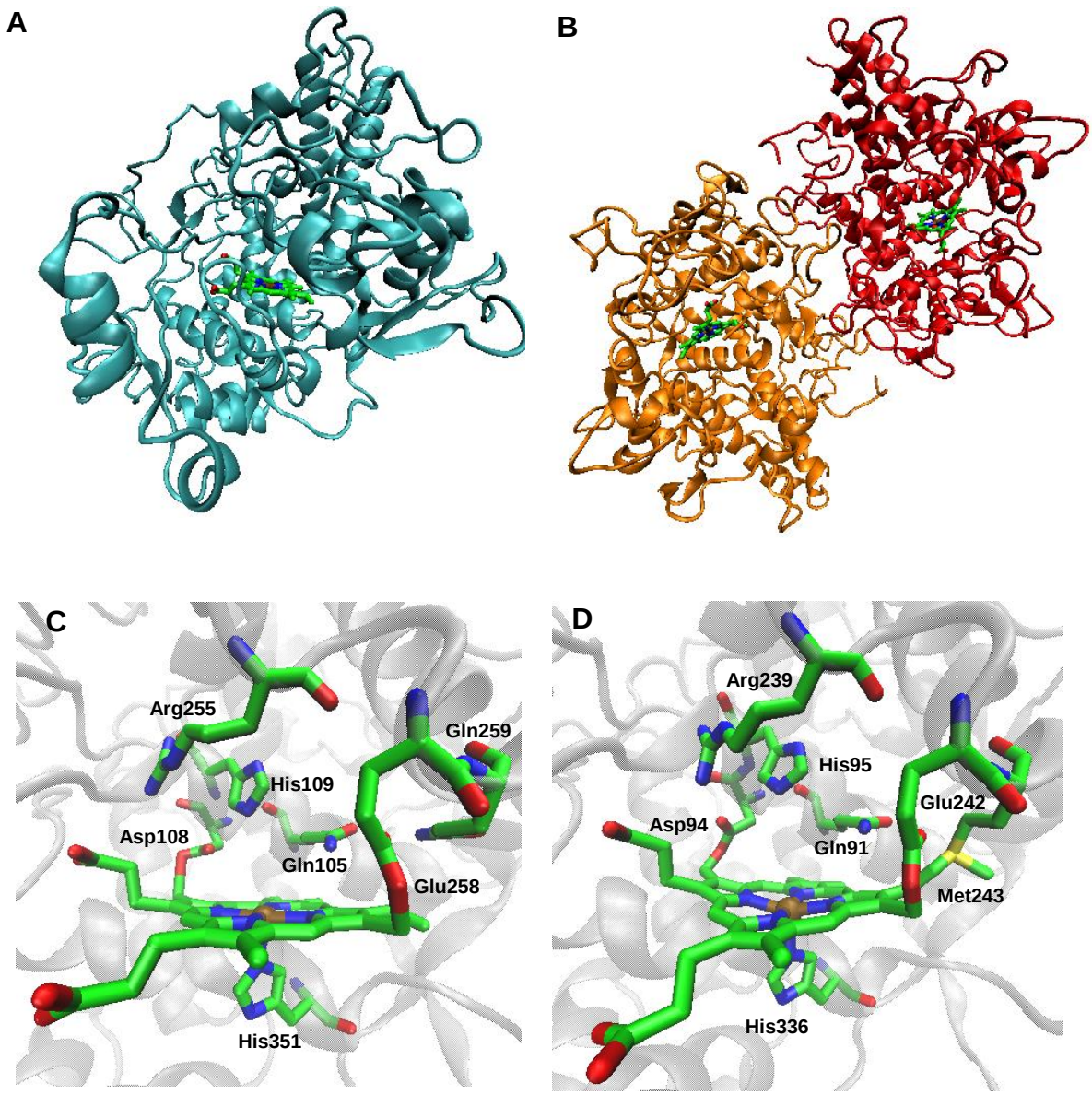

Figure 1-8. Structure and active site of the hemeperoxidases LPO and MPO. Structure of (A) LPO (Image by Singh et. al., November 2006. PDB:2NQX) and (B) MPO (PDB:1CXP) [106]. (C) and (D) Active site of LPO and MPO respectively highlighting covalent bindings of amino acid residues to the porphyrin ring.

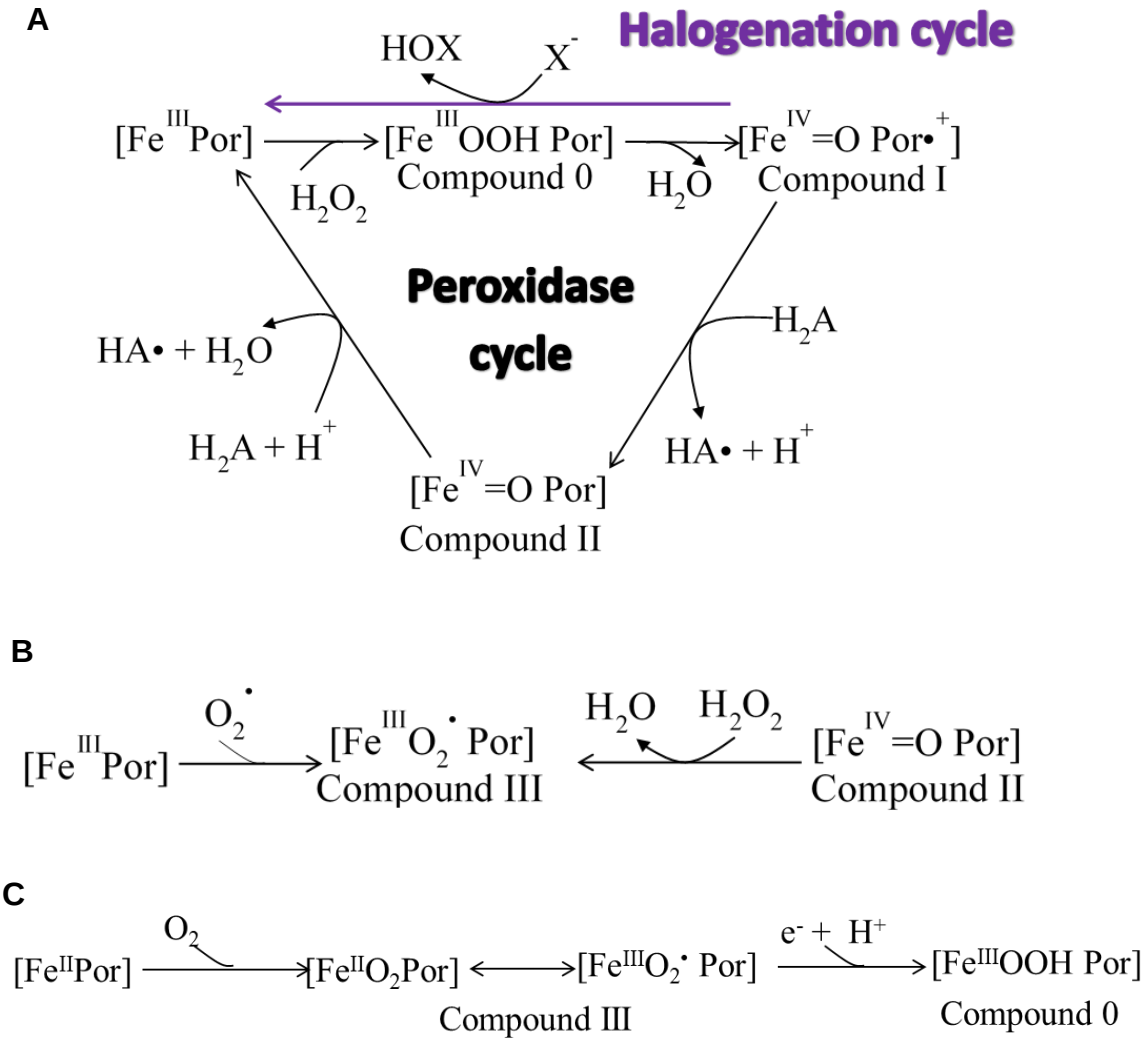

Figure 1-9. Oxoferryl intermediates formation. (A) Peroxidase and halogenation catalytic cycle. (B) Formation of compound III from superoxide and excess of H_2O_2. (C) Formation of compound 0 under an acidic environment through Compound III.

are oxidized to hypohalous acids (HOX) to return the enzyme to resting state from compound I (Figure 1-9 A) [113]. In the presence of superoxide and excess of H_2O_2, LPO and MPO forms compound III (ferric-superoxide/ferrous-dioxygen complex) state (Fe(III)-$O_2^{\bullet-}$ Por/Fe(II)-O_2 Por) (Figure 1-9B) [109–112]. Figure 1-9C shows that a more direct route to compound III is achieved through the reaction between deoxy-heme and O_2. Under an acidic environment, compound III upon accepting a proton and electron, leads to the subsequent formation of compound 0 [109].

The catalytic activity of LPO is inhibited by sulfhydryl compounds such as methylmercaptoimidazole (MMI) and thiouracil [114]. Ohtaki and coworkers suggested that the irreversible inactivation of the enzyme was induced by the reaction of compound II with the antithyroid drug MMI [115]. In 1984, Nakamura and coworkers also evaluated the interactions of LPO with H_2S, MMI, cysteine and dithiothreitol in the presence of H_2O_2 [50]. They found that as Mb, Hb and catalase, the reaction of H_2S with the enzyme in the presence of H_2O_2, yielded a sulfheme derivative, which they named sulflactoperoxidase (sulfLPO). The ferrous sulfLPO has a characteristic band at approximately 638 nm whereas the ferric sulfLPO has bands at 605 nm and 727 nm [50]. The ferrous sulfLPO has a second order rate constant of $1.5 \times 10^5\ M^{-1}s^{-1}$ from the reaction of compound II with H_2S. Reaction of MMI with LPO compound II yielded a spectrum with visible bands at 592 nm and 635 nm. Based on the similarity with the one obtained with H_2S, the authors suggested that sulfLPO was also formed with MMI.

Although the molecular mechanism of sulfLPO formation from H_2S have not been described, the analogous processes have been well evaluated with the sulfur-containing compound MMI [50,114–117]. Ohtaki in 1982 and Nakamura in 1984, suggested that LPO compound II was reduced to the ferric state by one electron transfer from MMI with the concomitant formation of a MMI radical [50,115]. In 1986, Doerge proposed by kinetics studies suicidal inactivation of LPO

by MMI. It is known by works by Ortiz Montellano that suicidal substrates of peroxidases inactive the enzyme by a generation of a radical which interact with the specific heme site [117–119]. The presence of the MMI radical was later confirmed by EPR studies and it was also shown that the radical did not interact directly with the heme iron [116]. The authors suggested that the MMI radical must bind to a specific site of heme porphyrin ring and that the unpaired electron of the radical was then transferred to the heme ferryl group [116]. It was also proposed in that study that the distal His might influence MMI oxidation and subsequent binding to the heme porphyrin. Remarkably, this supports the unique role of the distal His in sulfheme formation as suggested previously [45]. Overall, it is now believed that MMI interacts with the LPO compound II, inducing the formation of a thiyl radical that inhibits LPO irreversibly by reacting directly with the heme porphyrin system. Based on the optical spectra reported by Nakamura it is plausible that the MMI radical interacts with the heme and generates sulfLPO, which inhibits the enzyme activity [50]. A similar mechanism can be invoked for the interaction of LPO with H_2S. Moreover, the fact that the optical spectra of LPO in the presence of H_2S and H_2O_2, as shown in Figure 1-10, presents bands similar to sulfHb and sulfMb, strongly suggest that the heme group of the sulflactoperoxidase derivative is a chlorin type structure in which the sulfur atom is incorporated across the β-β double bond of the pyrrole B [39,94,95].

MPO activity is inhibited in the presence of H_2S and H_2O_2 [120–122]. The interaction of H_2S with MPO compound II exhibit a UV-Vis band at 625 nm with a second-order rate constant of 2.0 $x10^5$ $M^{-1}s^{-1}$ [120]. The complex assigned to this band warrants further investigation. Although we focused in human peroxidase, MPO and LPO, horseradish peroxidase (HRP) is an enzyme found in the roots of horseradish (plant) that also has a histidine (His42) in the active site (Figure 1-11) [123]. Like MPO, HRP is inhibited by thiols in the presence of oxo ferryl

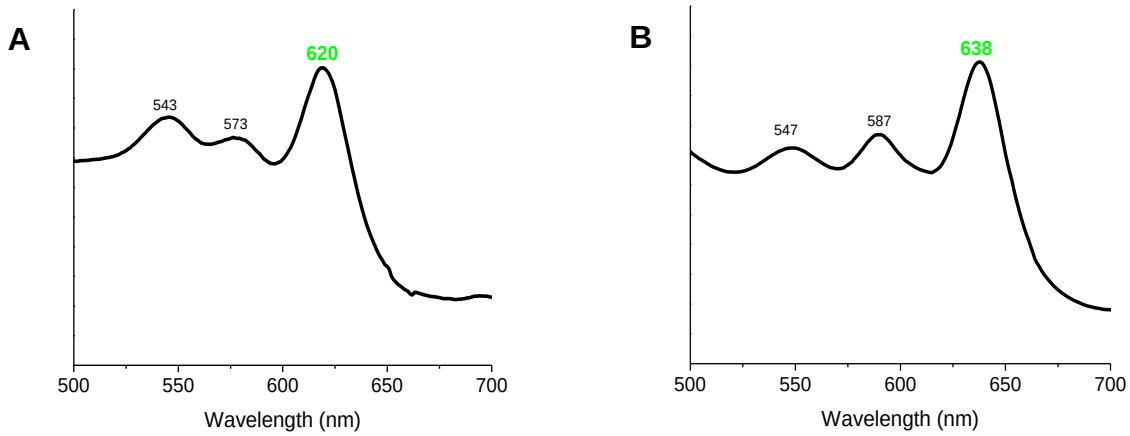

Figure 1-10. UV-Vis spectra of the sulfheme derivative formation upon the reaction H_2O_2 and H_2S. Characteristic UV-Vis band of (A) sulfMb and (B) sulfLPO formation.

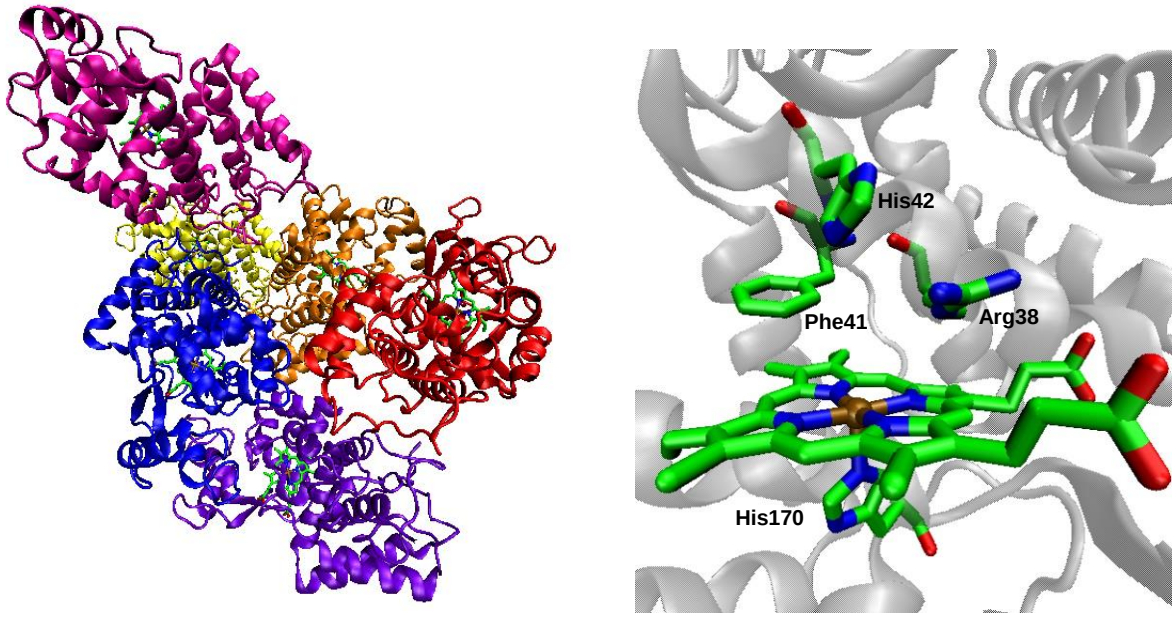

Figure 1-11. Structure and active site of HRP. Structure of (A) HRP (PDB:1ATJ) [123] and active site of (B) HRP.

intermediates [124,125]. The formation of the sulfheme derivative has not yet been demonstrated experimentally in MPO and HRP but the fact that these hemeperoxidases have a histidine residue in the heme distal site can contribute to the possibility of sulfheme formation.

The distal residues have been determined to play an important role in the sulfheme derivatives formation since the reactivity of H_2S with hemeproteins are controlled by the polarity of the distal heme cavity, the stereo orientation of the distal side residues and the concentration of H_2S [46]. HbI mutants that mimic the Mb distal site were made and the resulted showed that His is crucial for sulfheme derivates formation [45]. The first part of this research focused in new HbI single and double mutants to confirm that His with the correct orientation and position in the presence of H_2O_2 and/or O_2 and H_2S is essential for the formation of sulheme derivatives. Also, these new mutants will elucidate how the polarity of the distal site affects the H_2S reactivity with hemeproteins and hemeperoxidases, and the sulfheme derivative formation.

In spite of these efforts, there is a need to generate new data that can help to further understand the sulfheme development in hemeperoxidases. The data of the sulheme formation in LPO and the interactions of H_2S with MPO and HRP is limited and requires further attention. This work focuses in the: a) species involved in the sulfLPO generation, b) interactions of H_2S with ferric and ferrous hemeperoxidases in the absence and presence of oxidizing agents like H_2O_2 and O_2, c) effect of conformational changes in the distal active site in the reactivity with H_2S, and d) turnover of sulfLPO to the native state and the possible products in it. This work will contribute to propose a general mechanism and the physiological implications of the sulfheme generation in peroxidases.

Chapter 2: Materials and Methods

CHAPTER 2: MATERIALS AND METHODS

2.1 Site Directed Mutagenesis for the preparation of the HbI mutants (Gln64Arg HbI, Phe68His HbI, and Gln64His and Phe68Val HbI)

To perform site directed mutagenesis of the cDNA that codifies for *Lucina pectinata* HbI, the Quick Change Site-Directed Mutagenesis kit (Strategene, La Jolla, Ca, USA) was used. The Site-Directed Mutagenesis method was performed using PfuTurbo DNA polymerase and a thermal cycler. The method consists first in designing oligonucleotide primers with the desired mutation, each complementary to opposite strands of the cDNA. The pET-28a(+) vector with the HbI cDNA insert (25 -50 ng) [76,126] and two the oligonucleotides primers (125 ng each) were mixed. Then, the oligonucleotides were extended during temperature cycling by PfuTurbo DNA polymerase. The parameters used for cycling were at first an incubation at 95 ^{o}C for 30 sec followed by 16 cycles of 95 ^{o}C for 30 sec, 55 ^{o}C for 1 min and 68 ^{o}C for 6 min. The reaction was left on ice for 2 min and then treated with Dpn I restriction enzyme (10 U/µL) by mixing gently and microcentrifuge for 1 min. The mixture was incubated at 37 ^{o}C for 1 hour to digest the parental DNA template and was not cut the synthesized DNA containing the mutation. Finally, the nicked vector DNA with the mutation is transformed into XL1-Blue supercompetent cells by heat shock leaving the reactions at 42 ^{o}C for 45 sec and then put in ice for 2 minutes. Then 500 µL of NZY^{+} broth was added to the transformation reaction and incubated at 37 ^{o}C for 1 hour with shaking at 225-250 rpm. The cells were spread on LB agar plates containing 50 µg/mL of kanamycin.

2.2 Purification of the plasmid or vector with the desired mutation

After site-directed mutagenesis a plasmid purification process is made to verify that the desired mutation was obtained. Colonies are selected from the transformation of the vector with the mutation. Each colony is grown in 5.00 mL of LB medium containing kanamycin in 50 mL

falcon tubes for 12 hour at 37 ^{o}C with vigorous shaking (225 rpm). The bacterial cells were harvested by centrifugation for 10 min at 4000 rpm. The plasmids were purified using the QIAprep Spin Miniprep kit from QIAGEN. The plasmid purity (ratio of 260/280 absorbance) and quantification were verified using Nanodrop. The plasmids were digested at 37 ^{o}C overnight with the restriction enzymes XhoI and NdeI. Agarose gel electrophoresis of the digested plasmids were done to verify integrity using ethidium bromide to stain the plasmid DNAs and molecular weight standards.

2.3 Transformation of purify plasmid with the mutation into Escherichia coli Bli5 competent cells

The purified plasmids were sent to sequence with the T7 promoter (5' TAATACGACTCACTATAGGGG 3') and T7 reverse (5' CTAGTTATTGCTCAGCGGTGG 3') primers to the RCMI Molecular Biology facility at the University of Puerto Rico Medical Science Campus, using Sanger dye terminator chemistry. These segments of DNA are close to the coding sequence for HbI in the pET-28a(+) plasmid. The DNA sequence of the mutated plasmid was compared by using the Blast software the rHbI sequence to know if the desired mutation was obtained. If the mutation was achieved, the mutated plasmid was transformed into *Escherichia coli* Bli5 competent cells by heat shock as described earlier. These cells have another vector called pDIA 17 resistance to chloramphenicol that is essential for expression control.

2.4 Small scale expression of Gln64His and Phe68Val HbI

Low scale expressions of Gln64His and Phe68Val HbI in *Escherichia coli* Bli5 cells were conducted to determine the optimum induction temperature. An overnight culture was grown in 1/10 volume of the total expression culture volume using LB broth, the rest of the expression was done in TB medium. The 1.0 L TB medium was supplemented with the antibiotics, 30 µg/mL

chloramphenicol and 50 µg/mL kanamycin, 30 µg/mL hemin chloride and 1 % glucose. The induction at different temperatures, 25 ^{o}C, 30 ^{o}C, and 37 ^{o}C, was carried with 1 mM IPTG at an OD_{600nm} of 1.4 -1.8. The expression time was carried for approximately three and a half hours. The culture was centrifuged at 4000 rpm for 15 min and 4 ^{o}C and the pellet was stored for purification.

2.5 Large scale expression of the HbI mutants

The single and double HbI mutants were expressed and purified as described in previous studies [126] with slight modifications. Briefly, the HbI mutants in *Escherichia coli* Bli5 cells were expressed after induction with 1mM IPTG (OD_{600nm} 1.4-1.8) at 30 ^{o}C in a Bioflo 110 Modular Benchtop fermentator. The 4.0 L TB medium was supplemented with the antibiotics, 30 µg/mL chloramphenicol and 50 µg/mL kanamycin, 30 µg/mL hemin chloride, 500 mL of phosphate buffer (0.17 M KH_2PO_4 and 0.72 M K_2HPO_4) and 1 % glucose. During the fermentation process, the pH of 7.0 was maintained with an acidic solution of 1.5 M of KH_2PO_4 and an alkaline solution of 30% per volume of ammonium hydroxide. All the equipment, glassware and solutions were sterilized except for the antibiotics, IPTG and the ammonium hydroxide. The fermentation was carried until the cell growth reach the stationary phase between 18 hours to 26 hours. The culture was centrifuged at 4000 rpm for 20 min and 4 ^{o}C. The supernatant was discarded and the pellet was stored.

2.6 Lysis of Escherichia coli Bli5 cells

The pellets obtained from the expression were lysed to obtain the HbI mutant protein. The pellet was re-suspended in a native binding buffer (NBB) for lysis that consist 17 mM NaH_2PO_4, 68 mM NaCl and 58 mM Na_2HPO_4 at pH of 7.5. The quantity of NBB for lysis used should be three times the grams of pellet. Then 1 mg of chicken egg white lysozyme per gram of bacteria cell was added and 1 tablet of protease inhibitor (cOmplete, EDTA-free Protease Inhibitor Cocktail

from Roche) for every 50 mL of NBB. The mixture was incubated by homogenizing for 1 min and 5 min rest for half an hour at 10,000 rpm on ice and then sonicated, in a Fisher Scientific 550 sonic dismembrator, ten times at 25 % for 1 min 15 sec and rest for 45 sec. Then the lysate was centrifuged for 1 hour at 12,000 rpm and 4 ^{o}C using a Beckman J2-HS centrifuge to separate the soluble protein from the insoluble fractions.

2.7 Purification process for the HbI mutants

The soluble fractions, the HbI mutant His-tagged protein, were purified in Co^{2+} affinity columns (His-Select Cobalt Affinity Gel, Sigma H8162). A second step of purification was achieved by fast performance liquid chromatography (FPLC) in a Hi Load 26/60 Superdex 200 gel filtration column.

2.7.1 Affinity chromatography

The His-tagged HbI mutants were bound to the affinity resin to allow the separation of the protein from other impurities. The column was filled with 10 mL of the resin. The process consists in first equilibrating the column with 10 column volume (CV) of buffer at pH of 7.0 containing 50 mM NaH_2PO_4 and 300 mM NaCl. The lysate was added to the column and was mixed to allow interaction of the His-tagged protein with the resin. After the resin settle, the wash buffer (50 mM Na_2HPO_4, 300 mM NaCl and 10 mM imidazole) at pH 7.6 was added to remove other protein and impurities. To elute the HbI mutant from the column, a 7.0 pH elution buffer of 50 mM Na_2HPO_4, 300 mM NaCl and 150 mM imidazole was used. The protein fraction was concentrated and washed with distillated water using 10 KDa YM 10 membrane in a amicon ultrafiltration cell. Then put the HbI mutant in the buffer used for equilibrating the Co^{2+} affinity columns to move to the second purification step. The columns were washed with 6 M of guaninidium chloride or 20 mM of 2-

morpholinoethanesulfonic acid (MES) at a pH of 5 for rigorous cleaning and regular cleaning, respectively. The Talon columns were stored for later use in an ethanol solution at 20 %.

2.7.2 Size exclusion chromatography

The concentrated protein (5.0 mL) was passed through a Hi Load 26/60 Superdex 200 gel filtration column to separate the HbI mutant from traces of imidazole and other impurities. The fractions were collected in a Frac-950 fraction collector. The protein sample passed through a column from Amersham Bioscience with a matrix of dextran, covalently bound to highly cross-linked agarose, using a 50 mM NaH_2PO_4 and 300 mM NaCl with pH of 7.0 at a flow rate of 1.5 mL/min under 0.3 MPa pressure. The selection of the desired fraction with the HbI mutant was made by the photometric chromatogram at 280 nm sonce the instrument is equipped with a UV-Vis detector. The protein was concentrated using an amicon ultrafiltration with YM 10 membrane. The buffer was exchanged in the Amicon to the H_2S buffer (100 mM succinic acid, 100 mM K_2HPO_4 and 1 mM ethylenediaminetetraacetic acid (EDTA) at a pH of 6.5 to proceed with the UV-Vis experiments.

2.8 Sodium dodecyl sulphate-polyacrylamide gel electrophoresis (SDS-PAGE)

The purity of the HbI mutant was verified by SDS-PAGE analysis. The gel used was prepared by making a resolving gel at 15 % using the following solutions: 30 % acrylamide mix, 1.5 M Tris (pH 8.8), 10 % SDS, 10% ammonium persulfate and TEMED, and a 5 % stacking gel with 30 % acrylamide mix, 1.0 M Tris (pH 6.8), 10 % SDS, 10 % ammonium persulfate and TEMED. The samples were prepared by mixing the protein and a SDS gel-loading buffer. The quantity of each will depend of the concentration of the protein. The SDS gel-loading buffer consisted of 0.05 M Tris-HCl at a pH of 6.8, 2 % SDS, 0.1% bromophenol blue, 10% glycerol and β-mercaptoethanol. The mixture was heated for 3 minutes in a sand bath at 95 ^{o}C. Then, first

pipette 5 µL of the EZ RUN Pre-Stained Rec Protein Ladder (Fisher Scientific) with a molecular range from 11.0-170 kDa in one of the wells and put the 20 µL of the sample in each well. The migration of the protein was initiated by applying a voltage of 200 V for approximately one hour using Biorad PowerPac 3000 as power supply. The gel was carefully removed and stained with Coomasie Blue for 20 minutes. The excess of stain was removed with a solution of water, acetic acid and methanol (ratio of 1:4:5) for 5 minutes. The gel was left in distilled water for 24 hour period.

2.9 UV-Vis measurements of HbI mutants with H_2S in the presence of H_2O_2

The concentration for ferric equine skeletal muscle Mb and HbI were determined using the extinction coefficient ε_{408}=179 $mM^{-1}cm^{-1}$ and ε_{407}=178 $mM^{-1}cm^{-1}$. The concentration for oxy HbI was determined spectrophotometrically using extinction coefficient of ε_{416}=135 $mM^{-1}cm^{-1}$ The horse heart Mb (Sigma M0630) and the LPO (Sigma type L-2005) was purchased from Sigma-Aldrich. HbI protein from *Lucina pectinata* was isolated and purified using the method described by Kraus and Wittenberg [43] and Navarro and coworkers [127]. The approximate concentration of the HbI mutants were determined using the extinction coefficient of the HbI. If necessary, the proteins were oxidized with potassium ferricyanide to start the reaction with the heme proteins in the ferric state. The excess of potassium ferricyanide was removed using Amicon ultrafiltration with YM 10 membrane. The H_2O_2 solution was prepared from a 30 % solution and the H_2S were prepared daily from Na_2Sx9H_2O in tightly sealed ambar glass bottles. The working solutions (H_2O_2 and H_2S solutions) and the protein sample were prepared using 100 mM succinic acid, 100 mM K_2HPO_4 and 1 mM EDTA at pH 6.5 and 25 ^oC.

In UV-Vis absorption spectra the heme proteins exhibit electronic transitions of the porphyrin heme macro cycle. The heme proteins spectra are characterized by an intense band near

the ultraviolet region known as the Soret, and the Q bands between 500 nm and 650 nm. The spectra of the interactions were monitored using an Agilent 8453 spectrophotometer emphasizing in the 620 nm region to detect possible formation of the sulfheme derivative. The interactions of the heme proteins, Mb, HbI, LPO and HbI mutants (Phe29His HbI, Phe68His HbI, Gln64His HbI and Gln64His and Phe68Val HbI) with H_2O_2 and H_2S were performed in sealed quartz cuvettes with septum (1cm path length). At first the oxo ferryl intermediates were obtained by adding three fold excess of H_2O_2 to the ferric heme protein. Then twenty fold excess of H_2S was added to the protein sample except for the HbI double mutant, Gln64His and Phe68Val HbI, which was a ninety fold excess. Following the same procedure as the other mutants, 3.7 µM Gln64Arg HbI was reacted with 6.2 µM of H_2O_2 and the subsequent addition of 150 µM of H_2S.

2.10 UV-Vis measurements of the interactions hemeperoxidases with H_2S

All the reagents and proteins were purchased from Sigma-Aldrich unless otherwise indicated. LPO (Sigma type L-2005) was purchased as a lyophilized powder, MPO was purchased from Planta Natural Products, HRP Type XII (Sigma P8415) and HRP Type II (Sigma P8250). The concentration of LPO, MPO and HRP were determined using the extinction coefficient ε_{412}=114 $mM^{-1}cm^{-}1$, ε_{428} = 91 $mM^{-1}cm^{-1}$ per heme and ε_{403}=102 $mM^{-1}cm^{-1}$, respectively. The H_2O_2 was obtained as a 30 % solution. The working solutions were prepared using a 0.1 M KH_2PO_4/Na_2HPO_4 buffer. H_2S solutions were prepared daily from Na_2Sx9H_2O in tightly sealed ambar glass bottles. These solutions were diluted in the KH_2PO_4/Na_2HPO_4 buffer containing 1 mM EDTA. All other chemicals were ACS reagent grade or better.

2.10.1 UV-Vis measurements of LPO reactions with O_2 and H_2O_2 in the presence of H_2S

The interactions of H_2S with LPO were measured with an Agilent 8453 spectrophotometer using sealed quartz cuvettes with septum (1cm path length). The reactions were made titrating 1

µL of the reagents with a gastight syringe into the sample in the cuvette. All the measurements were performed at 25 ^{o}C and pH 7.0 in 0.1M KH_2PO_4/Na_2HPO_4 buffer. To evaluate the interactions of native LPO with H_2S in the presence of O_2, H_2S was added to the sample in a gastight syringe. In ferrous LPO, the buffer, Na_2Sx9H_2O, sodium dithionite (DT), and protein solutions were prepared anaerobically by degassing for 30 min and flushing with nitrogen for at least 20 min. To accomplish the reduction of LPO a seven fold excess of DT was added from a freshly prepared anaerobic stock solution. The reaction with H_2S was made when the DT was consumed, monitored by the absorbance decrease at 315 nm, and the LPO remains in the ferrous oxidation state. After the H_2S addition to LPO, the sample was purge for 1 min with O_2 and the associated spectral changes were obtained. The experimental turnover of sulfLPO was followed upon the reaction of LPO with 10.5 µM of H_2O_2 and 375 µM of H_2S. Initially, the formations of the ferryl species were obtained from the addition of three fold excess of H_2O_2 to native LPO. After two minutes, H_2S was added to the reaction. The spectral changes of the formation of 638 nm were observed for periods of 10 sec, 4 min, 6 min and 8 min. The reaction proceeds until the LPO returned to the electronic transition characteristics of the proteins' native state. Then a second aliquot of 21 µM of H_2O_2 was added to the sample leading to a new increase of the 638 nm intensity. The process was repeated several times until all H_2S was used and the reaction products are only related to the classical peroxidative reaction and the 638 nm band was completely absent.

2.10.2 UV-Vis measurements of LPO reaction with H_2O_2 and hydralazine

The reaction started by adding 10.5 µM of H_2O_2 to 3.5 µM LPO. After the oxo-ferryl species were formed, 300 µM of hydralazine were added from a freshly prepared stock solution.

2.10.3 UV-Vis measurements of HRP reactions with H_2S

The interaction with 9.6 µM HRP type II was investigated by the addition of 29 µM H_2O_2 and the consequently addition 192 µM of H_2S. Initially the formations of the oxo-ferryl species were obtained from the addition of three fold excess of H_2O_2 to native HRP. After three minutes, H_2S was added to the reaction. The spectral changes were recorded at 5 seconds and 10 minutes. The reaction proceeds until the HRP returned to the native state. The interaction of 192 µM of H_2S to 9.6 µM HRP was performed under aerobic conditions. The spectra were taken at 5 minutes and 10 minutes. The interactions of 11.52 µM H_2O_2 and 716 µM H_2S was evaluated with other HRP isoform (6.07 µM HRP type XII). The reactions with HRP type XII were performed using a Smimadzu UV-2600 spectrophotometer. The reactivity of H_2S with ferric HRP type XII was studied by adding 288 µM of H_2S to 5.76 µM of HRP under anaerobic conditions.

2.10.4 UV-Vis measurements of MPO aerobic and anaerobic reaction with H_2S

The interactions of H_2S with ferrous MPO and with ferric MPO under anaerobic conditions were measured with an Agilent 8453 spectrophotometer using sealed quartz cuvettes with septum (1 cm path length). The reactions were made titrating 1 µL of the reagents with a gastight syringe into the sample in the cuvette. All measurements were performed at 25 ^oC and pH 7.0 in 0.1 M KH_2PO_4/Na_2HPO_4 buffer. Ferric MPO, buffer, Na_2Sx9H_2O, DT, and protein solutions were prepared anaerobically by degassing for 30 min and flushing with nitrogen for at least 20 min. To investigate the interaction of ferric MPO with H_2S, 115 µM of H_2S was added to 2.5 µM of ferric MPO. Following 36 min incubation time samples were purged with O_2 for 30 sec. For the ferrous MPO experiments, to accomplish the reduction of 2.7 µM MPO a fivefold excess of DT was used from a freshly prepared anaerobic stock solution. When the reduction was complete, 115 µM of H_2S was added to start the reactions. Pure O_2 was introduced by purging the solutions for 30 sec.

All reactions were followed by monitoring the absorbance changes in the Soret band region of MPO, collecting time resolved polychromatic data in the 200 - 800 nm range.

2.11 Stopped-flow spectrophotometry of LPO aerobic and anaerobic reaction with H_2S

The interactions of native LPO with H_2S were measured using a π* 180 stopped flow instrument from Applied Photophysics Inc. (Leatherhead, UK) equipped with a photodiode array detection. All measurements were performed at 25 ^oC and pH 7.0 in 0.1 M KH_2PO_4/Na_2HPO_4 buffer. H_2S interaction to native LPO was performed under but both aerobic and anaerobic conditions. These measurements were made by purging with nitrogen gas for at least 30 min the KH_2PO_4/Na_2HPO_4 buffer (0.1M), H_2S, and protein solutions. Then 12 μM of native LPO sample and 560 μM H_2S solution were transported to the stopped-flow instrument in gas-tight syringes.

2.12 EPR spectroscopy of LPO reactions with H_2O_2 in the presence of H_2S

Electron paramagnetic resonance (EPR) measurements were carried out on a Varian E-112 spectrometer equipped with a TE_{102} cavity operating at X-band (9 Ghz) frequencies. The sample temperature was held at 77 K using an immersion finger Dewar flask. EPR spectra were recorded using 1mW microwave power, modulation amplitude 1.00 x 10.00 Gs, 0.5 s time constant and 2000 points. The samples were prepared at pH of 7 in 0.1M KH_2PO_4/Na_2HPO_4 buffer. The different reactions of H_2S with and without H_2O_2 with LPO at 300 μM under aerobic conditions were made in sealed glass bottles and then 200 μL were immediately transferred into quartz EPR tubes (4 mm OD) and frozen in liquid nitrogen. Previously adding the solution, the EPR tube was degassed with N_2.

2.13 Measurement of sulfur derivatives, i.e. sulfate production, upon LPO turnover

The reaction was performed as described in section 2.10.1, here, after 3 and half hour of the turnover of LPO in the presence of H_2O_2 and H_2S, the sample was centrifuge for 30 thirty

minutes in intervals of 10 minutes in a 10 kDa concentrator. The permeate fraction was recover to measure the sulfate production in the reaction following a procedure established in the literature [64]. The 900 µL aliquot was acidified with a conditioning reagent (450 µL) containing concentrated HCl. Barium sulfate was obtained as a precipitate by adding barium chloride to the solution. Then 1mL of the solution was transferred to a quartz cuvette to measure the optical density at 420 nm. The concentration of sulfate was determined using a calibration curve (Figure 2-12) previously made in a range concentration of 10 ppm – 80 ppm of sulfate with a 1,000 ppm sodium sulfate stock.

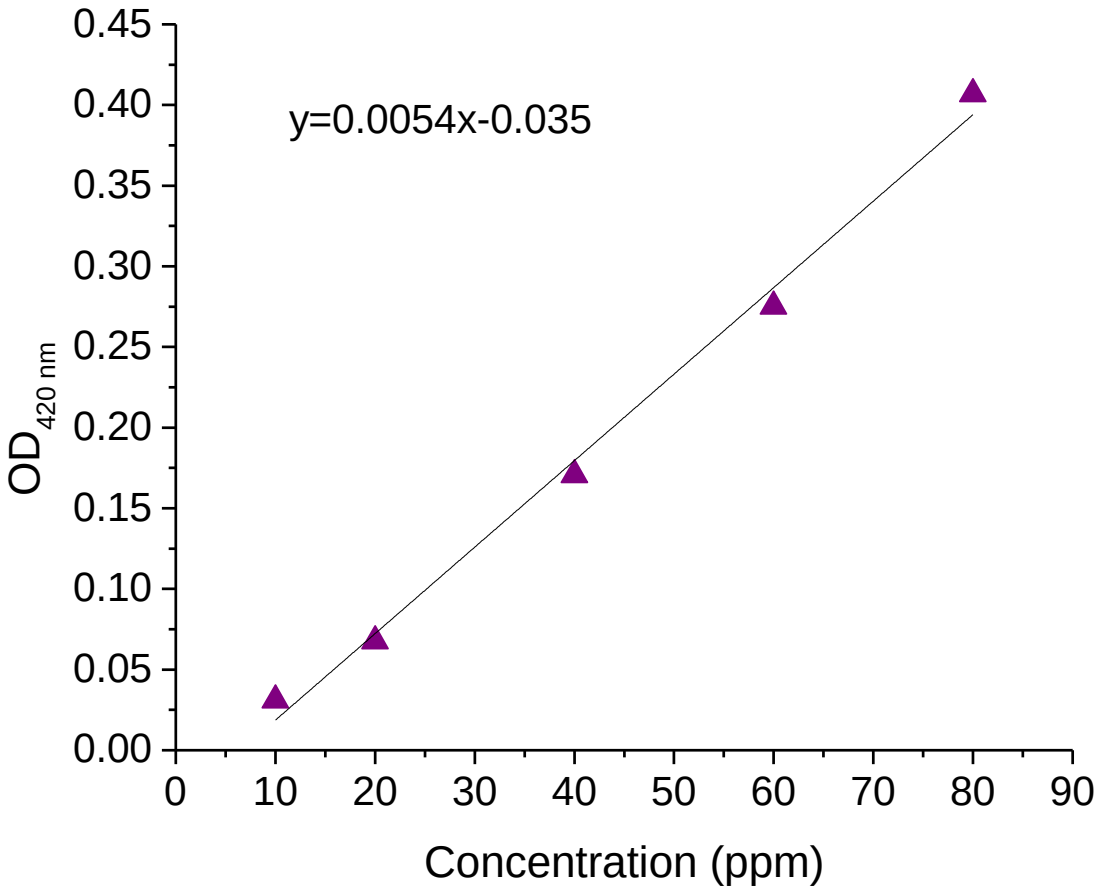

Figure 2-12. Calibration curve to determine sulfate concentration. The curve was prepared using a 1,000 ppm sodium sulfate stock.

Chapter 3: Results

CHAPTER 3: RESULTS

3.1 HbI mutant's preparation and interactions with H_2S

3.1.1 Single and double HbI mutations by Site Directed Mutagenesis

The mutagenic oligonucleotide primers used to generate the HbI mutants are described in Table 3-1. After the site directed mutagenesis, the integrity of the HbI single mutant was verify with a 1.2% agarose gel showing the linearized digested plasmid of approximately 5 Kb and the insert of 430 b (Figure 3-13). Figures 3-14, 3-15 and 3-16 show the Blast alignment of the changes in the nucleotide sequence between the rHbI and the mutated plasmids Gln64Arg HbI, Phe68His HbI and Gln64His and Phe68Val HbI, respectively. Sanger DNA sequencing confirmed that the HbI mutated plasmids had the desire mutation. It is worth mentioning that for the HbI double mutant the Gln64His HbI mutant construct was used to make construct harboring of the second mutation of valine in the position 68.

3.1.2 Small-scale expression of Gln64His and Phe68Val HbI

The expression of Gln64His and Phe68Val HbI in *Escherichia coli* Bli5 cells was performed at 25 ^{o}C, 30 ^{o}C and 37 ^{o}C induction temperatures. The pellets weight were 3.73 g, 4.56 g and 4.03 g for the inductions temperatures of 25 ^{o}C, 30 ^{o}C and 37 ^{o}C, respectively. The highest protein yield (1.16 mg) was obtained at 30 ^{o}C (Table 3-2). At 25 ^{o}C the protein obtained was 0.536 mg and at 37 ^{o}C the yield decreases to 0.282 mg. The protein yield in grams of protein mass per grams of dry cell mass reiterate that the optimum temperature for induction was 30 ^{o}C. Given this result, the large-scale expression of the HbI mutant was performed at 30 ^{o}C induction temperature.

Mutated residue	Oligonucleotide primer sequence
TTC → CAC (Phe → His)	5' GCCCAGGCACAGTCTCACAAGGGTTTGGTCAGC 3'
CAG → AGG (Gln → Arg)	5' CCAGAAATGGCAGCCAGGGCAGCACAGTCTTTCAAG 3'
CAG → CAC (Gln → His)	5' CCAGAAATGGCAGCCCACGCACAGTCTTTCAAG 3'

Table 3-1. Oligonucleotides used for the single and double HbI mutations.

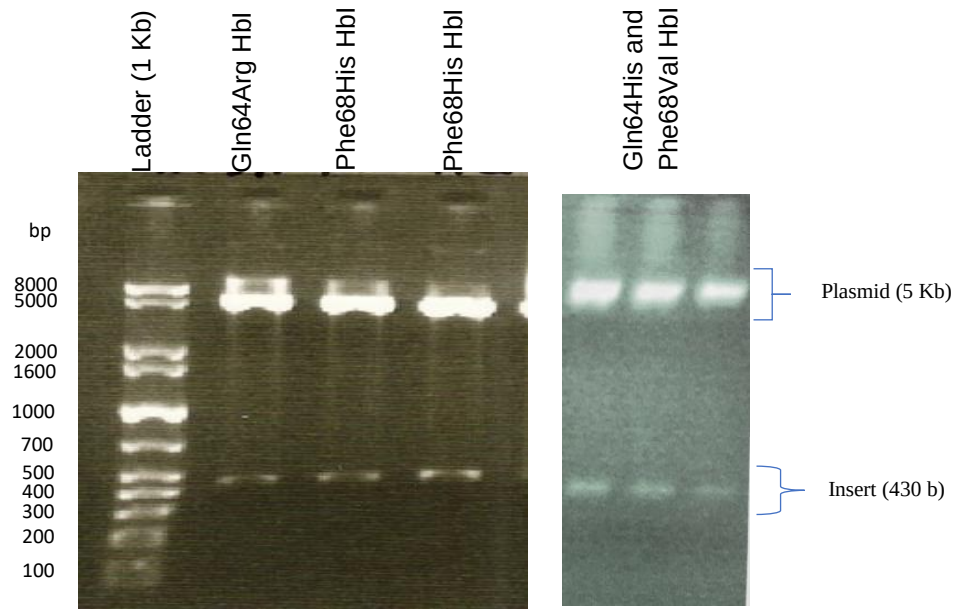

Figure 3-13. Digital image of a 1.2% agarose gel of the digested mutated pET-28(a+) with HbI insert.

Sequence ID: lcl|Query_93405Length: 1045Number of Matches: 1

Score	Expect	Identities	Gaps	Strand
787 bits(426)	0.0	430/432(99%)	0/432(0%)	Plus/Minus

```
Query  1    ATGTCTCTCTCTGCTGCACAGAAGGACAACGTGAAATCCAGCTGGGCAAAGGCTAGTGCT  60
            ||||||||||||||||||||||||||||||||||||||||||||||||||||||||||||
Sbjct  481  ATGTCTCTCTCTGCTGCACAGAAGGACAACGTGAAATCCAGCTGGGCAAAGGCTAGTGCT  422

Query  61   GCCTGGGGAACCGCTGGTCCCGAATTCTTCATGGCTCTTTTCGATGCCCATGATGATGTG  120
            ||||||||||||||||||||||||||||||||||||||||||||||||||||||||||||
Sbjct  421  GCCTGGGGAACCGCTGGTCCCGAATTCTTCATGGCTCTTTTCGATGCCCATGATGATGTG  362

Query  121  TTCGCCAAGTTCAGCGGGCTATTCAAGGGGGCAGCAAAGGGCACCGTGAAGAACACACCA  180
            ||||||||||||||||||||||||||||||||||||||||||||||||||||||||||||
Sbjct  361  TTCGCCAAGTTCAGCGGGCTATTCAAGGGGGCAGCAAAGGGCACCGTGAAGAACACACCA  302

Query  181  GAAATGGCAGCCCAGGCACAGTCTTTCAAGGGTTTGGTCAGCAACTGGGTAGACAATCTT  240
            ||||||||||||  ||||||||||||||||||||||||||||||||||||||||||||||
Sbjct  301  GAAATGGCAGCCAGGGCACAGTCTTTCAAGGGTTTGGTCAGCAACTGGGTAGACAATCTT  242

Query  241  GACAACGCCGGAGCTCTTGAGGGTCAGTGCAAGACATTCGCAGCAAACCACAAAGCCAGA  300
            ||||||||||||||||||||||||||||||||||||||||||||||||||||||||||||
Sbjct  241  GACAACGCCGGAGCTCTTGAGGGTCAGTGCAAGACATTCGCAGCAAACCACAAAGCCAGA  182

Query  301  GGCATTTCAGCTGGCCAGCTTGAGGCTGCTTTTAAAGTACTCGCAGGATTCATGAAAAGT  360
            ||||||||||||||||||||||||||||||||||||||||||||||||||||||||||||
Sbjct  181  GGCATTTCAGCTGGCCAGCTTGAGGCTGCTTTTAAAGTACTCGCAGGATTCATGAAAAGT  122

Query  361  TATGGCGGAGATGAGGGCGCATGGACCGCAGTCGCCGGAGCATTGATGGGCATGATCAGA  420
            ||||||||||||||||||||||||||||||||||||||||||||||||||||||||||||
Sbjct  121  TATGGCGGAGATGAGGGCGCATGGACCGCAGTCGCCGGAGCATTGATGGGCATGATCAGA  62

Query  421  CCAAACATGTGA  432
            ||||||||||||
Sbjct  61   CCAAACATGTGA  50
```

Figure 3-14. Blast alignment between the nucleotide sequence of rHbI and the Gln64Arg HbI mutation.

Sequence ID: lcl|Query_28045Length: 988Number of Matches: 1

Score	Expect	Identities	Gaps	Strand
787 bits(426)	0.0	430/432(99%)	0/432(0%)	Plus/Plus

```
Query  1    ATGTCTCTCTCTGCTGCACAGAAGGACAACGTGAAATCCAGCTGGGCAAAGGCTAGTGCT  60
            ||||||||||||||||||||||||||||||||||||||||||||||||||||||||||||
Sbjct  96   ATGTCTCTCTCTGCTGCACAGAAGGACAACGTGAAATCCAGCTGGGCAAAGGCTAGTGCT  155

Query  61   GCCTGGGGAACCGCTGGTCCCGAATTCTTCATGGCTCTTTTCGATGCCCATGATGATGTG  120
            ||||||||||||||||||||||||||||||||||||||||||||||||||||||||||||
Sbjct  156  GCCTGGGGAACCGCTGGTCCCGAATTCTTCATGGCTCTTTTCGATGCCCATGATGATGTG  215

Query  121  TTCGCCAAGTTCAGCGGGCTATTCAAGGGGGCAGCAAAGGGCACCGTGAAGAACACACCA  180
            ||||||||||||||||||||||||||||||||||||||||||||||||||||||||||||
Sbjct  216  TTCGCCAAGTTCAGCGGGCTATTCAAGGGGGCAGCAAAGGGCACCGTGAAGAACACACCA  275

Query  181  GAAATGGCAGCCCAGGCACAGTCTTTCAAGGGTTTGGTCAGCAACTGGGTAGACAATCTT  240
            |||||||||||||||||||||||  ||||||||||||||||||||||||||||||||||
Sbjct  276  GAAATGGCAGCCCAGGCACAGTCTCACAAGGGTTTGGTCAGCAACTGGGTAGACAATCTT  335

Query  241  GACAACGCCGGAGCTCTTGAGGGTCAGTGCAAGACATTCGCAGCAAACCACAAAGCCAGA  300
            ||||||||||||||||||||||||||||||||||||||||||||||||||||||||||||
Sbjct  336  GACAACGCCGGAGCTCTTGAGGGTCAGTGCAAGACATTCGCAGCAAACCACAAAGCCAGA  395

Query  301  GGCATTTCAGCTGGCCAGCTTGAGGCTGCTTTTAAAGTACTCGCAGGATTCATGAAAAGT  360
            ||||||||||||||||||||||||||||||||||||||||||||||||||||||||||||
Sbjct  396  GGCATTTCAGCTGGCCAGCTTGAGGCTGCTTTTAAAGTACTCGCAGGATTCATGAAAAGT  455

Query  361  TATGGCGGAGATGAGGGCGCATGGACCGCAGTCGCCGGAGCATTGATGGGCATGATCAGA  420
            ||||||||||||||||||||||||||||||||||||||||||||||||||||||||||||
Sbjct  456  TATGGCGGAGATGAGGGCGCATGGACCGCAGTCGCCGGAGCATTGATGGGCATGATCAGA  515

Query  421  CCAAACATGTGA  432
            ||||||||||||
Sbjct  516  CCAAACATGTGA  527
```

Figure 3-15. Blast alignment between the nucleotide sequence of rHbI and the Phe68His HbI mutation

Sequence ID: lcl|Query_30813Length: 729Number of Matches: 1

Score	Expect	Identities	Gaps	Strand
776 bits(420)	0.0	426/429(99%)	0/429(0%)	Plus/Plus

```
Query  1    CATGTTTGGTCTGATCATGCCCATCAATGCTCCGGCGACTGCGGTCCATGCGCCCTCATC  60
            ||||||||||||||||||||||||||||||||||||||||||||||||||||||||||||
Sbjct  33   CATGTTTGGTCTGATCATGCCCATCAATGCTCCGGCGACTGCGGTCCATGCGCCCTCATC  92

Query  61   TCCGCCATAACTTTTCATGAATCCTGCGAGTACTTTAAAAGCAGCCTCAAGCTGGCCAGC  120
            ||||||||||||||||||||||||||||||||||||||||||||||||||||||||||||
Sbjct  93   TCCGCCATAACTTTTCATGAATCCTGCGAGTACTTTAAAAGCAGCCTCAAGCTGGCCAGC  152

Query  121  TGAAATGCCTCTGGCTTTGTGGTTTGCTGCGAATGTCTTGCACTGACCCTCAAGAGCTCC  180
            ||||||||||||||||||||||||||||||||||||||||||||||||||||||||||||
Sbjct  153  TGAAATGCCTCTGGCTTTGTGGTTTGCTGCGAATGTCTTGCACTGACCCTCAAGAGCTCC  212

Query  181  GGCGTTGTCAAGATTGTCTACCCAGTTGCTGACCAAACCCTTGAAAGACTGTGCCTGGGC  240
            |||||||||||||||||||||||||||||||||||||||||| | |||||||| ||||||
Sbjct  213  GGCGTTGTCAAGATTGTCTACCCAGTTGCTGACCAAACCCTTCACAGACTGTGCGTGGGC  272

Query  241  TGCCATTTCTGGTGTGTTCTTCACGGTGCCCTTTGCTGCCCCCTTGAATAGCCCGCTGAA  300
            ||||||||||||||||||||||||||||||||||||||||||||||||||||||||||||
Sbjct  273  TGCCATTTCTGGTGTGTTCTTCACGGTGCCCTTTGCTGCCCCCTTGAATAGCCCGCTGAA  332

Query  301  CTTGGCGAACACATCATCATGGGCATCGAAAAGAGCCATGAAGAATTCGGGACCAGCGGT  360
            ||||||||||||||||||||||||||||||||||||||||||||||||||||||||||||
Sbjct  333  CTTGGCGAACACATCATCATGGGCATCGAAAAGAGCCATGAAGAATTCGGGACCAGCGGT  392

Query  361  TCCCCAGGCAGCACTAGCCTTTGCCCAGCTGGATTTCACGTTGTCCTTCTGTGCAGCAGA  420
            ||||||||||||||||||||||||||||||||||||||||||||||||||||||||||||
Sbjct  393  TCCCCAGGCAGCACTAGCCTTTGCCCAGCTGGATTTCACGTTGTCCTTCTGTGCAGCAGA  452

Query  421  GAGAGACAT  429
            |||||||||
Sbjct  453  GAGAGACAT  461
```

Figure 3-16. Blast alignment between the reverse nucleotide sequence of rHbI and the Gln64His and Phe68Val HbI mutation.

Protein	Induction temperatures	Weight (mg)	Yield (g protein/ g dcw)
Gln64His and Phe68Val HbI	25 ºC	0.536	1.44×10^{-04}
Gln64His and Phe68Val HbI	30 ºC	1.16	2.54×10^{-04}
Gln64His and Phe68Val HbI	37 ºC	0.282	0.701×10^{-04}

Table 3-2. Weight and yield (grams of protein mass per grams of dry cell mass) of the Gln64His and Phe68Val HbI resulting from the expression in *Escherichia coli* Bli5 cells at different induction temperatures.

3.1.3 Expression of the HbI mutants (Gln64Arg HbI mutant, Phe68His HbI mutant and Gln64His and Phe68Val HbI)

Figure 3-17 shows the growth curve of the expression of the HbI mutants in *Escherichia coli* BLi5. The summarized data of the weight and color of pellet obtained for each expression of the HbI mutants is shown in Table 3-3. From the pellets obtained there we took 298.08 grams, 150 grams, and 150 grams of Gln64Arg HbI mutant, Phe68His HbI mutant and Phe68Val and Gln64His HbI, respectively. The pellets of the HbI mutants were lysed, homogenized, and centrifuge to separate the soluble protein from the cell debris. The supernatant was color red or yellow, depending of the concentration of the protein, characteristic of hemoglobin's presence. After the purification process, Figure 3-18 shows the elution profile of separation of the HbI mutants from impurities, salts and imidazole. The purification of the proteins was verified by electrophoresis as show in the sodium dodecyl sulphate-polyacrylamide gel (Figure 3-19). As seen in the gel, the lanes with the HbI mutants samples show a band around ~16,981 Da, which is the molecular weight reported for the recombinant HbI [126], demonstrating a good purification process. The faster migration of the Gln64Arg HbI can be explained by the fact that the denaturation process of the protein was affected by the large quantities of protein (79 µg) added to the well in comparison with Phe68His HbI (0.59 µg) and Phe68Val and Gln64His HbI (17 µg). This causes a change in the globular structure of Gln64Arg HbI and to migrate to lower molecular weights. The protein yield obtained from each pellet are presented in Table 3-4. The expression of the Gln64Arg HbI showed a higher yield in comparison with Phe68HisHbI and Gln64His and Phe68Val HbI. This result agrees with the pellet's color obtained for the cells containing the Gln64Arg HbI that showed a dark chocolate color. The other two HbI mutants, Phe68HisHbI, and Gln64His and Phe68Val HbI, expressions resulted in lower yields as evidenced by the brown and

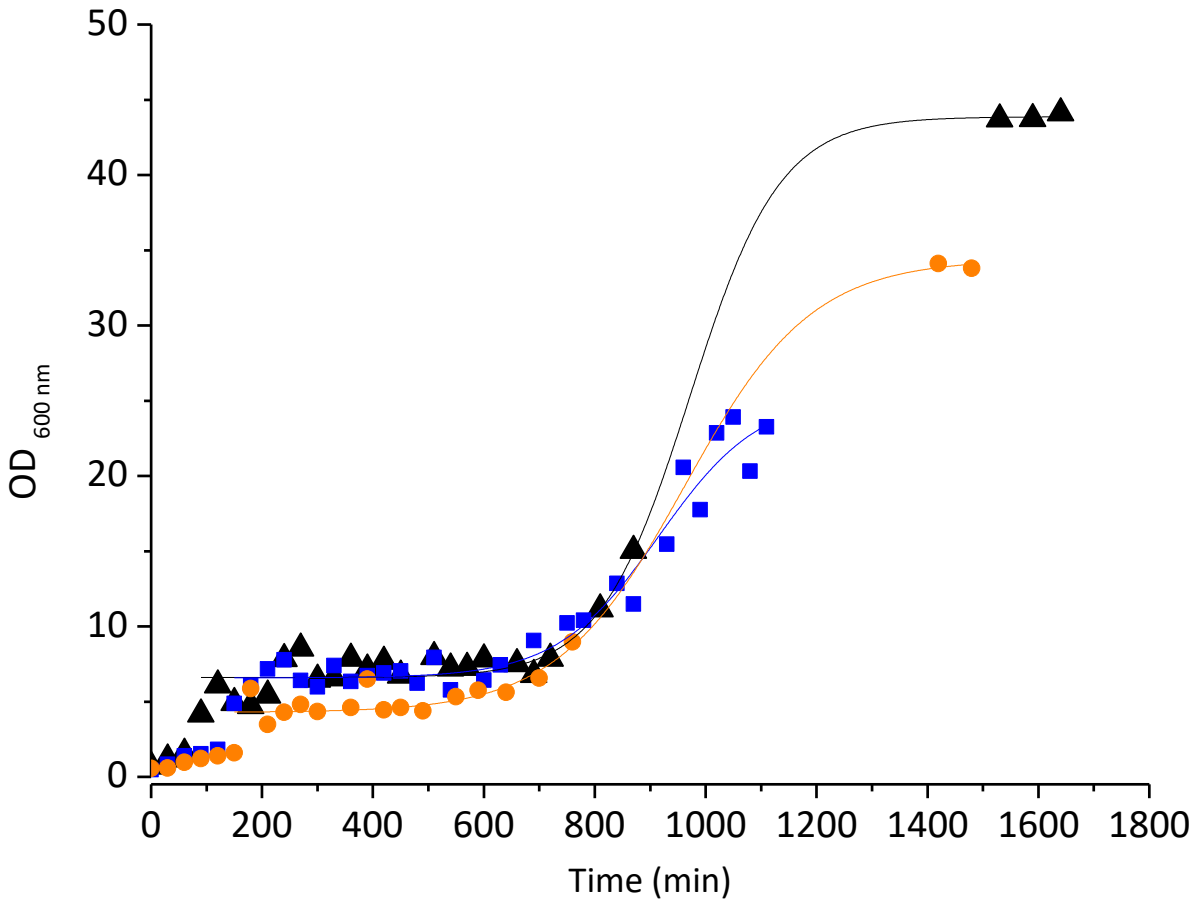

Figure 3-17. Growth curve of the expression of HbI mutants in *Escherichia coli Bli5* cells. OD at 600 nm as a function of time of Gln64ArgHbI (▲), Phe68HisHbI (●), and Gln64His and Phe68Val HbI (■) expression.

HbI mutant	Pellet	
	Weight (grams)	**Color**
Gln64Arg HbI	298.08	dark chocolate
Phe68His HbI	312.77	brown-beige
Gln64His and Phe68Val HbI	282.33	dark chocolate with beige

Table 3-3. Weight and color of the pellets after the expression of the mutated HbI protein in *Escherichia coli* Bli5.

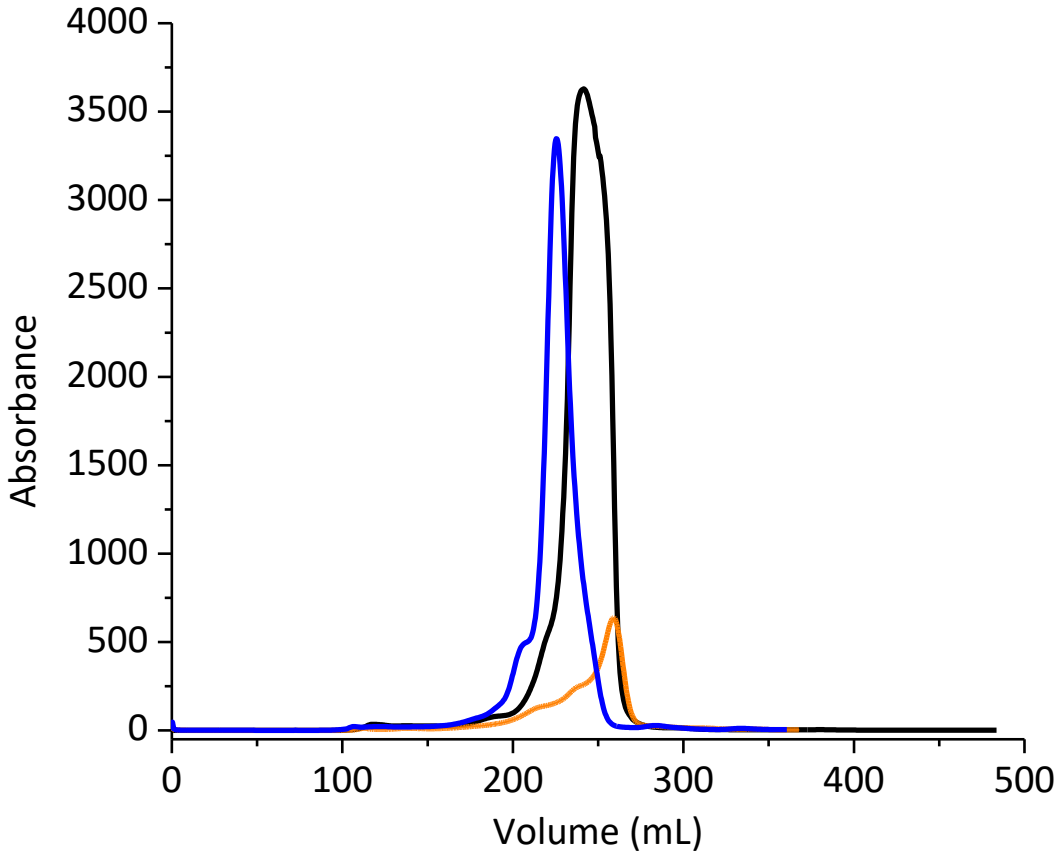

Figure 3-18. Elution profile of the size exclusion chromatography at 280 nm for the purification of the HbI mutants: Gln64ArgHbI (—), Phe68HisHbI (—), and Gln64His and Phe68Val HbI (—) expression.

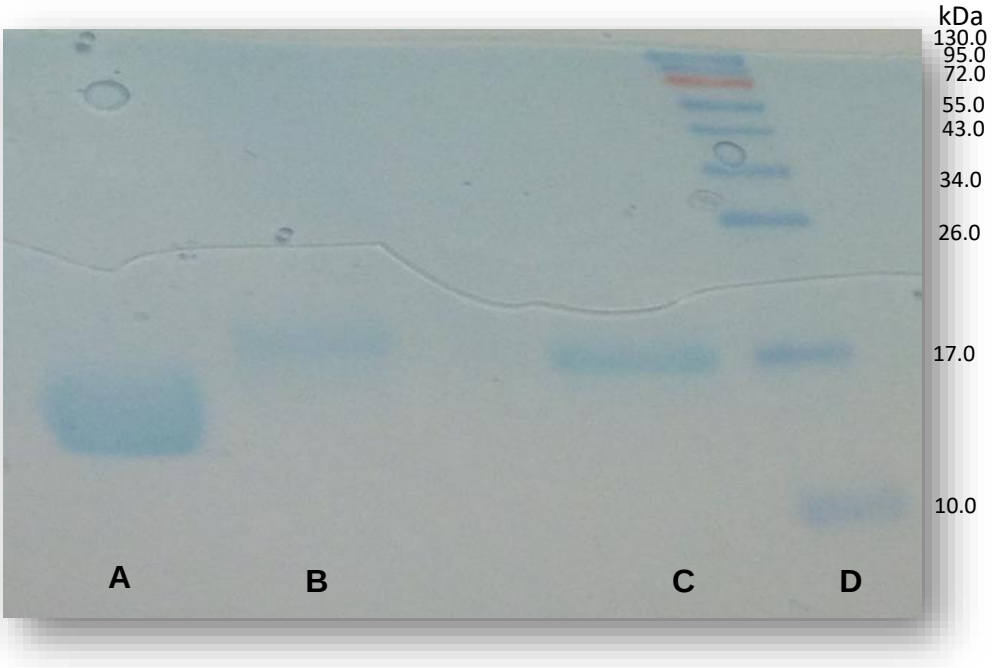

Figure 3-19. Protein separation by SDS-PAGE electrophoresis. (A) GlnE7Arg HbI, (B) PheE11His HbI, (C) PheE11Val and GlnE7His HbI and (D) EZ RUN Pre-Stained Rec Protein ladder.

Protein	**Weight (mg)**	**Yield (g protein/ g dcw)**
Gln64Arg HbI	287	9.62×10^{-04}
Phe68His HbI	0.47	0.031×10^{-04}
Gln64His and Phe68Val HbI	53	3.5×10^{-04}

Table 3-4. Weight and yield (grams of protein mass per grams of dry cell mass) of the HbI mutants resulting from the expression in *Escherichia coli* Bli5 cells.

beige color of the pellets. Additional to these new HbI mutants, a double mutant, Gln64His and Phe68Arg HbI, that mimics the active site of LPO was tried but unsuccessfully achieved.

3.1.4 Interaction of H_2S with HbI mutants in the presence of H_2O_2

To investigate the possible sulfheme formation in the HbI mutants (GlnE7Arg HbI mutant, PheE11His HbI mutant and PheE11Val and GlnE7His HbI), interactions with H_2O_2 and H_2S were studied. As mention before the Mb, LPO and Gln64His HbI are capable of forming the sulfheme derivative with a distinctive band at 620 nm, 638 nm and 624 nm, respectively. However, HbI from *Lucina pectinata* cannot form the derivative as seen in Figure 3-20. The spectrum shows the bands of H_2S complex with ferric HbI at 425 nm, 544 nm and 574 nm (blue line) [43]. Table 3-5 show the UV-Vis absorption bans of the new HbI mutant at the resting state at pH 6.5. Previous studies reported that His in the position 29 didn't form the sulfheme derivative [45] as the new HbI mutant, Phe68His HbI (green line). Both HbI mutants do not show a band in the 620 nm region. However, at the addition of H_2S to Phe68His HbI with H_2O_2 show the characteristic Q bands of H_2S complex with HbI and through time the protein returns to the native state. On the other hand, the double mutant, PheE11Val and GlnE7His HbI (yellow line) mimicking the active site of Mb show the formation of the sulfheme derivative with a band at 627 nm. These results indicate that only the histidine in the position 64 at the active site can form the sulfheme derivative.

UV-Vis spectrum of 3.7 µM of Gln64Arg HbI upon the reaction 6.2 µM of H_2O_2 and 150 µM of H_2S was recorded as showed in Figure 3-21. Initially, the Gln64Arg HbI showed a Soret band at 412 nm and the Q bands were at 502 nm, 541 nm, 576 nm and 633 nm. The addition of H_2O_2 caused a decreased in the intensity of the Soret band and the 502 nm band vanished and the 633 nm band decreases. Other two bands appear at 540 nm and 575 nm. After the formation of the

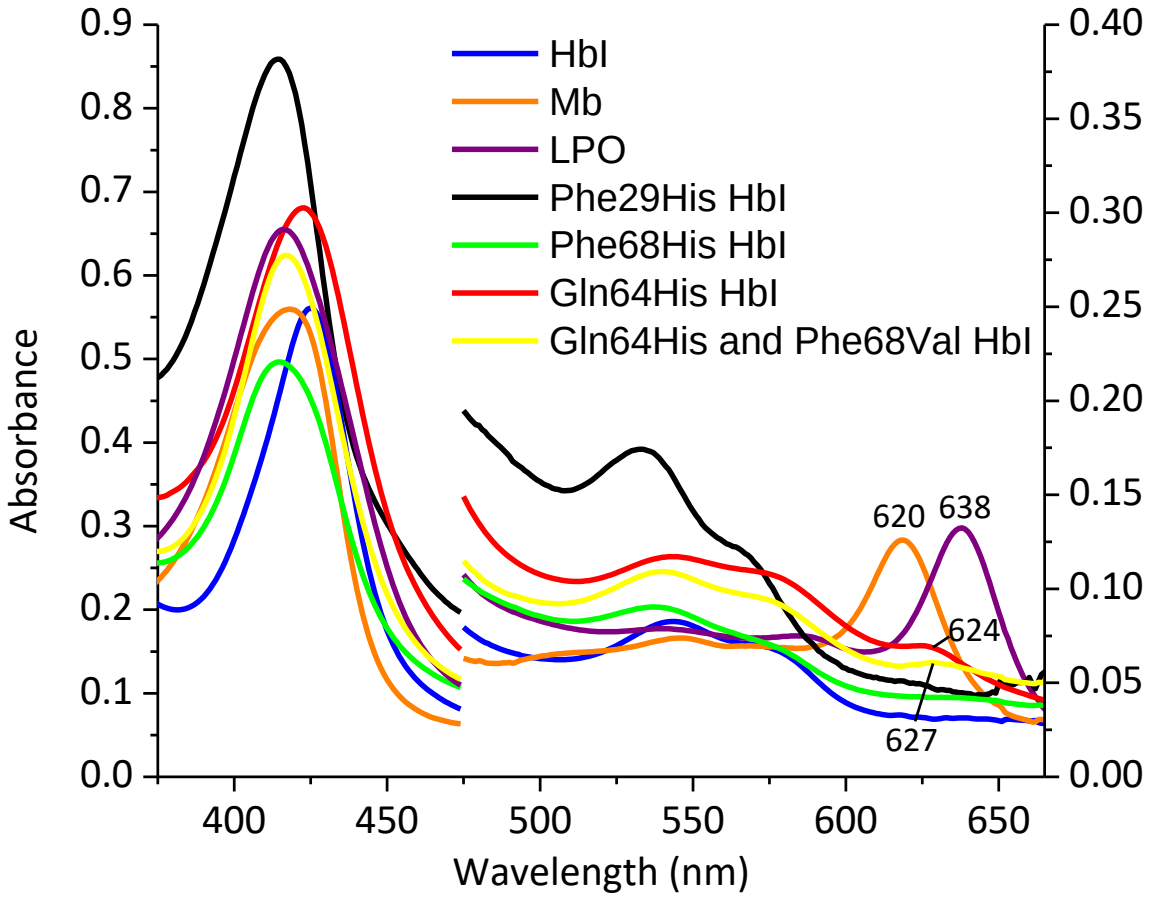

Figure 3-20. UV-Vis spectra of the interaction of hemeproteins with H_2S in the presence of H_2O_2.

Protein	Soret band (nm)	Visible bands (nm)
HbI	408	502, 540, 576 633
Phe68His HbI	409	532, 566, 633
Gln64His and Phe68Val HbI	412	533, 574, 633
Gln64Arg HbI	412	502, 541, 576, 633

Table 3-5. UV-Vis absorption bands of the ferric HbI mutants.

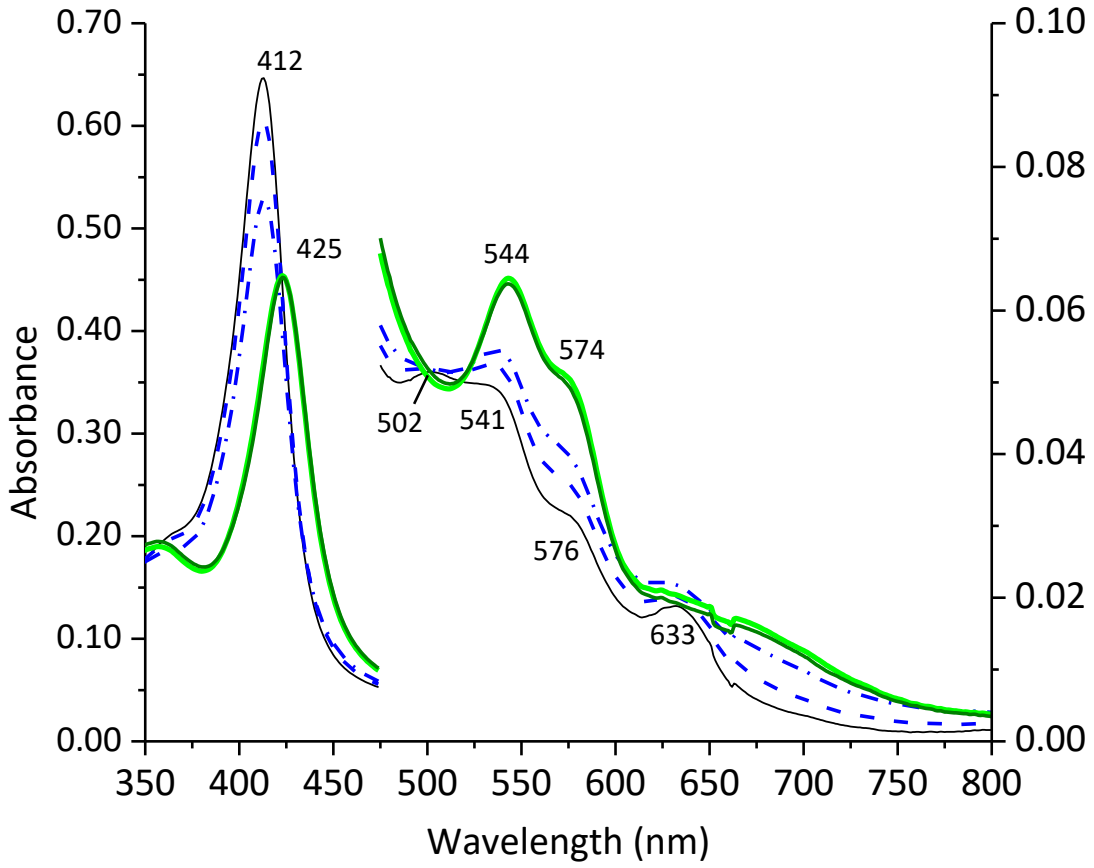

Figure 3-21. UV-Vis spectra of the reaction of Gln64Arg HbI with H_2O_2 and the subsequent addition of H_2S. Oxo-ferryl species at 1 min (- - -) and 2min(-·-·-) was formed by adding 6.2 µM H_2O_2 to 3.7 µM Gln64Arg HbI (—). Addition of 150 µM H_2S recorded at 1 min (▬) and 10 min (—) to the sample generated the H_2S complex with the protein.

oxo-ferryl intermediates the addition of H_2S show the Soret band shifted to 425 nm and the Q bands appear at 544 nm and 574 nm. The Gln64Arg HbI not reveal any band in the region of 620 nm but the changes in the spectrum indicates the H_2S bind to the ferric iron as a ligand.

3.2 Interactions of H_2S with hemeperoxidases

3.2.1 Aerobic and anaerobic interactions of native and ferrous LPO with H_2S

Figure 3-22A shows the classic UV-Vis spectra of LPO in the native state (thin black line), with characteristic transitions at 412 nm, 501 nm, 541 nm, 589 nm and 631 nm [110]. Upon addition of 150 µM H_2S under aerobic conditions, the Soret band shifts from 412 nm to 416 nm and new bands appear at 547 nm, 587 nm, 638 nm and 727 nm. This first spectrum was recorded at 30 sec, with the subsequent spectra taken at 60 sec, 121 sec, 241 sec and 356 sec, respectively. Arrows indicate the spectral changes associated with the dominant increase in intensity of the 638 nm and 727 nm transitions, corresponding to ferrous sulfLPO and ferric sulfLPO sulfheme species, respectively based on literature data [50]. Interestingly, stopped-flow spectra presented in Figure 3-22B (inset) show that under strict anaerobic conditions the addition of 280 µM H_2S to native LPO does not generate the formation of the dominant 638 nm and 727 nm sulfheme derivatives, indicating the need of molecular oxygen to produce these sulfLPO products. To further define the oxygen requirement for the reaction, ferrous LPO was reacted with sulfide with and without subsequent addition of oxygen to the reaction mixture. Figure 3-23 shows the spectra of native and ferrous LPO (orange line) with Soret and Q bands at 412 nm and 501 nm, 541 nm, 589 nm and 631 nm and 444 nm and 561 nm and 593 nm, respectively [111]. The addition of 50 µM H_2S at 5 sec (green line) and at 1 min (olive dotted line) to ferrous LPO show no spectral changes. However, subsequent addition of O_2 to this sample generates the species (red bold line) dominated by the 638 nm transition. Notice, however, that the 727 nm band is not present in this Figure 3-23

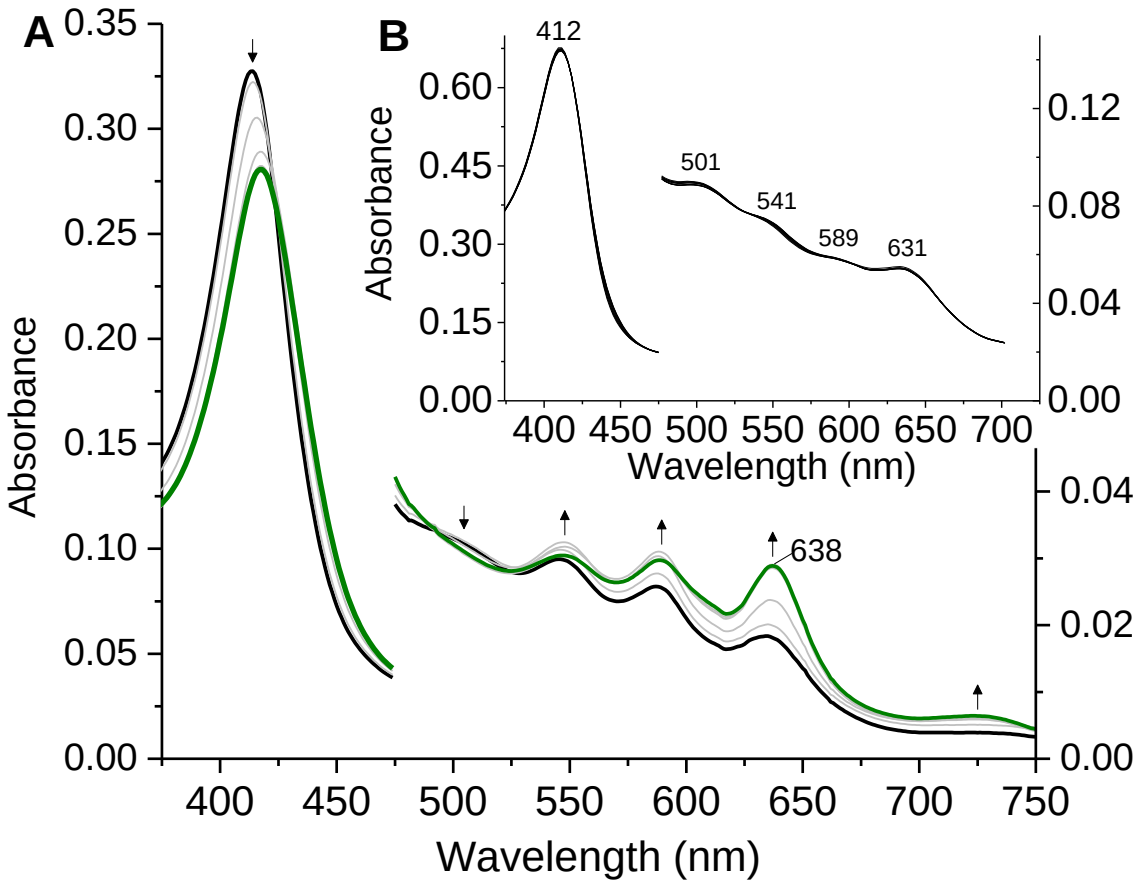

Figure 3-22. H_2S interaction with native LPO. (A) Spectral changes of the interaction of 3 µM native LPO (—) with 150 µM H_2S under aerobic conditions. The first spectrum upon addition of H_2S was recorded at 30 sec, with the subsequent spectra taken at 60 sec, 121 sec, 241 sec and 356 (—) sec. Arrows indicate direction of the spectra changes. (B, inset) Stopped-flow spectra of the interaction of 6 µM native LPO with 280 µM H_2S under anaerobic conditions. The spectra were recorded at 0.81 sec after mixing, with the subsequent spectra taken at 5.6 sec, 9.3 sec, 21.0 sec, 30.0 sec, 49.9 sec, 69.1 sec, 81.1 sec, and 100.0 sec. respectively.

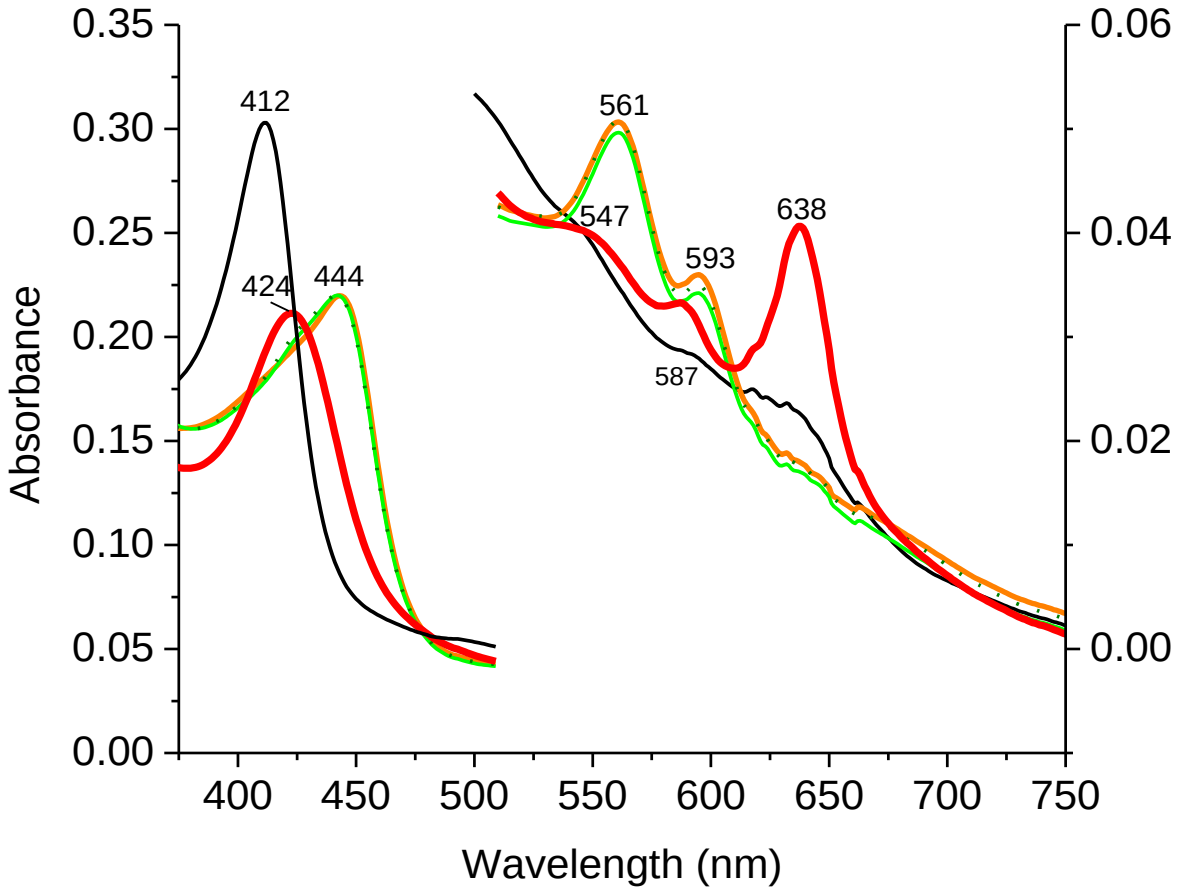

Figure 3-23. Interaction of ferrous LPO with H_2S and the subsequent addition of O_2. Ferrous LPO (—) was formed upon adding DT to 2.7 μM native LPO (—). The addition of 50 μM H_2S at 5 sec (—) and at 1min (· · ·) show no spectral changes, while the addition of O_2 generated sulfLPO (▬).

spectrum, since it is dominated by the ferrous LPO derivative. Figure 3-24 presents a red shift of the Soret band upon the addition of 150 μM H_2S to native LPO under anaerobic conditions and the appearance of two bands at 561 nm and 593 nm. These are characteristic to ferrous LPO indicating sulfide-mediated reduction of ferric LPO to ferrous LPO. Notice, that the spectrum did not show a complete transition of the native LPO to the ferrous state under these conditions. Consistent with this, subsequent addition of O_2 (Figure 3-24 Inset) results in bands at 416 nm, 547 nm, 587 nm, 638 nm and 727 nm, indicating the formation of both ferric- and ferrous-sulfLPO. Through time, the ferrous and ferric sulfLPO bands decrease in intensity and the protein returns to the native state. Overall, the data indicate that for LPO the formation of the 638 nm and 727 nm derivative directly depends on the presence of both O_2 and H_2S, leading to the conclusion that under oxidative conditions LPO forms the corresponding sulfLPO derivatives in line with a previous proposal [50].

3.2.2. Aerobic and anaerobic interactions of ferric and ferrous MPO with H_2S

Previous studies shown that ferric MPO reacts with H_2S to give a low spin complex of MPO with H_2S [51]. Palinkas and coworkers reported that the reaction of H_2S with MPO in the prescence of O_2 exhibit characteristic spectroscopic features with a distinct band at 625 nm and a shoulder at 472 nm [51]. However, these derivatives were not characterized in detail. Figure 3-25A shows the distinctive bands of ferric MPO at 429 nm, 570 nm and 690 nm (black thin line). Interestingly, after the addittion of H_2S under strictly anaerobic conditions, the Soret band shift from 429 nm to 472 nm and new band s appear at 590 nm and 638 nm. The complete transition to 472 nm ocurred at approximately thirty minutes (green line). These peaks resemble the spectrophotometric feautures of ferrous MPO [128,112] which indicate the reduction of MPO by excess of H_2S. Subsequent addition of O_2 to the ferrous MPO showed a shift from 638 nm to 625

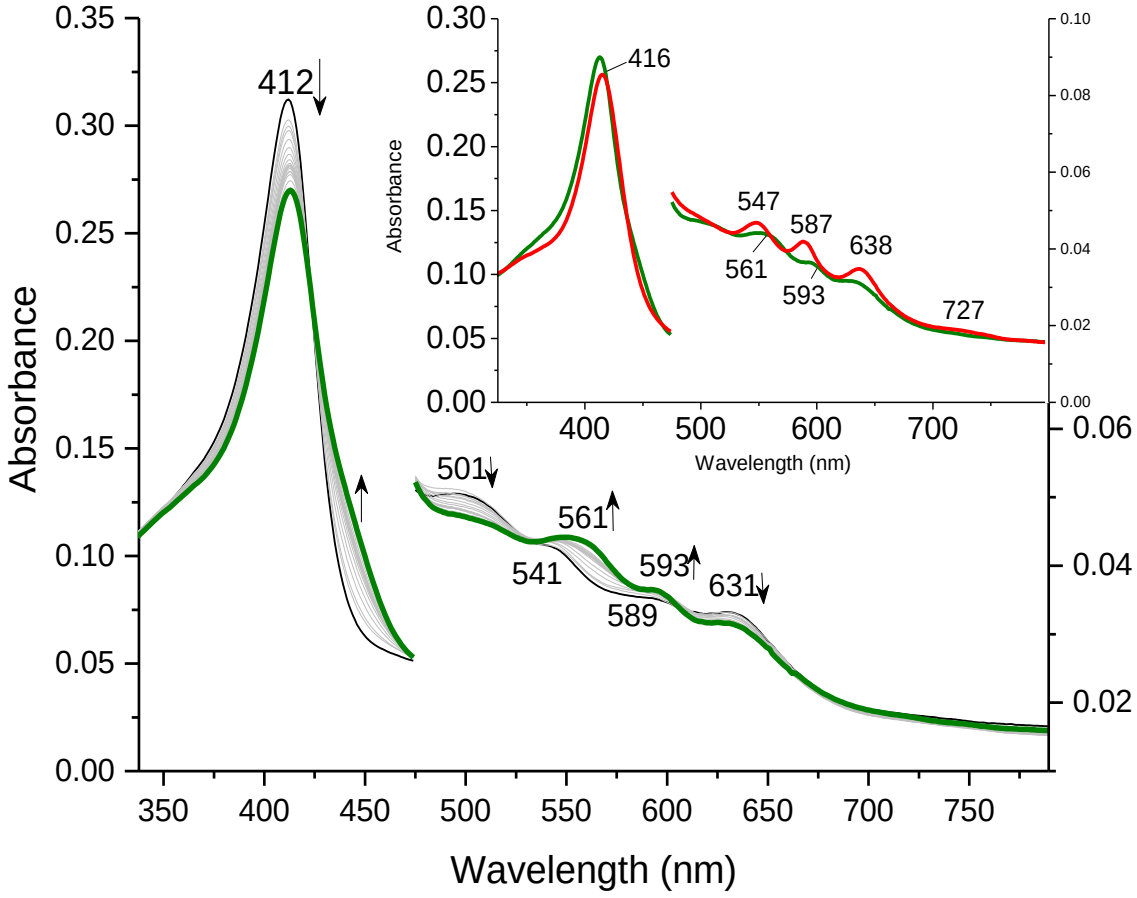

Figure 3-24. Interaction of ferric LPO with H_2S under anaerobic conditions and subsequent addition of O_2. Ferrous LPO (—) was partially form upon adding 150 µM H_2S to 2.7 µM ferric LPO (—). (Inset) The subsequent addition of O_2 generated sulfLPO (—).

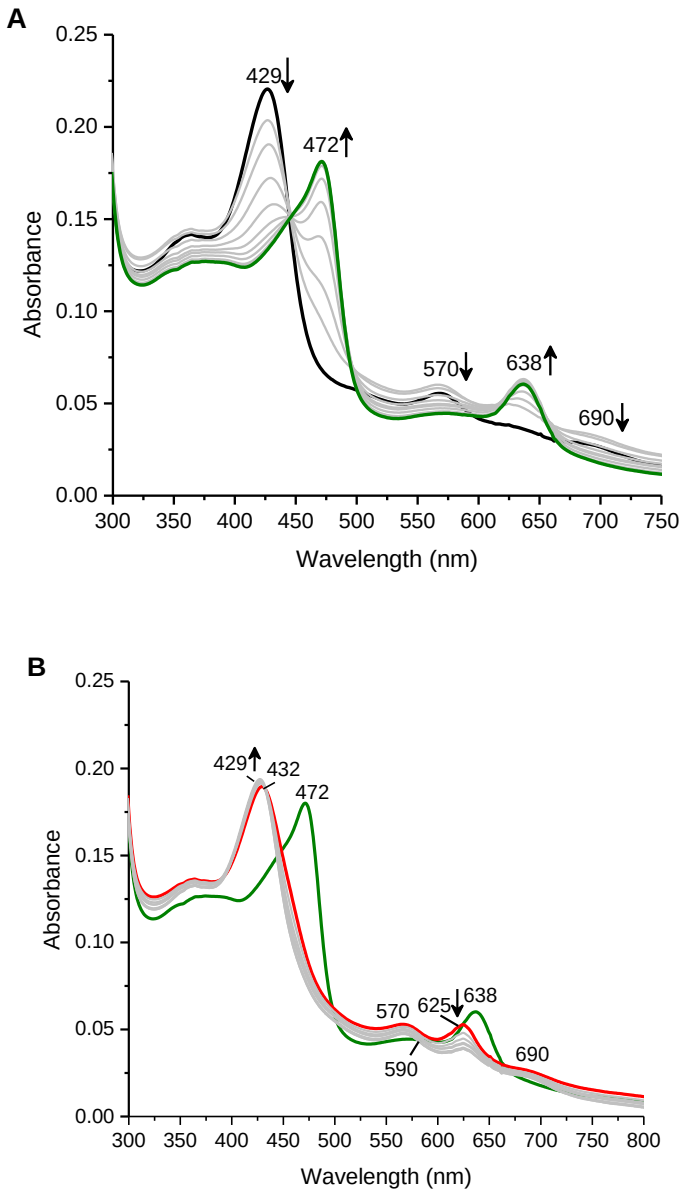

Figure 3-25. Interactions of H_2S with ferric MPO. (A) Spectral changes for the reactions of 2.5 µM native MPO (—) with 115 µM H_2S under anaerobic conditions. The spectra were taken at 35 sec, 215 sec, 395 sec, 575 sec, 755 sec, 935 sec, 1105 sec, 1305 sec, 1545 sec and 1715 sec. Green spectrum shows the formation of ferrous MPO at 1835 sec. (B) Spectral changes upon the addition of O_2 to the reaction mixture after completion of the reactions that are shown on Figure 3-25A. Red spectrum shows the addition of O_2 (30 sec) to ferrous MPO (—) in the presence of H_2S. The subsequent spectra were recorded at 150 sec, 330 sec, 450 sec, 750 sec, 1050 sec, 1350 sec and 3150 sec. Arrows indicate direction of the spectral changes.

nm and the Soret band shifted from 472 nm to 432 nm (Figure 3-25B). This spectrum is similar to the one obtained from the reaction of MPO with H_2S under aerobic conditions and in the prescence of H_2O_2 [51]. Through time the 625 nm band decayed and the protein slowly returned to the native state (Figure 3-25B). These results indicate the need of molecular oxygen to form the 625 nm species.

Ferrous MPO was formed by the reduction of ferric MPO with a fivefold excess of DT under anaerobic conditions. Figure 3-26A shows the spectra of ferrous MPO with a Soret band at 472 nm and two additional bands at 570 nm and 638 nm. Absorbance at 315 nm is due to DT. No spectral changes were observed upon the addition of 115 µM H_2S (for up to 24 min), with the exception of a decrease at 315 nm, which is due to the consumption of O_2 by DT (Figure 3-26A), where O_2 (in small amounts) was introduced to the reaction mixture upon the addition of H_2S. Subsequent addition with O_2 (Figure 3-26B) of the sample causes an immediate formation of the 432 nm and 625 nm band. At longer incubation times the 625 nm band decreased in intensity and the distinctive bands of ferric MPO appeared (429 nm, 570 nm, and 690 nm) suggesting a slow turnover of the enzyme until the exhaustion O_2 or H_2S (Figure 3-25B and 3-26C). Although the 625 nm band is similar to the spectroscopic features of the sulfheme derivative in Hb (618 nm) [41], Mb (620 nm) [37,44,56], catalase (635 nm) [48] and LPO (638 nm) [50], in MPO this band is attibuted in literature to the reaction of MPO with O_2, superoxide or excess of H_2O_2 to form compound III [112,129,130]. This suggest that the sulfheme derivative is not form in MPO.

3.2.3 Reaction of LPO with H_2O_2 in the presence of H_2S

Figure 3-27 presents the characteristic band displacements from native LPO (solid line), with transitions 412 nm, 501 nm, 541 nm, 589 nm and 631 nm to ferryl heme derivatives (430 nm, 535 nm and 567 nm), where compound II is accumulated upon reaction of LPO with an excess of

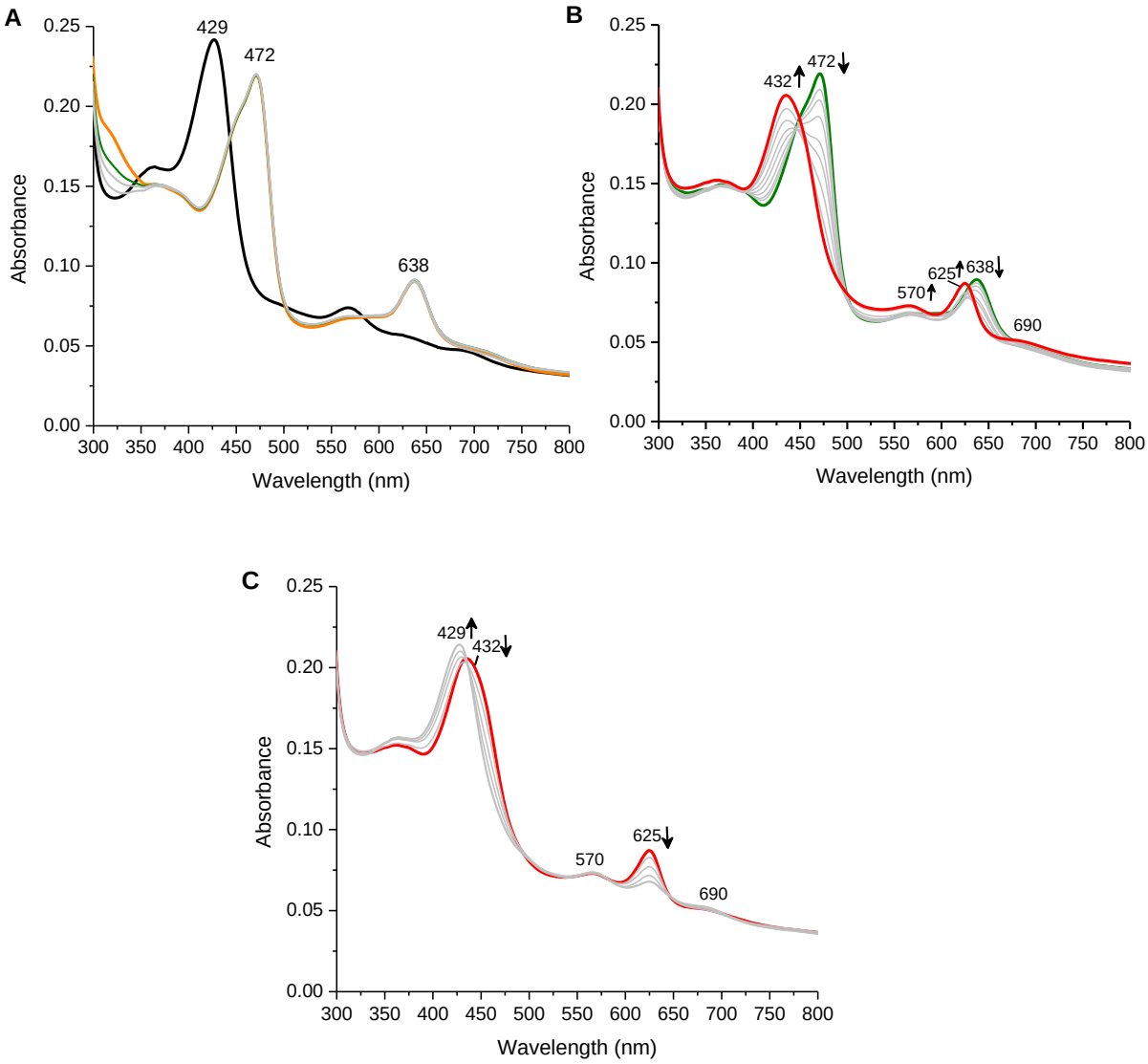

Figure 3-26. Interaction of ferrous MPO with H_2S under anaerobic conditions and subsequent addition of O_2. (A) Ferrous MPO was formed upon the addition of a fivefold excess of DT (—) to 2.7 µM native MPO (—). Subsequent addition of 115 µM H_2S did not result in substantial spectral changes in a 24 min timescale. (B) Introducing O_2 to the sample that was generated in Figure 3-26A (—) caused a shift in the Soret bands from 638 nm to 625 nm and 472 nm to 432 nm. The spectra were recorded at 10 sec, 12 sec, 14 sec, 15 sec, 16 sec, 20 sec, 25 sec, 30 sec, 31 sec and 32 sec (—). (C) Time resolved spectra demonstrate the slow return of MPO to its native ferric state after the interaction of O_2 with ferrous MPO in the presence of H_2S (sample in Figure 3-26B; red line). The spectra were taken at 32 sec, 40 sec, 78 sec, 210 sec, 240 sec and 630 sec. Arrows indicate direction of the spectral changes.

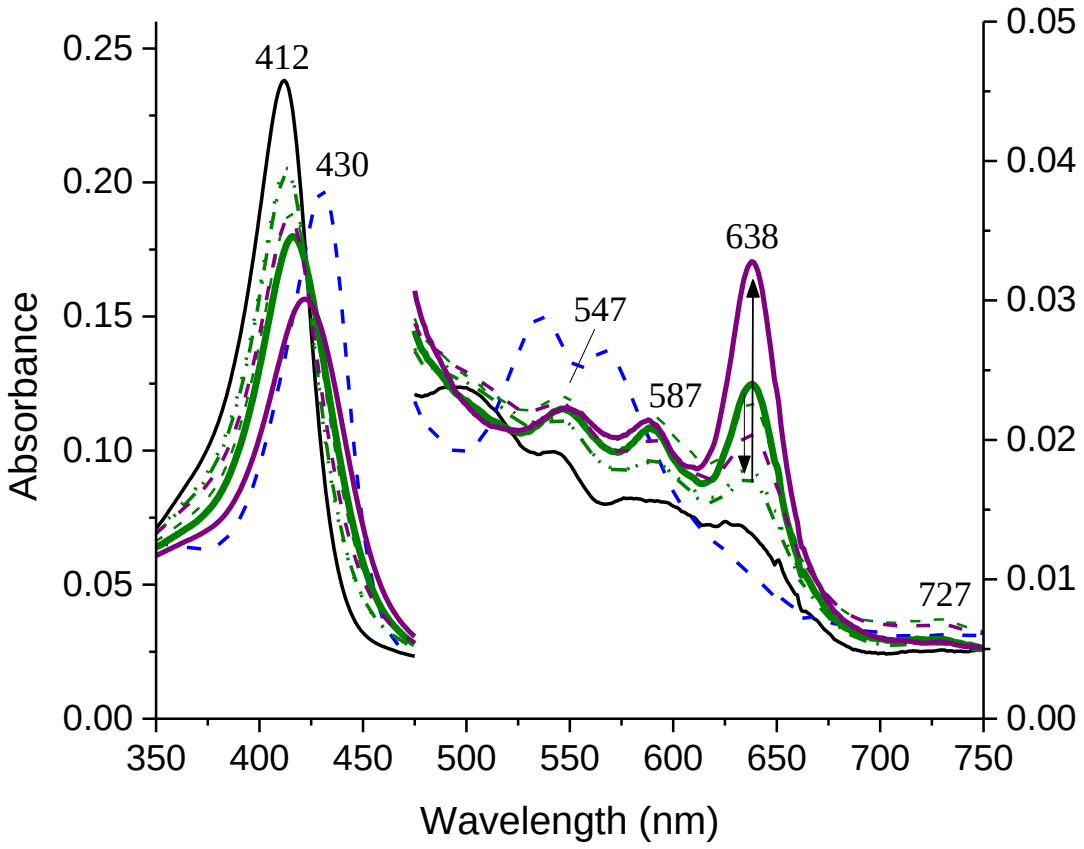

Figure 3-27. UV-Vis spectra of sulfLPO formation upon addition of H_2O_2 and H_2S to the native LPO. Oxo-ferryl species (- - -) was formed by adding 10.5 µM H_2O_2 to 2.1 µM native LPO (—). Addition of 375 µM H_2S to the sample generated sulfLPO with the spectra taken at 10 sec (▬), 4 min (- - -), 6 min (· · ·) and 8 min (-·-·-). At this last time was added 21 µM of H_2O_2 increasing the intensity of the 638 nm band (▬) and the subsequent spectra recorded at 12 min 30 sec (- - -). Arrows indicate direction of the spectra changes.

H_2O_2 (blue dashed line) [110]. The addition of 375 µM H_2S to this sample generates both the ferrous and ferric sulfLPO derivative (green bold line) with absorbance peaks at 424 nm, 547 nm, 587 nm, 638 nm and 727 nm. The transitions are identical to those present in the reaction, under aerobic conditions, between native LPO and H_2S (Figure 3-22A). Here, the 631 nm transition of the LPO native state has very low intensity or is almost absent, while the 638 nm dominates this spectral region. Subsequent spectra, without further addition of H_2S (which regardless remains in excess), at 4 min (green dashed line) and 8 min (green dashed-dotted line) show a shift of the Soret band from 424 nm to 416 nm, the Q bands at 547 nm and 587 nm remain constant and the intensity of the 638 nm band decreases with a concomitant slight increase at 727 nm. Through time the native state transitions appear, indicating that the protein has consumed all available H_2O_2 and returned to the original state, which was observed in the presence of excess H_2S (i.e. representing a mixture of ferrous and ferric LPO derivatives). Upon addition of a second aliquot of 21 µM H_2O_2, without the addition of more H_2S, Figure 3-27 shows again the formation of sulfLPO (purple bold line) transitions at 638 nm and 727 nm, which once more decreases with time. This behavior is repeated each time an aliquot of H_2O_2 was added to the protein-sulfide mixture, for a total period of 1500 sec, until all the H_2S was consumed as indicated by the absence of the ferrous and ferric sulfLPO bands at the longest time point. Overall, the data in Figure 3-27 shows that the turnover of the 638 nm and 727 nm species are directly dependent on both H_2O_2 and H_2S. Figure 3-28 shows consecutive increase and decrease periods in the 638 band upon addition of H_2O_2 aliquots and subsequent short incubation times, indicating constant turnover of LPO via sulfLPO at excess H_2S. Each new jump is the addition of another aliquot of H_2O_2 to the recovered LPO spectrum in the presence of the remaining H_2S. When all the H_2S has been consumed the remaining absorption spectrum belongs to native LPO. These LPO turnovers indicate that the formation of ferrous and

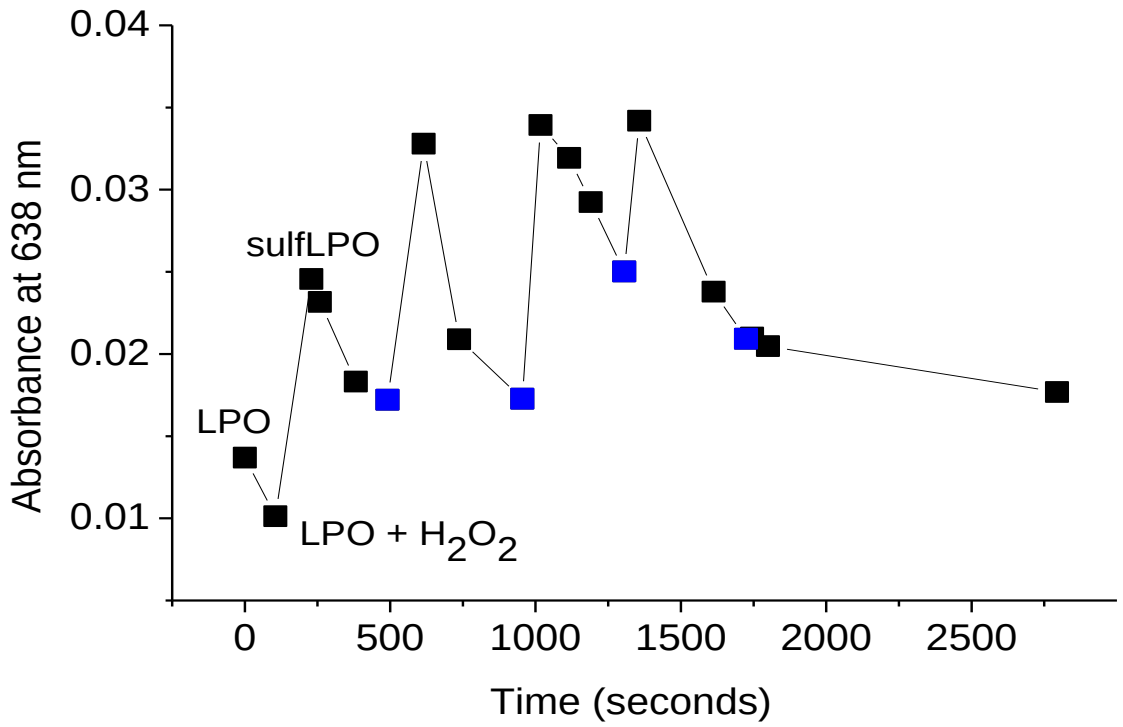

Figure 3-28. Turnover of LPO-sulfLPO formation. Absorbance trend (increase and decrease) at 638 nm upon the addition of H_2O_2 to LPO (bottom) in the presence of H_2S to from sulfLPO (top). Blue squares indicated each time H_2O_2 was added to the recuperate LPO native spectrum.

ferric sulfLPO derivatives is a reversible process and does not result in the recovery of H_2S from the sulfheme species, rather induce catalytic oxidation of sulfide.

3.2.4 Reaction of LPO with H_2O_2 and hydralazine

Comprehensive analyses of the catalytic cycles of MPO with H_2S indicated no sulfheme formation during MPO turnover, but the Compound III state was found to be the central intermediate species in that system with similar UV-Vis characteristics to sulfheme species [131]. It was also found that hydralazine oxidation by MPO proceeds via the Compound III state in the absence of H_2S. Compound III of LPO has a completely different spectral signature than the sulfheme of LPO. The Soret band of LPO Compound III is at 423 nm with two intensive bands in the visible range at 550 nm and 584 nm [111,132]. Whereas the sulfheme in LPO shows two intensive bands in the visible range at 638 nm and 727 nm [50]. Therefore, we investigated whether hydralazine oxidation by LPO catalyzed processes would induce similar spectral changes in the electronic spectra to the sulfheme derivatives of LPO. Figure 3-29 shows the interaction of native LPO with hydralazine in the presence of H_2O_2. Ferric LPO interacts with H_2O_2 to generate the oxo-ferryl intermediate species compound II with transitions at 430 nm, 535 nm, 567 nm and 589 nm (blue dashed line). The addition of hydralazine to the system returned the protein to the native state represented by the 412 nm, 501 nm, 541 nm, 589 nm and 631 nm transitions (yellow solid line), without any transient change in absorbance at 638 or 727 nm. This result indicates that hydralazine acts as a substrate and reacts with the oxo-ferryl intermediates by donating electrons to the heme and return LPO to its ferric form. In addition, the absence of the formation of the 638 and 727 nm bands support the notion that these electronic transitions are characteristic of sulfLPO.

3.2.5 Reaction of horseradish peroxidase with H_2S

To get further insight into the similarities and differences of peroxidase catalyzed oxidation

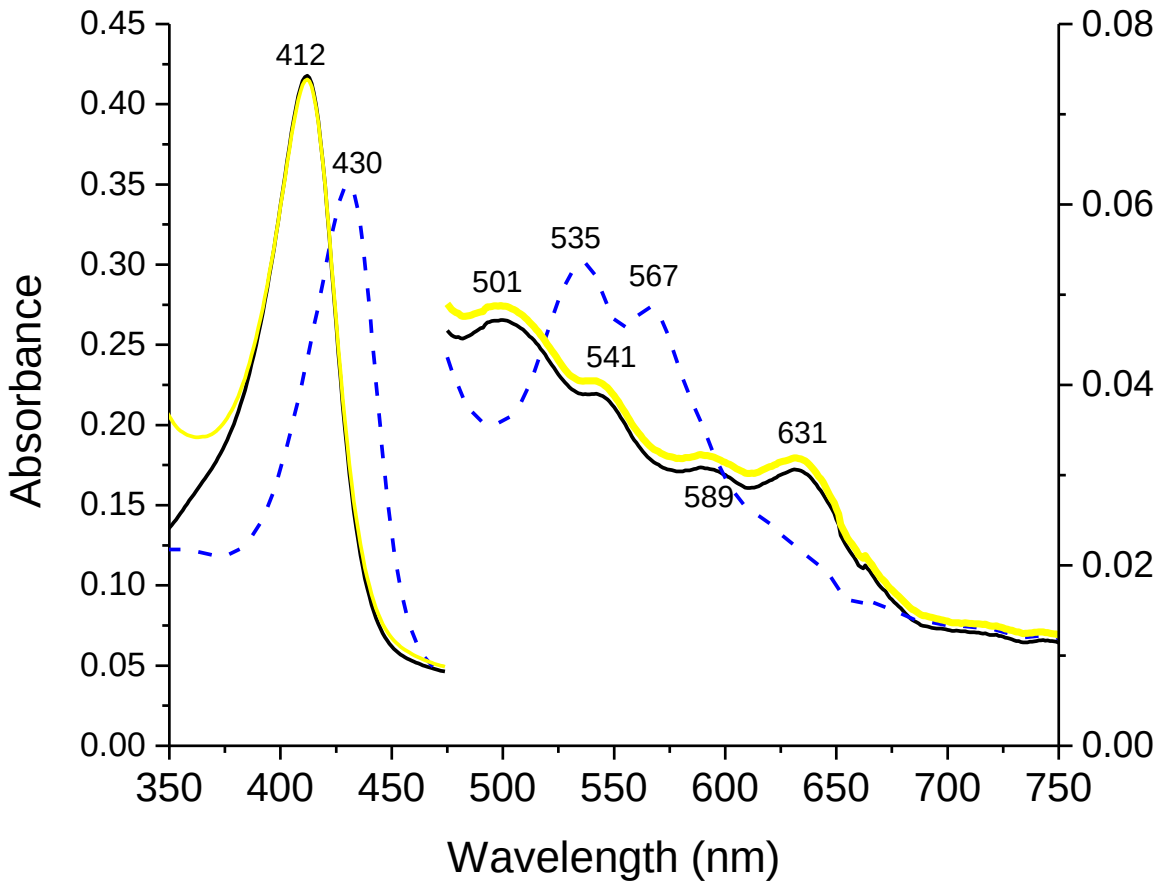

Figure 3-29. Interaction of native LPO with hydralazine in the presence of H_2O_2. Oxo-ferryl species (- - -) was formed by adding 10.5 µM H_2O_2 to 3.5 µM native LPO (—). Addition of 300 µM hydralazine (—) return the LPO to the native state.

of sulfide focusing on sulfheme formation, we also investigated the interactions of two types horseradish peroxidase isoforms with H_2S. Figure 3-30 and Figure 3-31 presents the typical peaks of metaquo-HRP at 403 nm, 495 nm and 641 nm [133]. The addition of H_2O_2 leads to a mixture of the oxoferryl intermediates, compound I and compound II with bands at 407 nm, 527 nm, 552 nm and 646 nm. Upon addition of H_2S to the reaction mixture the majority of the protein returns to the native ferric state, without any indication of sulfHRP formation. In other words, HRP did not show in any moment the classical 638 nm or 620 nm band, which can be attributed to the formation of the sulfheme derivative. Therefore, it is likely that sulfheme formation at the HRP heme is not favorable. Curiously two peaks appear at 544 nm and 576 nm with low intensity which resemble those observed for compound III [134]. Moreover, under anaerobic conditions the addition of H_2S to HRP triggers no spectral changes as indicated in Figure 3-32, suggesting that the protein remains in the native state and the heme may not react with H_2S.

3.2.6 EPR measurements for the reaction of LPO with H_2S under aerobic conditions

Figure 3-33 shows the spectra of LPO reacting with 300 µM and 15000 µM of H_2S under aerobic conditions. EPR spectrum of ferric LPO with water as ligand in buffer solution is shown in Figure 3-33a, with a distinctive high spin ferric signal as reported by Lukat et al. [135]. The spectrum with the addition of 300 µM of H_2S remains unaltered (Figure 3-33b). However, the addition of an excess of H_2S (15000 µM) show a low-spin ferric signal at 2.27 g (Figure 3-33c). This can be due to the excess of H_2S that causes the reduction of the LPO permitting the oxygen to bind to the iron and with the H_2S present in the active site trigger the sulfheme derivative formation.

3.2.7 EPR measurements for the reaction of LPO with H_2O_2 in the presence of H_2S

Figure 3-34 shows the spectra of LPO reacting with H_2O_2 in the presence of two different

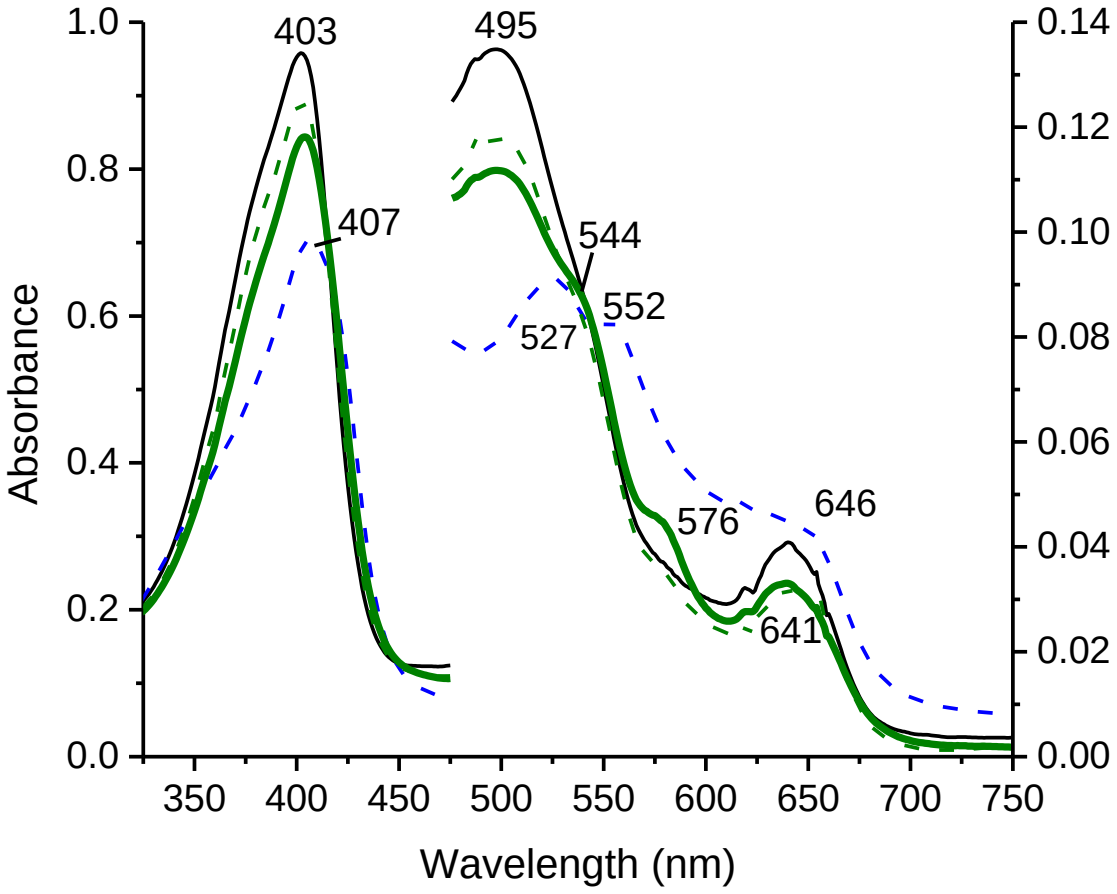

Figure 3-30. UV-Vis spectra of the interaction of ferric HRP Type II with H_2S in the presence H_2O_2. Oxo-ferryl species (- - -) were formed by adding 29 µM H_2O_2 to 9.6 µM native HRP (—). Addition of 192 µM H_2S to the sample does not generate the sulfheme derivative with the spectra taken at 5 sec (▬), and 10 min (- - -).

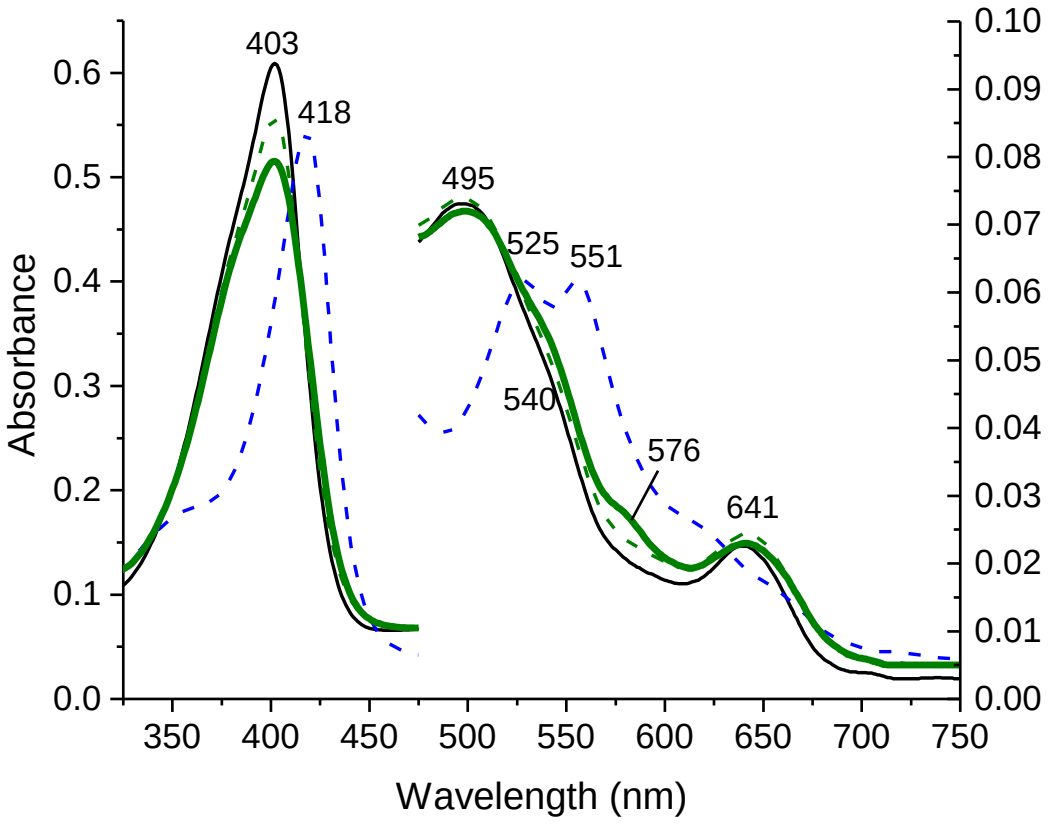

Figure 3-31. UV-Vis spectra of the interaction of ferric HRP Type XII with H_2S in the presence H_2O_2. Oxo-ferryl species (- - -) were formed by adding 11.52 µM H_2O_2 to 6.07 µM native HRP (—). Addition of 716 µM H_2S to the sample does not generate the sulfheme derivative with the spectra taken at 10 sec (▬), and 5 min (- - -).

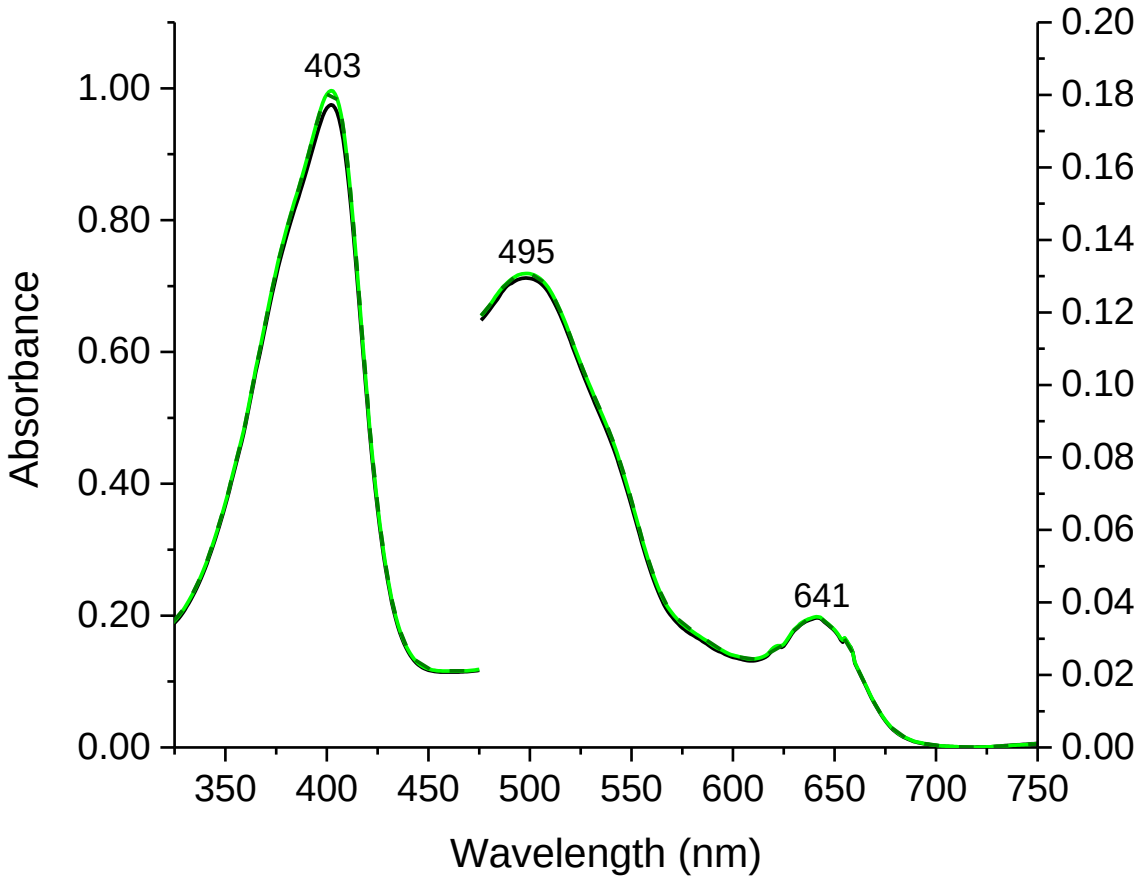

Figure 3-32. Interaction of H_2S with HRP. The spectrum were recorded at 5 min (—) and 10 min (- - -) after the addition of 192 µM H_2S to 9.6 µM HRP (—).

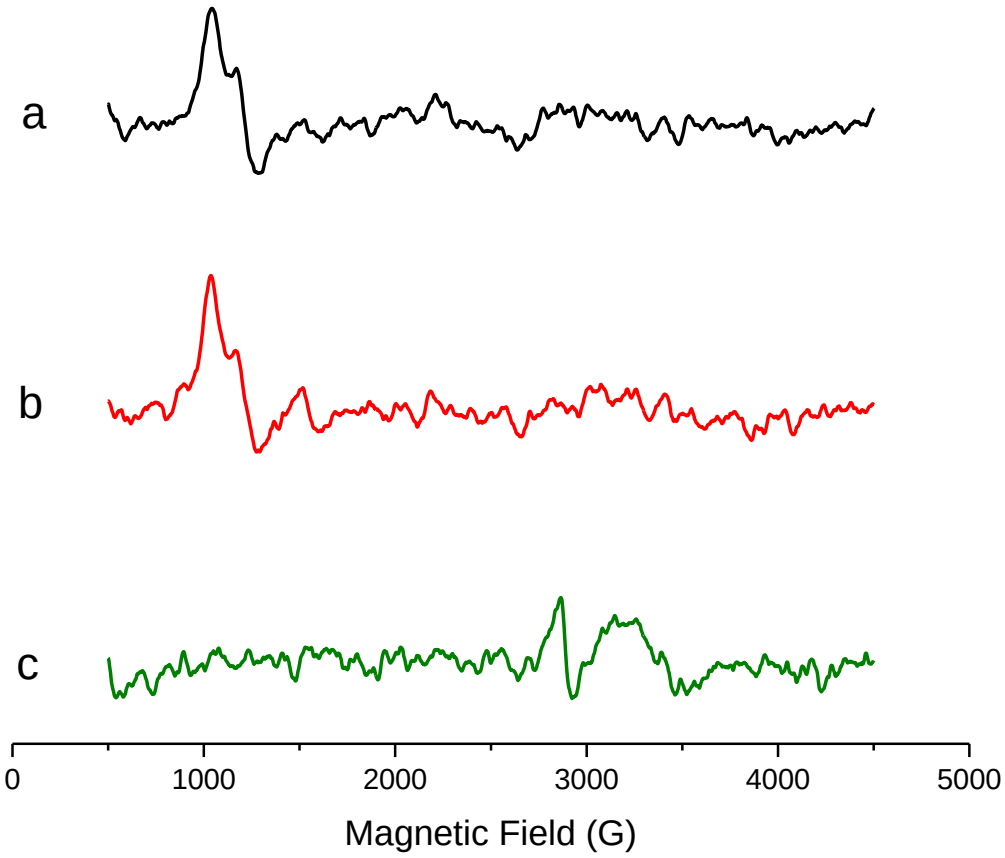

Figure 3-33. Spectra of LPO reacting with two different concentrations of H_2S. (a) EPR spectra 300 µM native LPO, (b) 300 µM native LPO reacting with 300 µM H_2S, and (c) 300 µM native LPO with 15000 µM H_2S.

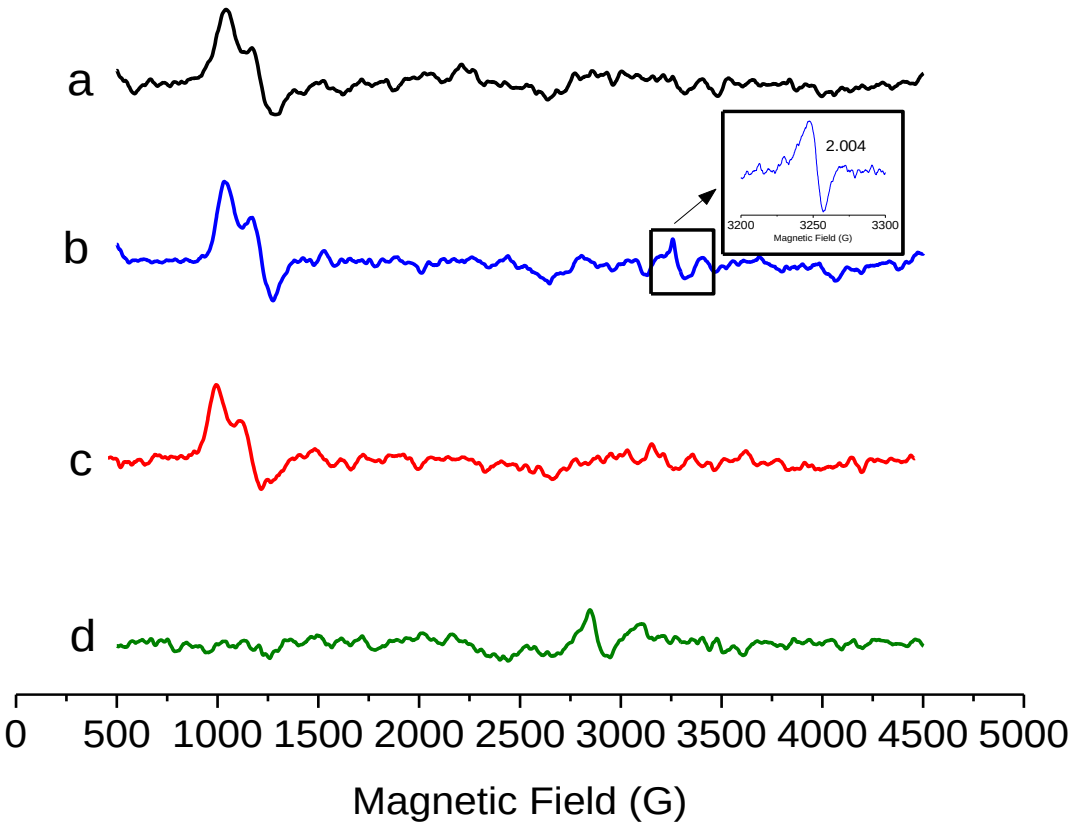

Figure 3-34. Spectra of LPO reacting with H_2O_2 at two different concentrations of H_2S. (a) EPR spectra 300 µM native LPO, (b) 300 µM native LPO reacting with 900 µM H_2O_2, (c) 300 µM native LPO reacting with 900 µM H_2O_2 upon the addition of 300 µM H_2S, and (d) 300 µM native LPO with 900 µM H_2O_2 and 15000 µM H_2S. The inset shows the enhancement of the signal in the magnetic field of 3200 to 3300 with the 2.004 g LPO radical centered in the protein amino acids.

concentrations of H_2S. Figure 3-34a shows the EPR spectrum of LPO in buffer solution, while Figure 3-34b demonstrates the EPR spectrum, upon the addition of three fold excess of H_2O_2, where a high spin ferric iron signal and a free radical peak at 2.004 g were observed. The reactions of LPO with H_2O_2 and the subsequent addition of H_2S were carried out at two different concentration ratios: LPO:H_2O_2:H_2S = 1:3:1 (Figure 3-34c) and 1:3:50 (Figure 3-34d). At the lower concentration of H_2S (Figure 3-34c) the spectrum only shows a high-spin Fe (III) signal and it does not show the free radical peak at 2.004 g. This observation not necessarily means that the radical is not generated; alternatively the radical may have a lifetime which is too short to be trapped in the timescale of sample mixing and freezing. At 50 fold excess of H_2S the spectrum (Figure 3-34d) only shows a weak low-spin Fe (III) signal.

The free radical peak with the obtained g value of 2.004 upon addition of H_2O_2 to LPO is characteristic of a carbon centered radical. Previously this radical was suggested to be a tyrosyl radical derived from oxoferryl intermediates [136]. The high spin ferric signal remains transiently stable during LPO cycling in the presence of H_2O_2. The addition of 300 µM of H_2S to the reaction mixture (300 µM LPO and 900 µM H_2O_2) vanishes the amino acids radical peak at 2.004 g. The observed high spin ferric signal is most likely the result of H_2S consumption by the excess H_2O_2. In Figure 3-34d, a low-spin ferric signal at 2.27 g appears in the spectrum following the addition of an excess sulfide (15000 µM) to a similar mixture of LPO and H_2O_2. Based on the observed and reported [137] characteristic UV-Vis bands at 727 nm, 416 nm, 547 nm and 587 nm (Figure 3-27) in a similar reaction mixture this peak can tentatively be assigned to a sulfLPO-Fe(III)-oxygen complex. In agreement with this assignment, the observed g-value of 2.27 is similar to those reported for oxygenated Mb, HRP and chloroperoxidase species [138]. The relatively low intensity of the signal is in line with formation of a mixture of ferrous (EPR silent) and ferric

sulfLPO under these conditions. This ferrous contribution was also observed by UV-Vis spectrophotometry with a characteristic band at 638 nm. Moreover, similar to the observations at the lower H_2S concentration (300 µM), the EPR spectra at 15000 µM of H_2S also did not contain any detectable peak in the 2.004 g region. Again, this does not necessarily mean that it is not formed, but it is not detectable on the timescale of the freezing of the sample after the reactants are mixed. Independently, the data shows the impact of H_2S in the observable amino acid radical at 2.004 g of the reaction of LPO and H_2O_2 (Figure 3-34b) since upon addition of H_2S the amino acid radical is not observable (Figure 3-34c and 3-34d). A thiol radical (•SH) is suggested to be involved in the mechanism for the sulfheme derivative [44]. Although any signal is observed in the thiol radical region is not discarded since the life time of the radical is to short that is difficult and it will be needed traps or lower temperatures to acquire the signals.

3.2.8 Products of LPO-sulfLPO turnover

We made an attempt to obtain some insight into the nature of the sulfide oxidation products as a result of LPO-SulfLPO turnover. Motivated by the data which demonstrated that sulfheme decomposes to protohemin, with first order kinetics to produce $SO_4^{=}$ as the major product [64], we tried to semi quantitatively investigate sulfate production in the H_2S-H_2O_2-LPO system. Figure 3-35A shows an increase in sulfate production as a function of the initial sulfide concentration at 5 µM native LPO and 25 µM H_2O_2 using three different concentration of H_2S: 600 µM (black), 800 µM (dark gray) and 1000 µM (gray), respectively. The experiment was repeated at 50 µM H_2O_2 (Figure 3-35B, inset), where a similar trend was observed, the amount of detected sulfate increases as function of the H_2S concentration. Alternatively polysulfides can also be formed in these systems as in the case of MPO [131], which upon acidification would result in S_8 precipitation and an increase in turbidity [139–141]. Thus, there is a need for additional experiments to determine

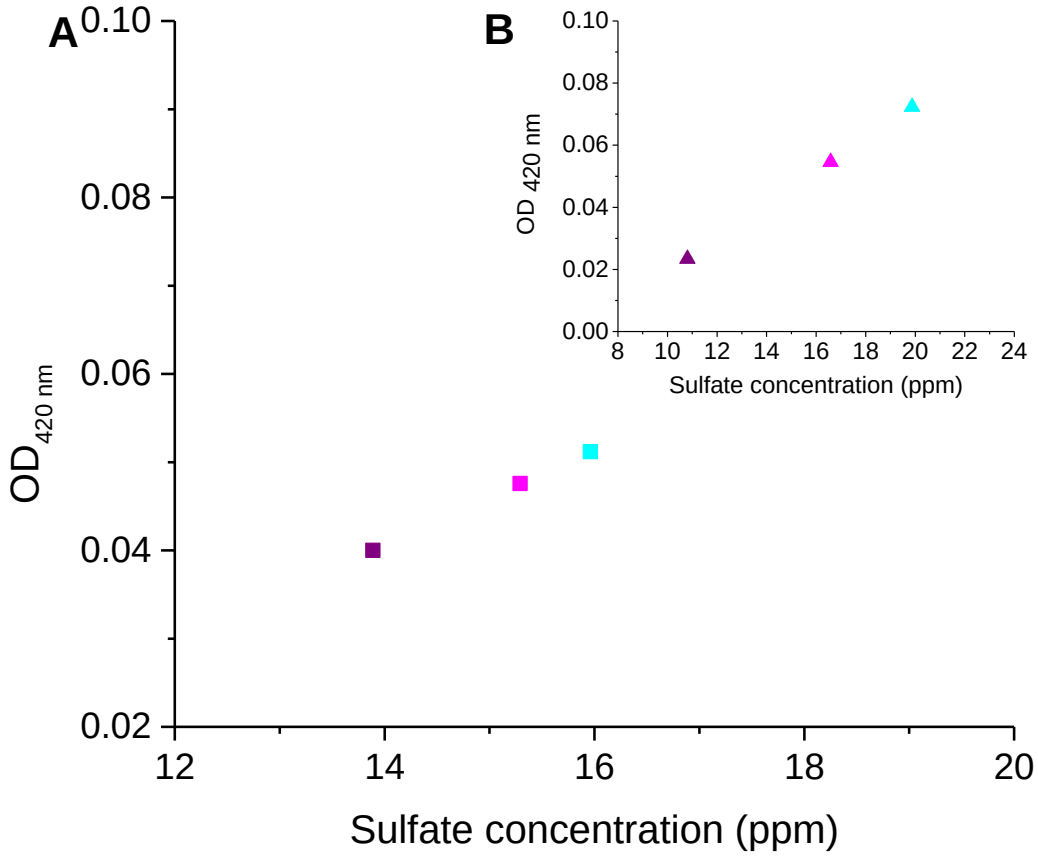

Figure 3-35. Sulfate concentration after sulfLPO formation at different concentrations of H_2O_2 and H_2S. (A) Sulfate concentration of the interaction of 5 µM native LPO with 25 µM H_2O_2 and different concentration of H_2S. (B) Sulfate concentration of the interaction of 5 µM native LPO with 50 µM H_2O_2 and different concentration of H_2S. The different concentrations of H_2S used were 600 µM (purple), 800 µM (magenta) and 1000 µM (cyan).

the potential presence of sulfane sulfur species in order to better understand the mechanism of LPO-mediated sulfide oxidation.

Chapter 4: Discussion

CHAPTER 4: DISCUSSION

The reactions of H_2S with hemeproteins in the presence of O_2 and H_2O_2 have been extensively studied resulting in distinct models to explain sulfheme chemistry [38,44,45,47,56,64,95]. Although several mechanistic aspects of sulfheme formation remain unknown, there is sufficient experimental evidence to provide insight into the characteristics of sulfheme generation. For example, the orientation and position of the His residue at the heme active site is crucial for the production of the sulfheme product [45]. Thus, with the exception of a limited group of heme proteins, such as cytochrome c oxidase, HRP, MPO and the phosphodiesterase His mutant (Ec DOS-PAS Met95His) which do not form sulfheme, the distal His seems to be essential for the formation of the heme modification [44,45]. These observations and the tautomeric nature of distal His [142] are in agreement with the Figure 1-9 showing the importance of LPO histidine protonation toward the formation of compound 0 and compound III, in the ferryl heme O−O bond cleavage, under two different scenarios dominated by H_2O_2 and O_2, respectively [109].

4.1 Insights into the HbI mutants reactions with H_2S in the presence of H_2O_2

Distal residues play an important role in functionality of hemeproteins. Earlier studies with HbI mutant mimicking the human hemoglobin active site suggest that the distal histidine plays an important role in the sulfheme derivate formation [45]. This reason inspires to performed new HbI mutants (Gln64ArgHbI, Phe68HisHbI and Gln64His and Phe68Val HbI) to evaluate the effect of the residues changes in the sulfheme derivative formation (Figure 4-36). All the HbI mutants were obtained after a good expression and purification process. The conformational changes of the HbI due to the incorporated residues can be seen in shifts in the UV-Vis band (Table 3-5). This shifts in the band can be due to a low spin contribution of the hydrogen bonding between the water

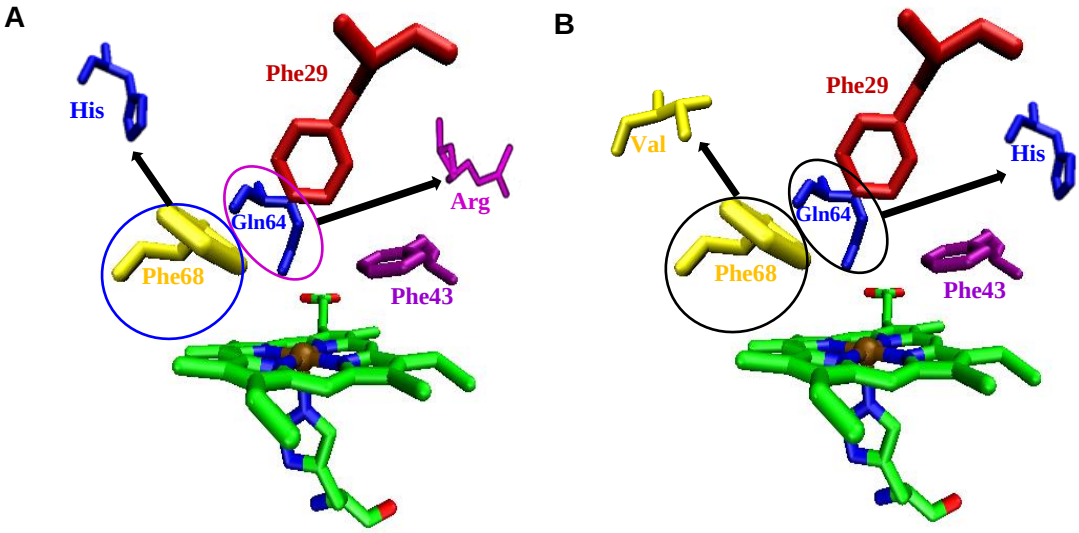

Figure 4-36. Amino acid residue substitution in the active site of HbI: (A) single HbI mutations (Gln64ArgHbI and Phe68His HbI) and (B) double HbI mutant (Gln64His and Phe68Val HbI).

molecule attached as a ligand and the distal residues as stipulated by Ruth and coworkers [46]. These changes will affect the ligand binding and stability. The HbI mutants interactions with H_2O_2 and H_2S show that definitively His with the adequate orientation and position plays an important role in the sulfheme derivative formation. The only mutant capable of forming the sulfheme derivative are the ones with His in the position 64 like Gln64His and Phe68Val HbI mutant. The Phe68HisHbI bind H_2S as a ligand and through a short period of time return to the native. As mentioned before the affinity of H_2S for ferric HbI is very high with an association constant of 2.3 x 10^5 $M^{-1}s^{-1}$ and a very slow dissociation constant of 0.22 x 10^{-3} s^{-1}. The insertion of His to the position 68 (Phe68His HbI) diminish the affinity of the HbI to H_2S inducing the protein to return to the native state. In contrast the insertion of Arg, a polar amino acid as His, to the position 64 do not form the sulfheme derivative. However, binds H_2S directly to the iron as ligand with high affinity.

4.2 Insight into the LPO reactions with H_2S in the presence and absence of O_2

The reaction of native LPO under anaerobic conditions present the reduction of the LPO heme iron by excess of H_2S, as in other met-aquo heme proteins [46] due to the hydrogen bonding environment, and no band at 638 nm or 620 nm are observed. Curiously, both, in native and ferrous LPO reaction with H_2S in the absence of O_2, the UV-Vis spectrum remains unaltered indicating that H_2S does not bind directly to the iron. However in the reaction of native and ferrous LPO with H_2S in the presence of oxygen, generates products with UV-Vis peaks at 638 nm and 727 nm which have been assigned previously to the ferrous sulfheme and ferric sulfheme derivative, respectively [50]. The EPR results of the reaction of LPO with H_2S under aerobic conditions present a low ferric spin signal attributed to an oxygenated intermediary in the ferric sulfLPO formation, discuss in detail in the next section. These observations support the behavior of H_2S to

reduce the LPO letting the O_2 bind to the iron and form the sulfheme derivative with UV-Vis band at 638 nm and 727 nm. Furthermore in Mb and Hb sulfheme derivatives show a 620 nm and 717 nm transition with the same O_2 and H_2S dependence but with a very slow turnover to the native protein [37,38,56,67,83,143]. In this Q region, the optical spectra of sulfLPO is very similar to sulfMb and sulfHb strongly suggesting that the modification in the heme group is a chlorin type structure in which the sulfur atom is incorporated across the β-β double bond of the pyrrole B [50,94,95]. The data indicate that in the presence of O_2, H_2S modifies directly the LPO heme group producing ferrous sulfLPO and ferric sulfLPO species, while species such as SCN^-, Br^- and Cl^-, do not result in altered UV-Vis spectra [144]. Therefore, the observations and the data presented experimentally, in Figure 3-22, Figure 3-23 and Figure 3-24 support the discussion that the ferrous sulfLPO and ferric sulfLPO derivatives return slowly to native LPO. Thus, H_2S in the presence of O_2 is a non-classical LPO substrate that forms the sulfheme derivative which then subsequently turns over to generate the native LPO heme. Therefore, H_2S in the presence of O_2 does not lead to an irreversible inhibition of the LPO enzymes, as is the case with other sulfur derivatives such as MMI [116].

4.3 Insights into the LPO reactions with H_2S in the presence of H_2O_2

Figure 3-27 presents the UV-Vis spectra of LPO reactions with H_2O_2 in the presence of H_2S and, analogous to the oxygen scenario, the Q region is dominated by the 638 nm transition. Similarly, Figure 3-28, shows the same behavior in the transition upon formation of sulfheme. Regarding this, Figure 3-27 demonstrates the changes in the intensity of the 638 nm transition, ferrous sulfheme LPO, as consumes H_2O_2 in the presence of an H_2S excess. At the end point of the reaction, additional H_2O_2 was added until all of the H_2S was consumed and the classical peroxidative reaction was observed (Figure 3-28). This behavior suggests that the 638 nm species

or sulfLPO does not lead to any H_2S generation or transport mechanism, rather, H_2S in LPO acts as a substrate to scavenge excess of H_2O_2 protecting the enzyme from the classical peroxidative reactions. These in vitro results indicates that H_2S can regulate the ROS species produced by the excess of H_2O_2 thus protecting the turnover of LPO. This observation is supported by the data in Figure 3-34, which indicates a significant difference between the EPR spectra of LPO plus H_2O_2 in the absence of H_2S (Figure 3-34b) and with H_2S added (Figures 3-34c and 3-34d). Under this scenario, LPO EPR results show that during the sulfheme turnover, there is not an observable aromatic amino acids radical formation or that the radical lifetime is too short to allow its trapping upon sample freezing after mixing. Apparently, H_2S can scavenge H_2O_2 without the presence of any carbon center radicals protecting also the LPO system.

4.4 Insights into the HRP reactions with H_2S in the presence of H_2O_2

Interestedly, HRP reaction with H_2O_2 and H_2S does not form sulfheme. Figure 3-30 show that H_2S, similar to other heme proteins, inactivates the HPR, indicating that H_2S acts as a reversible peroxidase inhibitor via the generation of compound III. It has been reported that a substrate can trigger the formation of compound III and the subsequent suicidal inactivation of HRP [145,146]. In this case the inactivation from compound III can followed any of these pathways: a) the substrate acts as an electron donor to form H_2O_2 and subsequently the protein returns to the native state and b) the generation of reactive oxygen species can inactivate the protein by oxidizing an amino acid near the heme group and the protein return to the native state [145]. However, under identical condition, LPO shows a continuous turnover. Nevertheless, both peroxidases do not bind H_2S to the ferric iron. The distal environments in these peroxidases are very selective to the substrates that bind to the iron. Structurally, Figure 4-37 shows both LPO and HRP have a His and Arg in their active site, which are important for their enzymatic activity, but

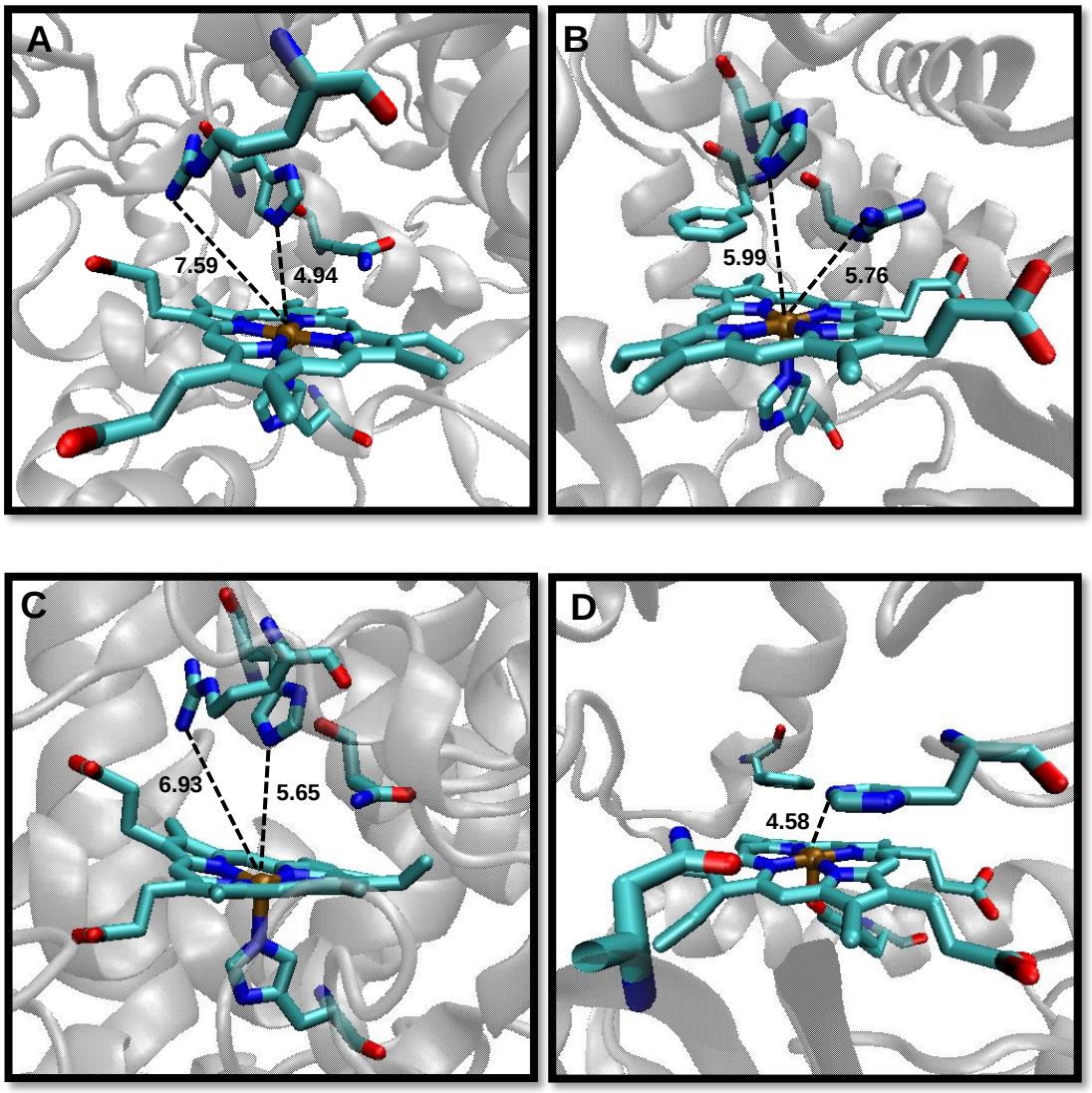

Figure 4-37. Distal active site of (A) LPO (PDB:2NQX), (B)HRP (PDB:1ATJ), (C) MPO (PDB:1CXP) and (D) catalase (PDB:3RGP).

only the former generates sulfheme, while the latter does not [44]. Furthermore, under the same oxidative conditions, H_2S allows LPO to turnover, while it inactivates HRP. This exclusive behavior and the fine tuning of the His, Arg and the heme iron centers generates two completely different scenarios. The crystallographic data in Figure 4-37 shows the distances between the His, Arg and the heme iron. In the case of His is shorter in LPO (4.94 Å), as opposed to HRP (5.99 Å), while Arg case are 7.59 Å and 5.76 Å, respectively, being the former longer that the latter. The data indicate that orientation and position of the His residue at the heme active site are crucial for the synthesis of the sulfheme product. The importance of this His residue is also supported by site directed mutagenesis in HbI, where His 64 was changed to Arg led to the inhibition of sulfheme formation as discussed in section 4.1.

4.5 Insight into the MPO reactions with H_2S in the presence and absence of O_2

Previous studies demonstrated that H_2S with the MPO oxo-ferryl intermediates, compound I and compound II, form a UV-Vis peak at 625 nm [51]. This study shows that the ferric and ferrous MPO reaction with H_2S in the absence of O_2 indicates that H_2S does not bind directly to the iron. Furthermore, we demonstrated that H_2S efficiently reduced the MPO heme iron. However the presence of O_2 in the reaction of ferric and ferrous MPO with H_2S, generates a species with a UV-Vis peak at 625 nm. The 625 nm band can be generated of the interaction of oxo-ferryl intermediates under aerobic conditions with hydralazine in the absence of H_2S [131]. Hydralazine is a substrate that acts as peroxidase inhibitor in MPO via the generation of compound III. The inactivation via compound III can occur via the hydralazine radicals a) activating O_2 and forming superoxide or by b) reducing the ferric MPO which can bind O_2 to give compound III [131,147]. In contrast the interaction of LPO with H_2O_2 and hydralazine does not generate the 638 nm band and 727 nm band. The hydralazine in LPO acts as a classical substrate returning the protein to the

native state. This points towards the idea that compound III is the species formed in the interaction of MPO with O_2 and/or H_2O_2 and H_2S instead of the sulfheme derivative. Then H_2S acts as a substrate returning the enzyme to the resting state by reverting the inhibition cause by compound III.

The reactivity of H_2S with hemeproteins was found to be controlled by the positions and orientations of distal residues [44,46]. Many hemeproteins like Hb, Mb, catalase and LPO the position and orientation of the His in the active site is crucial for the generation of the sulfheme derivative. Although MPO with His in the active site under oxidative conditions generate a band at 625 nm which is the region of the sulfheme derivatives, this research argue against the sulfheme derivative formation and supports the production of compound III. The hemeperoxidases LPO and MPO via the methyl groups on pyrrole rings A and C form two ester linkages with the carboxyl groups of glutamate and aspartate residues, respectively (Figure 1-8) [97,106]. This perturb the planarity and rigidity of heme groups. Nevertheless, MPO, in addition of these ester bonds, forms a sulfonium ion linkage with the β-carbon of the vinyl pyrrole ring A via the sulfur of Met243 (Figure 1-8), which is crucial to the effectiveness of MPO to catalyze the oxidation of chloride to HOCl [148]. The sulfonium ion linkage in MPO not only introduces a strong electron withdrawing effect on the porphyrin ring, but also causes a distortion in the heme group which displaced the iron center to the proximal site [106,107]. These effects weaken the interactions of the iron center with the pyrrol rings [149] and makes the iron located further away from the distal histidine (5.65 Å, compared to the 4.94 Å and 4.58 Å position of the histidine in LPO and catalase respectively, see Figure 4-37). The sulfur atom of the methionine responsible of the sulfonium ion linkage reduce the electron density on the heme iron, contributing to the MPO preference to form compound III instead of a sulfheme derivative.

4.6 Role of distal residues in sulfheme formation and H_2S reactivity in hemeproteins

As shown in Table 4.6, hemeproteins with His in the distal site, except for MPO and HRP, form the sulfheme derivative reiterating the essential role of His in the reaction of sulfheme. This behavior in MPO and HRP can be attributed to the distance between the His and the heme iron. which in HRP (5.99 Å) and MPO (5.65 Å) is larger in comparison with LPO (4.94 Å). In addition, in HRP the distance of Arg distal residue (5.76 Å) to the heme iron is shorter than the distance between the His and the iron. The sulfonium ion linkage in MPO introduces an electron withdrawing effect on the porphyrin ring causing that this protein does not generate the sulfheme derivative. The HbI and Gln64Arg HbI with Gln and Arg, respectively, in its distal site does not induce the sulfheme formation This demonstrates that Gln and Arg are not involve in the sulfheme formation and emphasizes that the orientation and position of His residue is vital for the synthesis of sulfheme.

The unique features of Arg and His residues in the active site of hemeperoxidases, LPO, MPO and HRP, causes that the H_2S does not bind with the ferric iron (Table 4-6). On the contrary, HbI with Gln in the active site accounts for the ferric iron high affinity for H_2S. Hemeproteins, like Mb and Hb, with His in the active site binds H_2S to the ferric iron but with low affinity. These results showed the importance of the distal residues in these hemeproteins in the reactivity with H_2S.

4.7 Events in the turnover of sulfLPO-LPO

Early on [50] it was suggested that LPO in the ferryl state (compound II) reacts with sulfide to form a typical sulfheme-containing hemeprotein. Despite this mechanism being supported today by several groups in the field of typical sulfheme-containing hemeproteins such as Hb, Mb, and catalase, there is the need to explain why H_2S does not inactivate the enzyme as observed by other

Hemeprotein	**Key distal residues**	**Sulfheme**	**Bind H_2S to the iron**
Myoglobin	His	Yes (620 nm)	Yes
Human hemoglobin	His	Yes (618 nm)	Yes
Lactoperoxidase	His, Arg	Yes (638 nm)	No
Myeloperoxidase	His, Arg	No	No
Horseradish peroxidase	Arg, His	No	No
Hemoglobin I	Gln	No	Yes
Gln64Arg HbI	Arg	No	Yes
Gln64His HbI	His	Yes (624 nm)	Yes
Phe68His HbI	Gln, His	No	Yes

Table 4-6. Sulfheme formation and H_2S reactivity in hemeproteins.

sulfur derivatives [37,38,41,44,50,56]. The process of reversion of sulfheme to the native proteins is not new and has been observed in proteins such as Mb, Hb, and catalase under a diversity of oxidizing and reducing agents [38,83,150]. However, it is interesting that under oxidative conditions and H_2S (Figures 3-22, 3-23 and 3-24), LPO continues its function until all the H_2S is consumed and the classical peroxidative reaction dominates. Thus, the LPO-sulfLPO going to LPO process does not lead to any H_2S regeneration, transport, or enzyme inactivation.

Curiously, aromatic desulfurization reaction has been studied for many years and literature has been generated on the subject [151–153] indicating for example, that the desulfurization of alkyl and organic aromatic sulfides in the presence of oxidizing agents, like O_2 and H_2O_2, leads to the production of sulfate [154,155]. In fact, an early work in sulfMb, using radioactive ^{35}S indicated that the decomposition of the isolated sulfheme produces sulfate as the major product, while H_2S, SO_2 and elemental sulfur were ruled out as possible products [64]. Regarding this, Figure 3-35 showed an increase in sulfate production after the disappearance of sulfLPO formed upon the interaction of 5 µM native LPO with 25 µM and 50 µM H_2O_2 and three different concentration of H_2S 600 µM (black), 800 µM (dark gray) and 1000 µM (gray), respectively. The results show the same behavior, the amount of detected sulfate increases as function of the H_2S concentration. Overall the results indicate that approximately 20% of the initially added H_2S converts to sulfate. Although it cannot be discerned the direct contributions to the total $SO_4^=$ comes from the reaction H_2O_2 and H_2S or from the turnover of sulfLPO [156]. Furthermore other sulfur species that are also produced [139–141]. Thus, there is a need for additional experiments to determine the products and mechanism of sulfur species generated by the turnover of sulfPLO. Additional turnover reactions which produce oxidized sulfur species could generate polysulfides [36,40,139,157,158]. Thus, the suggestion that desulfurization of the sulfLPO can generate only

$SO_4^=$ and native LPO, needs further quantitative studies with more precise techniques other than Ba_2SO_4 precipitation. However, the desulfuration process of heme to generate LPO from sulfLPO, the turnover process is faster in LPO that Mb and Hb suggesting that the positively charged Arginine in the heme pocked of LPO facilitates the desulfurization of sulfLPO returning the protein to its native state.

4.8 Formation of sulfheme by H_2S and under different oxidative conditions

The reactions between LPO with H_2S in the presence of O_2 or H_2O_2 show different formation rates to sulfheme. This suggests (Figure 4-38) that the rate determining step of sulfheme formation in the presence O_2 is the formation of compound III, while with H_2O_2 it is the formation of heme compound 0. For example, Figure 4-38B shows the reaction pathway form sulfLPO based on recent DFT/MM potential energy scans method coupled to the CHARMM force field in the doublet, quartet and sextet states indicated that hydrogen transfer from H_2S to Fe(III)-H_2O_2 complex results in homolytic cleavage of the O-O and S-H bond to form •SH, ferryl heme compound II, and a water molecule [47]. Subsequent addition of •SH to pyrrole B carbon of the heme compound II specie leads to a metastable ring-opened episulfide, which become the 3-membered episulfide ring and met-aquo Fe (III). Finally, the 5-membered thiochlorin structure is formed from the 3-membered episulfide ring with very favorable energy drop of 140 Kcal/mol [47]. Overall, these results are in agreement with a wide range of experimental NMR data [95]. Figure 4-38A shows that intermediates in sulfheme formation can be postulated based on recent work on LPO indicating that compound III ($Fe^{III}O_2^{\bullet}$ Por) accepts the transfer of an electron and a proton from His 109 (Figure 1-9), to form heme compound 0 (Figure 1-9C) [109]. Given this observation and taking in consideration the ability of H_2S to undergo homolytic cleavage [47], the route to sulfLPO from native LPO and H_2S in the presence of O_2 is very possible through the

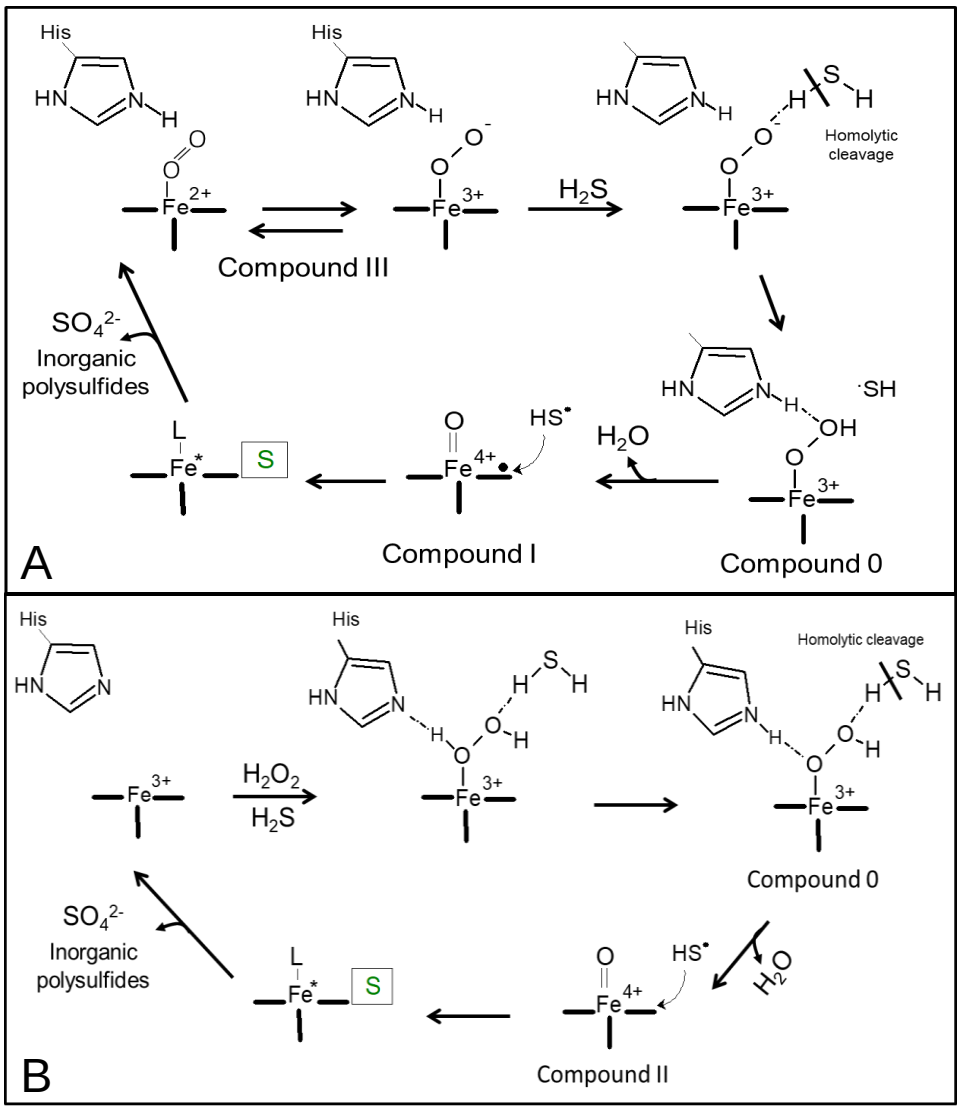

Figure 4-38. Proposed mechanism for sulfheme formation and turnover to the native state in the presence of (A) oxygen and (B) hydrogen peroxide.

compound III intermediate. Here, in Figure 4-38A, compound III accepts an electron and a proton from H_2S, the substrate, leading to the formation of compound I (*via* Figure 1-9C), water and •SH. The downhill reaction, similar to these two radical species, compound I and •SH, leads to the subsequent formation of sulfLPO. Since oxyMb also forms compound III [109,159] and previous studies suggest that the •SH radical is involved in the sulfheme derivative [38,44–47], maybe in the case compound III triggers the formation •SH, which interact with the porphyrin ring as the route for the sulfheme formation in the presence of O_2. Apparently, in the mechanism for the sulfheme derivative formation either with O_2 or H_2O_2, the rate limiting step is the generation of compound III or compound 0, respectively.

4.9 Physiological Relevance of LPO and sulfLPO turnover

The *in vivo* significance of the *in vitro* results presented here will require further research regarding: (1) the biological reversibility of LPO and sulfLPO and the role that H_2S may play in scavenging H_2O_2 and preventing the generation carbon center radical in the LPO system; and (2) the possibility of $SO_4^{=}$ and other sulfur species as possible product of the turnover. The observations that H_2S is required in both of these circumstances and that H_2S is not a product of the reaction are consistent with the physiological functions of LPO and H_2S as anti-inflammatory agents in airways [160]. This can be due to the action of H_2S as a substrate to reverse the LPO inhibition caused by the high levels of H_2O_2 in inflammation sites [161]. The *in vitro* H_2O_2 depletion in the LPO to sulfheme LPO conversion opens a route to explore the *in vivo* prevention of the toxic effects of H_2O_2 in patients with asthma and chronic obstructive pulmonary disease (COPD) and the relationship between LPO and CBS and CSE enzymes in the antioxidant nature of H_2S. On the other hand, from the toxic view of H_2S scenarios [157], the primary entrance of H_2S to the body is through the human airway and upon exposure to relatively high concentrations

of H_2S, LPO can use sulfLPO turnover as a "sink" for H_2S to protect human body to certain degree from reactive oxygen species (ROS) and sulfide toxicity.

Chapter 5: Conclusion

CHAPTER 5: CONCLUSION

The results presented elucidate the importance of the conformational changes in the active site and the oxidative conditions in the generation of sulfheme derivatives in hemeproteins like peroxidases. The experimental data of the HbI mutants demonstrated the influence of the distal residues changes in the reactivity with H_2S. This highlight the crucial role of the distal histidine (position 64) with the adequate position and orientation in the sulfheme formation. The insertion of a polar residue, His, in the position 68 similar to localization of the Arg in the hemeperoxidases do not generate the sulfheme derivative but show a decrease of affinity to H_2S reconverting the protein to the ferric metaquo state.

The data with LPO indicate that the presence of O_2 or H_2O_2 is an absolute requirement for the formation of these sulfheme derivatives. Interestingly, in the presence of H_2S, during the reactions of LPO with H_2O_2 a continuous turnover with the formation of ferrous and ferric sulfLPO followed by a recovery of native LPO was observed, indicating LPO catalyzed oxidation of H_2S by peroxide. This catalytic oxidation of H_2S is not consistent with sulfheme decomposition to regenerate H_2S, in other words H_2S trafficking via sulfLPO. Pilot product analysis suggest that the turnover process indeed generates oxidized sulfur species, most likely $SO_4^{=}$ and/or inorganic polysulfides (HS_x^- x=2-9) as products. These results indicate that H_2S is a non-classical LPO substrate, because the porphyrin ring of the heme group is reversibly modified during turnover via intermediate formation of sulfheme derivatives. This also implies that LPO is an unusual heme protein in the sense that its sulfheme derivative can be rapidly converted back to the active native form of the enzyme in contrast to Hb or Mb, where sulfheme derivatives are stable. Additionally, EPR data suggest that during sulfheme turnover, H_2S can act as a scavenger of H_2O_2 in the presence of LPO without detectable formation of any carbon centered globin radical species, suggesting that

H_2S might be capable to protect the enzyme from radical-mediated damage in the presence of H_2O_2. Sulfheme formation was shown to be slower in the reaction between oxyLPO and H_2S compared to the LPO catalyzed oxidation of sulfide by H_2O_2. Based on the results and available literature data on heme proteins, we speculate that this might be due to intermediate formation of compound III in the reaction of oxyLPO with H_2S during the process of generating the compound 0 state, which is a proposed central intermediate in the formation of sulfheme derivatives. On the other hand, heme compound 0 can be generated by direct coordination of H_2O_2 to ferric LPO in the presence of H_2O_2.

Surprisingly, the hemeperoxidases LPO, MPO and HRP do not bind H_2S to the ferric iron suggesting that this behavior is due to the unique features of His and Arg in the distal active site of peroxidases. Although these enzymes have His, conformational changes in the active site in comparison to LPO causes MPO and HRP to not generate the sulfheme derivative. Both proteins instead produce compound III from the interactions of H_2S under oxidative conditions. In MPO and HRP, H_2S acts as a peroxidase inhibitor via compound III with low turnover to the native state. Nevertheless, high H_2S concentrations induces the heme reductions of the ferric MPO and LPO. These results emphasize in how structural changes and the presence of H_2O_2 and/or oxygen in hemeproteins affect the generation of the sulfheme derivative, and the products in the sulfheme turnover. Also remarks the species involve in the interaction of H_2S with hemeperoxidases.

References

[1] L.L. Barton, G.D. Fauque, Chapter 2 Biochemistry, physiology and biotechnology of sulfate-reducing bacteria, Adv. Appl. Microbiol. 68 (2009) 41–98. doi:10.1016/S0065-2164(09)01202-7.

[2] K.R. Olson, K.D. Straub, The role of hydrogen sulfide in evolution and the evolution of hydrogen sulfide in metabolism and signaling, Physiology. 31 (2016) 60–72. doi:10.1152/physiol.00024.2015.

[3] M.M. Halmer, H.U. Schmincke, H.F. Graf, The annual volcanic gas input into the atmosphere, in particular into the stratosphere: A global data set for the past 100 years, J. Volcanol. Geotherm. Res. 115 (2002) 511–528. doi:10.1016/S0377-0273(01)00318-3.

[4] D.W. Layton, R.T. Cederwall, Assessing and managing the risks of accidental releases of hazardous gas: A case study of natural gas wells contaminated with hydrogen sulfide, Environ. Int. 12 (1986) 519–532. doi:10.1016/0160-4120(86)90146-7.

[5] S.F. Watts, The mass budgets of carbonyl sulfide, dimethyl sulfide, carbon disulfide and hydrogen sulfide, Atmos. Environ. 34 (2000) 761–779. doi:10.1016/S1352-2310(99)00342-8.

[6] D.M. Leahey, M.B. Schroeder, Predictions of maximum ground-level hydrogen sulfide concentrations resulting from two sour gas well blowouts, J. Air Pollut. Control Assoc. 36 (1986) 1147–1149.

[7] L. Chénard, S.P. Lemay, C. Laguë, Hydrogen sulfide assessment in shallow-pit swine housing and outside manure storage, J. Agric. Saf. Health. 9 (2003) 285–302.

[8] J.F. Beck, C.M. Bradbury, A.J. Connors, J.C. Donini, Nitrite as antidote for acute hydrogen sulfide intoxication?, Am. Ind. Hyg. Assoc. J. 42 (1981) 805–809.

[9] W.M. Grant, J.S. Schuman, Hydrogen sulfide. Toxicology of the eye. Effects on the eyes and visual system from chemicals, drugs, metals and minerals, plants, toxins and venoms; also, systemic side effects from eye medications, 4th ed., Charles C. Thomas, Springfield, IL, 1993.

[10] M. Sitting, Handbook of toxic and hazardous chemicals and carcinogens, Noyes Publications, Park Ridge, NJ, 2002.

[11] I. Devai, R.D. DeLaune, Emission of reduced malodorous sulfur gases from wastewater treatment plants, Water Environ. Res. 71 (1999) 203–208.

[12] B.K. Takemoto, R.D. Noble, H.M. Harrington, Differential sensitivity of duckweeds (Lemnaceae) to sulfite: II. Thiol production and hydrogen sulphide emission as factors influencing sulphite phytotoxicity under low and high irradiance, New Phytol. 103 (1986) 541–548.

[13] L.G. Wilson, R. a Bressan, P. Filner, Light-dependent emission of hydrogen sulfide from plants., Plant Physiol. 61 (1978) 184–9. doi:10.1104/pp.61.2.184.

[14] H. Rennenberg, P. Filner, Developmental changes in the potential for H2S emission in cucurbit plants, Plant Physiol. 71 (1983) 269–275. doi:10.1104/pp.71.2.269.

[15] D. Julian, J.L. Statile, S.E. Wohlgemuth, A.J. Arp, Enzymatic hydrogen sulfide production in marine invertebrate tissues, Comp. Biochem. Physiol. Part A Mol. Integr. Physiol. 133 (2002) 105–115. doi:10.1016/S1095-6433(02)00122-8.

[16] S. Panthi, H.J. Chung, J. Jung, N.Y. Jeong, Physiological importance of hydrogen sulfide: Emerging potent neuroprotector and neuromodulator, Oxid. Med. Cell. Longev. 2016 (2016). doi:10.1155/2016/9049782.

[17] R. Wang, Physiological implications of hydrogen sulfide: A whiff exploration that blossomed, Physiol. Rev. 92 (2012) 791–896. doi:10.1152/physrev.00017.2011.

[18] J.C. Mathai, A. Missner, P. Kugler, S.M. Saparov, M.L. Zeidel, J.K. Lee, P. Pohl, No facilitator required for membrane transport of hydrogen sulfide, Proc. Natl. Acad. Sci. 106 (2009) 16633–16638. doi:10.1073/pnas.0902952106.

[19] S. Singh, R. Banerjee, PLP-dependent H2S biogenesis, Biochim. Biophys. Acta. 1814 (2011) 1518–1527.

[20] D.G. Searcy, S.H. Lee, Sulfur reduction by human erythrocytes, J. Exp. Zool. 282 (1998) 310–22.

[21] M. Whiteman, S. Le Trionnaire, M. Chopra, B. Fox, J. Whatmore, Emerging role of hydrogen sulfide in health and disease: critical appraisal of biomarkers and pharmacological tools, Clin. Sci. 121 (2011) 459–488. doi:10.1042/CS20110267.

[22] O. Kabil, R. Banerjee, Enzymology of H2S biogenesis, decay and signaling, Antioxid. Redox Signal. 20 (2014) 770–782.

[23] S. Tang, D. Huang, N. An, D. Chen, D. Zhao, A novel pathway for the production of H2S by DAO in ratjejunum, Neurogastroenterol Motil. 28 (2016) 687–692.

[24] M. Meier, M. Janosik, V. Kery, J.P. Kraus, P. Burkhard, Structure of human cystathionine beta-synthase: a unique pyridoxal 5'-phosphate-dependent heme protein, EMBO J. 20 (2001) 3910–3916. doi:10.1093/emboj/20.15.3910.

[25] Q. Sun, R. Collins, S. Huang, L. Holmberg-Schiavone, G.S. Anand, C.-H. Tan, S. Van-den-Berg, L.-W. Deng, P.K. Moore, T. Karlberg, J. Sivaraman, Structural basis for the inhibition mechanism of human cystathionine gamma-lyase, an enzyme responsible for the production of H(2)S, J. Biol. Chem. 284 (2009) 3076–85. doi:10.1074/jbc.M805459200.

[26] T. Kawazoe, H. Tsuge, M.S. Pilone, K. Fukui, Crystal structure of human D-amino acid oxidase: context-dependent variability of the backbone conformation of the VAAGL hydrophobic stretch located at the si-face of the flavin ring., Protein Sci. 15 (2006) 2708–2717. doi:10.1110/ps.062421606.

[27] K. Abe, H. Kimura, The possible role of hydrogen sulfide as an endogenous

neuromodulator., Off. J. Soc. Neurosci. 16 (1996) 1066–1071.

[28] X. Zhang, J.S. Bian, Hydrogen sulfide: A neuromodulator and neuroprotectant in the central nervous system, ACS Chem. Neurosci. 5 (2014) 876–883. doi:10.1021/cn500185g.

[29] N.L. Kanagy, C. Szabo, A. Papapetropoulos, Vascular biology of hydrogen sulfide, Am. J. Physiol. - Cell Physiol. 312 (2017) C537–C549. doi:10.1152/ajpcell.00329.2016.

[30] M. Bucci, A. Papapetropoulos, V. Vellecco, Z. Zhou, A. Zaid, P. Giannogonas, A. Cantalupo, S. Dhayade, K.P. Karalis, R. Wang, R. Feil, G. Cirino, cGMP-dependent protein kinase contributes to hydrogen sulfide-stimulated vasorelaxation, PLoS One. 7 (2012). doi:10.1371/journal.pone.0053319.

[31] G. Tang, L. Zhang, G. Yang, L. Wu, R. Wang, Hydrogen sulfide-induced inhibition of L-type Ca2+ channels and insulin secretion in mouse pancreatic beta cells, Diabetologia. 56 (2013) 533–541. doi:10.1007/s00125-012-2806-8.

[32] J.L. Wallace, J.G.P. Ferraz, M.N. Muscara, Hydrogen sulfide: an endogenous mediator of resolution of inflammation and injury., Antioxid. Redox Signal. 17 (2012) 58–67. doi:10.1089/ars.2011.4351.

[33] A. Papapetropoulos, A. Pyriochou, Z. Altaany, G. Yang, A. Marazioti, Z. Zhou, M.G. Jeschke, L.K. Branski, D.N. Herndon, R. Wang, C. Szabó, Hydrogen sulfide is an endogenous stimulator of angiogenesis., Proc. Natl. Acad. Sci. U. S. A. 106 (2009) 21972–21977. doi:10.1073/pnas.0908047106.

[34] C. Szabó, A. Papapetropoulos, Hydrogen sulphide and angiogenesis: Mechanisms and applications, Br. J. Pharmacol. 164 (2011) 853–865. doi:10.1111/j.1476-5381.2010.01191.x.

[35] V. Yadav, X.-H. Gao, B. Willard, M. Hatzoglou, R. Banerjee, O. Kabil, Hydrogen sulfide modulates eukaryotic translation initiation factor 2? (eIF2?) phosphorylation status in the integrated stress response pathway, J. Biol. Chem. 292 (2017) 13143–13153.

[36] H. Kimura, Hydrogen sulfide and polysulfides as signaling molecules, Proc. Jpn. Acad. Ser. B. Phys. Biol. Sci. 91 (2015) 131–159.

[37] B.Y.H. Michel, A study of sulfhemoglobin, J. Biol. Chem. 126 (1938) 323–348.

[38] P. Nicholls, The formation and properties of sulphmyoglobin and sulphcatalase, Biochem. J. 81 (1961) 374–383.

[39] J.A. Berzofsky, J. Peisach, J.O. Albem, Sulfheme Proteins III. Carboxysulfmyoglobin: the relation between electron withdrawal from iron and ligand binding, J. Biol. Chem. 247 (1972) 3774–3782.

[40] T. Bostelaar, V. Vitvitsky, J. Kumutima, B.E. Lewis, P.K. Yadav, T.C. Brunold, M. Filipovic, N. Lehnert, T.L. Stemmler, R. Banerjee, Hydrogen sulfide oxidation by myoglobin, J. Am. Chem. Soc. 138 (2016) 8476–8488. doi:10.1021/jacs.6b03456.

[41] R.J. Carrico, J. Peisach, J.O. Alben, The preparation and some physical properties of sulfhemoglobin, J. Biol. Chem. 253 (1978) 2386–2391.

[42] D.W. Kraus, J.B. Wittenberg, Hemoglobins of the lucina pectinata/bacteria symbiosis, J. Biol. Chem. 265 (1990) 16054–16059.

[43] D.W. Kraus, J.B. Wittenberg, Hemoglobins of the Lucina pectinata/bacteria symbiosis. I. Molecular properties kinetics and equilibria of reactions with ligands, J. Biol. Chem. 265 (1990) 16043–16053.

[44] B.B. Ríos-González, E.M. Román-Morales, R. Pietri, J. López-Garriga, Hydrogen sulfide activation in hemeproteins: The sulfheme scenario, J. Inorg. Biochem. 133 (2014) 78–86.

[45] E. Román-Morales, R. Pietri, B. Ramos-Santana, S.N. Vinogradov, A. Lewis-Ballester, J. López-Garriga, Structural determinants for the formation of sulfhemeprotein complexes, Biochem. Biophys. Res. Commun. 400 (2010) 489–492.

[46] R. Pietri, A. Lewis, R.G. León, G. Casabona, L. Kiger, S.-R. Yeh, S. Fernandez-Alberti, M.C. Marden, C.L. Cadilla, J. López-Garriga, Factors controlling the reactivity of hydrogen sulfide with hemeproteins, Biochemistry. 48 (2009) 4881–4894.

[47] H.D. Arbelo-Lopez, N.A. Simakov, J.C. Smith, J. Lopez-Garriga, T. Wymore, Homolytic cleavage of both heme-bound hydrogen peroxide and hydrogen sulfide leads to the formation of sulfheme, J. Phys. Chem. B. 120 (2016) 7319–7331. doi:10.1021/acs.jpcb.6b02839.

[48] D. Padovani, A. Hessani, F.T. Castillo, G. Liot, M. Andriamihaja, A. Lan, C. Pilati, F. Blachier, S. Sen, E. Galardon, I. Artaud, Sulfheme formation during homocysteine S-oxygenation by catalase in cancers and neurodegenerative diseases, Nat. Commun. 7 (2016) 13386. doi:10.1038/ncomms13386.

[49] K.R. Olson, Y. Gao, E.R. DeLeon, M. Arif, F. Arif, N. Arora, K.D. Straub, Catalase as a sulfide-sulfur oxido-reductase: An ancient (and modern?) regulator of reactive sulfur species (RSS), Redox Biol. 12 (2017) 325–339. doi:10.1016/j.redox.2017.02.021.

[50] S. Nakamura, M. Nakamura, I. Yamazaki, M. Morrison, Reactions of ferryl lactoperoxidase (compound II) with sulfide and sulfhydryl compounds, J. Biol. Chem. 259 (1984) 7080–7085.

[51] Z. Pálinkás, P.G. Furtmüller, A. Nagy, C. Jakopitsch, K.F. Pirker, M. Magierowski, K. Jasnos, J.L. Wallace, C. Obinger, P. Nagy, Interactions of hydrogen sulfide with myeloperoxidase, Br. J. Pharmacol. 172 (2015) 1516–1532.

[52] A.L. Lehninger, D.L. Nelson, M.M. Cox, Lehninger Principles of Biochemistry, 4th editio, W. H. Freeman & Co., 2004.

[53] J.R.H. Tame, B. Vallone, The structures of deoxy human haemoglobin and the mutant Hb Tyrα42His at 120 K, Acta Crystallogr. Sect. D Biol. Crystallogr. 56 (2000) 805–811. doi:10.1107/S0907444900006387.

[54] M. Bolognesi, C. Rosano, R. Losso, A. Borassi, M. Rizzi, J.B. Wittenberg, A. Boffi, P. Ascenzi, Cyanide binding to Lucina pectinata hemoglobin I and to sperm whale myoglobin: An x-ray crystallographic study, Biophys. J. 77 (1999) 1093–1099. doi:10.1016/S0006-3495(99)76959-6.

[55] F. Hoppe, Ueber das verhalten des blutfarbstoffes im spectrum des sonnenlichtes, Arch. F??r Pathol. Anat. Und Physiol. Und F??r Klin. Med. 23 (1862) 446–449. doi:10.1007/BF01939277.

[56] J.A. Berzofsky, J. Peisach, W.E. Blumberg, Sulfheme Proteins. I. Optical and magnetic properties of sulfmyoglobin and its derivatives, J. Biol. Chem. 246 (1971) 3367–3377.

[57] M. Noor, E. Beutler, Acquired sulfhemoglobinemia. An underreported diagnosis?, West. J. Med. 169 (1998) 386–389.

[58] L. Gharahbaghian, B. Massoudian, G. Dimassa, Methemoglobinemia and sulfhemoglobinemia in two pediatric patients after ingestion of hydroxylamine sulfate., West. J. Emerg. Med. 10 (2009) 197–201.

[59] C. Wu, M.A. Kenny, A case of sulfhemoglobinemia and emergency measurement of sulfhemoglobin with an OSM3 CO-oximeter, Clin. Chem. 43 (1997) 162–166.

[60] E.M. Román-Morales, E. López-Alfonzo, R. Pietri, J. López-Garriga, Sulfmyoglobin conformational change: A role in the decrease of oxy-myoglobin functionality, Biochem. Biophys. Reports. 7 (2016) 386–393.

[61] R. Pietri, E. Román-Morales, J. López-Garriga, Hydrogen sulfide and hemeproteins: knowledge and mysteries, Antioxid. Redox Signal. 15 (2011) 393–404.

[62] A. George, D. Goetz, A case of sulfhemoglobinemia in a child with chronic constipation, Respir. Med. Case Reports. 21 (2017) 21–24. doi:10.1016/j.rmcr.2017.03.009.

[63] A. Tangerman, G. Bongaerts, R. Agbeko, B. Semmekrot, R. Severijnen, The origin of hydrogen sulfide in a newborn with sulfhaemoglobin induced cyanosis., J. Clin. Pathol. 55 (2002) 631–633. doi:10.1136/jcp.55.8.631.

[64] J.A. Berzofsky, J. Peisach, B.L. Horecker, Sulfheme Proteins IV. The stoichiometry of sulfur incorporation and the isolation of sulfhemin, the prosthetic group of sulfmyoglobin, J. Biol. Chem. 247 (1972) 3783–3791.

[65] M.J. Chatfield, G.N. La Mar, R.J. Kauten, Proton NMR characterization of isomeric sulfmyoglobins: preparation, interconversion, reactivity patterns, and structural features, Biochemistry. 26 (1987) 6939–6950.

[66] S. V Evans, B.P. Sishta, A.G. Mauk, G.D. Brayer, Three-dimensional structure of cyanomet-sulfmyoglobin C, Proc. Natl. Acad. Sci. U. S. A. 91 (1994) 4723–4726.

[67] J.A. Berzofsky, J. Peisach, W.E. Blumberg, Sulfheme Proteins II. The reversible oxygenation of ferrous sulfmyoglobin, J. Biol. Chem. 246 (1971) 7366–7372.

[68] R. Timkovich, M.R. Vavra, Proton NMR spectroscopy of sulfmyoglobin, Biochemistry. 24 (1985) 5189–5196.

[69] L.L. Bondoc, M.H. Chau, M.A. Price, R. Timkovich, Structure of a stable form of sulfheme, Biochemistry. 25 (1986) 8458–8466.

[70] M.J. Chatfield, G.N. La Mar, J.T.J. Lecomte, A.L. Balch, K.M. Smith, K.C. Langry, Identification of the altered pyrrole in sulfmyoglobin and an extractable "sulfhemin": participation of the 4-vinyl group in the saturation of the pyrrole in one form of sulfmyoglobin, J. Am. Chem. Soc. 108 (1986) 7108–7110. doi:10.1021/ja00282a048.

[71] M.J. Chatfield, G.N. La Mar, A.L. Balch, K.M. Smith, D.W. Parish, T.J. LePage, Proton NMR study of the influence of heme vinyl groups on the formation of the isomeric forms of sulfmyoglobin, FEBS Lett. 206 (1986) 343–346. doi:10.1016/0014-5793(86)81009-2.

[72] M.J. Chatfield, G.N. La Mar, A.L. Balch, J.T.J. Lecomte, Multiple forms of sulfmyoglobin as detected by 1H nuclear magnetic resonance spectroscopy, Biochem. Biophys. Res. Commun. 135 (1986) 309–315. doi:10.1016/0006-291X(86)90978-2.

[73] S.H. Libardi, H. Pindstrup, D.R. Cardoso, L.H. Skibsted, Reduction of ferrylmyoglobin by hydrogen sulfide. Kinetics in relation to meat greening, J. Agric. Food Chem. 61 (2013) 2883–2888.

[74] R.E. Weber, S.N. Vinogradov, Nonvertebrate hemoglobins: functions and molecular adaptations, Physiol. Rev. 81 (2001) 569–628.

[75] D.W. Kraus, Heme proteins in sulfide-oxidizing bacteria/mollusc symbioses, Am. Zool. 35 (1995) 112–120. doi:10.1093/icb/35.2.112.

[76] F.M. Antommattei-Pérez, T. Rosado-Ruiz, C.L. Cadilla, J. López-Garriga, The cDNA-derived amino acid sequence of hemoglobin I from Lucina pectinata, J Protein Chem. 18 (1999) 831–836.

[77] M. Rizzi, J.B. Wittenberg, A. Coda, M. Fasano, P. Ascenzi, M. Bolognesi, Structure of the sulfide-reactive hemoglobin from the clam Lucina pectinata. Crystallographic analysis at 1.5 A resolution., J. Mol. Biol. 244 (1994) 86–99. doi:10.1006/jmbi.1994.1706.

[78] M. Rizzi, J.B. Wittenberg, A. Coda, P. Ascenzi, M. Bolognesi, Structural bases for sulfide recognition in Lucina pectinata hemoglobin I, J Mol Biol. 258 (1996) 1–5. doi:10.1006/jmbi.1996.0228.

[79] W. De Jesús-Bonilla, J.E. Cortés-Figueroa, F. a Souto-Bachiller, L. Rodríguez, J. López-Garriga, Formation of compound I and compound II ferryl species in the reaction of hemoglobin I from Lucina pectinata with hydrogen peroxide., Arch. Biochem. Biophys. 390 (2001) 304–308.

[80] T. Egawa, H. Shimada, Y. Ishimura, Formation of compound I in the reaction of native myoglobins with hydrogen peroxide, J. Biol. Chem. 275 (2000) 34858–34866. doi:10.1074/jbc.M004026200.

[81] T. Matsui, S.I. Ozaki, E. Liong, G.N. Phillips, Y. Watanabe, Effects of the location of distal histidine in the reaction of myoglobin with hydrogen peroxide, J. Biol. Chem. 274 (1999) 2838–2844. doi:10.1074/jbc.274.5.2838.

[82] T. Brittain, A.R. Baker, C.S. Butler, R.H. Little, D.J. Lowe, C. Greenwood, N.J. Watmough, Reaction of variant sperm-whale myoglobins with hydrogen peroxide: the effects of mutating a histidine residue in the haem distal pocket, Biochem. J. 326 (1997) 109–115.

[83] E.A. Johnson, The reversion to haemoglobin of sulphhaemoglobin and its coordination derivatives, Biochim. Biophys. Acta - Protein Struct. 207 (1970) 30–40.

[84] W. Schroeder, J.R. Shelton, J.B. Shelton, B. Robberson, G. Apell, R.S. Fang, J. Bonaventura, The complete amino acid sequence of bovine liver catalase and the partial sequence of bovine erythrocyte catalase, Arch. Biochem. Biophys. 214 (1982) 397–421.

[85] J.B. Summer, A.L. Dounce, Crystalline catalase, J Biol Chem. 121 (1937) 417–424.

[86] J.B. Summer, N. Gralén, The molecular weight of crystalline catalase, J. Biol. Chem. 125 (1938) 33–36.

[87] N. Purwar, J.M. McGarry, J. Kostera, A.A. Pacheco, M. Schmidt, Interaction of nitric oxide with catalase: Structural and kinetic analysis, Biochemistry. 50 (2011) 4491–4503. doi:10.1021/bi200130r.

[88] C. Michiels, M. Raes, O. Toussaint, J. Remacle, Importance of Se-glutathione peroxidase, catalase, and Cu/Zn-SOD for cell survival against oxidative stress, Free Radic. Biol. Med. 17 (1994) 235–248. doi:10.1016/0891-5849(94)90079-5.

[89] G.C. Brown, Reversible binding and inhibition of catalase by nitric oxide, Eur. J. Biochem. 232 (1995) 188–191. doi:10.1111/j.1432-1033.1995.tb20798.x.

[90] B. Chance, The reaction of catalase and cyanide, J. Biol. Chem. 179 (1949) 1299–1309.

[91] D. Keilin, E.F. Hartree, Properties of azide-catalase, Biochem. J. 39 (1945) 148–157.

[92] E. Margoliash, A. Novogrodsky, A study of the inhibition of catalase by 3-amino-1:2:4-triazole, Biochem. J. 68 (1958) 468–475.

[93] R.F. Beers, I.W. Sizer, Sulfide inhibition of catalase, Science (80-.). 120 (1954) 32.

[94] M.. Chatfield, G.N. La Mar, K.M. Smith, H.K. Leung, R.K. Pandey, Identification of the altered pyrrole in the isomeric sulfmyoglobins: hyperfine shift patterns as indicators of ring saturation in ferric chlorins, Biochemistry. 27 (1988) 1500–1507.

[95] M.J. Chatfield, G.N. La Mar, 1H nuclear magnetic resonance study of the prosthethic group in sulfhemoglobin, Arch. Biochem. Biophys. Biochem Biophys. 295 (1992) 289–296.

[96] K.D. Kussendrager, A.C. Van Hooijdonk, Lactoperoxidase: physico-chemical properties, occurrence, mechanism of action and applications, Br. J. Nutr. 84 Suppl 1 (2000) S19–

S25.

[97] P.G. Furtmuller, M. Zederbauer, W. Jantschko, J. Helm, M. Bogner, C. Jakopitsch, C. Obinger, Active site structure and catalytic mechanisms of human peroxidases, Arch. Biochem. Biophys. 445 (2006) 199–213.

[98] M. Zamocky, C. Jakopitsch, P.G. Furtmüller, C. Dunand, C. Obinger, The peroxidase-cyclooxygenase superfamily: Reconstructed evolution of critical enzymes of the innate immune system, Proteins. 72 (2008) 589–605.

[99] J. Arnhold, J. Flemmig, Human myeloperoxidase in innate and acquired immunity, Arch. Biochem. Biophys. 500 (2010) 92–106. doi:10.1016/j.abb.2010.04.008.

[100] G. Battistuzzi, M. Bellei, C.A. Bortolotti, M. Sola, Redox properties of heme peroxidases, Arch. Biochem. Biophys. 500 (2010) 21–36.

[101] C. Wijkstrom-Frei, S. El-Chemaly, R. Ali-Rachedi, C. Gerson, M. a Cobas, R. Forteza, M. Salathe, G.E. Conner, Lactoperoxidase and human airway host defense, Am. J. Respir. Cell Mol. Biol. 29 (2003) 206–212.

[102] S.J. Klebanoff, Myeloperoxidase : friend and foe, J. Leukoc. Biol. 77 (2005) 598–625. doi:10.1189/jlb.1204697.1.

[103] S. Stanković, N. Majkić-Singh, Myeloperoxidase: New Roles for an old molecule, J. Med. Biochem. 30 (2011) 230–236. doi:10.2478/v10011-011-0033-3.

[104] K. Lemma, M.T. Ashby, Reactive sulfur species: Kinetics and mechanism of the reaction of hypothiocyanous acid with cyanide to give dicyanosulfide in aqueous solution, Chem. Res. Toxicol. 22 (2009) 1622–1628.

[105] A. Al Obaidi, Role of airway lactoperoxidase in scavenging of hydrogen peroxide damage in asthma, Ann. Thorac. Med. 2 (2007) 107–110.

[106] T.J. Fiedler, C.A. Davey, R.E. Fenna, X-ray crystal structure and characterization of halide-binding sites of human myeloperoxidase at 1.8 Å resolution, J. Biol. Chem. 275 (2000) 11964–11971. doi:10.1074/jbc.275.16.11964.

[107] A.K. Singh, N. Singh, S. Sharma, S.B. Singh, P. Kaur, A. Bhushan, A. Srinivasan, T.P. Singh, Crystal structure of lactoperoxidase at 2.4 A resolution, J. Mol. Biol. 376 (2008) 1060–1075.

[108] S. Watanabe, F. Varsalona, Y.C. Yoo, J.P. Guillaume, A. Bollen, K. Shimazaki, N. Moguilevsky, Recombinant bovine lactoperoxidase as a tool to study the heme environment in mammalian peroxidases, FEBS Lett. 441 (1998) 476–479.

[109] P.J. Mak, W. Thammawichai, D. Wiedenhoeft, J.R. Kincaid, Resonance Raman spectroscopy reveals pH-dependent active site structural changes of lactoperoxidase compound 0 and its ferryl heme O-O bond cleavage products, J. Am. Chem. Soc. 137 (2015) 349–361.

[110] E. Ghibaudi, E. Laurenti, Unraveling the catalytic mechanism of lactoperoxidase and myeloperoxidase: A reflection on some controversial features, Eur. J. Biochem. 270 (2003) 4403–4412.

[111] W. Jantschko, P.G. Furtmüller, M. Zederbauer, K. Neugschwandtner, C. Jakopitsch, C. Obinger, Reaction of ferrous lactoperoxidase with hydrogen peroxide and dioxygen: An anaerobic stopped-flow study, Arch. Biochem. Biophys. 434 (2005) 51–59.

[112] W. Jantschko, P.G. Furtmüller, M. Zederbauer, C. Jakopitsch, C. Obinger, Kinetics of oxygen binding to ferrous myeloperoxidase, Arch. Biochem. Biophys. 426 (2004) 91–97. doi:10.1016/j.abb.2004.03.019.

[113] I. Bertini, H.B. Gray, E.I. Stiefel, J.S. Valentine, Biological inorganic chemistry: structure and reactivity, 2007.

[114] J.L. Michot, J. Nunez, M.L. Johnson, G. Irace, H. Edelhoch, Iodide binding and regulation of lactoperoxidase activity toward thyroid goitrogens, J Biol Chem. 254 (1979) 2205–2209.

[115] S. Ohtaki, H. Nakagawa, M. Nakamura, I. Yamazaki, Reactions of purified hog thyroid peroxidase with H2O2, tyrosine, and methylmercaptoimidazole (goitrogen) in comparison with bovine lactoperoxidase, J Biol Chem. 257 (1982) 761–766.

[116] U. Bandyopadhyay, D.K. Bhattacharyya, R. Chatterjee, R.K. Banerjee, Irreversible inactivation of lactoperoxidase by mercaptomethylimidazole through generation of a thiyl radical: its use as a probe to study the active site, Biochem. J. 306 (Pt 3) (1995) 751–757.

[117] D.R. Doerge, Oxygenation of organosulfur compounds by peroxidases: Evidence of an electron transfer mechanism for lactoperoxidase, Arch. Biochem. Biophys. 244 (1986) 678–685. doi:10.1016/0003-9861(86)90636-3.

[118] M.A. Ator, P.R. Ortiz de Montellano, Protein control of prosthetic heme reactivity. Reaction of substrates with the heme edge of horseradish peroxidase, J. Biol. Chem. 262 (1987) 1542–1551.

[119] P.R. Ortiz de Montellano, Control of the catalytic activity of prosthetic heme by the structure of hemoproteins, Acc. Chem. Res. 20 (1987) 289–294. doi:10.1021/ar00140a004.

[120] Z. Pálinkás, P.G. Furtmüller, A. Nagy, C. Jakopitsch, K.F. Pirker, M. Magierowski, K. Jasnos, J.L. Wallace, C. Obinger, P. Nagy, Interactions of hydrogen sulfide with myeloperoxidase, Br. J. Pharmacol. (2014) 1–50.

[121] R. Claesson, M. Granlund-Edstedt, S. Persson, J. Carlsson, Activity of polymorphonuclear leukocytes in the presence of sulfide, Infect. Immun. 57 (1989) 2776–2781.

[122] H. Laggner, M.K. Muellner, S. Schreier, B. Sturm, M. Hermann, M. Exner, B.M.K. Gmeiner, S. Kapiotis, Hydrogen sulphide: A novel physiological inhibitor of LDL atherogenic modification by HOCl, Free Radic. Res. 41 (2007) 741–747. doi:10.1080/10715760701263265.

[123] M. Gajhede, D.J. Schuller, A. Henriksen, A.T. Smith, T.L. Poulos, Crystal structure of horseradish peroxidase C at 2.15 A resolution, Nat. Struct. Biol. 4 (1997) 1032–1038.

[124] B.E. Svensson, Myeloperoxidase oxidation states involved in myeloperoxidase-oxidase oxidation of thiols, Biochem. J. 256 (1988) 751–755.

[125] R. Sariri, R.H. Sajedi, V. Jafarian, Inhibition of horseradish peroxidase activity by thiol type inhibitors, J. Mol. Liq. 123 (2006) 20–23.

[126] R.G. León, H. Munier-Lehmann, O. Barzu, V. Baudin-Creuza, R. Pietri, J. López-Garriga, C.L. Cadilla, High-level production of recombinant sulfide-reactive hemoglobin I from Lucina pectinata in Escherichia coli: High yields of fully functional holoprotein synthesis in the BLi5 E. coli strain, Protein Expr. Purif. 38 (2004) 184–195. doi:10.1016/j.pep.2004.08.014.

[127] A.M. Navarro, M. Maldonado, J. González-Lagoa, R. López-Mejía, J. López-Garriga, J.L. Colón, Control of carbon monoxide binding states and dynamics in hemoglobin I of Lucina pectinata by nearby aromatic residues, Inorganica Chim. Acta. 243 (1996) 161–166. doi:10.1016/0020-1693(95)04903-7.

[128] R. Floris, Y. Kim, G.T. Babcock, R. Wever, Optical spectrum of myeloperoxidase: Origin of the red shift, Eur. J. Biochem. 222 (1994) 677–685. doi:10.1111/j.1432-1033.1994.tb18912.x.

[129] A. Hans Hoogland, A.O.M. and R.W. van Kuilenburg, Caroline van Riel, Spectral properties of myeloperoxidase Compounds II and III, Biochim. Biophys. Acta - Protein Struct. Mol. Enzymol. 916 (1987) 76–82.

[130] C.C. Winterbourn, R.C. Garcia, A.W. Segal, Production of the superoxide adduct of myeloperoxidase (compound III) by stimulated human neutrophils and its reactivity with hydrogen peroxide and chloride, Biochem. J. 228 (1985) 583–592.

[131] D. Garai, B.B. Ríos-González, P.G. Furtmuller, J.M. Fukuto, M. Xian, J. López-Garriga, C.C. Obinger, P. Nagy, Mechanisms of myeloperoxidase catalyzed oxidation of H2S by H2O2 or O2 to produce potent protein Cys-polysulfide-inducing species, Free Radic. Biol. Med. 113 (2017) 551–563.

[132] F. Courtin, D. Deme, A. Virion, J.L. Michot, J. Pommier, J. Nunez, The role of lactoperoxidase-H2O2 compounds in the catalysis of thyroglobulin iodination and thyroid hormone synthesis, Eur. J. Biochem. 124 (2005) 603–609.

[133] W.D. Hewson, L.P. Hager, Oxidation of horseradish peroxidase compound II to compound I., J. Biol. Chem. 254 (1979) 3182–3186.

[134] S.A. Adediran, A.M. Lambeir, Kinetics of the reaction of compound II of horseradish peroxidase with hydrogen peroxide to form compound III, Eur. J. Biochem. 186 (1989) 571–576. doi:10.1111/j.1432-1033.1989.tb15246.x.

[135] G.S. Lukat, K.R. Rodgers, H.M. Goff, Electron paramagnetic resonance spectroscopy of lactoperoxidase complexes: clarification of hyperfine splitting for the NO adduct of

lactoperoxidase, Biochemistry. 26 (1987) 6927–6932.

[136] M.L. McCormick, J.P. Gaut, T.S. Lin, B.E. Britigan, G.R. Buettner, J.W. Heinecke, Electron paramagnetic resonance detection of free tyrosyl radical generated by myeloperoxidase, lactoperoxidase, and horseradish peroxidase, J. Biol. Chem. 273 (1998) 32030–32037.

[137] S. Galijasevic, G.M. Saed, M.P. Diamond, H.M. Abu-Soud, High dissociation rate constant of ferrous-dioxy complex linked to the catalase-like activity in lactoperoxidase, J. Biol. Chem. 279 (2004) 39465–39470. doi:10.1074/jbc.M406003200.

[138] R. Davydov, M. Laryukhin, A. Ledbetter-Rogers, M. Sono, J.H. Dawson, B.M. Hoffman, Electron paramagnetic resonance and electron-nuclear double resonance studies of the reactions of cryogenerated hydroperoxoferric-hemoprotein intermediates, Biochemistry. 53 (2014) 4894–4903. doi:10.1021/bi500296d.

[139] P. Nagy, Mechanistic chemical perspective of hydrogen sulfide signaling, Methods Enzymol. 554 (2015) 3–29. doi:10.1016/bs.mie.2014.11.036.

[140] P. Nagy, C.C. Winterbourn, Rapid reaction of hydrogen sulfide with the neutrophil oxidant hypochlorous acid to generate polysulfides, Chem. Res. Toxicol. 23 (2010) 1541–1543.

[141] R. Greiner, Z. Pálinkás, K. Bäsell, D. Becher, H. Antelmann, P. Nagy, T.P. Dick, Polysulfides link H2S to protein thiol oxidation, Antioxid. Redox Signal. 19 (2013) 1749–1765.

[142] H. Shimahara, T. Yoshida, Y. Shibata, M. Shimizu, Y. Kyogoku, F. Sakiyama, T. Nakazawa, S.I. Tate, S.Y. Ohki, T. Kato, H. Moriyama, K.I. Kishida, Y. Tano, T. Ohkubo, Y. Kobayashi, Tautomerism of histidine 64 associated with proton transfer in catalysis of carbonic anhydrase, J. Biol. Chem. 282 (2007) 9646–9656. doi:10.1074/jbc.M609679200.

[143] R.J. Carrico, W.E. Blumberg, J. Peisach, The reversible binding of oxygen to sulfhemoglobin, J. Biol. Chem. 253 (1978) 7212–7215.

[144] R.P. Ferrari, E.M. Ghibaudi, S. Traversa, E. Laurenti, L. De Gioia, M. Salmona, Spectroscopic and binding studies on the interaction of inorganic anions with lactoperoxidase, J. Inorg. Biochem. 68 (1997) 17–26.

[145] B. Valderrama, M. Ayala, R. Vazquez-Duhalt, Suicide inactivation of peroxidases and the challenge of engineering more robust enzymes, Chem. Biol. 9 (2002) 555–565. doi:10.1016/S1074-5521(02)00149-7.

[146] S. Malomo, R. Adeoye, L. Babatunde, Suicide inactivation of horseradish peroxidase by excess hydrogen peroxide: The effects of reaction pH, buffer ion concentration, and redox mediation, Biokemistri. 23 (2011) 124–128. http://www.ajol.info/index.php/biokem/article/view/77688.

[147] J. Soubhye, M. Gelbcke, P. Van Antwerpen, F. Dufrasne, M.Y. Boufadi, J. Neve, P.G. Furtmüller, C. Obinger, K.Z. Boudjeltia, F. Meyer, From dynamic combinatorial

chemistry to in vivo evaluation of reversible and irreversible myeloperoxidase inhibitors, ACS Med. Chem. Lett. 8 (2017) 206–210.

[148] I.M. Kooter, N. Moguilevsky, A. Bollen, L.A. Van Der Veen, C. Otto, H.L. Dekker, R. Wever, The sulfonium ion linkage in myeloperoxidase. Direct spectroscopic detection by isotopic labeling and effect of mutation, J. Biol. Chem. 274 (1999) 26794–26502. doi:10.1074/jbc.274.38.26794.

[149] G. Battistuzzi, J. Stampler, M. Bellei, J. Vlasits, M. Soudi, P.G. Furtmüller, C. Obinger, Influence of the covalent heme-protein bonds on the redox thermodynamics of human myeloperoxidase, Biochemistry. 50 (2011) 7987–7994. doi:10.1021/bi2008432.

[150] A. Tomoda, A. Kakizuka, Y. Yoneyama, Oxidative and reductive reactions of sulphhaemoglobin with various reagents correlated with changes in quaternary structure of the protein, 221 (1984) 587–591.

[151] J. March, Advance Organic Chemistry, Third, Wiley, 1985.

[152] E.I. Stiefel, K. Matsumoto, Transition metal sulfur chemistry, ACS Symposium Series 653, 1996.

[153] E.S. Saltzman, W.J. Cooper, Biogenic sulfur in the environment, ACS Symposium Series 393, 1987.

[154] T. Omori, Y. Saiki, K. Kasuga, T. Kodama, Desulfurization of alkyl and aromatic sulfides and sulfonates by dibenzothiophene-desulfurizing Rhodococcus sp. strain SY1, Biosci. Biotechnol. Biochem. 59 (1995) 1195–1198. doi:10.1271/bbb.59.1195.

[155] R. Javadli, A. de Klerk, Desulfurization of heavy oil, Appl. Petrochemical Res. 1 (2012) 3–19. doi:10.1007/s13203-012-0006-6.

[156] M.R. Hoffmann, Kinetics and mechanism of oxidation of hydrogen sulfide by hydrogen peroxide in acidic solution, Environ. Sci. Technol. 11 (1977) 61–66.

[157] Q. Li, J.R. Lancaster, Chemical foundations of hydrogen sulfide biology, Nitric Oxide - Biol. Chem. 35 (2013) 21–34. doi:10.1016/j.niox.2013.07.001.

[158] V. Vitvitsky, P.K. Yadav, A. Kurthen, R. Banerjee, Sulfide oxidation by a noncanonical pathway in red blood cells generates thiosulfate and polysulfides, J. Biol. Chem. 290 (2015) 8310–8320. doi:10.1074/jbc.M115.639831.

[159] P.J. Mak, J.R. Kincaid, Resonance Raman spectroscopic studies of hydroperoxo derivatives of cobalt-substituted myoglobin, J. Inorg. Biochem. 102 (2008) 1952–1957.

[160] C. Hoi, K. Wu, Review article The role of hydrogen sulphide in lung diseases, Biosci. Horizons. 6 (2013) 1–8.

[161] H. Jenzer, W. Jones, H. Kohler, On the molecular mechanism of lactoperoxidase-catalyzed H2O2 metabolism and irreversible enzyme inactivation, J. Biol. Chem. 261 (1986) 15550–15556.

Appendix (Scientific Publications)

Appendix A.1 Hydrogen sulfide activation in hemeproteins: The sulfheme scenario

Appendix A.2 Mechanisms of myeloperoxidase catalyzed oxidation of H_2S by H_2O_2 or O_2 to produce potent protein Cys-polysulfide-inducing species

Appendix A.3 Lactoperoxidase catalytically oxidize hydrogen sulfide via the intermediate formation of sulfheme derivatives turnover (Submission Pending: February 2018)

Journal of Inorganic Biochemistry 133 (2014) 78–86

Contents lists available at ScienceDirect

Journal of Inorganic Biochemistry

journal homepage: www.elsevier.com/locate/jinorgbio

Hydrogen sulfide activation in hemeproteins: The sulfheme scenario

Bessie B. Ríos-González, Elddie M. Román-Morales, Ruth Pietri, Juan López-Garriga *

Department of Chemistry, University of Puerto Rico, Mayagüez Campus, PO Box 9019, Mayagüez 00681-9019, Puerto Rico

ARTICLE INFO

Article history:
Received 21 August 2013
Received in revised form 14 January 2014
Accepted 14 January 2014
Available online 25 January 2014

Keywords:
Sulfhemoglobin
Hydrogen sulfide
Sulfheme protein
Sulfperoxidase
Histidine
Ferryl intermediate

ABSTRACT

Traditionally known as a toxic gas, hydrogen sulfide (H_2S) is now recognized as an important biological molecule involved in numerous physiological functions. Like nitric oxide (•NO) and carbon monoxide (CO), H_2S is produced endogenously in tissues and cells and can modulate biological processes by acting on target proteins. For example, interaction of H_2S with the oxygenated form of human hemoglobin and myoglobin produces a sulfheme protein complex that has been implicated in H_2S degradation. The presence of this sulfheme derivative has also been used as a marker for endogenous H_2S synthesis and metabolism. Remarkably, human catalases and peroxidases also generate this sulfheme product. In this review, we describe the structural and functional aspects of the sulfheme derivative in these proteins and postulate a generalized mechanism for sulfheme protein formation. We also evaluate the possible physiological function of this complex and highlight the issues that remain to be assessed to determine the role of sulfheme proteins in H_2S metabolism, detection and physiology.

1. Introduction

Hydrogen sulfide (H_2S), historically viewed as a toxic gas, has emerged as a biologically relevant molecule with significant therapeutic potential [1–3]. Endogenous H_2S in humans is produced by cystathionine β-synthase (CBS), cystathionine γ-lyase (CSE), and 3-mercaptopyruvate sulfur transferase (3MST) [4]. Once generated, H_2S penetrates cell membranes by simple diffusion and acts on target biomolecules to modulate numerous biological responses. Several molecular targets have been identified, including proteins, enzymes, transcription factors, and membrane ion channels [1]. As with nitric oxide and carbon monoxide, the other two bioactive gases, H_2S can also interact with heme-containing proteins to regulate biological activities [5–7]. Remarkably, the reactivity of hemeproteins towards H_2S has been associated with relevant physiological processes in many invertebrate systems living in sulfide-rich environments.

The clam *Lucina pectinata*, which lacks a mouth and gut, lives in sulfide-rich mangroves and its nutritional needs are met by a symbiotic relationship with sulfide oxidizing bacteria. Bacteria living inside the gill oxidize H_2S in the presence of oxygen (O_2) and this energy is utilized to synthesize organic nutrients for the invertebrate. The protein responsible for delivering H_2S to the bacteria is a hemeprotein called hemoglobin I (HbI) [8], which binds H_2S in the ferric heme iron with very high affinity (Fig. 1a). The orientation of the vinyl and the flexibility of the propionate peripheral groups of the heme, together with its dynamic behavior facilitate H_2S binding in this hemeprotein [9–11]. Interaction of H_2S with nearby residues also contributes to the affinity of HbI for H_2S [8,12]. This protein has a glutamine (Gln) residue at the distal ligand-binding site, instead of the equivalent histidine (His) typically found in many invertebrate and vertebrate organisms. We have shown that H_2S is stabilized in part by a hydrogen bonding interaction with Gln. H_2S release is dictated by two competing processes involving slow dissociation of H_2S from the ferric adduct and heme iron reduction followed by H_2S liberation [13,14]. Heme reduction by H_2S has also been observed in porphyrinates [15] and in phosphodiesterase (Ec DOS-PAS) [16]. We have also shown that replacing Gln with His in HbI, H_2S not only induces heme reduction [17] but it also generates a sulfheme derivative where another sulfur atom is incorporated in one of the pyrrole rings of the heme [18]. It is plausible that His plays an essential role in sulfheme formation.

The giant tubeworm *Riftia pachyptila* is another invertebrate that lives in the sulfide-rich hydrothermal vents and is also characterized by the presence of symbiotic sulfide-oxidizing bacteria that need to be supplied with both H_2S and O_2 [19]. *Riftia* supplies H_2S and O_2 to the endosymbionts by binding both ligands simultaneously at two different sites in its extracellular hemoglobins (Hbs). The worm binds O_2 in the iron heme groups and H_2S in other sites of the proteins. It has been suggested that binding of H_2S occurs at "free cysteine" or cysteine residues (Cys) not involved in disulfide bonds [19]. Likewise, the marine worm *Oligobrachia mashikoi*, which harbors endosymbiotic bacteria and lives in a sulfide rich environment, has Hbs that bind O_2 and H_2S and similar to *Riftia* it can transport both ligands simultaneously [20]. Structural analyses of *Oligobrachia* and *Riftia* Hbs showed that their sulfide-binding Cys residues are well conserved and that these residues play a principal role in sulfide binding (Fig. 1b and c). These conserved Cys residues are found in other animals living in sulfide-rich habitats. These facts support the notion that Cys residues are involved in sulfide binding

* Corresponding author. Tel.: +1 787 265 5453; fax: +1 787 265 5476.
E-mail address: juan.lopez16@upr.edu (J. López-Garriga).

0162-0134/$ – see front matter © 2014 Elsevier Inc. All rights reserved.
http://dx.doi.org/10.1016/j.jinorgbio.2014.01.013

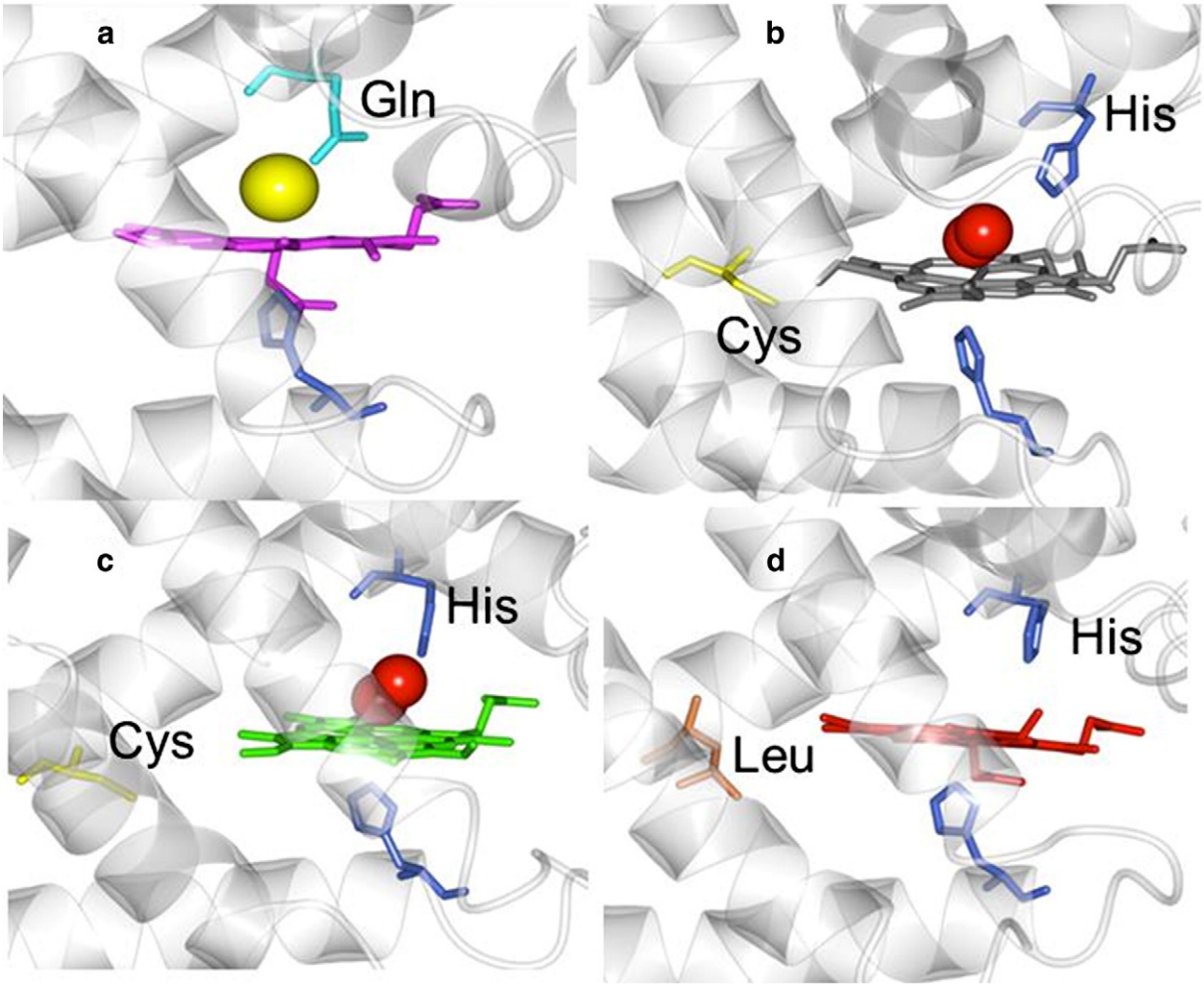

Fig. 1. Distal active site of: (a) *L. pectinata* (PDB:1MOH), (b) *R. pachyptila* (PDB:1YHU), (c) *O. mashikoi* (PBD:2ZS0), and (d) *L. terrestris* (PDB:1X9F). In *L. pectinata*, H_2S (shown as the sphere) binds to the ferric heme iron. *R. pachyptila* and *O. mashikoi* bind H_2S in the free Cys residue and O_2 in the heme iron center shown as spheres. In *L. terrestris*, the Cys residue is replaced by Leu, and in the presence of O_2, H_2S diffuses through the protein without encountering alternative binding sites and once at the heme site, it can interact directly with heme forming the sulfheme derivative.

and that this interactions would have the benefit of avoiding sulfheme formation. Although the hemoglobins in *Riftia* and *Oligobrachia* have a His residue near the heme (Fig. 1b and c), formation of a sulfheme complex has not been detected [19,21]. In contrast, sulfheme formation has been observed in the hemoglobins from *Lumbricus terrestris*, which inhabits sulfide-free environments and contains His at the ligand-binding site. Structural studies demonstrated that "free Cys residues" are absent in these Hbs (Fig. 1d), implying that in the presence of O_2, H_2S diffuses through these proteins without encountering alternative binding sites and once at the heme site, it can interact directly with the heme forming the sulfheme derivatives. These observations strongly suggest that His is required for the formation of the sulfheme derivatives. In *R. pachyptila* and *O. mashikoi*, the Cys residues transport H_2S to the symbiotic bacteria and protect the worms from sulfheme formation, which can limit O_2 transportation.

Human hemoglobin and myoglobin have His at the heme distal site and also form sulfheme in the presence of H_2S and O_2 or hydrogen peroxide (H_2O_2). Indeed, formation of these sulfheme complexes at moderate levels and their destruction by the physiologic turnover of red blood cells have been considered to be one of the pathways for H_2S degradation in humans [22]. The presence of these sulfheme derivatives has also been used as a marker of endogenous H_2S synthesis [23,24]. Remarkably, human catalases and peroxidases have His at their active site and also generate these sulfheme derivatives [25]. Thus, it is plausible that sulfheme derivatives might play a physiological role in vivo. This review focuses on the structural and functional characteristics of human sulfhemoglobin, sulfmyoglobin and other sulfheme proteins. We discuss the role of the distal His as a unique amino acid that triggers the formation of the sulfheme species and propose a mechanism that involves interaction of H_2S with ferric hydroperoxide and compound II intermediates.

2. Interaction of H_2S with myoglobin and hemoglobin

2.1. General aspects of sulfhemoglobin and sulfmyoglobin

Hemoglobin and myoglobin are globular hemeproteins whose functions involve the binding of O_2 to the ferrous iron (Fe^{II}) of the heme group (protoporphyrin IX). Hemoglobin (Hb) is a tetrameric protein that transports O_2 with cooperative structure fluctuations from lungs to muscles, while myoglobin (Mb) is monomeric and stores O_2 in the muscle cells. In the presence of sulfide, both Mb and Hb undergo two different chemical reactions. Both proteins are capable of binding H_2S in the open sixth position of the ferric heme iron (Fe^{III}) but with very low affinity [8,10]. H_2S can also react rapidly with the oxy and ferryl forms of Mb and Hb producing the so-called sulfheme derivatives.

In 1866, Hoppe-Seyler observed the formation of a green product after reacting Hb–O_2 with H_2S and called this green derivatives sulfhemoglobin (sulfHb). Michel et al. showed the formation of an analogous compound upon interaction of Mb–O_2 with H_2S and termed the

complex sulfmyoglobin (sulfMb) [25–27]. These derivatives have a sulfur atom incorporated in the heme pyrrole B with a characteristic optical band around 620 nm [26,28–31]. The displacement of the band depends on heme–Fe oxidation and ligation states, as well as the type of the sulfheme isomer [26,32–34]. These sulfheme derivatives exhibit lower affinity towards O_2 compared to the native proteins [33,35,36] and cannot be reverted to the normal functional proteins by natural mechanism in the red cells. High levels of sulfHb and sulfMb can be poisonous since they alter the protein O_2 transport or storage functionalities, causing a cyanosis known as sulfhemoglobinemia [14]. Possible symptoms are chocolate brown arterial blood, fatigue, chest pain and tightness, dizziness, pallor, livid discoloration of the skin and lips, bluish stain on finger tips, foul urine and breath, and tremor of the upper and lower extremities [37–39]. It is very common for sulfhemoglobinemia to be initially misdiagnosed as methemoglobinemia [37,38,40]. A helpful note for its diagnostic is the lack of respiratory distress for the degree of cyanosis [37], and near normal O_2 tension [41]. It can lead to end-organ damage and death when high sulfHb levels are reached (approximately 60%) [40]. In order to be clinically detectable the sulfHb concentration should be more than 5 g/L (approximately 80 μM) [37,38] while normal concentrations are below 0.37 g/L (approximately 5.8 μM) [38]. Its identification is usually performed by spectrophotometry, co-oximetry, gas chromatography or HPLC [37,40]. Treatment involves suspected chemical agent suspension, external O_2 supply [37] and in severe cases, blood transfusion [40].

2.2. Sulfhemoglobin and sulfmyoglobin formation

The mechanism for sulfHb and sulfMb formation is still unclear, however, it can be generated from the reaction of the Hb–O_2 and Mb–O_2 derivatives with H_2S, as well as in the presence of H_2O_2 and other thiol compounds [42]. In the case of H_2O_2, the heme ferryl species have been implicated in the formation of the sulfheme derivatives [18]. Fig. 2 shows that interaction of H_2O_2 with Hb and Mb leads to the formation of ferric hydroperoxide and the ferryl species compound I (Fe^{IV}═O $Por^{\bullet+}$) and compound II (Fe^{IV}═O), which generate reactive O_2 species that can damage cellular processes.

OxyHb and oxyMb can also generate these ferryl species. It has been suggested that the reaction of H_2S with ferryl compound II is crucial for sulfMb and sulfHb formation and two major overall reactions have been proposed [25,27]. In 1961, Nicholls proposed that sulfMb can be formed stoichiometrically by the reaction of heme ferryl compound II with H_2S and that a mixture of ferric sulfMb and small quantities of ferrous sulfMb were generated as final products (Reaction 1) [25,43]. He also observed that ferric sulfMb could then be reduced to ferrous sulfMb by H_2S excess. On the other hand, Berzofsky et al. observed that ferrous sulfMb (77%) was the major product of the reaction between 1 mol of H_2S and 1 mol of Mb ferryl compound II [44]. As shown in Reaction 2,

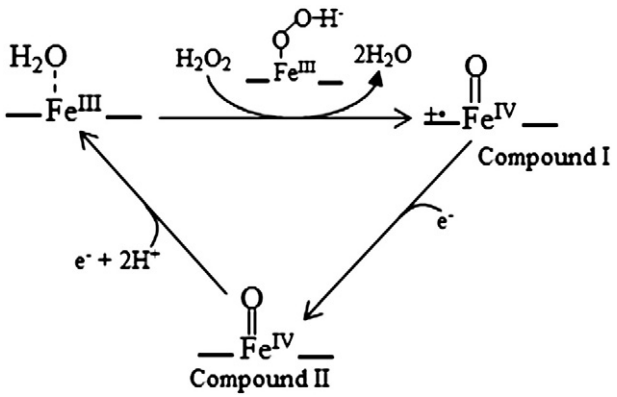

Fig. 2. Cyclic reaction of myoglobin with hydrogen peroxide.

Berzofsky also suggested that the hydrosulfide ion (HS^-) may be the initial reactant species since at physiological pH, 30% of H_2S is undissociated and ~70% dissociates to HS^- (pKa of 7.04) [44].

$$\text{Mb–compound II} + H_2S \rightarrow \begin{pmatrix} \text{sulfMbFe}^{II} + H_2O \\ \text{sulfMbFe}^{III} + H_2O + e^- \end{pmatrix} \quad (1)$$

$$\text{Mb–compound II} + HS^- \rightarrow \text{sulfMbFe}^{II} + HO^- \quad (2)$$

Nonetheless, in 1938, Michel demonstrated that at pH 6 about 20% of Hb was converted to sulfHb, while at pH 8 only 9% of the sulfHb product was obtained. In addition, it has been shown recently that the rate of sulfMb formation decreases 250-fold at basic pH values where the predominant species is HS^- [45]. Thus, in both Hb and Mb the effect of increasing the pH is to decrease the rate and amount of sulfheme formation. This inverse correlation between pH and sulfheme formation, suggests that at basic conditions (pH > 7) formation of the sulfheme product is slow and restricted, which reduces the possibility of HS^- as the reactive sulfur species. Accordingly, it is plausible that the initial reactants involved in sulfheme formation are ferryl compound II and undissociated H_2S.

In addition, we have proposed that His plays an essential role in sulfheme formation and that the interaction of H_2S with the His–ferryl–heme ternary complex triggers the formation of the sulfheme derivative [18]. As discussed in detail latter, we have observed that hemoglobins lacking a corresponding distal His are able to form the ferryl compound I and compound II species in the presence of H_2S but sulfheme formation is not seen. Thus, formation of sulfheme requires a concerted interaction between the reactants and the distal His. On these bases, sulfheme formation can be rationalized by the reaction scheme shown in Fig. 3a, which takes into account the role of His in sulfheme formation. Incorporating the His interaction, the first step is the formation of a ternary complex intermediate involving His, ferryl compound II and the heme–protein moiety. His donates a proton to the ferryl species, generating a highly reactive protonated ferryl compound II, which interacts with H_2S yielding in turn a sulfide radical (HS•) and ferric heme Mb or Hb. The HS• then attacks the porphyrin ring, producing the final sulfheme derivative. Romero and coworkers showed that Mb compound II also reacts with some thiols, yielding thiyl radical species and ferric Mb with the subsequent formation of sulfMb. It is important to mention that Nicholls, Berzofsky and others used catalase in their experiments to remove excess of H_2O_2 and to prevent the cyclic process shown in Fig. 2 [26,43,44]. In the absence of catalase, the cyclic reaction in Fig. 2 is operative and depending on the H_2O_2 concentration, ferric hydroperoxide can represent an additional initial reactant center for sulfheme complex formation. In this scenario, sulfheme formation can be described by the reaction scheme shown in Fig. 3b. Here, the ternary complex intermediate involves His, ferric hydroperoxide and the heme–protein moiety. The His–ferric hydroperoxide ternary complex in the presence of H_2S forms the {Fe(III)$OOHH_2S$} intermediate, which can trigger heterolytic or homolytic cleavage of the O – O bond. Heterolysis yields heme ferryl compound I and SH^-, while homolysis generates ferryl compound II and the HS• species. Since the rate of sulfMb formation decreases with the hydrosulfide HS^- ion, we suggest that the ferryl compound II and the HS• species are the predominant intermediates in the reaction of sulfheme formation. The HS• then attacks the ferryl compound II, producing the final sulfheme derivative. Curiously, Romero et al. also observed that in the absence of catalase the reaction of Mb compound II with thiols generated higher concentration of thiyl radicals [42], which accumulates during the cyclic reaction in Fig. 2 and can react with either the ferric hydroperoxide or the ferryl centers.

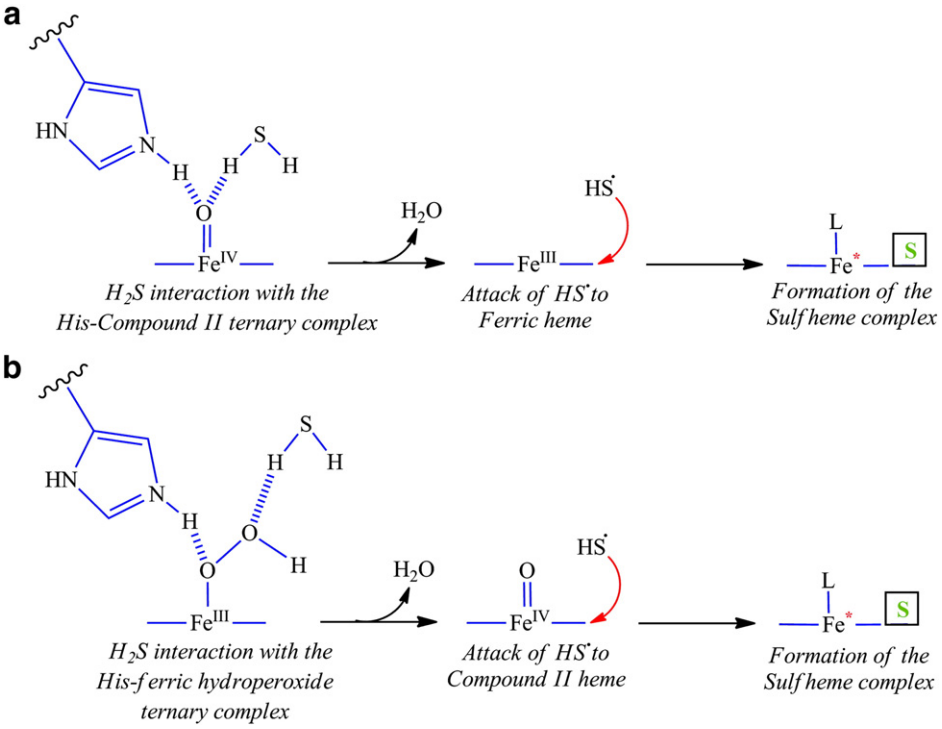

Fig. 3. Proposed mechanism for sulfheme protein formation.

2.3. Structural aspects of sulfHb and sulfMb

In sulfHb and sulfMb the sulfur atom is incorporated in one of the pyrrole rings of the heme, which lowers their affinity for O_2. The chemical nature of the modified heme in both sulfHb and sulfMb was a matter of debate for many years and the precise physiological structure of these derivatives remains elusive. It is now well accepted that sulfHb and sulfMb consist of a modified heme in which a sulfur atom adds to the pyrrole B of the porphyrin system. Using labeled sulfur (^{35}S) experiments it was first determined that only one atom of sulfur was incorporated into the heme group of sulfMb [26–28,44,46]. Later, proton NMR studies of sulfMb identified the sulfur atom on pyrrole B by analyzing the chemical shifts of the heme 1,3,5,8-methyls and the 2,4-vinyl substitutions [31,34,47]. Based on NMR and resonance Raman data it was then proved that the sulfur atom is incorporated across the double β–β bond of pyrrole B either as episulfide or thiochlorin, with a heme–chlorin type structure [26,28,30,31,34,44,47,48]. The band at 620 nm observed in the optical spectra of sulfHb and sulfMb reflects the nature of the chlorin structure. Heme–chlorin structure and other metallo-chlorin derivatives are characterized by a saturated $C_\beta - C_\beta$ bond in one of the pyrrole ring of the porphyrin, which reduces the symmetry of heme porphyrin from D_{4h}, typical of native Hb and Mb, to a C_{2v} system (Fig. 4a). This reduction induces a distortion of the macrocycle planarity and changes in the heme electronic properties, resulting in the activation of other electronic transitions at higher wavelengths. When a sulfur atom adds to the pyrrole B, the $C_\beta - C_\beta$ bond becomes saturated, adopting a chlorin like structure with a visible band at 620 nm. Therefore, it is clear that the incorporation of the sulfur atom involves disruption of the ring conjugation to that of chlorin, which reduces O_2 affinity in both sulfHb and sulfMb [18,33,35,36,48]. NMR and crystallographic studies demonstrated that in fact, conversion of Mb to sulfMb did not affect the heme cavity or the overall protein structure and that the observed changes in O_2 binding arise entirely from the local electronic changes of heme–chlorin structure [34,47,49].

Proton NMR studies of several sulfMbCN complexes revealed that there are at least three isomeric forms of the chlorin structure that may affect O_2 affinity [29,30]. As shown in Fig. 4b, each sulfheme isomer, named sulfMbA, sulfMbB and sulfMbC, has different chemical properties and hence, different reactivities and stabilities [29,34]. These differences reside in the porphyrin periphery alterations where the incorporated sulfur lays since all three isomers where observed at different pHs, temperatures and protein concentrations [29]. In general, the NMR spectra of all isomers showed symmetry reduction of the prosthetic group and alteration of the π conjugation of pyrrole B [34]. The sulfMbA structure is an episulfide across the β–β bond, which is rapidly reconverted to the protoheme when the heme is extracted from the protein [28,34,50,51]. SulfMbB is characterized by a "ring opened episulfide" [34], while sulfMbC is described as a thiochlorin structure. SulfMbA is converted to both sulfMbB and sulfMbC, but

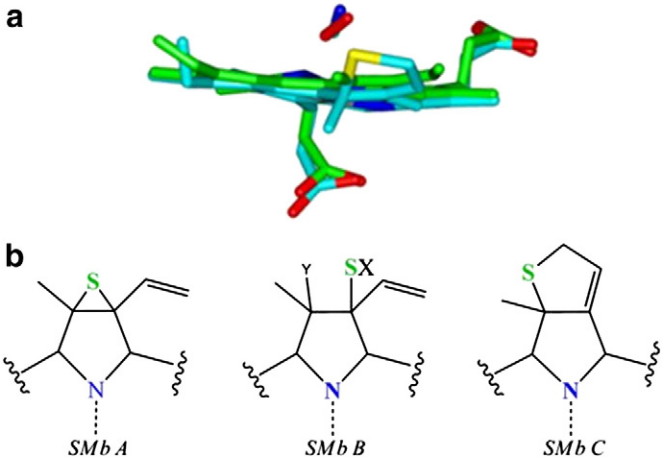

Fig. 4. Structure of: (a) Mb with bound oxygen (green, PDB:1MBO) and after exposure of H_2S (blue, PDB:1YMC), and (b) SulfMb isoforms. The final sulfheme product is a modified chlorin-type heme with a sulfur atom incorporated into one of the pyrrole rings. Several isoforms were identified in which sulfMbA is an episulfide, while sulfMbB and sulfMbC are characterized by a ring opened episulfide and a thiochlorin, respectively.

conversion from sulfMbB to sulfMbC has not been observed, indicating that sulfMbA is the precursor of the other two sulfheme species [28,34]. SulfMbC is the most stable isomeric form and is only observed when the 4-vinyl is on heme [30,52]. Replacing this vinyl group with hydrogen only yields sulfMbA and sulfMbB and two other red sulfMb isomers (D and E), which apparently forms from the former two isomers [52]. It is worthwhile to mention that the predominant isomeric species depends on experimental conditions such as pH and the nature of the oxidation and coordination states of the heme iron [28,34]. Nonetheless, the sulfMbC isomer is the terminal sulfMb product and it appears to predominate at physiological conditions, implying that the stability and reactivity of this compound may account for the reduced O_2 affinity in sulfMb.

SulfHb on the other hand, shows mainly the sulfHbA isomer with only a 10% of the sulfMbB counterpart [34]. In addition, sulfHbA does not go through isomeric interconversion probably due to internal flexibility limitation [28]. SulfMb and sulfHb isomers have different chemical reactivities, which can in principle influence O_2 affinity in both proteins.

2.4. Structural and functional implications of sulfHb and sulfMb

Similar to the native proteins, sulfMb and sulfHb bind numerous ligands at distal site of the heme iron [25,26,29,31–33,35]. Spontaneous autoxidation as well as oxidation state interconversion with different reducing and oxidation reagents are also maintained in these sulfheme derivatives without disturbing the sulfur ring. However, O_2 affinity is substantially reduced in both sulfMb and sulfHb. In this section we evaluate O_2 binding in sulfMb and sulfHb and the factors that may influence O_2 affinity in these proteins. Reconversion of the native proteins from the sulfheme derivatives and the possible physiological implications of sulfMb and sulfHb are also discussed.

The reversible reaction of O_2 with sulfMb was first recognized by Berzofsky et al., who observed that the 616 nm band, characteristic of ferrous sulfMb, shifted to 624 nm when deoxy sulfMb was exposed to O_2. Also, a shift of the Soret band from 424 nm (deoxy sulfMb) to 408 nm was detected. The authors observed that the shifts were completely reversed when the same sample was exposed to an argon atmosphere, and attributed the spectral displacements to the reversible binding of O_2 [33]. They also showed that the oxygen-binding curve of sulfMb was characterized by a rectangular hyperbolic shape, similar to native Mb, which led them to conclude that sulfMb was in fact able to bind O_2 reversibly in a concentration dependent manner. However, the concentration of O_2 required to saturate half of the sulfMb molecules, known as $p^{1/2}$ in the binding curve, was ~2500 higher than that of the native protein (530 mm Hg for sulfMb and 0.21 mm Hg for Mb), indicating much lower O_2 affinity for the former [33].

Following Berzofsky approach, Carrico et al. [35] studied the reversible binding of O_2 in sulfHb and observed that when the ferrous sulfHb complex was exposed to O_2, the band at 619 nm was displaced to 623 nm. They assigned these optical changes to formation of the oxy sulfHb derivative (sulfHb–O_2). As with native Hb, the O_2 binding curve was found to be sigmoidal, which supported the fact that sulfHb was able to reversibly bind O_2. The sigmoidal shape, a characteristic of cooperative behavior, also indicated that sulfHb retained some cooperative character of the native protein. Nonetheless, the $p^{1/2}$ of sulfHb was 63 mm Hg, while that of native Hb under similar conditions was 0.46 mm Hg. On this bases, it was concluded that the affinity of sulfHb for O_2 was 135 lower that the native protein [35].

The substantial decrease in O_2 affinity, in both sulfMb and sulfHb, has been attributed to the electron withdrawing character of the heme–chlorin structure. Incorporation of the sulfur atom to the β–β double bond of the pyrrole B removes electron density from the iron towards the periphery of the chlorine ring, reducing the ability of the iron to donate electron density back to the bound ligand and as a consequence, the iron affinity for O_2 decreases. It is well known that when O_2 binds to the ferrous heme in Mb and Hb, it donates two electrons to the heme iron, increasing in turn the electron density on the iron. To stabilize the complex, the iron donates electron density to the π orbital of the O_2, producing ferric superoxide ($Fe^{III}-OO^{\bullet-}$) [33]. Hence, the inability of sulfMb and sulfHb to effectively transfer electron density to O_2, destabilizes the complex and lowers their affinity for O_2. Although this interpretation sheds light on the reduced affinity of sulfMb and sulfHb for O_2, it does not explain the differences of O_2 affinity between sulfMb and sulfHb. As described above, sulfMb was shown to be ~2500-fold lower, whereas O_2 binding in sulfHb was reduced by a factor of ~135. The higher affinity of sulfHb for O_2 can be rationalized by the fact that not all four hemes are modified by H_2S and the protein is a partially sulfurated tetramer, leaving hemes available for normal O_2 binding [36]. The chemical nature of the sulfHb isomeric structure can also explain the observed higher O_2 affinity. The episulfide structure of the sulfHb isoform (sulfHbA) is more nucleophilic and less electronegative than the thiochlorin of sulfMb (sulfMbC), which can in principle decrease the electron withdrawing character of the chlorin structure in the former, resulting in higher O_2 affinity. This is consistent with the reduced intensity of the 620 nm band in the optical absorption spectra of sulfHb as opposed to sulfMb. This band arises from the forbidden electronic transition in the visible or Q region of the spectra that becomes partially allowed due to configuration interactions between the heme–chlorin orbitals. Distortion of the heme planarity increases the energy of heme orbitals and as a consequence the intensity of the band associated with the forbidden transition also increases. In sulfHb, the small intensity of the 620 nm band reflects less distortion of the heme macrocycle, which decreases the electron withdrawing characteristic of the typical chlorin derivative [18].

The reconversion of the sulheme products to the native functional proteins has been studied for many years. In 1961, Nicholls [25] was the first to observe the reconversion of sulfMb to native Mb, when he exposed the sulfMb sample to H_2O_2. Similar results were obtained when he exposed sulfMb to dithionite in the presence of O_2 or cyanide (CN^-), which also produces H_2O_2. Therefore, the reversion of sulfMb to Mb appears to be mediated by H_2O_2 in a reaction that may involve products associated with the spontaneous oxidation of H_2O_2. Photo-excitation of the sulfMb–CO complex also induced reconversion of the sulfheme derivative to the normal Mb–CO species. Berzofsky et al. [32] observed that when a sulfMb–CO sample was exposed to successive periods of irradiation, the Soret band shifted from 413 nm, typical of the sulfMb–CO complex, to 422 nm with a progressive disappearance of the 612 nm band. The results were explained in terms of the differences in activation energy, both in the ground and excite state of the chlorin structure. In the ground state, large activation energy is required to release the bound sulfur and to unsaturated the pyrrole ring. During photo-excitation, the structure reaches an electronic excited state that reduces the activation energy, resulting in a thermodynamically favored reconversion of the native Mb–CO complex [32].

The sulfMb reversion process was further studied by extracting the sulfheme prosthetic group of under various conditions [44]. The sulfhemin complex was unstable at all conditions and was rapidly converted to the protohemin and a mixture of sulfur containing molecules in which 50% was found to be SO_4^{2-}. The presence of peroxides increases the decomposition rate of sulfhemin, supporting the notion that H_2O_2 or products associated with its oxidation are probably required to initiate the reversibility process [25,44]. In addition to the peroxides, $HgCl_2$ and $Hg(OAc)_2$ were shown to decompose the sulfhemin derivative as well as. It appears that Hg^{2+} removes the sulfur atom from the sulfhemin molecule, generating the intact porphyrin system and a stable HgS compound [44]. Although reversion of the sulfheme products to the native derivatives has been observed under several experimental conditions, the analogous process has not been detected in vivo. This suggests that the only mechanism of sulfHb and sulfMb removal in our body is through the natural decomposition of these molecules in tissues and cells. Curiously, it was

demonstrated recently that H_2S diffuses rapidly across the red blood cell and that erythrocytes and plasma consume endogenous H_2S [53]. Klingerman et al. also showed that once in the blood, H_2S interacts primarily with Hb and not with proteins in the plasma [54]. Thus, it is plausible that oxyHb interacts with H_2S to form sulfHb, which is then eliminated by the natural destruction of red blood cells. Furthermore, the long normal life span of erythrocytes indicates that sulfHb can be detected and that indeed, it can be used as a biomarker for H_2S generation in cells.

3. Interaction of H_2S with enzymes

Enzymes are found in bacteria, fungi, plants and animals and their function is to serve as biological catalysts. They accelerate reactions that are necessary to sustain life but some inhibitors decrease the reaction rate and turnover of enzymes. Similar to human Hb and Mb, there is a set of some enzymes like lactoperoxidase and catalase that react with H_2S, forming analogous sulfheme derivatives. Nonetheless, published information about the interaction of H_2S with these enzymes is limited [25,43]. In this section we discuss the current knowledge about the interaction of H_2S with some heme peroxidases and catalase and correlate these interactions with human Hb and Mb.

3.1. Heme peroxidase (lactoperoxidase and myeloperoxidase)

Heme peroxidases are enzymes that catalyze the oxidation of a number of inorganic and organic compounds using H_2O_2 as the primary substrate. These enzymes turn reactive O_2 species like H_2O_2, which damage cell structure, to harmless product by adding hydrogen from a donor molecule. Lactoperoxidase (LPO) and myeloperoxidase (MPO) are two important heme-containing peroxidases involved in the immune defense system [55–58]. Both defend the system from invading microorganism by the bactericidal activities of the oxidized substrates [56,59]. For example, MPO catalyzes the formation of hypochlorous acid (HOCl) from chloride species and H_2O_2, which has antimicrobial activity and kills other pathogens in humans [59]. In the resting form, the heme groups of LPO and MPO are penta-coordinated with the iron in the high spin ferric state. As shown in Fig. 5, the distal sites of both enzymes have His and arginine (Arg) [57,60,61], which are important in their catalytic activities, specifically in the formation and stabilization of ferryl intermediates [62]. The generalized mechanism is similar to that shown in Fig. 2. Interaction of the enzymes with H_2O_2 generates the ferryl compound I and compound II intermediates. As opposed to Hb and Mb, compound I is quite stable in these enzymes. Compound II is generated by the donation of an electron from a reducing substrate to the porphyrin cation radical ($Por^{\bullet+}$) or compound I. The enzymes then return to their resting state by another electron transfer reaction from a second substrate, which reduces compound II with the concomitant formation of the ferric enzyme, a second radical substrate and a water molecule. The electron donor molecules vary from inorganic compounds such, as halides (X^-), to organic (AH_2) substrates, which are oxidized to hypohalous acids (HOX) and organic radicals ($^{\bullet}AH$), respectively [63].

The catalytic activity of LPO is inhibited by sulfhydryl compounds such as methylmercaptoimidazole (MMI) and thiouracil [64,65]. Ohtaki and coworkers suggested that the irreversible inactivation of the enzyme was induced by the reaction of compound II with the antithyroid drug MMI [66]. In 1984, Nakamura and coworkers also evaluated the interactions of LPO with H_2S, MMI, cysteine and dithiothreitol in the presence of H_2O_2 [43]. They found that as Hb and Mb, the reaction of H_2S with the enzyme in the presence of H_2O_2, yielded a sulfheme derivative, which they named sulflactoperoxidase. The ferrous sulflactoperoxidase complex has a characteristic band at approximately 638 nm whereas the ferric derivative has bands at 605 nm and 727 nm [43]. Reaction of MMI with resting LPO yielded a spectrum with visible band at 592 nm and 635 nm and based on the similarity with the one obtained with H_2S, the authors suggested that sulflactoperoxidase was also formed with MMI.

Although the molecular mechanism of sulflactoperoxidase formation from H_2S and the subsequent inactivation of the enzyme have not been described, the analogous processes have been well evaluated with the sulfur-containing compound MMI [43,64–68]. Ohtaki in 1982 and Nakamura in 1984, suggested that LPO compound II was reduced to

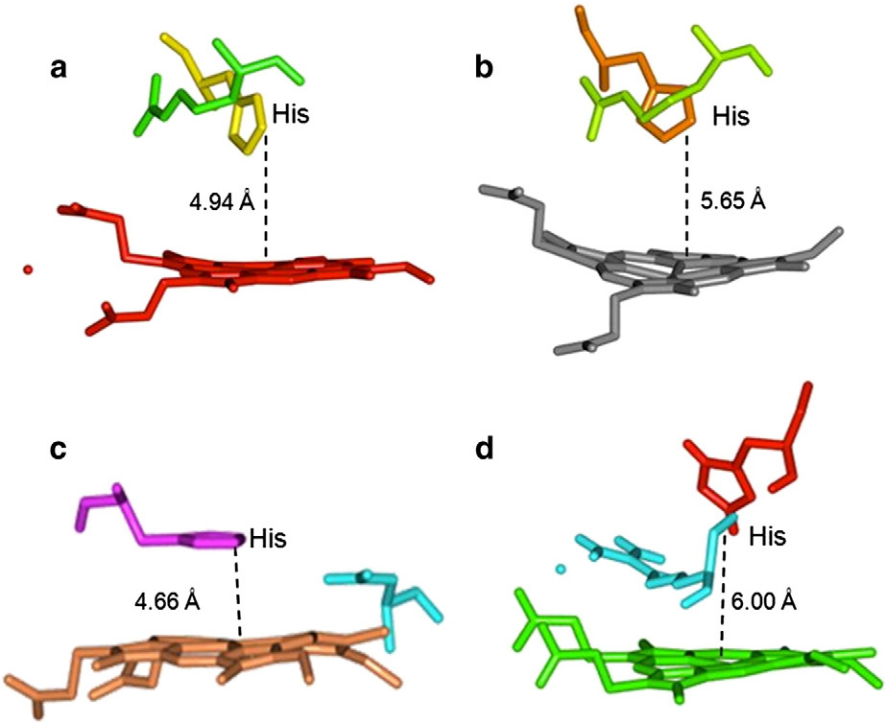

Fig. 5. Distal active site of: (a) LPO (PDB:2NQX), (b) MPO (PDB:1CXP), (c) catalase (PDB:3RGP) and (d) HRP (PDB:1ATJ). The structures show the distances from the iron to the NE2 of the distal His.

the ferric state by one electron transfer from MMI with the concomitant formation of a MMI radical [43,66]. The presence of the MMI radical was later confirmed by EPR studies and it was also shown that the radical did not interact directly with the heme iron. The authors suggested that the MMI radical must bind to a specific site of heme porphyrin ring and that the unpaired electron of the radical was then transferred to the heme ferryl group [67]. It was also proposed in that study that the distal His might influence MMI oxidation and subsequent binding to the heme porphyrin. Remarkably, this supports the unique role of the distal His in sulfheme formation as suggested previously [18]. Overall, it is now believed that MMI interacts with LPO ferryl compound II, inducing the formation of a thiyl radical that inhibits LPO irreversibly by reacting directly with the heme porphyrin system. Based on the optical spectra reported by Nakamura it is plausible that the MMI radical interacts with the heme and generates sulflactoperoxidase, which inhibit the enzyme activity [43]. A similar mechanism can be invoked for the inactivation of LPO by H_2S. Moreover, the fact that the optical spectra of LPO in the presence of H_2S and H_2O_2 show bands similar to sulfHb and sulfMb, strongly suggests that the heme group of the sulflactoperoxidase derivative is a chlorin type structure in which the sulfur atom is incorporated across the $\beta-\beta$ double bond of the pyrrole B [44,47,69].

Like LPO, MPO activity is inhibited in the presence of H_2S and H_2O_2 [70,71]. The mechanism of inhibition has not been described and warrants further investigation. It has been speculated that the inhibition may be mediated by the formation of the sulfheme derivative, which lowers the affinity of the enzyme for the substrates [25,70,71]. Although formation of the sulfheme derivative has not yet been demonstrated experimentally in MPO, the enzyme has a His residue in the heme distal site that in the presence of H_2S and the natural H_2O_2 substrate can contribute to sulfheme formation (Fig. 5b).

It has been suggested recently that H_2S interacts with HOCl, the enzymatic product of MPO, and prevents oxidative damage in vivo. As mentioned before HOCl possesses antimicrobial activity in cells. Nevertheless, excessive production of HOCl can cause oxidative stress to proteins, lipids, DNA and RNA. HOCl seems to contribute to the oxidative damage of these biomolecules in patients with Alzheimer's disease (AD) since high levels of MPO are found in the prefrontal cortex, hippocampal microglia and neurons. Whiteman et al. showed that H_2S prevents oxidative damage in neuronal cells exposed to HOCl and suggested that the direct interaction of both reactants could be an important mechanism for HOCl removal in vivo in AD patients [72]. Likewise, it has been suggested that HOCl can also modify low-density lipoproteins (LDL) associated with the formation of arteriosclerotic plaques. In 2007 Laggner and coworkers demonstrated the ability of H_2S to prevent modification of LDL by HOCl either via direct interaction with HOCl or inhibition of MPO [71]. Nonetheless, it has been suggested recently that the reaction of H_2S with HOCl is not favorable in vivo, unless it could accumulate at high local concentrations [73]. Thus, it is highly possible that H_2S stops HOCl oxidative damage by limiting MPO activity via sulfheme formation.

It is evident that LPO forms sulflactoperoxidase and that MPO must probably generate the analogous compound, however, the physiological implication of these derivatives remains unknown and warrants additional examination. Moreover, interaction of H_2S and the possible physiological role of these interactions should be further evaluated in other peroxidases, in particular those having His at the active site and are involved in H_2O_2 and O_2 chemistry. For example, thyroid peroxidase (TPO), an enzyme that participates in hormone biosynthesis and uses H_2O_2 as a substrate, is inactivated by MMI possibly through the formation of a sulfheme like derivative [43]. The sulfheme TPO complex may also be produced in the presence of H_2S. In fact, amino acid sequence alignment shows that TPO has His in the active distal site, which is involved in the enzyme catalytic activity and probably may play a crucial role in sulfheme formation [57,74]. Although we focus in human peroxidases, the dehaloperoxidase–hemoglobin from the invertebrate *Amphitrite ornata* forms the sulfheme product and has His near the heme [75]. Indeed, as we describe next, catalase has a His in the distal active site and generates the sulfheme derivative upon reaction with H_2S.

3.2. Catalase

Catalase is a heme-containing enzyme found in many bacteria and almost all plants and animals. The protein is a tetramer and each monomer contains a heme group [76–78]. As Reaction 3 shows, the enzyme protects the cells by converting H_2O_2 into water and O_2 [79]. The proposed mechanism occurs in two steps and involves the ferryl intermediates [80]. In the first step the enzyme reacts with H_2O_2 to form compound I. In the second step, compound I reacts with another molecule of H_2O_2 and the enzyme returns to the resting state. Two electrons are transferred to one molecule of H_2O_2 and then two electrons are accepted from a second H_2O_2. Catalase does not form compound II as part of the normal catalytic cycle but at low concentration of H_2O_2 and in the presence of one electron donor generation of compound II has been observed. The efficiency of the catalytic reactions is improved by the interaction of the active site His and Asn residues (His and Asn in the positions 74 and 147, respectively) with the ferryl intermediates.

$$\begin{aligned} &2H_2O_2 \rightarrow 2H_2O + O_2 \\ &\text{Step 1.} \quad \left[Fe^{III}Por\right] + H_2O_2 \rightarrow \left[Fe^{IV} = O \ \ Por^{\bullet +}\right] + H_2O \\ &\text{Step 2.} \quad \left[Fe^{IV} = O \ \ Por^{\bullet +}\right] + H_2O_2 \rightarrow \left[Fe^{III}Por\right] + H_2O + O_2 \end{aligned} \tag{3}$$

Catalase is inhibited by ligands like cyanide, azide, 3-amino-1,2,4-triazol and nitric oxide [81–84]. Also, as Beers and Sizer proposed, H_2S could inhibit catalase in two ways: it may form an inactive compound with the primary catalase peroxide complex and that it may react directly with either the protein moiety or with the heme group [85]. Nicholls then proposed that the interaction of H_2S with catalase was similar to that of Mb in which H_2S reacts with the ferryl compound II intermediate and modifies the heme porphyrin system to produce the analogous sulfheme derivatives [25]. The product of the reaction of catalase with H_2S and H_2O_2 yielded an optical spectrum with a characteristic band at 635 nm and was therefore ascribed to ferrous sulfcatalase. Ferric sulfcatalase was also observed with absorption bands at 585 nm and 710 nm. Based on this, Bersofsky suggested that the structure of sulfcatalase should be similar to sulfMb and sulfHb [26,44,47,69]. Therefore, these observations support the notion that the sulfheme product is generated in presence of O_2 and/or H_2O_2 and that the distal His residue near the iron regulates sulfheme formation. Interestingly, catalase can be regenerated from sulfcatalase by oxidizing agents like O_2 and ethyl hydroperoxide and by small molecules like cyanide and azide, and sodium dithionite [25].

4. Role of His in sulfheme protein formation

Several mechanistic aspects of sulfheme protein formation remain unknown. However, there are enough experimental evidences that can provide an insight into the characteristics of sulfheme protein generation. For example, as mentioned in this review, we have suggested that His is directly involved in sulfheme protein formation. In this respect, we have shown that the cytoplasmic HbI, HbII and HbIII from *L. pectinata*, which have Gln instead of His, do not form the sulfheme derivatives [18]. In addition to Gln, HbI has a cluster of Phe residues near the heme, while in HbII and HbIII one of the Phe is replaced with Tyr. Thus, it appears that neither Gln, Phe nor Tyr are involved in sulfheme protein formation. Moreover, as Table 1 shows, sulfheme was not detected in the HbI Gln/Val, Gln/Asn and Gln/Arg mutants, while the product was only observed in the Gln/His variant [14,18]. Similarly, it

Table 1
Sulfheme formation in different hemeproteins.

Protein	Key distal site residues	Sulfheme
Horse heart Mb	His	Yes (618 nm)
Human Hb	His	Yes (620 nm)
L. pectinata HbII and HbIII[a]	Gln	No
L. pectinata HbI	Gln	No
HbI Gln64Asn[b]	Asn	No
HbI Gln64His[b]	His	Yes (624 nm)
HbI Phe29His[b]	Gln	No
HbI Phe68His[b]	Gln	No
HbI Phe29Leu[b]	Gln	No
HbI Gln64Arg[b]	Arg	No
HbI Phe68Val[b]	Gln	No
Macrobdella decora Hbs[c]	His	Yes (620 nm)
Lumbricus terrestris Hbs[c]	His	Yes (620 nm)
Catalase	His	Yes (635 nm)
Lactoperoxidase	His	Yes (638 nm)
Dehaloperoxidase[d]	His	Yes (620 nm)
Horseradish peroxidase	Arg	No
Cytochrome c oxidase	His (cyt a_3)	No
Heme–O_2 sensor Ec DOS PAS	Met, Arg	No
Ec DOS PAS Met95Ala[e]	Ala	No
Ec DOS PAS Met95His[e]	His	No
Ec DOS PAS Met95Leu[e]	Leu	No
Ec DOS PAS Arg97Ala[e]	Ala	No
Ec DOS PAS Arg97Glu[e]	Glu	No
Ec DOS PAS Arg97Ile[e]	Ile	No

[a] HbII and HbIII are O_2 transport proteins found in *L. pectinata* [8].
[b] Point mutants of HbI from *L. pectinata*. The numbers represent the position of the amino acid in the polypeptide chain [17,18].
[c] *Macrobdella decora* and *Lumbricus terrestris* are invertebrates that live in sulfide-free environments and have large Hbs that transport O_2 [18].
[d] This enzyme is found in the marine worm *Amphitrite ornata* and is believed to be involved in H_2S catabolism [75].
[e] Point mutants of the heme sensor phosphodiesterase from *Escherichia coli* (Ec DOS PAS) [86].

was shown recently that the native Ec DOS-PAS heme sensor, which has Met and Arg in its distal site, does not form the sulfheme complex, supporting the role His in sulfheme formation [86]. Mutations of these residues by Ala, Ile, Leu and Glu did not induce formation of sulfheme, instead a verdoheme product was observed in the Arg/Ala and Arg/Ile mutants. Verdoheme is a modified heme that has oxygen incorporated in the α-meso heme position. It is known for being one of the heme degradation steps in heme oxygenase [86]. Thus, it is evident that amino acids with: (*i*) non-polar aliphatic groups like glycine, alanine, valine and isoleucine, (*ii*) polar uncharged groups like glutamine and asparagine, (*iii*) aromatic group like phenylalanine and tyrosine, and (*iv*) positively charged groups like lysine and arginine, are not involved in the synthesis of the sulfheme species.

As shown in Table 1, His is a common feature in those proteins that generate sulfheme, reiterating the role of His in the reaction of sulfheme. Thus, with the exception of cytochrome c oxidase, horseradish peroxidase, and the phosphodiesterase His mutant (Ec DOS-PAS Met95His), distal His seems to be essential for sulfheme formation. In cytochrome c oxidase, the catalytic center includes a heme porphyrin (a_3), a copper (Cu_B) center and three His residues, which are coordinated to Cu_B. The fact that heme a_3–Cu_B binuclear centers are directly involved in the catalytic activity of the enzyme precludes sulfheme formation. Interestingly, both LPO and horseradish peroxidase (HRP) have a His and Arg in their active site, which are important for their enzymatic activity, but only the former generates sulfheme, while the latter does not [25,43]. This exclusive behavior can be attributed to the distance between the His and the heme iron, which is shorter in LPO (4.94 Å), as opposed to HRP (6.00 Å) (Fig. 5a and d). On the other hand, the His residue in the Ec DOS-PAS Met95His mutant is coordinated to the heme iron, which blocks H_2O_2 binding and sulfheme formation [86]. Clearly, this shows that the orientation and position of the His residue at the heme active site are crucial for the synthesis of the sulfheme product. The fact that only proteins that have His at the distal site generate sulfheme, the reactivity of this residue should be taken into account when considering the mechanism of sulfheme protein formation.

5. Summary and future perspectives

In view of the current data we suggest that: (*a*) the formation of the sulfheme derivate requires a His residue in the heme distal site with an adequate orientation to form an active ternary complex; (*b*) the ternary complex intermediate involves His, ferric hydroperoxide or compound II and the heme–protein moiety; (*c*) interaction of this heme cluster with H_2S triggers formation of the SH•, yielding the final ferrous or ferric sulfheme product. These observations and the tautomeric nature [87,88] and orientation of distal His, which can behave as an acid–base catalyst, allows suggesting the general mechanisms shown in Fig. 3. Due to the cyclic nature of the reaction between hemeproteins and H_2O_2 (Fig. 2), it is difficult to assign the initial peroxide adduct (ferric hydroperoxide or compound II) responsible for sulfheme formation. Assuming that in the presence of an H_2O_2 scavenger the end product of the reaction is compound II, then the predominant reaction can be summarized as shown in Fig. 3a. On the other hand if the cyclic reaction is operative, the reaction can be described as demonstrated in Fig. 3b. In both scenarios the SH• appears to be the reactive species that attack the double β–β bond of pyrrole B.

It is clear that much remains to be investigated before implicating sulfheme proteins in any physiological function. Nonetheless, the fact that this complex is also produced during the catalytic reaction of heme–peroxidases and catalases, strongly suggests that this derivative can also be generated in other heme-containing enzymes involved in O_2 chemistry. Also, albeit the concentration of endogenous H_2S may be too low to generate sulfheme in vivo, exposure of H_2S by donors can induce formation of the complex, which can be used in turn to assess the presence of exogenous H_2S in tissues and cells. Key issues that requires further investigation to address the above hypotheses include: (*a*) the precise peroxide adduct involved in sulfheme formation, (*b*) the subsequent reaction of the thiyl radical with the heme ferric or ferryl compound II intermediate, (*c*) the final sulfheme product (ferric versus ferrous) and (*d*) the stability, decay and reversibility of the sulfheme complex in vitro and in vivo. Insights into these issues will determine the role of sulfheme proteins in H_2S metabolism, detection and physiology.

Abbreviations

HbI	hemoglobin I
Hbs	hemoglobins
sulfHb	sulfhemoglobin
sulfMb	sulfmyoglobin
MMI	methylmercaptoimidazole
HRP	horseradish peroxidase
HS•	sulfide radical
(Fe^{IV}=O)	compound II
Fe^{III} – OO•	ferric superoxide
LPO	lactoperoxidase
MPO	myeloperoxidase
$Por^{\bullet+}$	porphyrin cation radical

Acknowledgment

We thank the NIH-RISE (Grant R25SGM088023) and the National Science Foundation (Grant 0843608) for their financial support.

References

[1] K. Kashfi, K.R. Olson, Biochem. Pharmacol. 85 (2013) 689–703.
[2] H. Kimura, N. Shibuya, Y. Kimura, Antioxid. Redox Signal. 17 (2012) 45–57.
[3] K.R. Olson, Am. J. Physiol. Regul. Integr. Comp. Physiol. 301 (2011) R297–R312.
[4] S. Singh, R. Banerjee, Biochim. Biophys. Acta 1814 (2011) 1518–1527.
[5] O. Kabil, R. Banerjee, J. Biol. Chem. 285 (2010) 21903–21907.
[6] M. Kajimura, R. Fukuda, R.M. Bateman, T. Yamamoto, M. Suematsu, Antioxid. Redox Signal. 13 (2010) 157–192.
[7] Q. Li, J.R. Lancaster Jr., Nitric Oxide 35C (2013) 21–34.
[8] D.W. Kraus, J.B. Wittenberg, J. Biol. Chem. 265 (1990) 16043–16053.
[9] J.F.C. Colón, E. Silfa, J.L. Garriga, J. Am. Chem. Soc. 120 (1998) 9312–9317.
[10] S. Fernandez-Alberti, D.E. Bacelo, R.C. Binning Jr., J. Echave, M. Chergui, J. Lopez-Garriga, Biophys. J. 91 (2006) 1698–1709.
[11] E. Silfa, M. Almeida, J. Cerda, S. Wu, J. Lopez-Garriga, Biospectroscopy 4 (1998) 311–326.
[12] M. Rizzi, J.B. Wittenberg, A. Coda, P. Ascenzi, M. Bolognesi, J. Mol. Biol. 258 (1996) 1–5.
[13] R. Pietri, R.G. Leon, L. Kiger, M.C. Marden, L.B. Granell, C.L. Cadilla, J. Lopez-Garriga, Biochim. Biophys. Acta 1764 (2006) 758–765.
[14] R. Pietri, E. Roman-Morales, J. Lopez-Garriga, Antioxid. Redox Signal. 15 (2011) 393–404.
[15] J.W. Pavlik, B.C. Noll, A.G. Oliver, C.E. Schulz, W.R. Scheidt, Inorg. Chem. 49 (2010) 1017–1026.
[16] H. Takahashi, M. Sekimoto, M. Tanaka, A. Tanaka, J. Igarashi, T. Shimizu, J. Inorg. Biochem. 109 (2012) 66–71.
[17] R. Pietri, A. Lewis, R.G. Leon, G. Casabona, L. Kiger, S.R. Yeh, S. Fernandez-Alberti, M.C. Marden, C.L. Cadilla, J. Lopez-Garriga, Biochemistry 48 (2009) 4881–4894.
[18] E. Roman-Morales, R. Pietri, B. Ramos-Santana, S.N. Vinogradov, A. Lewis-Ballester, J. Lopez-Garriga, Biochem. Biophys. Res. Commun. 400 (2010) 489–492.
[19] X. Bailly, S. Vinogradov, J. Inorg. Biochem. 99 (2005) 142–150.
[20] N. Numoto, T. Nakagawa, A. Kita, Y. Sasayama, Y. Fukumori, K. Miki, Proc. Natl. Acad. Sci. U. S. A. 102 (2005) 14521–14526.
[21] A.J. Arp, J.J. Childress, R.D. Vetter, J. Exp. Biol. 128 (1987) 139–158.
[22] B.L. Predmore, D.J. Lefer, G. Gojon, Antioxid. Redox Signal. 17 (2012) 119–140.
[23] A.F. Perna, M.G. Luciano, D. Ingrosso, P. Pulzella, I. Sepe, D. Lanza, E. Violetti, R. Capasso, C. Lombardi, N.G. De Santo, Nephrol. Dial. Transplant. 24 (2009) 3756–3763.
[24] M. Whiteman, S. Le Trionnaire, M. Chopra, B. Fox, J. Whatmore, Clin. Sci. (Lond.) 121 (2011) 459–488.
[25] P. Nicholls, Biochem. J. 81 (1961) 374–383.
[26] J.A. Berzofsky, J. Peisach, W.E. Blumberg, J. Biol. Chem. 246 (1971) 3367–3377.
[27] H.O. Michel, J. Biol. Chem. 126 (1938) 323–348.
[28] L.L. Bondoc, M.-H. Chau, M.A. Price, R. Timkovich, Biochemistry 25 (1986) 8458–8466.
[29] M.J. Chatfield, G.N. La Mar, A.L. Balch, J.T. Lecomte, Biochem. Biophys. Res. Commun. 135 (1986) 309–315.
[30] M.J. Chatfield, G.N. La Mar, J.T.J. Lecomte, A.L. Balch, K.M. Smith, K.C. Langry, J. Am. Chem. Soc. 108 (1986) 7108–7110.
[31] R. Timkovich, M.R. Vavra, Biochemistry 24 (1985) 5189–5196.
[32] J.A. Berzofsky, J. Peisach, J.O. Alben, J. Biol. Chem. 247 (1972) 3774–3782.
[33] J.A. Berzofsky, J. Peisach, W.E. Blumberg, J. Biol. Chem. 246 (1971) 7366–7372.
[34] M.J. Chatfield, G.N. La Mar, R.J. Kauten, Biochemistry 26 (1987) 6939–6950.
[35] R.J. Carrico, W.E. Blumberg, J. Peisach, J. Biol. Chem. 253 (1978) 7212–7215.
[36] C.M. Park, R.L. Nagel, W.E. Blumberg, J. Peisach, R.S. Magliozzo, J. Biol. Chem. 261 (1986) 8805–8810.
[37] M. Harangi, J. Matyus, E. Nagy, E. Nagy, G. Paragh, J. Balla, A.V. Olah, Clin. Toxicol. (Phila.) 45 (2007) 189–192.
[38] M. Noor, E. Beutler, West. J. Med. 169 (1998) 386–389.
[39] A. Tangerman, G. Bongaerts, R. Agbeko, B. Semmekrot, R. Severijnen, J. Clin. Pathol. 55 (2002) 631–633.
[40] G.V. Baranoski, T.F. Chen, B.W. Kimmel, E. Miranda, D. Yim, J. Biomed. Opt. 17 (2012) 97005.
[41] A.S. Gopalachar, V.L. Bowie, P. Bharadwaj, Ann. Pharmacother. 39 (2005) 1128–1130.
[42] F.J. Romero, I. Ordonez, A. Arduini, E. Cadenas, J. Biol. Chem. 267 (1992) 1680–1688.
[43] S. Nakamura, M. Nakamura, I. Yamazaki, M. Morrison, J. Biol. Chem. 259 (1984) 7080–7085.
[44] J.A. Berzofsky, J. Peisach, B.L. Horecker, J. Biol. Chem. 247 (1972) 3783–3791.
[45] S.H. Libardi, H. Pindstrup, D.R. Cardoso, L.H. Skibsted, J. Agric. Food Chem. 61 (2013) 2883–2888.
[46] D.B. Morell, Y. Chang, P.S. Clezy, Biochim. Biophys. Acta 136 (1967) 121–130.
[47] M.J. Chatfield, G.N. La Mar, K.M. Smith, H.K. Leung, R.K. Pandey, Biochemistry 27 (1988) 1500–1507.
[48] L.A. Andersson, T.M. Loehr, A.R. Lim, A.G. Mauk, J. Biol. Chem. 259 (1984) 15340–15349.
[49] S.V. Evans, B.P. Sishta, A.G. Mauk, G.D. Brayer, Proc. Natl. Acad. Sci. U. S. A. 91 (1994) 4723–4726.
[50] M.A. Scharberg, G.N. La Mar, J. Am. Chem. Soc. 115 (1993) 6513–6521.
[51] M.A. Scharberg, G.N. La Mar, J. Am. Chem. Soc. 115 (1993) 6522–6528.
[52] M.J. Chatfield, G.N. La Mar, A.L. Balch, K.M. Smith, D.W. Parish, T.J. LePage, FEBS Lett. 206 (1986) 343–346.
[53] M.J. Jennings, Am. J. Physiol. Cell Physiol. 305 (2013) C941–C950.
[54] C.M. Klingerman, N. Trushin, B. Prokopczyk, P. Haouzi, Am. J. Physiol. Regul. Integr. Comp. Physiol. 305 (2013) R630–R638.
[55] J. Arnhold, J. Flemmig, Arch. Biochem. Biophys. 500 (2010) 92–106.
[56] K.D. Kussendrager, A.C. van Hooijdonk, Br. J. Nutr. 84 (Suppl. 1) (2000) S19–S25.
[57] P.G. Furtmuller, M. Zederbauer, W. Jantschko, J. Helm, M. Bogner, C. Jakopitsch, C. Obinger, Arch. Biochem. Biophys. 445 (2006) 199–213.
[58] M. Zamocky, C. Jakopitsch, P.G. Furtmuller, C. Dunand, C. Obinger, Proteins 72 (2008) 589–605.
[59] S. Stanković, N. Majkić-Singh, J. Med. Biochem. 30 (2011) 230–236.
[60] T.J. Fiedler, C.A. Davey, R.E. Fenna, J. Biol. Chem. 275 (2000) 11964–11971.
[61] A.K. Singh, N. Singh, S. Sharma, S.B. Singh, P. Kaur, A. Bhushan, A. Srinivasan, T.P. Singh, J. Mol. Biol. 376 (2008) 1060–1075.
[62] G. Battistuzzi, M. Bellei, C.A. Bortolotti, M. Sola, Arch. Biochem. Biophys. 500 (2010) 21–36.
[63] I. Bertini, H.B. Gray, E.I. Stiefel, J.S. Valentine, Biological Inorganic Chemistry. Structure and Reactivity, First ed. University Science Books, United States of America, 2007.
[64] H. Edelhoch, G. Irace, M.L. Johnson, J.L. Michot, J. Nunez, J. Biol. Chem. 254 (1979) 11822–11830.
[65] J.L. Michot, J. Nunez, M.L. Johnson, G. Irace, H. Edelhoch, J. Biol. Chem. 254 (1979) 2205–2209.
[66] S. Ohtaki, H. Nakagawa, M. Nakamura, I. Yamazaki, J. Biol. Chem. 257 (1982) 761–766.
[67] U. Bandyopadhyay, D.K. Bhattacharyya, R. Chatterjee, R.K. Banerjee, Biochem. J. 306 (Pt 3) (1995) 751–757.
[68] D.R. Doerge, Arch. Biochem. Biophys. 244 (1986) 678–685.
[69] M.J. Chatfield, G.N. La Mar, Arch. Biochem. Biophys. 295 (1992) 289–296.
[70] R. Claesson, M. Granlund-Edstedt, S. Persson, J. Carlsson, Infect. Immun. 57 (1989) 2776–2781.
[71] H. Laggner, M.K. Muellner, S. Schreier, B. Sturm, M. Hermann, M. Exner, B.M. Gmeiner, S. Kapiotis, Free Radic. Res. 41 (2007) 741–747.
[72] M. Whiteman, N.S. Cheung, Y.Z. Zhu, S.H. Chu, J.L. Siau, B.S. Wong, J.S. Armstrong, P.K. Moore, Biochem. Biophys. Res. Commun. 326 (2005) 794–798.
[73] S. Carballal, M. Trujillo, E. Cuevasanta, S. Bartesaghi, M.N. Moller, L.K. Folkes, M.A. Garcia-Bereguiain, C. Gutierrez-Merino, P. Wardman, A. Denicola, R. Radi, B. Alvarez, Free Radic. Biol. Med. 50 (2011) 196–205.
[74] N.B. Loughran, B. O'Connor, C. O'Fagain, M.J. O'Connell, BMC Evol. Biol. 8 (2008) 101.
[75] F.P. Nicoletti, M.K. Thompson, S. Franzen, G. Smulevich, J. Biol. Inorg. Chem. 16 (2011) 611–619.
[76] W.A. Schroeder, J.R. Shelton, J.B. Shelton, B. Robberson, G. Apell, R.S. Fang, J. Bonaventura, Arch. Biochem. Biophys. 214 (1982) 397–421.
[77] J.B. Sumner, A.L. Dounce, Science 85 (1937) 366–367.
[78] J.B. Sumner, N. Gralen, Science 87 (1938) 284.
[79] C. Michiels, M. Raes, O. Toussaint, J. Remacle, Free Radic. Biol. Med. 17 (1994) 235–248.
[80] N. Purwar, J.M. McGarry, J. Kostera, A.A. Pacheco, M. Schmidt, Biochemistry 50 (2011) 4491–4503.
[81] G.C. Brown, Eur. J. Biochem. 232 (1995) 188–191.
[82] B. Chance, J. Biol. Chem. 179 (1949) 1299–1309.
[83] D. Keilin, E.F. Hartree, Biochem. J. 39 (1945) 148–157.
[84] E. Margoliash, A. Novogrodsky, Biochem. J. 68 (1958) 468–475.
[85] R.F. Beers Jr., I.W. Sizer, Science 120 (1954) 32–33.
[86] Y. Du, G. Liu, Y. Yan, D. Huang, W. Luo, M. Martinkova, P. Man, T. Shimizu, BioMetals 26 (2013) 839–852, http://dx.doi.org/10.1007/s10534-013-9640-4.
[87] H. Shimahara, T. Yoshida, Y. Shibata, M. Shimizu, Y. Kyogoku, F. Sakiyama, T. Nakazawa, S. Tate, S.Y. Ohki, T. Kato, H. Moriyama, K. Kishida, Y. Tano, T. Ohkubo, Y. Kobayashi, J. Biol. Chem. 282 (2007) 9646–9656.
[88] S. Li, M. Hong, J. Am. Chem. Soc. 133 (2011) 1534–1544.

Free Radical Biology and Medicine 113 (2017) 551–563

Contents lists available at ScienceDirect

Free Radical Biology and Medicine

journal homepage: www.elsevier.com/locate/freeradbiomed

Mechanisms of myeloperoxidase catalyzed oxidation of H_2S by H_2O_2 or O_2 to produce potent protein Cys-polysulfide-inducing species

Dorottya Garai[a,1], Bessie B. Ríos-González[b,1], Paul G. Furtmüller[c], Jon M. Fukuto[d], Ming Xian[e], Juan López-Garriga[b], Christian Obinger[c], Péter Nagy[a,*]

[a] Department of Molecular Immunology and Toxicology, National Institute of Oncology, Ráth György utca 7-9, Budapest 1122, Hungary
[b] Department of Chemistry, University of Puerto Rico, Mayagüez Campus, P.O. Box 9019, Mayagüez, PR 00681-9019, United States
[c] Division of Biochemistry, Department of Chemistry, Vienna Institute of BioTechnology, BOKU-University of Natural Resources and Life Sciences, Muthgasse 18, A-1190 Vienna, Austria
[d] Department of Chemistry, Sonoma State University, Rohnert Park, CA 94928, United States
[e] Department of Chemistry, Washington State University, Pullman, WA 99164, United States

ARTICLE INFO

Keywords:
Myeloperoxidase
Hydrogen sulfide
Sulfane sulfur species
Persulfidation
Sulfhydration
Redox signaling
Lactoperoxidase

ABSTRACT

The interaction of heme proteins with hydrogen sulfide is gaining attention as an important element in sulfide-mediated protection against oxidative stress and in regulation of redox signaling. In our previous study we reported the efficient reversible inhibition of myeloperoxidase (MPO) activity by sulfide and the kinetics of the reactions of sulfide with ferric MPO, Compound I and Compound II. Here we provide several lines of evidence that a central intermediate species in the turnover of MPO by sulfide is the Compound III state. Compound III is formed in the reactions of sulfide with ferric or ferrous MPO in the presence of oxygen or via the reductions of Compound I or Compound II by sulfide. The regeneration of active ferric MPO from Compound III is slow - representing the rate-limiting step during turnover - but facilitated by ascorbate or superoxide dismutase. These catalytic cycles produce inorganic sulfane sulfur species, which were shown to promote protein Cys persulfidation. Based on compiling experimental data we propose that in contrast to hemoglobin, myoglobin, catalase or lactoperoxidase the formation of a sulfheme derivative in the oxidative interactions of sulfide with MPO is not a major pathway. Using the Met243Val mutant we demonstrated that the sulfonium ion linkage of the Met243 sulfur to the heme pyrrole ring A, which is a unique feature of MPO, is pivotal in the catalytic oxidation of sulfide via Compound III. The proposed novel MPO-catalyzed sulfide oxidation model does not require the initial presence of hydrogen peroxide, only oxygen to provide a slow flux of sulfane sulfur species generation, which could be important in sulfide-mediated endogenous signaling. Furthermore, peroxide-induced formation of sulfane sulfur species by MPO may have a role in protection of regulatory or functional Cys residues during (for example neutrophil induced) inflammatory oxidative stress.

1. Introduction

The diverse biological actions of the small signaling molecule hydrogen sulfide[2] have triggered increasing attention in the last two decades on evolutionary, physiological as well as pathophysiological grounds [1–5]. An important element of the underlying molecular mechanisms of the biological actions of sulfide is its interactions with heme proteins [6]. For example, the oxidative stress alleviating effects of sulfide were associated with i) inhibition of ROS producing heme protein functions (e.g. myeloperoxidase [7]) or ii) with reduction of highly oxidizing heme protein redox intermediate species [6,7]. In addition, it is becoming increasingly appreciated that a number of

Abbreviations: 3MST, 3-Mercaptopyruvate sulfurtransferase; ABTS, 2,2'-azino-bis(3-ethylbenzothiazoline-6-sulphonic acid); BSA, bovine serum albumin; CBS, cystathione β-synthase; CHO, chinese hamster ovary; CSE, cystathione γ-lyase; DTNB, 5-5'-dithiobis(2-nitrobenzoic acid); DTT, dithiothreitol; EPR, electron paramagnetic resonance; HSA, human serum albumin; IAB, EZ-Link Iodoacetyl-PEG2- biotin; MPO, myeloperoxidase enzyme; NADPH, Nicotinamide adenine dinucleotide phosphate; PVDF, polyvinylidene fluoride; ROS, reactive oxigen species; SDS PAGE, sodium dodecyl sulfate polyacrylamide gel electrophoresis; SOD, superoxide dismutase; SSP4, 3',6'-Di(O-thiosalicyl)fluorescein or Sulfane Sulfur Probe 4; TCEP, Tris(2-carboxyethyl)phosphin; tRNA, transfer RNA; TTBS, tris-buffered saline and Tween 20 buffer; UV-vis, ultraviolet-visible; WT, wild type

* Corresponding author.
E-mail address: peter.nagy@oncol.hu (P. Nagy).

[1] These authors contributed equally to this study.

[2] From now on we will use the term sulfide to refer to the sum of its different protonated forms that exist in solution, i.e. H_2S, HS^- and S^{2-}.

http://dx.doi.org/10.1016/j.freeradbiomed.2017.10.384
Received 20 June 2017; Received in revised form 12 October 2017; Accepted 26 October 2017
Available online 31 October 2017
0891-5849/

important biological actions of sulfide are apparently due to sulfide-derived oxidation products, which contain zero-valent sulfur (often referred to as sulfane sulfur species[3]) including inorganic polysulfide and protein per/polysulfide species [6,8–11]. Consistent with the idea that poly sulfur species are biologically relevant and important signaling/effector species, sulfide exists at relatively low endogenous concentrations [12], while intracellular Cys per- and polysulfides were recently demonstrated to be highly abundant (including low molecular weight [13] and protein persulfides [14]). Protein persulfides can be generated post translationally via the reactions of sulfide with oxidized Cys residues (such as disulfides [15,16] or sulfenic acids [17]), oxidation of protein thiols by inorganic sulfane sulfur species [18,19] or enzymatically without the direct involvement of H_2S by 3-mercaptopyruvate sulfurtransferase (3MST) [20], cystathione β-synthase (CBS) [13] or cystathione γ-lyase (CSE) [21]. Furthermore, we recently demonstrated that protein Cys persulfides can be produced translationally by generating and incorporating Cys-SSH into nascent polypeptides by cysteinyl tRNA synthetase [22]. Protein persulfide speciation is highly regulated by selective and specific NADPH driven reduction mechanisms orchestrated by the thioredoxin and glutathione systems [14]. These recent mechanistic insights gave credence to the previous proposal [6,8,11] that persulfide formation on regulatory or functional protein Cys residues is an important element of sulfide signaling.

In this contribution we found a link between post-translational oxidative generation of protein persulfides and the interactions of sulfide with the heme enzyme human myeloperoxidase (MPO).

Based on a thorough kinetic study we previously reported efficient reversible inhibition of MPO peroxidase activity by sulfide and demonstrated that sulfide can also serve as a substrate for MPO in the presence of added H_2O_2 [7]. In that report we provided evidence for efficient interactions between different MPO enzyme forms and sulfide including coordination of sulfide to ferric MPO, reduction of ferric MPO by excess sulfide to ferrous MPO or fast oxidation of sulfide in its reactions with MPO Compound I and Compound II. Based on our pre-steady-state and steady-state enzyme kinetic studies we proposed a mechanism to explain both the turnover of MPO with sulfide using H_2O_2 and the reversible inhibition of MPO peroxidase activity in the presence of sulfide.

In this work we aimed at providing further insights into the reactions of MPO with sulfide by 1) investigating sulfide oxidation products and 2) further characterizing MPO intermediate species that form during turnover. We demonstrate that MPO can catalytically produce sulfane sulfur species even in the absence of added H_2O_2 by utilizing oxygen in a concerted action with superoxide dismutase (SOD) or ascorbate via the involvement of its Compound III (ferric-superoxide/ferrous-dioxygen complex) state. These MPO-induced sulfane sulfur species can oxidize protein Cys residues to their corresponding per/polysulfide derivatives. Therefore, we propose that this novel mechanism could play an important role in sulfur biology by providing a slow flux of sulfane sulfur production via MPO catalyzed sulfide oxidation by oxygen that can lead - among other biological actions - to protein persulfidation.

On the other hand, activated neutrophils excrete large amounts of H_2O_2 and MPO at sites of inflammation, which were associated with a number of inflammatory diseases via the production of promiscuous hypohalous acids and radical species [23,24]. Interestingly, sulfide was found to be protective in a number of these pathologies (see Ref. [7] for more info). We propose that this can potentially be due to inhibiting MPO-mediated oxidant production and/or due to sulfane sulfur production (via MPO catalyzed sulfide oxidation by neutrofil-produced H_2O_2). The latter can induce temporary per/polysulfidation on functional and/or regulatory protein Cys to protect these oxidant sensitive residues from irreversible excessive oxidation [9].

[3] "Sulfane sulfur species" is used herein as a collective term for oxidized sulfide derivatives, which, contain sulfur(s) at the zero valent oxidation state. Hence, sulfane sulfur, as we view it, regarding its oxidation state is equivalent to sulfur atom (a sulfur, containing 6 valence electrons).

2. Materials and methods

2.1. Materials

All reagents were purchased from Sigma-Aldrich unless otherwise indicated. Sulfide stock solutions were prepared as described previously [12]. Briefly, $Na_2S \times 9H_2O$ crystals were thoroughly washed and dissolved in ultrapure water. To determine the concentration of the stock solution, appropriate dilutions were made and their absorbances were measured at 230 nm ($\varepsilon_{230} = 7700\ M^{-1}\ cm^{-1}$). The purity of the solution was checked by measuring the absorbance at 412 nm after the addition of 5-5'-dithiobis(2-nitrobenzoic acid) (DTNB) ($\varepsilon_{412} = 14{,}100\ M^{-1}\ cm^{-1}$) (for details see Ref. [16]). Stock solutions were stored on ice in tightly closed and covered plastic containers to avoid oxidation and working solutions were prepared right before use by dilution with the appropriate assay buffer. Experiments were carried out in 100 mM (KH_2PO_4/K_2HPO_4) phosphate buffer at pH 7.4 unless otherwise specified.

Human leukocyte myeloperoxidase enzyme with a purity index ($A_{428\ nm}/A_{280\ nm}$) of at least 0.85 was purchased from Planta Natural Products (http://www.planta.at) The concentration of MPO, hydrogen peroxide (at pH 7.4) and hypochlorite (at pH 12) were determined spectrophotometrically using extinction coefficients of $\varepsilon_{428} = 91{,}000\ M^{-1}\ cm^{-1}$ per heme, $\varepsilon_{240} = 43.6\ M^{-1}\ cm^{-1}$ and $\varepsilon_{292} = 350\ M^{-1}\ cm^{-1}$, respectively.

2.2. Production of the Met243Val MPO mutant

Transfection, selection, CHO cell culture procedures, and protein purification protocols were described previously [25,26]. The Met243Val mutant had a purity index (A_{412}/A_{280}) of about 0.7 and the concentration was determined by using an extinction coefficient (ε) of $84{,}000\ M^{-1}\ cm^{-1}$ at 412 nm [27].

2.3. UV-vis measurements

The interactions of H_2S with ferrous MPO and with ferric MPO under anaerobic conditions were measured with an Agilent 8453 spectrophotometer using sealed quartz cuvettes with septum (1 cm path length). Reagents were added in 1 μL aliquots to the samples (in the cuvette) using gastight syringes. All measurements were performed at 25 °C and pH 7.0 in 0.1 M KH_2PO_4/Na_2HPO_4 buffer. Ferric MPO, buffer, $Na_2S \times 9H_2O$, sodium dithionite ($Na_2S_2O_4$), and protein solutions were prepared anaerobically by degassing for 30 min and flushing the headspace with nitrogen for at least 20 min. To investigate the interaction of ferric MPO with H_2S, 115 μM of H_2S was added to 2.5 μM of ferric MPO. Following a 36 min incubation time, samples were purged with O_2 for 30 s. For the ferrous MPO experiments, to accomplish the reduction of 2.7 μM MPO a fivefold excess of sodium dithionite was used from a freshly prepared anaerobic stock solution. When the reduction was complete, 115 μM of H_2S was added to start the reactions. Pure O_2 was introduced by purging the solutions for 30 s. All reactions were followed by monitoring the absorbance changes in the Soret band and in the visible region of MPO, collecting time resolved polychromatic data from 300 to 800 nm.

Spectral changes upon the addition of sulfide and SOD (from bovine erythrocytes) to ferric MPO derivatives were measured on a Zeiss Specord S10 photometer. In a typical experiment 2 μM MPO was mixed with 500 μM sulfide and after 500 s 3 μM SOD was added.

Sulfide-mediated reversible and irreversible inhibition of MPO and of the MPO Met243Val mutant, respectively was investigated by measuring the peroxidase activity using 2,2'-azino-bis(3-ethylbenzothiazoline-6-

sulphonic acid) (ABTS). In a typical experiment 2 μM MPO or 2 μM Met243Val mutant were incubated with or without 100 μM sulfide for 10 min and then the peroxidase activity was determined with 1 mM ABTS by measuring absorbance changes at 414 nm ($\varepsilon_{414\,nm}$ = 3.11 × $10^4\ M^{-1}\ cm^{-1}$). Conditions: 50 mM phosphate buffer pH 7.0 at 25 °C. The reaction was started by the addition of 100 μM hydrogen peroxide. In a similar experiment 2 μM MPO or Met243Val mutant were incubated with or without 100 μM hydrogen sulfide for 10 min. Then the samples were diluted 33 fold and the peroxidase activity was measured as described before.

2.4. Stopped-flow spectrophotometry

The stopped-flow apparatus (model SX-18MV) equipped for both conventional and sequential stopped-flow measurements was from Applied Photophysics (UK). A 20 μL optical observation cell with 10 mm light path length was used and the dead time of the instrument was 1.2 ms. All measurements were performed at 25 °C and pH 7.0 in 100 mM phosphate buffer, using a diode-array detector (Applied Photophysics PD.1). At least three determinations were performed for each sample.

Sulfide binding was measured in the conventional stopped-flow mode. In a typical sulfide binding experiment, one syringe contained 2 μM MPO (200 mM phosphate buffer, pH 7.0), and the second syringe contained 250 μM sulfide. The formation of the species absorbing at 625 nm was monitored using a diode array detector over 100 s. Cyanide binding to the 625 nm species was measured with the sequential stopped-flow method. (The formation of the 625 nm species was followed on the diode array detector over 100 s.)4 μM MPO in 200 mM phosphate buffer, pH 7.0 was incubated with or without 250 μM sulfide in the aging loop for 100 s and then mixed with various concentrations of cyanide.

The reaction of the 625 nm species with ascorbic acid was measured by mixing 2 μM MPO with 500 μM sulfide by hand and after a delay time of 10 min the formed 625 nm species was mixed with different concentration of ascorbic acid in conventional stopped-flow mode. Final concentrations: 1 μM MPO, 250 μM (or 25 mM in the experiment of Fig. 8) sulfide 40 μM − 5 mM ascorbic acid, 100 mM phosphate buffer, pH 7.0.

Because of the inherent instability of Compound I, the sequential stopped-flow (multi-mixing) technique was used to follow the reaction of Compound I with hydralazine. Typically, MPO (4 μM) was premixed with 40 μM H_2O_2 and incubated in the aging loop for 20 ms before the subsequent mixing with 200 μM hydralazine solutions in the second mixing cycle.

Polychromatic data were analyzed with Pro-Kineticist from Applied Photophysics (UK). The program simultaneously fits the kinetic traces at all wavelengths to the proposed reaction mechanism and simulates the spectra of all reactant, product and intermediate species as well as their time dependent distribution on the reaction coordinate.

2.5. Production of sulfane sulfur species by MPO

Hydrogen sulfide stock solutions were prepared as described above. The 3',6'-Di(O-thiosalicyl)fluorescein (Sulfane Sulfur Probe 4 or SSP4) fluorescent dye (Dojindo) that is specific to sulfane sulfur containing sulfide oxidation products was dissolved in dimethyl sulfoxide and used at a final concentration of 500 μM (for a schematic of sulfane sulfur detection by SSP4 see Scheme S1). Production of sulfane sulfur species by 100 nM MPO in the presence or absence of added H_2O_2 was determined by spectrofluorimety in flat bottom, black plates using an Optima Star fluorescent plate reader at the emission and excitation wavelengths of 485 nm and 515 nm, respectively. Fluorescence intensity values of the samples were measured every 45 s for 30 min.

The data in Table 1 was collected by adding 2.5 mM hydrogen sulfide and different concentrations of H_2O_2 (5–50 μM) to 100 nM MPO. Appropriate controls to test the interference of MPO, H_2O_2 and the SSP4 fluorescent probe were measured simultaneously with the samples.

Table 1
Production of sulfane sulfur species in the MPO catalyzed oxidation of sulfide by H_2O_2 ~40–70% of the added hydrogen peroxide is converted to the formation of sulfane sulfur species at different peroxide concentrations. Conditions: 100 nM MPO was mixed with 2.5 mM hydrogen sulfide, different concentrations of hydrogen peroxide (5–50 μM) and 500 μM SSP4. The production of sulfane sulfur species were measured by spectrofluorimetry after 30 min incubation based on a calibration curve that was developed using measured amounts of sulfane sulfur equivalents in inorganic polysulfides that were prepared by the reaction of sulfide with Gly-Cl at an excess of sulfide. Sulfane sulfur species concentrations and their errors represent the average and standard deviations of 3 independent experiments.

Hydrogen sulfide (H_2S)	Hydrogen peroxide (H_2O_2)	Sulfane sulfur species (HS_X)	HS_X/H_2O_2 (%)
2.5 mM	50 μM	17.4 ± 0.9 μM	34.8 ± 1.8
2.5 mM	25 μM	10.4 ± 0.4 μM	41.4 ± 1.7
2.5 mM	10 μM	4.6 ± 0.4 μM	45.5 ± 4.1
2.5 mM	5 μM	3.4 ± 0.2 μM	68.6 ± 4.8

Sulfane sulfur measurements by SOD mediated turnover of MPO in the presence of sulfide was investigated using 100 nM MPO, 3 μM SOD and different concentrations of sulfide (0.5–5 mM). Sulfide oxidation in the presence of SOD and absence of MPO was also determined in order to subtract non-MPO catalyzed sulfane sulfur production from the kinetic curves.

Sulfane sulfur measurements in the presence of different concentrations of ascorbic acid (1–10 mM) to reduce the Compound III state of 100 nM MPO was carried out as described for SOD using 2.5 mM H_2S. For semi-quantitative analysis of sulfane sulfur production using SSP4 a calibration curve was developed for each experiment using known concentrations of inorganic polysulfides. Stock polysulfide solutions were made by mixing sulfide (5 mM) and glycine chloramine (500 μM). A polysulfide dilution series (1–50 μM) then were mixed with the fluorescent probe and incubated for 30 min before measurement. Results were evaluated using Mars Data Analysis Software.

2.6. Measurement of sulfide consumption in the MPO-catalyzed oxidation of sulfide by H_2O_2

$FeCl_3$ and N, N-dimethyl-p-phenylenediamine sulfate (DPD) were dissolved in 1.2 M and 7.2 M HCl, respectively, and zinc-acetate solutions were made using distilled water. MPO (100 nM) was mixed with hydrogen sulfide (20 μM) in 10 mM degassed (by bubbling with nitrogen for 30 min) phosphate buffer KH_2PO_4/K_2HPO_4), pH 7.4, at 25 °C and reactions were started by adding 10 μM hydrogen peroxide. The control sample contained sulfide with peroxide at similar concentrations. 100 μL aliquots of the samples were taken from the reaction solutions repeatedly for 5 min and mixed with 50 μL of zinc-acetate (54.5 mM) to precipitate the sulfide content. After thorough mixing with zinc-acetate, 26.6 μL of DPD (31 mM) and 26.6 μL of $FeCl_3$ (18 mM) were added to the samples and the solutions were incubated for an additional 15 min in the dark. The concentrations of the generated methylene blue were determined spectrophotometrically by measuring the absorbance at 670 nm. Calibration curves were developed by a serial dilution (5–40 μM) of sulfide standard solutions under similar conditions using the same procedure [12].

2.7. Persulfidation of purified human serum albumin (HSA) by MPO catalyzed sulfide oxidation products in the absence of added H_2O_2

Lyophilised powder of human serum albumin (HSA) was dissolved in 100 mM phosphate buffer, pH 7.4, and protein concentration was determined using a BCA protein assay (Biorad). Pre-reduction of the Cys34 of HSA (10 mg/mL) was carried out by incubation with

dithiothreitol (DTT) for 30 min on ice. The reducing agent was then removed using desalting spin columns (Thermo Zeba Spin). Persulfidating sulfide oxidation products were produced by mixing MPO (100 nM), hydrogen sulfide (2 mM) and SOD (3 μM) or ascorbic acid (10 mM) under aerobic conditions. After 10 min of incubation the reaction mixtures (100 μL) were added to HSA (20 μL) and carefully mixed. After 1 min inorganic sulfide oxidation products were separated from HSA-solutions using desalting columns.

2.8. Persulfidation of human blood plasma by sulfide oxidation products produced by MPO in the absence of added H_2O_2

Blood samples from healthy donors were collected into sterile tubes containing lithium heparin. (The procedure was approved by the Hungarian National Ethics Committee under file number BPR-021/00084-2/2014.) The plasma was separated from the cell components by centrifugation (1500 × *g*) and total protein concentration was measured using BCA protein assay (Biorad). Plasma samples were diluted with phosphate buffer, pH = 7.4, to a final total protein concentration of 10 mg/mL. Sulfide oxidation products were produced by MPO as described previously without adding hydrogen peroxide. 100 μL of reaction mixture containing the sulfide oxidation products was added to 20 μL of diluted plasma (final total protein concentration of 1.67 mg/mL) and mixed carefully (for ~10 s). After mixing, persulfidating agents were eliminated from the plasma using desalting columns.

2.9. Detection of human serum albumin persulfidation

Inorganic polysulfide induced HSA per/polysulfidation in purified protein and plasma samples was detected using the ProPerDP method, as described earlier [14]. Briefly, treated protein samples were alkylated with 1 mM EZ-Link Iodoacetyl-PEG2- biotin (IAB) for 1 h in the dark at room temperature. The alkylating agents were removed by careful desalting with Thermo Zeba Desalting Spin Columns followed by 3 concentration-dilution steps using Amicon Ultraconcentrators (Merck) with a concomitant buffer exchange from 100 mM phosphate to 100 mM Tris–HCl buffer pH 7.4 containing 100 μM diethylenetriaminepentaacetic acid (DTPA). Affinity pull-down of 300 μg total protein was carried out using streptavidin coated magnetic beads. The beads were thoroughly washed with tris-buffered saline and Tween 20 buffer (TTBS) and then resuspended in 5 mM Tris(2-carboxyethyl) phosphin (TCEP). The supernatant of this reduction step is the per/polysulfidated protein fraction (S3), which was submitted to SDS-PAGE and Western blot analyses.

2.10. Western blotting conditions

Persulfide fractions of 500 ng total protein was subjected to 12% SDS-PAGE after a 10-fold dilution with loading buffer and then transferred to a PVDF membrane. The membranes were blocked overnight in 3% (w/v) bovine serum albumin (BSA) dissolved in TTBS at 4 °C and incubated with polyclonal anti-HSA antibody produced in rabbit (Sigma-Aldrich), diluted 1:10,000 in 3% BSA solution. After 30 min washing with TTBS buffer, the membranes were subjected to an appropriate secondary antibody, anti-Rabbit IgG conjugated with (whole molecule-alkaline phosphatase produced in goat, diluted 1:10,000 in 3% BSA solution. The signal was developed using ready-to-use BCIP/NBT substrate solution (Merck).

3. Results

3.1. Distinct reactions of ferric MPO with sulfide under aerobic and anaerobic conditions

As we have shown previously [7] ferric MPO reacts with sulfide to first give a low spin MPO-Fe(III)-H_2S complex. In a subsequent reaction

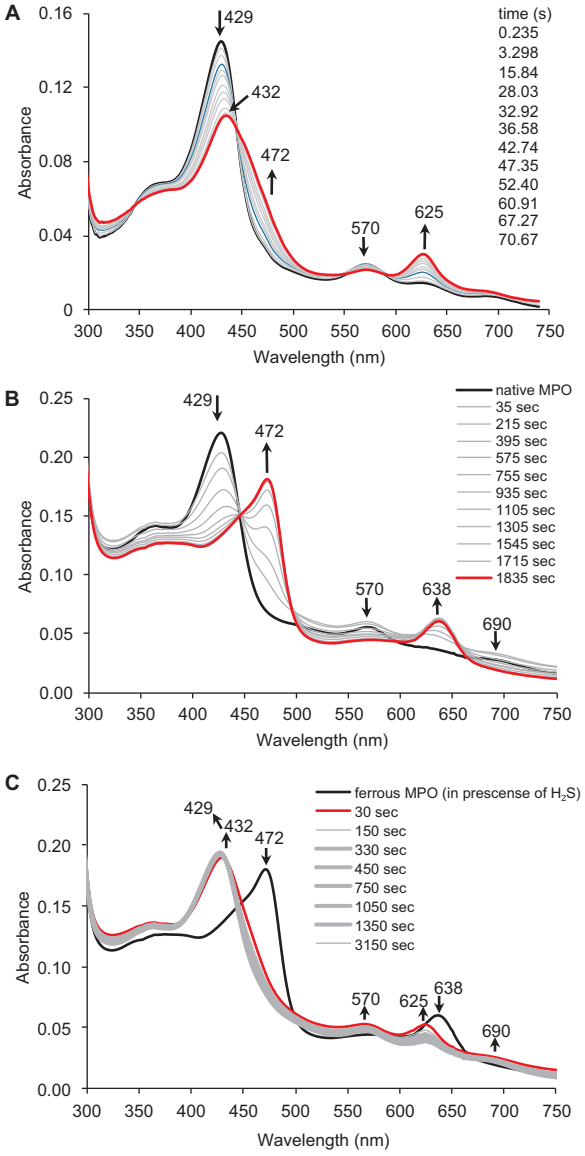

Fig. 1. Interactions of H_2S with native MPO. (A) Spectral changes for the reactions of 2 μM native MPO (black line) with 125 μM H_2S under aerobic conditions in phosphate buffer, pH 7.0. Blue spectrum shows the MPO-Fe(III)-H_2S complex and the red spectrum represent the final product mixture. (B) Spectral changes for the reactions of 2.5 μM native MPO (black line) with 115 μM H_2S under anaerobic conditions in phosphate buffer, pH 7.0. Red spectrum shows the formation of ferrous MPO at 1835 s. (C) Spectral changes upon the addition of O_2 to the reaction mixture after completion of the reactions that are shown on B. Red spectrum shows the addition of O_2 (at 30 s) to the ferric MPO-sulfide mixture (black line). The subsequent spectra were recorded at 150 s, 330 s, 450 s, 750 s, 1050 s, 1350 s and 3150 s. Arrows indicate direction of the spectral changes. Measurements were carried out by a diode array UV-vis spectrophotometer (For interpretation of the references to color in this figure legend, the leader is referred to the web version of this article.).

the Fe(III) center is reduced to give electron paramagnetic resonance (EPR) silent Fe(II) derivatives. However, these derivatives were not characterized in detail. Under aerobic conditions the product(s) exhibit characteristic spectroscopic features with a distinct band at 625 nm and a shoulder at ~472 nm (Fig. 1A). On the contrary, a more thorough investigation of this system revealed that when ferric MPO was reacted with sulfide under strictly anaerobic conditions, distinct peak maxima were observed in the visible range at 638 and 472 nm (Fig. 1B), resembling more to the spectrophotometric signatures of ferrous MPO [28,29]. Under the applied experimental conditions the formation of the new 638 and 472 nm bands occurred in approximately thirty

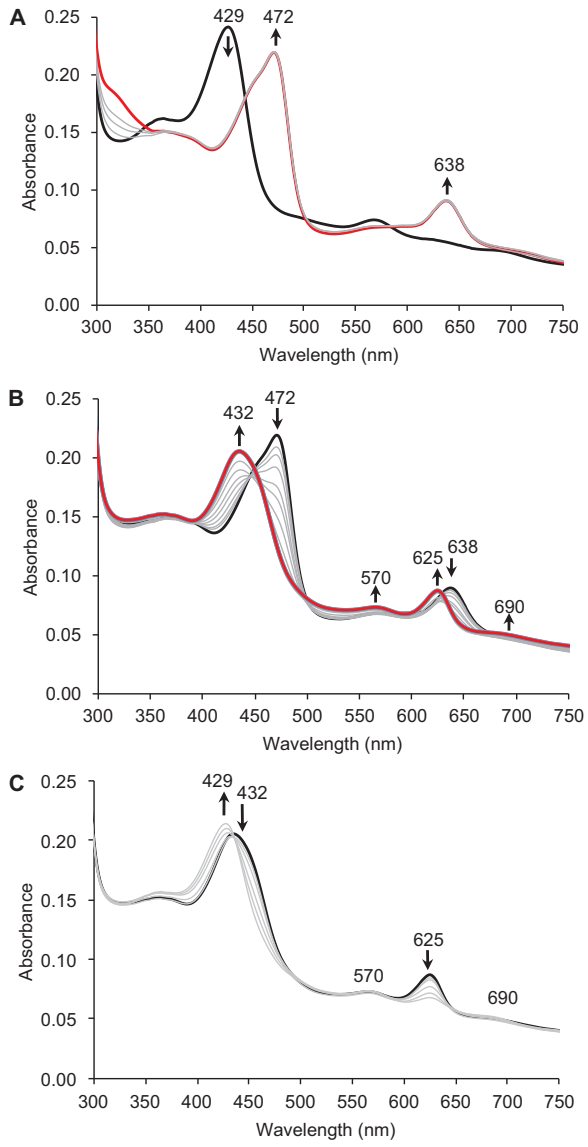

Fig. 2. Interaction of ferrous MPO with H_2S under anaerobic conditions and subsequent addition of O_2. (A) Ferrous MPO was formed upon the addition of a fivefold excess of $Na_2S_2O_4$ (red line) to 2.7 μM native MPO (black line) in phosphate buffer, pH 7.0. Subsequent addition of 115 μM H_2S did not result in substantial spectral changes in a 24 min timescale. (B) Introducing O_2 to the sample that was generated in A (black line) caused a shift in the visible band from 638 nm to 625 nm and a Soret shift from 472 nm to 432 nm. The spectra were recorded at 10 s, 12 s, 14 s, 15 s, 16 s, 20 s, 25 s, 30 s, 31 s and 32 s (red line). (C) Time resolved spectra demonstrate the slow return of MPO to its native ferric state after the interaction of O_2 with ferrous MPO in the presence of H_2S (sample in B; black line). The spectra were taken at 32 s, 40 s, 78 s, 210 s, 240 s and 630 s. Arrows indicate direction of the spectral changes. Measurements were carried out by a diode array UV-vis spectrophotometer (For interpretation of the references to color in this figure legend, the reader is referred to the web version of this article.).

minutes. Subsequent addition of O_2 showed a clear shift from 638 to 625 nm (Fig. 1C) and final spectra similar to that on Fig. 1A (i.e. when the whole reaction was carried out under aerobic conditions). Through time the 625 nm band decayed and the protein slowly returned to the native state (Fig. 1C). These results indicate the need of molecular oxygen to form the MPO redox state that exhibits an absorption maximum at 625 nm (from now on this enzyme form will be called "the 625 nm species").

3.2. Reactions of ferrous MPO with sulfide under anaerobic conditions and subsequent reaction with oxygen

Ferrous MPO was formed by the reduction of ferric MPO with a fivefold excess of $Na_2S_2O_4$. Fig. 2A shows the spectrum of ferrous MPO with a Soret band at 472 nm and two additional bands at 570 nm and 638 nm. Absorbance at 315 nm is due to $Na_2S_2O_4$. No spectral changes were observed upon the addition of 115 μM H_2S (for up to 24 min), with the exception of a decrease at 315 nm, which is due to the consumption of O_2 by $Na_2S_2O_4$ (Fig. 2A), where O_2 (in small amounts) was introduced to the reaction mixture upon the addition of H_2S. Subsequent purging with O_2 (Fig. 2B) of the sample causes an immediate formation of the MPO state that exhibits absorbance maxima at 432 nm and 625 nm. At longer incubation times the 625 nm band decreased in intensity and the distinctive bands of ferric MPO appeared (429 nm, 570 nm, and 690 nm) suggesting a slow turnover of the enzyme until the exhaustion O_2 or H_2S (Figs. 1C and 2C).

3.3. Sulfheme or Compound III

A band around 620 nm for hemoglobin or myoglobin in the presence of sulfide is characteristic of sulfheme formation [30]. In these sulfheme derivatives sulfur is incorporated into the pyrrole B ring of the porphyrin to form a thiochlorin like heterocyclic structure as the most stable isomer (Fig. 3) [31,32]. On the other hand, for MPO the 625 nm band is characteristic to Compound III formation. Compound III is a resonance form of the Fe(II)-dioxygen complex, where the electrons are shifted towards oxygen to give a ferric-superoxide-complex like species [29,33].

$$\text{MPO-Fe(II)—O}_2 \leftrightarrow \text{MPO-Fe(III)—O}_2^{\bullet-} \quad (1)$$

Compound III can be generated by the reactions of 1) ferric MPO with superoxide, 2) Compound II with excess peroxide or 3) ferrous MPO with oxygen [29,33,34]. This enzyme form is often produced during the turnover of various peroxidase inhibitors. For example when hydralazine is used as a classical MPO substrate, it reacts with Compound I and Compound II in one-electron reactions thereby generating hydralazine radicals. Hydralazine radicals can activate oxygen and the resulting superoxide can react with ferric MPO to produce Compound III. Alternatively, hydralazine radicals can reduce ferric MPO to its ferrous state, which can capture dioxygen to give Compound III (Fig. 4A). [35]

The UV-vis spectra (see Fig. 1A) that were recorded upon the reaction of sulfide with ferric MPO (or the reaction of sulfide with Compound I and/or Compound II, see Ref. [7]) under aerobic conditions were similar to the spectra that was obtained in the reactions of MPO with hydralazine in the absence of sulfide (see Fig. 4B) including the formation of the 625 nm band. This observation indicated that in

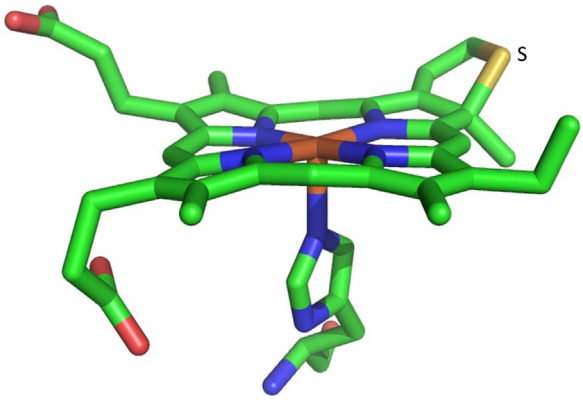

Fig. 3. Structure of a sulfheme prostetic group. Figure shows the heme group from the crystal structure of sulfhemoglobin using 1YMC from PDB.

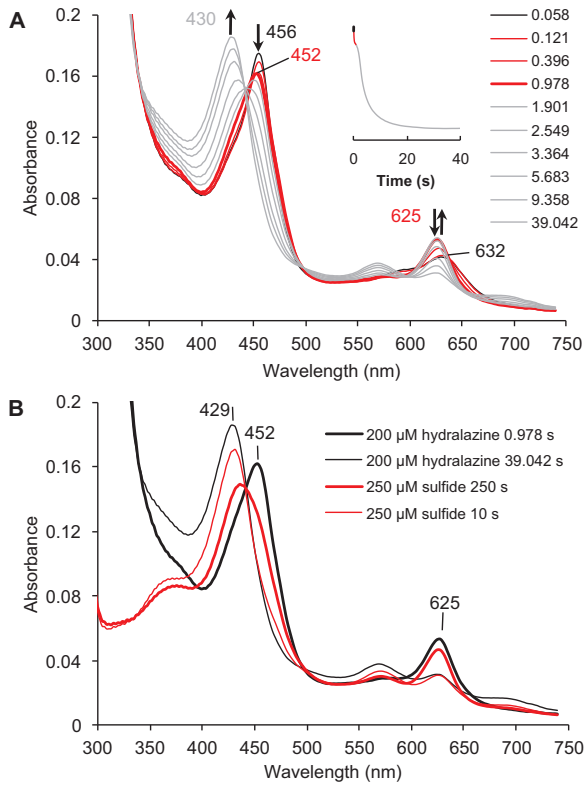

Fig. 4. Reaction of MPO Compound I with 200 µM hydralazine. (A) Black spectrum corresponds to Compound II; red spectra correspond to Compound III formation and gray spectra show the decay to ferric MPO. Red bold spectrum represents Compound III. Compound I was generated by the reaction of 4 µM ferric MPO with 40 µM H_2O_2 in the aging loop. After a delay time of 20 ms, Compound I was reacted with 200 µM hydralazine. Final concentrations: 2 µM MPO, 20 µM hydrogen peroxide and 200 µM hydralazine in 100 mM phosphate buffer pH 7.0. (B) Overlay of spectra obtained in the reaction of MPO with hydralazine (black lines) or with sulfide (red lines). Conditions are the same as in Fig. 1A (sulfide) and in A (hydralazine). Measurements were carried out by stopped-flow spectrophotometry (For interpretation of the references to color in this figure legend, the reader is referred to the web version of this article.).

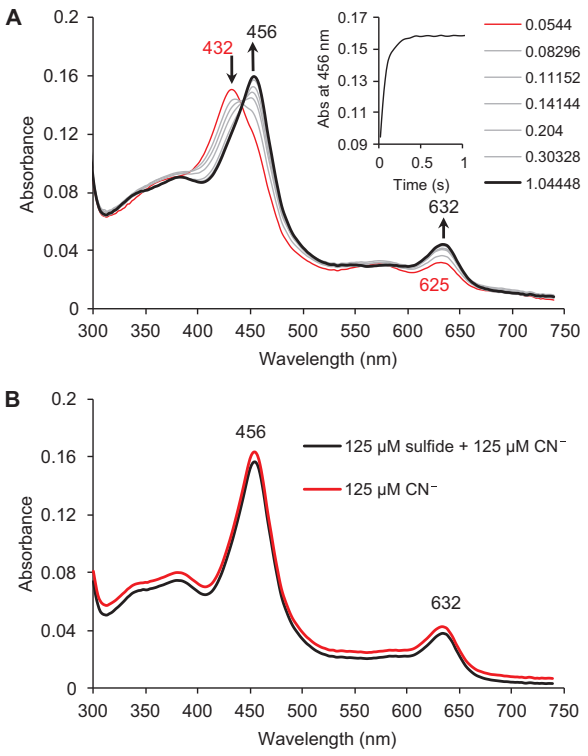

Fig. 5. Reaction of the aerobic MPO-sulfide product mixture with cyanide. (A) Spectral changes upon addition of 10 µM cyanide to an aerobic MPO-sulfide product mixture. (4 µM MPO was mixed with 250 µM sulfide in the aging loop for 100 s. In a subsequent mixing cycle the product mixture was reacted with 10 µM cyanide. Final concentrations: 2 µM MPO, 125 µM H_2S, 10 µM cyanide in 100 mM phosphate buffer pH 7.0. B) Overlay of the final spectrum (after 1.04448 s) from A (black line) with the spectrum of a ferric MPO-cyanide-complex, which was obtained in the absence of sulfide by mixing 2 µM MPO with 10 µM cyanide in 100 mM phosphate buffer pH 7.0 (red line). Measurements were carried out by stopped-flow spectrophotometry (For interpretation of the references to color in this figure legend, the reader is referred to the web version of this article.).

the case of MPO the formation of the enzyme form exhibiting the characteristic 625 nm absorption maximum can be generated in the absence of sulfide.

3.4. Reaction of the "625 species" with cyanide

Addition of cyanide to the aerobic product mixture of ferric MPO with sulfide (see Fig. 1A) resulted in a the formation of the MPO-Fe(III)-CN^--complex (Fig. 5A). The obtained spectra was identical to the spectrum of MPO-Fe(III)-CN^--complex that was generated upon the addition of cyanide to ferric MPO in the absence of sulfide (Fig. 5B)

This result is consistent with previous observations that the addition of cyanide to Compound III shifts the equilibrium of reaction 2 to the right resulting in superoxide release and ferric MPO, where the latter binds cyanide to give the MPO-Fe(III)-CN^--complex (reaction 3).

$$\text{MPO-Fe(III)—}O_2^{\bullet-} \rightleftharpoons \text{MPO –Fe(III)} + O_2^{\bullet-} \quad (2)$$

$$\text{MPO –Fe(III)} + CN^- \rightarrow \text{MPO –Fe(III)—}CN^- \quad (3)$$

Again this observation points towards the idea that the majority of the 625 nm species most likely represents Compound III. Although some reports suggest reversibility of sulfheme formation [36–40], such a rapid formation of the ferric-cyanide complex (see Fig. 5A inset) together with the previously observed full recovery of MPO peroxidase activity upon dilution-, oxidation- or evaporation-mediated loss of sulfide [7] argue against a major contribution of a sulfheme-like MPO derivative to the 625 nm absorbing species.

3.5. Reaction of the "625 nm species" with SOD

Marquez and Dunford reported that SOD is able to scavenge superoxide from Compound III, based on a faster decay of the 625 nm band when SOD was added to the reaction mixture (see Fig. 6 in Ref. [41]). Therefore, we added SOD to the reaction mixture of MPO with sulfide to see if the sulfide induced 625 nm species behaves the same way. The observed relatively fast decay of the 625 nm band (compared to samples without SOD) and concomitant absorbance increase at 429 nm is again consistent with Compound III representing the majority of the 625 nm absorbing species (Fig. 6A-C).

3.6. Reaction of the "625 nm species" with ascorbate

Compound III reacts with ascorbate to give ferric MPO [41]. Therefore, we investigated the kinetics of the reaction of the 625 nm absorbing species (that was generated in the reaction of ferric MPO with sulfide in the presence of oxygen) with increasing amounts of excess ascorbate over sulfide. Addition of ascorbate to the sulfide-MPO reaction mixture resulted in a fast decline of the 625 nm and 472 nm bands and an absorbance increase at 429 nm, with a final UV-vis spectrum indicative of ferric MPO formation (Fig. 7A). The exponential behavior of the obtained kinetic traces at both 625 nm and 429 nm (Figs. 7B and 7C, respectively) indicated first-order dependency of the rate on the concentration of the 625 species. Furthermore, the linear correlation of the obtained pseudo-first-order rate constants with the ascorbate concentration suggested first-order dependency of the rate law on the ascorbate concentration too (see insets of Figs. 7B and 7C).

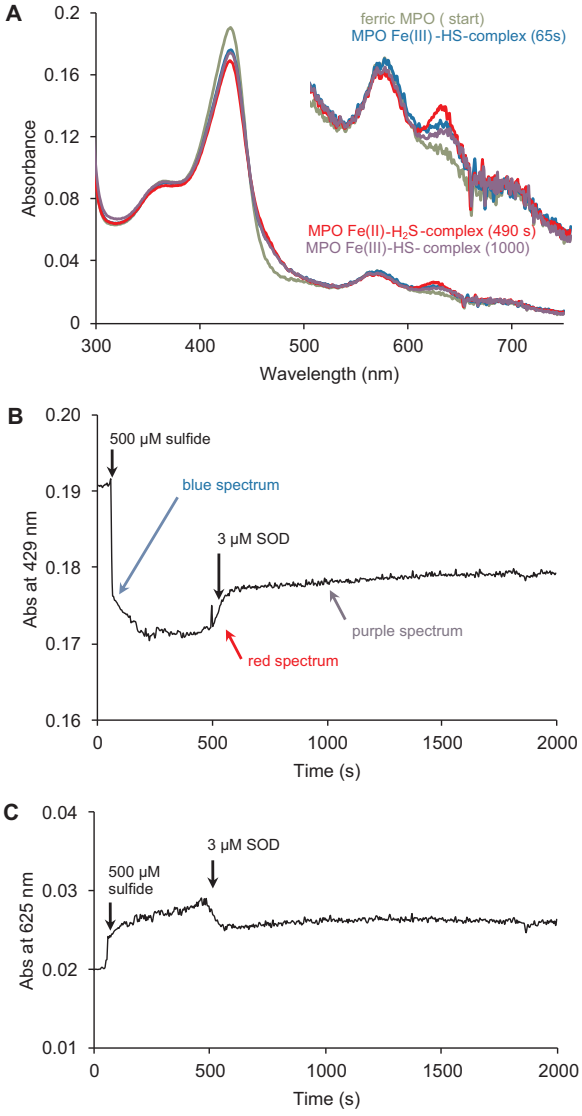

Fig. 6. Spectral changes upon consequtive addition of sulfide and SOD to ferric MPO. (A) Green spectrum was taken before adding sulfide to ferric MPO, blue spectrum was taken immediately after sulfide addition (65 s), red spectrum was taken before addition of SOD (490 s) and purple spectrum was taken at 1000 s. Conditions: 100 mM phosphate buffer pH 7.0, 2 µM MPO, addition of 500 µM sulfide after 60 s, addition of 3 µM SOD after 500 s. (B, C) Time traces at 429 nm and 625 nm. Black arrows indicate the addition of sulfide and SOD and the colored arrows indicate the time at which the spectra in A were taken. Measurements were carried out by a diode array UV-vis spectrophotometer (For interpretation of the references to color in this figure legend, the reader is referred to the web version of this article.).

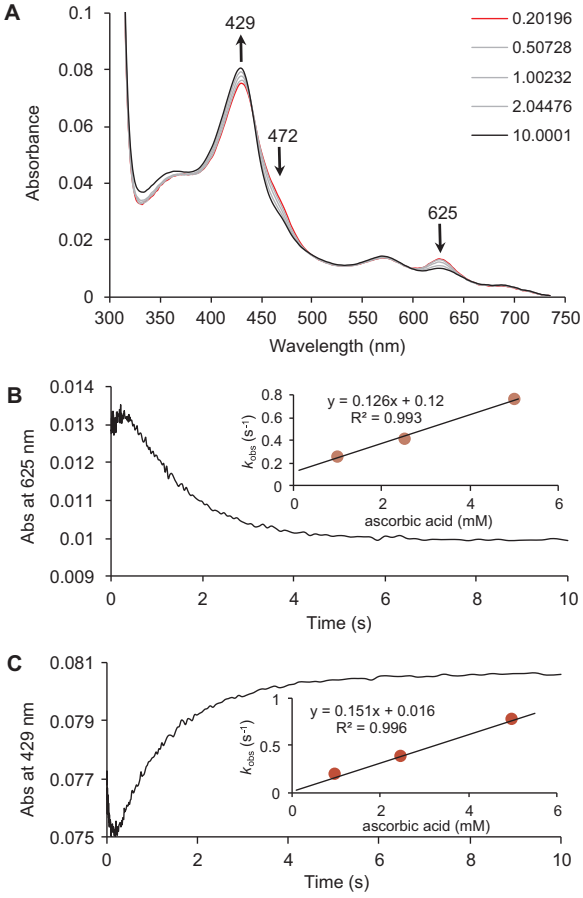

Fig. 7. Reaction of the aerobic MPO-sulfide product mixture with ascorbic acid. (A) Spectral transitions after adding 5 mM ascorbic acid to the aerobic MPO-sulfide product mixture. (B) Time trace at 625 nm; Inset shows the plot of k_{obs} determined at 625 nm as a function of the ascorbic acid concentration. (C) Time trace at 429 nm; Inset shows the plot of k_{obs} determined at 429 nm as a function of the ascorbic acid concentration. Final concentrations: 100 mM phosphate buffer pH 7.0, 1 µM MPO, 250 µM sulfide, 1, 2.5 and 5 mM ascorbic acid. Measurements were carried out by stopped-flow spectrophotometry (For interpretation of the references to color in this figure legend, the leader is referred to the web version of this article.).

The apparent second-order rate constant for the reaction at pH 7.0 was estimated from the slope of the line to be ~151 $M^{-1} s^{-1}$ (inset to Fig. 7C). This number is similar to the reported apparent second-order rate constant of 400 $M^{-1} s^{-1}$ [41] for the reaction of bovine MPO Compound III with ascorbate at pH 7.1, again consistent with the 625 species representing Compound III. The observed faster reaction (see the beginning of the kinetic traces on Figs. 7B and 7C) was also observed by Marquez and Dunford in the reaction of Compound III with ascorbate (see Fig. 8 in [41]). In their interpretation these initial fast phases were assigned to the reactions of residual Compound II (which is always present in Compound III preparations) with ascorbic acid. This is consistent with our model shown in Scheme 1, and explained by the following reaction sequence: 1) During the reaction of Compound III with ascorbic acid, hydrogen peroxide and ferric MPO is generated. 2) Hydrogen peroxide reacts rapidly with ferric MPO to give Compound I. 3) Compound I is rapidly consumed by sulfide to give Compound II. Compound II can either react with an additional sulfide to give ferrous MPO or with ascorbate as suggested by Marquez and Dunford. In light of these conclusions it is important to emphasize that the evaluation of the exponential parts of the obtained kinetic traces can only be considered semi-quantitative on strict kinetic grounds.

Polychromatic data that were collected at excess ascorbate over sulfide indicated the formation of ferric MPO at later time points. However, when sulfide was used in excess over ascorbate, the final spectrum indicated the partitioning of MPO in its Compound III and ferrous MPO-sulfide-complex states (Fig. 8). These results are consistent with the turnover of the system until the limiting substrate is exhausted.

3.7. Role of the MPO-typical sulfonium ion linkage in the catalytic oxidation of sulfide by MPO

In MPO there is a sulfonium ion linkage between the sulfur atom of Met243 and the β-carbon of the vinyl group on pyrrole ring A (see Fig. 12A). We hypothesized that this unique feature is associated with the unusual behavior of MPO among heme proteins to not form a sulfheme derivative in its oxidative interactions with sulfide, but rather serve as a catalyst of sulfide oxidation. In order to test this hypothesis we compared some of the reactions of the recombinant Met243Val mutant form of MPO with the wild type (WT) enzyme. Upon the

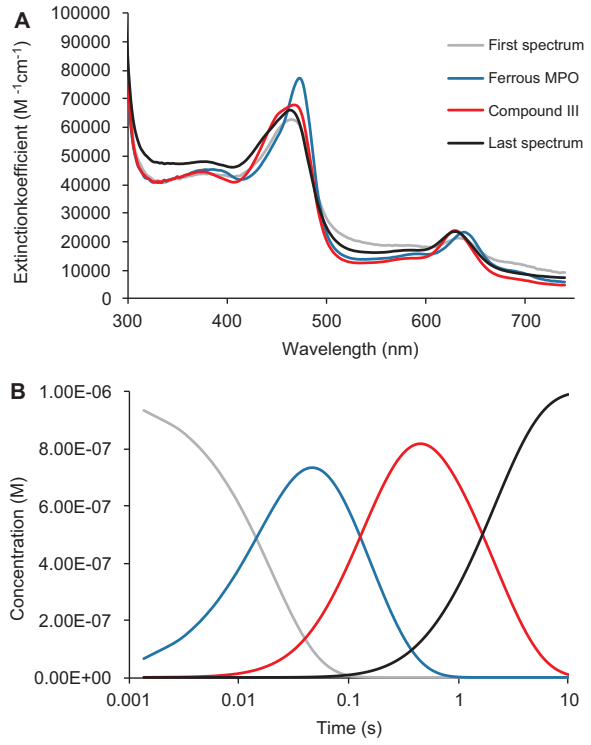

Fig. 8. Deconvoluted spectra of intermediate and product species for the reaction of Compound III with ascorbate at excess sulfide over ascorbate. (A) Spectra were obtained by singular value decomposition analyses of the polychromatic data that were collected for the reaction of Compound III with ascorbate at excess sulfide over ascorbate. Compound III was prepared by mixing 2 μM MPO with 25 mM sulfide under aerobic conditions. After a delay time of 10 min the reaction mixture was reacted with 20 μM ascorbic acid in the stopped-flow instrument. Conditions: 100 mM phosphate buffer pH 7.0, final MPO concentration was 1 μM. (B) Time dependent speciation of the enzyme forms for which the corresponding deconvoluted spectra are shown in (A) (For interpretation of the references to color in this figure legend, the leader is referred to the web version of this article.).

reaction of the Met243Val mutant with sulfide a delayed addition of SOD failed to induce the recovery/increase in the Soret band (Fig. 9A) that was observed in the case of the wild type enzyme (see Fig. 6B; note, that the soret band of the Met243Val mutant enzyme is different from the Soret band of the WT protein, 429 vs 413 nm, respectively). In contrast to WT MPO this observation speaks against the formation of a Compound III-like species in the reactions of the Met243Val mutant enzyme with sulfide.

The inhibition of the peroxidase activity of WT MPO by sulfide is fully reversible [7]. The complete inhibition of the peroxidase activity of MPO at 100 μM sulfide (Fig. 9B) can be reversed by a dilution step (Fig. 9C), representing reversible interactions between sulfide and the enzyme. In Fig. 9B-D we used the ABTS assay to follow the peroxidase activity of MPO, but it gave similar results for WT MPO to the previously published data using the TMB assay [7]. Notwithstanding, the peroxidase activity was completely and irreversibly inhibited by sulfide in the case of the Met243Val mutant (Fig. 9B&D). This observation strongly supports the hypothesis that the sulfonium ion linkage of Met243 to the heme has a major role in the sulfide oxidizing activity of MPO.

3.8. Products of MPO catalyzed oxidation of sulfide by H_2O_2 and by O_2

The slow decrease of a 20 μM initial sulfide concentration that was observed by the methylene blue assay [12] in solutions containing 10 μM H_2O_2 is consistent with the very slow oxidation of sulfide by H_2O_2 in the absence of any catalysis [42,43]. However, when 100 nM MPO was added to the H_2O_2-sulfide reaction mixture an immediate drop in the sulfide concentration indicated a rapid MPO-catalyzed reaction of sulfide with H_2O_2 (Fig. 10A). Using a sulfane sulfur specific fluorescent probe (SSP4 developed by Chen et al. [44]) we confirmed the production of sulfane sulfur species in the MPO-catalyzed oxidation of sulfide by H_2O_2 (Table 1). Semi-quantitative analyses of sulfane sulfur species formation in a H_2O_2 dependent manner suggested that a major portion (40–70%) of the oxidizing equivalents under the applied conditions were converted to sulfane sulfur containing product generation.

Sulfane sulfur product formation was also observed in the reaction of the 625 nm species (generated by the sulfide-mediated reduction of ferric MPO under aerobic conditions) with ascorbate or SOD in the absence of added peroxide (Figs. 10B and 10C). This is consistent with our previous proposal that MPO is turned over via the intermediate formation of Compound III in reactions with sulfide and oxygen facilitated by the presence of ascorbate or SOD. Notice that the initial rates of the fluorescence signal-intensity-increases on Figs. 10B and 10C (that is due to the reaction of sulfane sulfur products with SSP4) show a correlation with the ascorbate and sulfide concentrations, respectively.

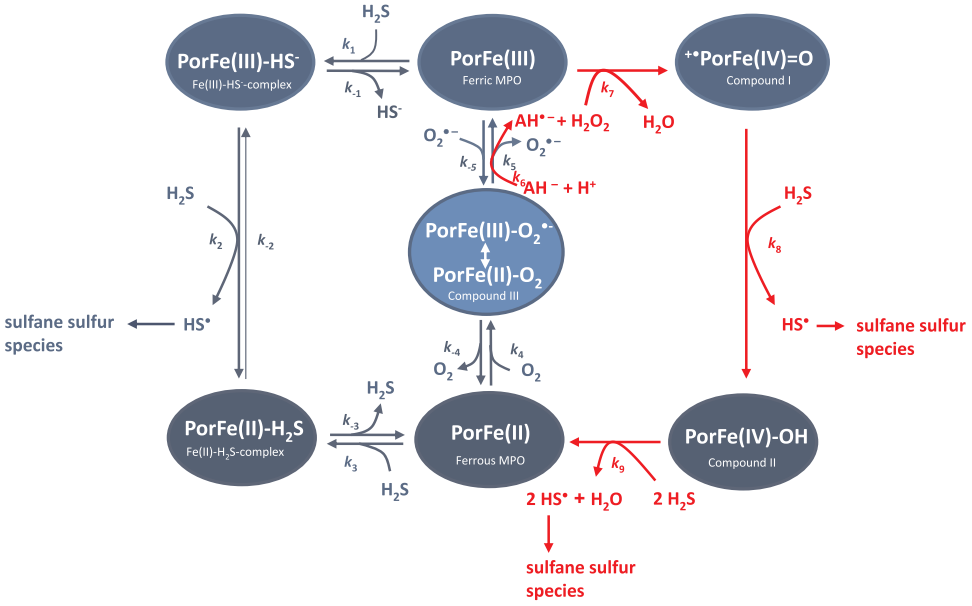

Scheme 1. Proposed model for the turnover of MPO by sulfide, aided by ascorbic acid or SOD in the absence of added H_2O_2. Sulfide efficiently reduce the Fe(III) center of native MPO. The generated Fe(II)-H_2S complex is in equilibrium with the "naked" ferrous MPO form; where the latter react with O_2 to give Compound III. Compound III is in equilibrium with the MPO-Fe(III)-superoxide complex (PorFe(III)-$O_2^{\bullet-}$). SOD can catalyze the dissociation of PorFe(III)-$O_2^{\bullet-}$ to restitute ferric MPO. Alternatively ascorbic acid (AH) can react with Compound III to give ferric MPO and H_2O_2. The generated H_2O_2 can turn MPO over via Compounds I and II by the oxidation of 2 additional molar equivalents of sulfide (or AH depending on the concentration conditions) (For interpretation of the references to color in this figure legend, the leader is referred to the web version of this article.).

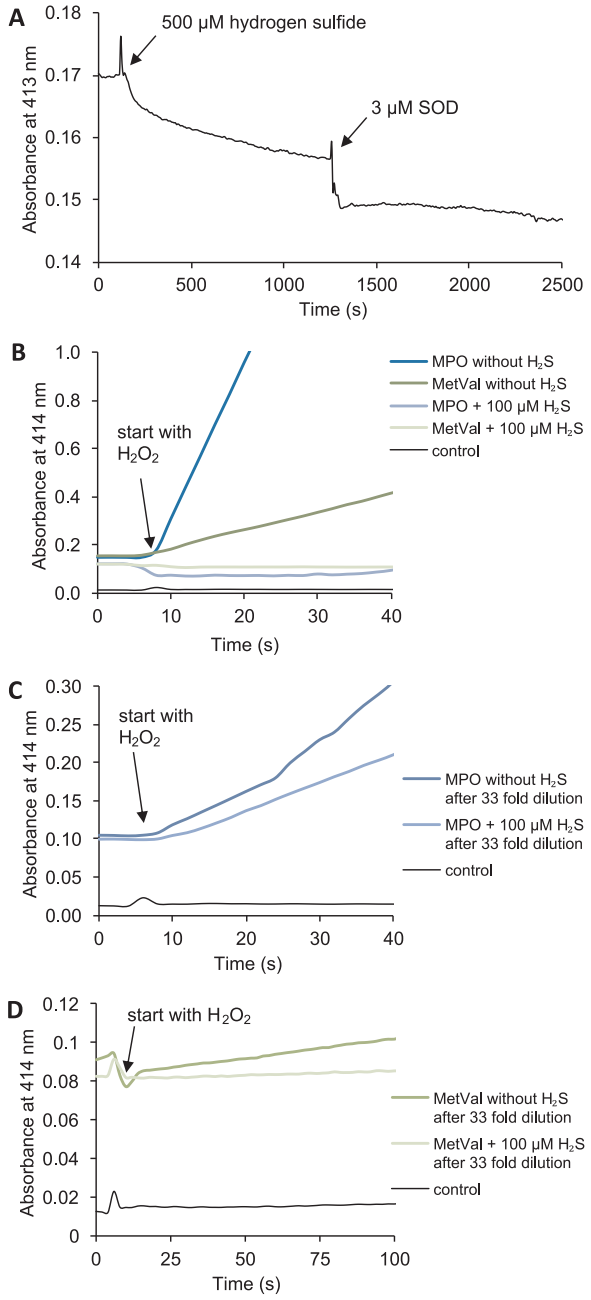

Fig. 9. Interactions of sulfide with the Met243Val mutant MPO. (A) The reaction of 2 μM Met243Val mutant MPO with 500 μM sulfide in 50 mM phosphate buffer pH 7.0 was followed at the Soret maximum (413 nm) of the enzyme. Addition of 3 μM SOD at 20 min had negligible effect on the kinetic trace. (B-D) Sulfide-mediated inhibition of the peroxidase activities of the WT and Met243Val mutant MPO. 2 μM WT or Met243Val mutant MPO was incubated in the presence or absence of 100 μM sulfide for 10 min, followed by measurements of the peroxidase activities using ABTS either directly (B) or after a 33 fold dilution (C-D). Conditions: (B) Reactions were started by the addition of 100 μM hydrogen peroxide to 1 mM ABTS, 2 μM Met243Val mutant MPO with or without 100 μM sulfide in 50 mM phosphate buffer pH 7.0 at 25 °C. (C-D) Reaction mixtures described in B were diluted 33 fold by 50 mM phosphate buffer pH 7 before the addition of 1 mM ABTS followed by 100 μM H_2O_2. Controls represent similar reaction mixtures without MPO. Measurements were carried out by a diode array UV-vis spectrophotometer (For interpretation of the references to color in this figure legend, the leader is referred to the web version of this article.).

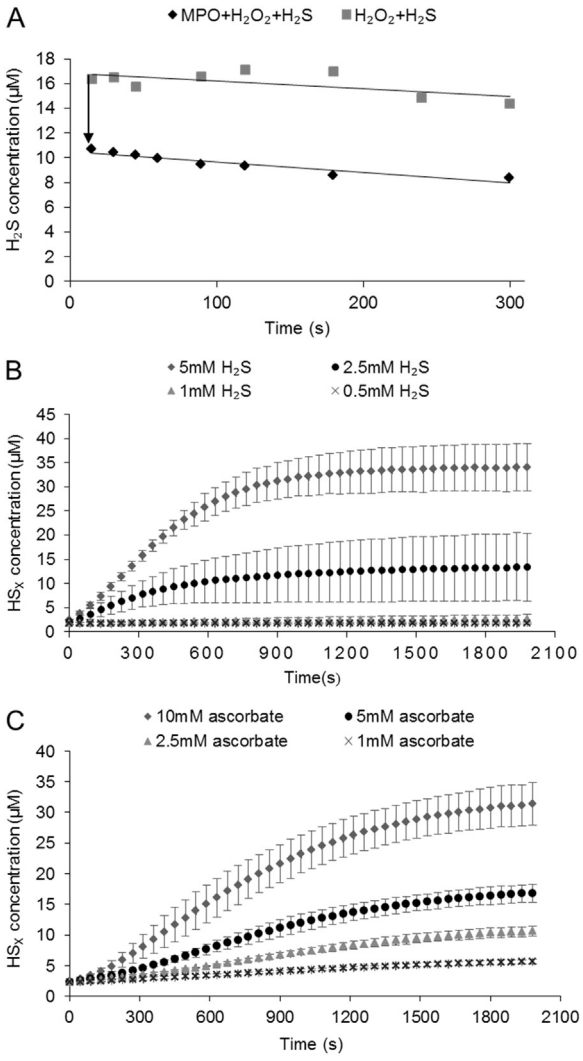

Fig. 10. MPO-mediated oxidation of sulfide in the presence and absence of hydrogen peroxide. (A) Solid line represent nonlinear least square fit of the observed sulfide consumption in the presence of H_2O_2 (squares). Rapid drop of hydrogen sulfide levels (represented by rhombs and the arrow) upon addition of 10 μM H_2O_2 in the presence of 100 nM MPO indicates fast catalytic oxidation of sulfide under these (high enzyme and substrate concentration) conditions. (B) Catalytic oxidation of sulfide by MPO in the presence of SOD using dissolved oxygen as the oxidizing agent at 100 nM MPO, 3 μM SOD and 0.5–5 mM sulfide in 100 mM phosphate buffer at pH 7.4 in the presence of 500 μM SSP4. Kinetic traces indicate the formation of the fluorescent product upon the reaction of SSP4 with sulfane sulfur species. Sulfane sulfur quantitation is based on calibration curves that were developed by reacting known amounts of inorganic polysulfide species with SSP4. (C) Catalytic oxidation of sulfide by MPO in the presence of ascorbate using dissolved oxygen as the oxidizing agent at 100 nM MPO, 1–10 mM ascorbate and 2.5 mM sulfide in 100 mM phosphate buffer at pH 7.4 in the presence of 500 μM SSP4. Kinetic traces were recorded as described at B. Data points and error bars represent the average and standard deviation of 4–6 independent experiments. Measurements were carried out by spectrofluorimetry.

However, interpretation of the traces should be handled with care due to the fact that they represent a composite of events. For example the kinetics of SSP4 with sulfane sulfur species under the applied conditions is on this timescale (not shown) and different sulfane sulfur species (i.e. different chain length polysulfides, thiosulfate tetrathionate etc) should exhibit different reaction rates with SSP4. This data does not allow a quantitative estimation for the efficacy of sulfane sulfur production in this system either because of many reasons. For example, the limiting reagent under the applied concentration conditions is O_2 (~200 μM in air saturated aqueous solutions), which can be consumed not only in its reaction with ferrous MPO to give Compound III, but also in reactions with thiyl radicals ($HS^{\bullet}$ is the proposed product of the reduction of ferric MPO to ferrous MPO by sulfide and the reaction of Compound I with sulfide). That oxygen was the limiting reagent under these conditions was demonstrated by the fact that in oxygen depleted solutions the rates and amounts of sulfane sulfur species production were diminished

(see Fig. S1). Furthermore, the generated superoxide/hydrogen peroxide (in the reaction of Compound III with ascorbate or SOD) can react with different enzyme forms and thereby alter the mechanism under different conditions [45,46]. Therefore, these systems are likely to exhibit highly complicated kinetics and a thorough kinetic investigation of the different enzymatic reaction steps and turnover pathways under different concentration conditions is outside the scope of the present study. However, the trace at the highest ascorbate concentration on Fig. 10C show > 30 μM sulfane sulfur production indicating that under these conditions a fair proportion of the dissolved oxygen is converted to sulfane sulfur species formation.

3.9. Per/polysulfidation of protein Cys residues by sulfane sulfur species that are generated in the catalytic, oxygen-mediated oxidation of sulfide by MPO in the presence of SOD or ascorbate

We previously demonstrated that inorganic polysulfide species can oxidize protein Cys residues to generate the corresponding Cys-persulfide derivatives [18].

$$R\text{-}SH + HS_x^- \rightarrow R\text{-}SS_nH + HS_{x-n}^- \quad (4)$$

Using our recently developed persulfide detection method ProPerDP [14,47] we investigated whether the sulfane sulfur species that are generated in the catalytic oxidation of sulfide by MPO in the presence of SOD or ascorbate induce persulfidation on human serum albumin. Indeed, aerobic reaction mixtures of sulfide with MPO and SOD or ascorbate induced the formation of per/polysulfide formation on the active site Cys residue of isolated HSA (Figs. 11A and B, respectively). In addition, these reaction mixtures also triggered HSA-persulfidation in human blood plasma (Fig. 11C).

4. Discussion

Previously we demonstrated that the ferric, Compound I and Compound II enzyme forms of MPO can rapidly oxidize sulfide [7]. All reactions proceed via the ferrous enzyme form to give a mixture of MPO derivatives that were not fully characterized. In this study we obtained compelling evidence that a common product of these reactions under aerobic conditions with the characteristic absorbance at 625 nm is MPO Compound III. Compound III formation was absent under anaerobic conditions, it was rapidly converted to the ferric-MPO-CN complex upon addition of cyanide, reacted with previously reported rates in the presence of ascorbate and its decomposition to the ferric form was facilitated by SOD. In addition, when Compound III was generated in the absence of sulfide in reactions with hydralazine, it exhibited identical spectral characteristics to the 625 nm species that was generated upon the interactions of MPO with sulfide. These results are all consistent with Compound III indeed being a central intermediate species in the catalytic cycles of MPO when it uses sulfide as substrate (Scheme 1). Compound III formation can also explain the previously observed reversible inhibition of MPO peroxidase activity by sulfide, representing the resting state of the enzyme during turnover.

The reaction of H_2S with heme proteins was found to be controlled by the positions and orientations of distal residues [30,48]. Formation of a sulfheme derivative, in which sulfide is covalently incorporated into pyrrole ring B on the heme porphyrin (see Fig. 3), in oxidative interactions with sulfide is a common feature of heme proteins [30] (reported for example in hemoglobin [49,50], myoglobin [50,51], catalase [40] and lactoperoxidase (LPO) [52]). Although, during the oxidative interactions of MPO with sulfide a UV-vis absorption maximum is observed at 625 nm, which is in the characteristic range of sulfheme derivatives, our data argue against a substantial amount of MPO sulfheme derivative formation and supports a mechanism that proceeds via Compound III (see Scheme 1), which can apparently account for the formation of the 625 nm band in the UV-vis spectra.

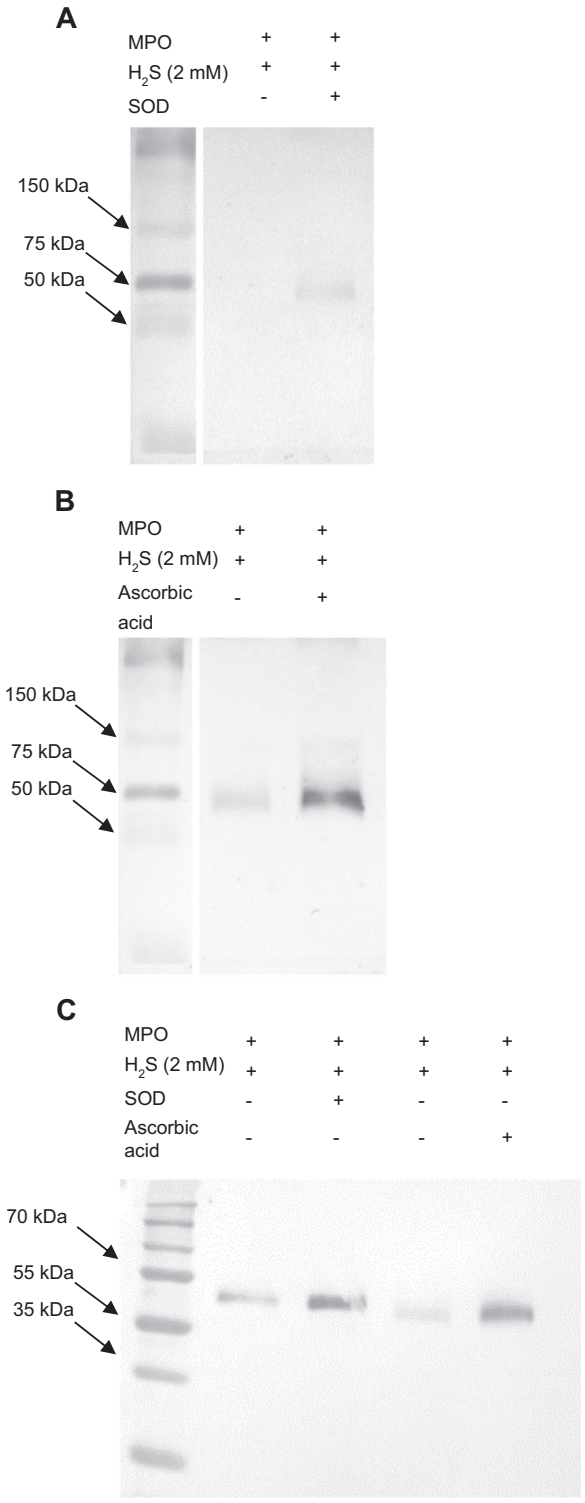

Fig. 11. Persulfidation of human serum albumin by MPO-mediated sulfide oxidation products that were generated using oxygen as the oxidizing agent in the presence of SOD or ascorbate. A) 2 mM sulfide was oxidized in the presence of 100 nM MPO and 3 μM SOD (A) or 10 mM ascorbate (B) upon a 10 min incubation in 100 mM phosphate buffer at pH 7.4, followed by the addition of 1.67 mg/mL pre-reduced HSA to the reaction mixture. After 1 min incubation, the formation of HSA-per/polysulfide species were detected by ProPerDP using western-blot analysis as described previously [14,47]. C) Human plasma samples containing 1.67 mg/mL total protein were treated with similar reaction mixtures (containing the sulfide oxidation products) as described above. HSA-per/polysulfide species were detected by ProPerDP [14,47].
The bands on the blots represent the persulfidated fractions of HSA. Blots are representative of 3 independent experiments with similar results.

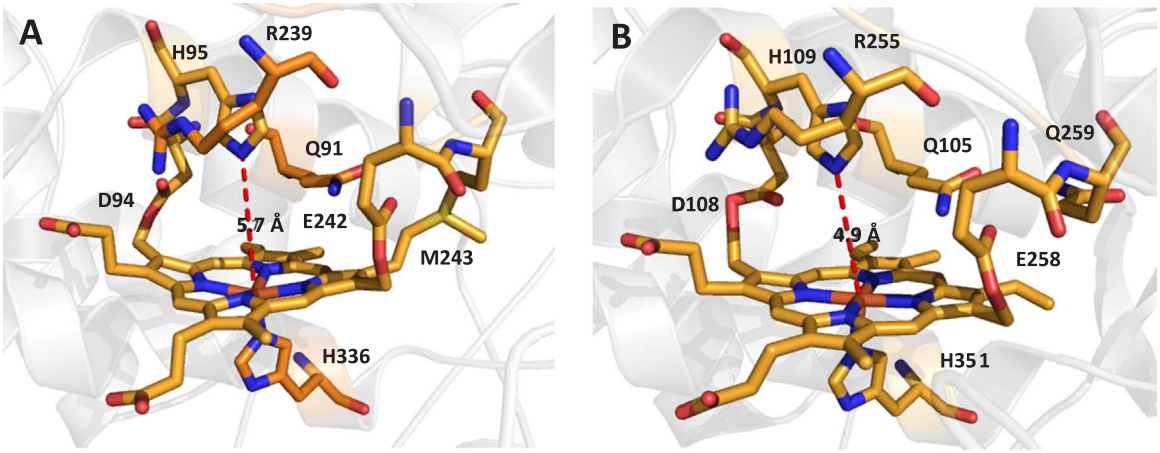

Fig. 12. Active site of heme peroxidases highlighting covalent bindings of amino acid residues to the porphyrin ring. (A) MPO (3F9P) and (B) LPO (PDB:2NQX).

Therefore, it is interesting to speculate, why LPO can engage in sulfheme production in contrast to MPO, which catalyze sulfide oxidation via the intermediate formation of Compound III instead. Both LPO and MPO via the methyl groups on pyrrole rings A and C form two ester linkages with the carboxyl groups of glutamate and aspartate residues, respectively [53–56](see Figs. 12A and 12B). This makes the heme groups of these peroxidases more rigid and distorted compared to the globins. However, MPO, in addition to these ester bonds, forms an electron-withdrawing sulfonium ion linkage with the β-carbon of the vinyl pyrrole ring A via the sulfur of methionine 243 (Fig. 12A), which was proposed to be pivotal in the unique redox and catalytic features of MPO among peroxidases. Myeloperoxidase is for example the only human enzyme that is able to catalyze the oxidation of chloride to HOCl at reasonable rates [27,57–59]. Our results that the Met243Val MPO mutant is irreversibly and completely inhibited by sulfide demonstrated that this sulfonium linkage is also essential in the sulfide oxidizing capacity of MPO. Moreover, SOD failed to accelerate the turnover of the Met243Val mutant of MPO in the presence of sulfide and oxygen suggesting that in this case sulfide-mediated inhibition is not due to (reversible) Compound III formation. The sulfonium ion linkage in MPO not only introduces a strong electron withdrawing effect on the porphyrin ring, but also further increases its rigidity and results in a bow-like distortion of the heme from planarity [54,60]. As a result of this distortion the iron center is placed in an out-of-plane position and displaced to the proximal site. These effects weaken the interactions of the iron center with the pyrrole rings [57] and makes the iron located further away from the distal histidine (5.65 Å, compared to the 4.94 Å position of the histidine in LPO, see Fig. 12). Because the distal histidine with the adequate orientation and position in heme proteins was found to be essential for the formation of sulfheme derivatives [30] and the positive charge of the sulfur atom in the sulfonium ion linkage influences the basicity of the pyrrole nitrogens and reduces the electron density on the heme iron, the Met243-heme linkage could be the major reason behind the preference of MPO to form Compound III instead of a sulfheme derivative.

Our results are suggestive that this unique feature may also be responsible for the SOD or ascorbate facilitated catalytic oxidation of sulfide by MPO even in the absence of added peroxide, using dissolved oxygen in aqueous solutions as the oxidizing agent. We proposed a kinetic model to explain our observations (see Scheme 1), where the catalytic reaction sequence is initiated by the reduction of ferric MPO by sulfide to give ferrous MPO and $HS^{\bullet}$. Ferrous MPO reacts with oxygen to give Compound III (reaction sequence k_1 k_2 k_{-3} and k_4 on Scheme 1). Compound III reacts with ascorbate as proposed by Marques and Dunford [41] to give ferric MPO and H_2O_2 (reaction k_6 on Scheme 1). The generated H_2O_2 can then turn over the ferric enzyme in the presence of sulfide via Compound I and II as we reported previously [7] (reaction sequence k_7 k_8 k_9 and k_4 on Scheme 1). The ferric enzyme that is produced in the reaction of ascorbate and Compound III can alternatively react with another sulfide molecule to regenerate Compound III by the above described reaction sequence k_1, k_2 k_{-3} and k_4. In the absence of ascorbate, SOD can also turn this system around by catalyzing the release of superoxide from Compound III to give the ferric enzyme (reaction k_5 on Scheme 1). These represent novel catalytic cycles for MPO to oxidize sulfide in the absence of added peroxide.

A number of reaction steps on Scheme 1 can generate sulfane sulfur species. For example $HS^{\bullet}$, that is produced in the reactions of ferric MPO or Compound I with sulfide is expected to react rapidly with another sulfide molecule (or in biological systems with a Cys thiolate) to give the corresponding disulfide radical anion species (reaction 5). $RSSH^{\bullet-}$ reacts with oxygen in rates that are diffusion controlled to produce the sulfane sulfur RSS^- species (Cys persulfide or inorganic polysulfide) and superoxide (reaction 6).

$$HS\bullet + RS^- \rightarrow RSSH^{\bullet-} \text{ (R = H or Cys)} \quad (5)$$

$$RSSH^{\bullet-} + O_2 \rightarrow RSS^- + H^+ + OO_2^{\bullet-} \quad (6)$$

In the experiments where SOD was used to facilitate the decomposition of Compound III (and hence the catalytic oxidation of sulfide), the relatively large applied SOD concentrations should be considered. We demonstrated that the catalytic activity of SOD is required to facilitate the reactions (see Fig. S2) by showing that i) the effect of SOD on sulfane sulfur production by the MPO-sulfide-O_2 system was dose dependent and ii) similar amounts of partially inactivated SOD (by incubation with H_2O_2 as reported previously [61]) had a diminished effect on sulfane sulfur production compared to non-treated SOD (Fig. S2). However, SOD catalyzed sulfide oxidation by superoxide was suggested to generate one mol equivalent peroxide [62], which in turn could contribute to sulfide oxidation processes by MPO-catalyzed pathways (depicted by red arrows on Scheme 1). In addition, O_2-induced sulfide oxidation by SOD can potentially contribute to sulfane sulfur production [63], but the rate of these reactions under the applied experimental conditions is much slower compared to MPO-mediated pathways. In fact the kinetic traces on Fig. 10B were obtained via subtracting the background sulfane sulfur production by the SOD-sulfide-O_2 system (which was ~20% of the total sulfane sulfur production at the latest time point) in the absence of MPO for each runs. Furthermore, we observed similarly prominent sulfane sulfur species production (and protein polysulfidation both in purified protein and plasma samples, see below) when ascorbic acid or SOD was used to facilitate the recovery of ferric MPO from Compound III. This corroborates our proposal that the majority of sulfide oxidation in these systems is due to MPO-mediated reactions.

We demonstrated that MPO-produced sulfane sulfur species can

interact with protein Cys residues to produce per/polysulfide derivatives. This posttranslational modification was proposed to exhibit a regulatory effect on specific protein activities in a number of proteins (for a review of a few examples see [6]). In fact, many of the biological actions of sulfide were associated with this protein posttranslational modification [8,64,65]. However, as we argued previously the generation of per/polysulfides on protein Cys residues by H_2S require oxidation of the Cys or sulfide [6,19].

Slow releasing sulfide donors were demonstrated to be more potent agents to induce sulfide-mediated biological events in *in vitro* as well as *in vivo* studies compared to administration of bolus sulfide in the form of sulfide salts [66]. Therefore, our findings that MPO can promote a relatively slow steady-state flux of sulfane sulfur species by oxygen-mediated sulfide oxidation, which induce protein per/polysulfide formation, can potentially contribute to previously observed sulfide-mediated protein persulfidation in certain physiological and pathophysiological conditions.

Furthermore, based on our findings, at sights of inflammation, neutrophil released MPO can use Nox2 produced hydrogen peroxide to rapidly generate sulfane sulfur species from sulfide (as indicated by the data in Table 1) and trigger more potent protein Cys persulfide formation as we demonstrated here and in a previous report [18]. This could potentially be a protein protecting mechanism (especially when administered sulfide was observed to alleviate inflammatory side effects), because excessive Cys oxidation (by for example the promiscuous neutrophil oxidant hypochlorous acid) can cause damage to proteins by the generation of non-reducible Cys-sulfinic or sulfonic acid derivatives ($CySO_2H$ and $CySO_3H$, respectively) in their reactions with Cys thiols. These irreversible Cys oxidations can be prevented by prior Cys per/polysulfidation, because overoxidation reactions of persulfides are expected to give reducible Cys-persulfinic ($CyS\text{-}SO_2H$) and persulfonic acid ($CyS\text{-}SO_3H$) species [9].

Further to our previous report on the interactions of sulfide with myeloperoxidase [7], the potential roles of heme proteins, such as hemoglobin [67], myoglobin [68] or catalase [40] in the endogenous oxidation of sulfide were proposed recently. In addition, an interesting recent study proposed that catalase can not only serve as a sulfide oxidase but under hypoxic conditions it may also contribute to H_2S producing pathways [69]. Although the globins are generally more abundant than MPO and hence may play a major role in the oxidative catabolism of sulfide, due to the formation of sulfheme derivatives (that is well documented for both enzymes), it is expected that they will exhibit transient catalytic capacities. On the other hand, the fact that sulfheme formation is retarded in the case of MPO a continuous slow oxidation of sulfide could potentially play a role in sulfide/polysulfide-mediated cellular signaling. In addition, as we argued above, MPO-mediated sulfide oxidation could be important in the protection of functional or regulatory protein Cys residues during oxidative stress, in particular at sites of inflammation, where increasing amounts of MPO and its primary substrate H_2O_2 (which reacts with MPO preferentially compared to the globins) are released by neutrophil white blood cells.

In conclusion, we propose that the sulfonium ion linkage of Met243 to the heme in MPO may not only be important for the ability of the protein to generate HOCl, but could also be the reason behind the slow sulfide oxidizing activity of MPO and preventing its inactivation via formation of a sulfheme derivative. The novel turnover models to oxidize sulfide (Scheme 1) even in the absence of added H_2O_2 via oxygen to provide a slow flux of sulfane sulfur generation could be important in protein Cys persulfidation-mediated signaling and sulfide-protection of Cys residues during oxidative stress.

Acknowledgments

Financial support from FP7-PEOPLE-2010-RG Marie Curie Actions (International Reintegration Grant, grant no.: PIRG08-GA-2010–277006) and the Hungarian Scientific Research Fund (OTKA; grant No.: K 109843) for P.N. is acknowledged. P.N. is a János Bolyai Research Scholar of the Hungarian Academy of Sciences. Financial supports from the Austrian Science Fund (FWF project P20664) to C.O. and P.G.F are also acknowledged. Dojindo Molecular Technologies Inc. is greatly acknowledged for their kind support of high quality chemical supplies.

Appendix A. Supporting information

Supplementary data associated with this article can be found in the online version at http://dx.doi.org/10.1016/j.freeradbiomed.2017.10.384.

References

[1] L. Li, P.K. Moore, Putative biological roles of hydrogen sulfide in health and disease: a breath of not so fresh air? Trends Pharmacol. Sci. 29 (2008) 84–90.
[2] K.R. Olson, K.D. Straub, The role of hydrogen sulfide in evolution and the evolution of hydrogen sulfide in metabolism and signaling, Physiology 31 (2016) 60–72.
[3] C. Szabo, Gasotransmitters in cancer: from pathophysiology to experimental therapy, Nat. Rev. Drug Discov. 15 (2016) 185–203.
[4] J.L. Wallace, R. Wang, Hydrogen sulfide-based therapeutics: exploiting a unique but ubiquitous gasotransmitter, Nat. Rev. Drug Discov. 14 (2015) 329–345.
[5] R. Wang, Physiological implications of hydrogen sulfide: a whiff exploration that blossomed, Physiol. Rev. 92 (2012) 791–896.
[6] P. Nagy, Mechanistic chemical perspective of hydrogen sulfide signaling, Methods Enzymol. 554 (2015) 3–29.
[7] Z. Palinkas, P.G. Furtmuller, A. Nagy, C. Jakopitsch, K.F. Pirker, M. Magierowski, K. Jasnos, J.L. Wallace, C. Obinger, P. Nagy, Interactions of hydrogen sulfide with myeloperoxidase, Br. J. Pharmacol. 172 (2015) 1516–1532.
[8] B.D. Paul, S.H. Snyder, H_2S signalling through protein sulfhydration and beyond, Nat. Rev. Mol. Cell Biol. 13 (2012) 499–507.
[9] K. Ono, T. Akaike, T. Sawa, Y. Kumagai, D.A. Wink, D.J. Tantillo, A.J. Hobbs, P. Nagy, M. Xian, J. Lin, J.M. Fukuto, Redox chemistry and chemical biology of H_2S, hydropersulfides, and derived species: implications of their possible biological activity and utility, Free Radic. Biol. Med. 77 (2014) 82–94.
[10] H. Kimura, Signaling molecules: hydrogen sulfide and polysulfide, Antioxid. Redox Signal. 22 (2015) 362–376.
[11] J.I. Toohey, Sulfur signaling: is the agent sulfide or sulfane? Anal. Biochem. 413 (2011) 1–7.
[12] P. Nagy, Z. Palinkas, A. Nagy, B. Budai, I. Toth, A. Vasas, Chemical aspects of hydrogen sulfide measurements in physiological samples, Biochim. Biophys. Acta 2014 (1840) 876–891.
[13] T. Ida, T. Sawa, H. Ihara, Y. Tsuchiya, Y. Watanabe, Y. Kumagai, M. Suematsu, H. Motohashi, S. Fujii, T. Matsunaga, M. Yamamoto, K. Ono, N.O. Devarie-Baez, M. Xian, J.M. Fukuto, T. Akaike, Reactive cysteine persulfides and S-polythiolation regulate oxidative stress and redox signaling, Proc. Natl. Acad. Sci. USA 111 (2014) 7606–7611.
[14] E. Doka, I. Pader, A. Biro, K. Johansson, Q. Cheng, K. Ballago, J.R. Prigge, D. Pastor-Flores, T.P. Dick, E.E. Schmidt, E.S. Arner, P. Nagy, A novel persulfide detection method reveals protein persulfide- and polysulfide-reducing functions of thioredoxin and glutathione systems, Sci. Adv. 2 (2016) e1500968.
[15] N.E. Francoleon, S.J. Carrington, J.M. Fukuto, The reaction of H_2S with oxidized thiols: generation of persulfides and implications to H_2S biology, Arch. Biochem. Biophys. 516 (2011) 146–153.
[16] A. Vasas, E. Doka, I. Fabian, P. Nagy, Kinetic and thermodynamic studies on the disulfide-bond reducing potential of hydrogen sulfide, Nitric Oxide 46 (2015) 93–101.
[17] E. Cuevasanta, M. Lange, J. Bonanata, E.L. Coitino, G. Ferrer-Sueta, M.R. Filipovic, B. Alvarez, Reaction of hydrogen sulfide with disulfide and sulfenic acid to form the strongly nucleophilic persulfide, J. Biol. Chem. 290 (2015) 26866–26880.
[18] R. Greiner, Z. Palinkas, K. Basell, D. Becher, H. Antelmann, P. Nagy, T.P. Dick, Polysulfides link H_2S to protein thiol oxidation, Antioxid. Redox Signal. 19 (2013) 1749–1765.
[19] P. Nagy, C.C. Winterbourn, Rapid reaction of hydrogen sulfide with the neutrophil oxidant hypochlorous acid to generate polysulfides, Chem. Res. Toxicol. 23 (2010) 1541–1543.
[20] N. Nagahara, T. Okazaki, T. Nishino, Cytosolic mercaptopyruvate sulfurtransferase is evolutionarily related to mitochondrial rhodanese. Striking similarity in active site amino acid sequence and the increase in the mercaptopyruvate sulfurtransferase activity of rhodanese by site-directed mutagenesis, J. Biol. Chem. 270 (1995) 16230–16235.
[21] T. Yamanishi, S. Tuboi, The mechanism of the L-cystine cleavage reaction catalyzed by rat liver gamma-cystathionase, J. Biochem. 89 (1981) 1913–1921.
[22] T. Akaike, et al., Cysteinyl-tRNA synthetase governs cysteine polysulfidation and mitochondrial bioenergetics, Nat. Commun. 8 (2017) 1177, , http://dx.doi.org/10.1038/s41467-017-01311-y.
[23] C. Nussbaum, A. Klinke, M. Adam, S. Baldus, M. Sperandio, Myeloperoxidase, A. Leukocyte-Derived Protagonist, of inflammation and cardiovascular disease, Antioxid. Redox Signal. 18 (2013) 692–713.
[24] S.J. Klebanoff, Myeloperoxidase: friend and foe, J. Leukoc. Biol. 77 (2005)

598–625.
[25] I.M. Kooter, N. Moguilevsky, A. Bollen, N.M. Sijtsema, C. Otto, R. Wever, Site-directed mutagenesis of Met243, a residue of myeloperoxidase involved in binding of the prosthetic group, J. Biol. Inorg. Chem. 2 (1997) 191–197.
[26] N. Moguilevsky, L. Garciaquintana, A. Jacquet, C. Tournay, L. Fabry, L. Pierard, A. Bollen, Structural and biological properties of human recombinant myeloperoxidase produced by Chinese hamster ovary cell lines, Eur. J. Biochem. 197 (1991) 605–614.
[27] M. Zederbauer, P.G. Furtmuller, B. Ganster, N. Moguilevsky, C. Obinger, The vinyl-sulfonium bond in human myeloperoxidase: impact on compound I formation and reduction by halides and thiocyanate, Biochem. Biophys. Res. Commun. 356 (2007) 450–456.
[28] R. Floris, Y. Kim, G.T. Babcock, R. Wever, Optical spectrum of myeloperoxidase. Origin of the red shift, Eur. J. Biochem. 222 (1994) 677–685.
[29] W. Jantschko, P.G. Furtmuller, M. Zederbauer, C. Jakopitsch, C. Obinger, Kinetics of oxygen binding to ferrous myeloperoxidase, Arch. Biochem. Biophys. 426 (2004) 91–97.
[30] B.B. Rios-Gonzalez, E.M. Roman-Morales, R. Pietri, J. Lopez-Garriga, Hydrogen sulfide activation in hemeproteins: the sulfheme scenario, J. Inorg. Biochem. 133 (2014) 78–86.
[31] M.J. Chatfield, G.N. La Mar, A.L. Balch, K.M. Smith, D.W. Parish, T.J. LePage, Proton NMR study of the influence of heme vinyl groups on the formation of the isomeric forms of sulfmyoglobin, FEBS Lett. 206 (1986) 343–346.
[32] M.J. Chatfield, G.N. La Mar, J.T.J. Lecomte, A.L. Balch, K.M. Smith, K.C. Langry, Identification of the altered pyrrole in sulfmyoglobin and an extractable "sulfhemin": participation of the 4-vinyl group in the saturation of the pyrrole in one form of sulfmyoglobin, J. Am. Chem. Soc. 108 (1986) 7108–7110.
[33] H. Hoogland, A. van Kuilenburg, C. van Riel, A.O. Muijsers, R. Wever, Spectral properties of myeloperoxidase compounds II and III, Biochim. Biophys. Acta 916 (1987) 76–82.
[34] C.C. Winterbourn, R.C. Garcia, A.W. Segal, Production of the superoxide adduct of myeloperoxidase (compound III) by stimulated human neutrophils and its reactivity with hydrogen peroxide and chloride, Biochem. J. 228 (1985) 583–592.
[35] J. Soubhye, M. Gelbcke, P. Van Antwerpen, F. Dufrasne, M.Y. Boufadi, J. Neve, P.G. Furtmuller, C. Obinger, K. Zouaoui Boudjeltia, F. Meyer, From dynamic combinatorial chemistry to *in vivo* evaluation of reversible and irreversible myeloperoxidase inhibitors, ACS Med. Chem. Lett. 8 (2017) 206–210.
[36] J.A. Berzofsky, J. Peisach, J.O. Alben, Sulfheme proteins. III. Carboxysulfmyoglobin: the relation between electron withdrawal from iron and ligand binding, J. Biol. Chem. 247 (1972) 3774–3782.
[37] J.A. Berzofsky, J. Peisach, B.L. Horecker, Sulfheme proteins. IV. The stoichiometry of sulfur incorporation and the isolation of sulfhemin, the prosthetic group of sulfmyoglobin, J. Biol. Chem. 247 (1972) 3783–3791.
[38] E.A. Johnson, The reversion to haemoglobin of sulphhaemoglobin and its co-ordination derivatives, Biochim. Biophys. Acta 207 (1970) 30–40.
[39] P. Nicholls, The formation and properties of sulphmyoglobin and sulphcatalase, Biochem. J. 81 (1961) 374–383.
[40] D. Padovani, A. Hessani, F.T. Castillo, G. Liot, M. Andriamihaja, A. Lan, C. Pilati, F. Blachier, S. Sen, E. Galardon, I. Artaud, Sulfheme formation during homocysteine S-oxygenation by catalase in cancers and neurodegenerative diseases, Nat. Commun. 7 (2016) 13386.
[41] L.A. Marquez, H.B. Dunford, Reaction of compound-III of myeloperoxidase with ascorbic-acid, J. Biol. Chem. 265 (1990) 6074–6078.
[42] M.R. Hoffmann, Kinetics and mechanism of oxidation of hydrogen-sulfide by hydrogen-peroxide in acidic solution, Environ. Sci. Technol. 11 (1977) 61–66.
[43] S. Carballal, M. Trujillo, E. Cuevasanta, S. Bartesaghi, M.N. Moller, L.K. Folkes, M.A. Garcia-Bereguiain, C. Gutierrez-Merino, P. Wardman, A. Denicola, R. Radi, B. Alvarez, Reactivity of hydrogen sulfide with peroxynitrite and other oxidants of biological interest, Free Radic. Biol. Med. 50 (2011) 196–205.
[44] W. Chen, C. Liu, B. Peng, Y. Zhao, A. Pacheco, M. Xian, New fluorescent probes for sulfane sulfurs and the application in bioimaging, Chem. Sci. 4 (2013) 2892–2896.
[45] A.J. Kettle, R.F. Anderson, M.B. Hampton, C.C. Winterbourn, Reactions of superoxide with myeloperoxidase, Biochemistry 46 (2007) 4888–4897.
[46] A.J. Kettle, A. Maroz, G. Woodroffe, C.C. Winterbourn, R.F. Anderson, Spectral and kinetic evidence for reaction of superoxide with compound I of myeloperoxidase, Free Radic. Biol. Med. 51 (2011) 2190–2194.
[47] E. Doka, E.S.J. Arner, E.E. Schmidt, P. Nagy, ProPerDP, a Protein Persulfide Detection Protocol, in: J. Beltowski (Ed.), Methods Mol. Biol. Springer, 2017.
[48] R. Pietri, A. Lewis, R.G. Leon, G. Casabona, L. Kiger, S.R. Yeh, S. Fernandez-Alberti, M.C. Marden, C.L. Cadilla, J. Lopez-Garriga, Factors controlling the reactivity of hydrogen sulfide with hemeproteins, Biochemistry 48 (2009) 4881–4894.
[49] F. Hoppe-Seyler, Zentralbl. Med. Wiss. 4 (1866) 436–438.
[50] H.O. Michel, A study of sulfhemoglobin, J. Biol. Chem. 126 (1938) 323–348.
[51] J.A. Berzofsky, J. Peisach, W.E. Blumberg, Sulfheme proteins. I. optical and magnetic properties of sulfmyoglobin and its derivatives, J. Biol. Chem. 246 (1971) 3367–3377.
[52] S. Nakamura, M. Nakamura, I. Yamazaki, M. Morrison, Reactions of ferryl lactoperoxidase (compound II) with sulfide and sulfhydryl compounds, J. Biol. Chem. 259 (1984) 7080–7085.
[53] X. Carpena, P. Vidossich, K. Schroettner, B.M. Calisto, S. Banerjee, J. Stampler, M. Soudi, P.G. Furtmuller, C. Rovira, I. Fita, C. Obinger, Essential role of proximal histidine-asparagine interaction in mammalian peroxidases, J. Biol. Chem. 284 (2009) 25929–25937.
[54] T.J. Fiedler, C.A. Davey, R.E. Fenna, X-ray crystal structure and characterization of halide-binding sites of human myeloperoxidase at 1.8 A resolution, J. Biol. Chem. 275 (2000) 11964–11971.
[55] P.G. Furtmuller, M. Zederbauer, W. Jantschko, J. Helm, M. Bogner, C. Jakopitsch, C. Obinger, Active site structure and catalytic mechanisms of human peroxidases, Arch. Biochem. Biophys. 445 (2006) 199–213.
[56] I.A. Sheikh, Ethayathulla, A.S., Singh, A.K., Singh, N., Sharma, S., Singh, T.P., Crystal structure of Buffalo lactoperoxidase at 2.75A resolution, PDB Data Bank entry 2GJM, 2006.
[57] G. Battistuzzi, J. Stampler, M. Bellei, J. Vlasits, M. Soudi, P.G. Furtmuller, C. Obinger, Influence of the covalent heme-protein bonds on the redox thermodynamics of human myeloperoxidase, Biochemistry 50 (2011) 7987–7994.
[58] I.M. Kooter, N. Moguilevsky, A. Bollen, L.A. van der Veen, C. Otto, H.L. Dekker, R. Wever, The sulfonium ion linkage in myeloperoxidase. Direct spectroscopic detection by isotopic labeling and effect of mutation, J. Biol. Chem. 274 (1999) 26794–26802.
[59] M. Zederbauer, P.G. Furtmuller, S. Brogioni, C. Jakopitsch, G. Smulevich, C. Obinger, Heme to protein linkages in mammalian peroxidases: impact on spectroscopic, redox and catalytic properties, Nat. Prod. Rep. 24 (2007) 571–584.
[60] A.K. Singh, Singh, N., Sharma, S., Bhushan, A., Singh, T.P., Crystal structure of Bovine lactoperoxidase at 2.3A resolution, PDB data bank entry 2GJ1, 2006.
[61] D.C. Salo, R.E. Pacifici, S.W. Lin, C. Giulivi, K.J.A. Davies, Superoxide-dismutase undergoes proteolysis and fragmentation Following oxidative modification and inactivation, J. Biol. Chem. 265 (1990) 11919–11927.
[62] D.G. Searcy, J.P. Whitehead, M.J. Maroney, Interaction of Cu,Zn superoxide-dismutase with hydrogen-sulfide, Arch. Biochem. Biophys. 318 (1995) 251–263.
[63] D.G. Searcy, HS-: O-2 oxidoreductase activity of Cu,Zn superoxide dismutase, Arch. Biochem. Biophys. 334 (1996) 50–58.
[64] A.K. Mustafa, M.M. Gadalla, N. Sen, S. Kim, W. Mu, S.K. Gazi, R.K. Barrow, G. Yang, R. Wang, S.H. Snyder, H_2S signals through protein S-sulfhydration, Sci. Signal. 2 (2009) ra72.
[65] B.D. Paul, S.H. Snyder, H_2S, A. Novel Gasotransmitter, that Signals by Sulfhydration, Trends Biochem. Sci. 40 (2015) 687–700.
[66] M. Whiteman, S. Le Trionnaire, M. Chopra, B. Fox, J. Whatmore, Emerging role of hydrogen sulfide in health and disease: critical appraisal of biomarkers and pharmacological tools, Clin. Sci. 121 (2011) 459–488.
[67] V. Vitvitsky, P.K. Yadav, A. Kurthen, R. Banerjee, Sulfide oxidation by a non-canonical pathway in red blood cells generates thiosulfate and polysulfides, J. Biol. Chem. 290 (2015) 8310–8320.
[68] T. Bostelaar, V. Vitvitsky, J. Kumutima, B.E. Lewis, P.K. Yadav, T.C. Brunold, M. Filipovic, N. Lehnert, T.L. Stemmler, R. Banerjee, Hydrogen sulfide oxidation by myoglobin, J. Am. Chem. Soc. 138 (2016) 8476–8488.
[69] K.R. Olson, Y. Gao, E.R. DeLeon, M. Arif, F. Arif, N. Arora, K.D. Straub, Catalase as a sulfide-sulfur oxido-reductase: an ancient (and modern?) regulator of reactive sulfur species (RSS), Redox Biol. 12 (2017) 325–339.

Lactoperoxidase catalytically oxidize hydrogen sulfide via the intermediate formation of sulfheme derivatives turnover

Bessie B. Ríos-González[a], Leishka D. Crespo[a], Gary J. Gerfen[b], Paul G. Furtmüller[c], Péter Nagy[d] and Juan López-Garriga*[a]

[a]Department of Chemistry, University of Puerto Rico, Mayagüez Campus, P.O. Box 9019, Mayagüez, Puerto Rico 00681-9019

[b]Department of Physiology & Biophysics, Albert Einstein College of Medicine, Bronx, NY 10461

[c]Division of Biochemsitry, Universität für Bodenkultur Wien, Muthgasse 18, 1190 Vienna

[d]Department of Molecular Immunology and Toxicology, National Institute of Oncology, Ráth György utca 7-9, Budapest, Hungary, 1122

E-mail: bessie.rios@upr.edu, gary.gerfen@einstein.yu.edu, paul.furtmueller@boku.ac.at, peter.nagy@oncol.hu, and juan.lopez16@upr.edu

Corresponding author: Juan López-Garriga

Address: Department of Chemistry, University of Puerto Rico, Mayagüez Campus, PO Box 9019, Mayagüez, Puerto Rico 00681-9019

Telephone: (787) 265-5453

Fax: (787) 265-5476

E-mail: juan.lopez16@upr.edu

Abstract

The chemistry of hydrogen sulfide (H_2S) has as targets physiologically important hemeproteins, such as myoglobin, hemoglobin, lactoperoxidase (LPO) or myeloperoxidase. However, despite extensive efforts, today there is a need to further comprehend the species involved in the reaction between LPO and molecular oxygen (O_2) or hydrogen peroxide (H_2O_2) in the presence of H_2S. Our results show that under strict anaerobic conditions the addition of H_2S to native LPO does not induce the formation of heme derivatives that form under aerobic conditions with characteristic bands at 638 nm and 727 nm in the electronic spectrum. These species were tentatively assigned to the ferrous and ferric states of the sulfheme derivative of LPO, respectively. Further data indicate that the presence of O_2 or H_2O_2 is an absolute requirement for the formation of these sulfheme derivatives. Interestingly, in the presence of H_2S, during the reactions of LPO with H_2O_2 a continuous turnover with the formation of ferrous and ferric sulfLPO followed by a recovery of native LPO was observed, indicating LPO catalyzed oxidation of sulfide by peroxide. This catalytic oxidation of sulfide is not consistent with sulfheme decomposition to regenerate sulfide, in other words sulfide trafficking via sulfLPO. Pilot product analysis suggest that the turnover process indeed generates oxidized sulfur species, most likely sulfate (SO_4^{2-}) and/or inorganic polysulfides (HS_x^- x = 2-9) as products. These results indicate that H_2S is a non-classical LPO substrate, because the porphyrin ring of the heme group is reversibly modified during turnover via intermediate formation of sulfheme derivatives. This also implies that LPO is an unusual heme protein in the sense that its sulfheme derivative can be rapidly converted back to the active native form of the enzyme in contrast to Hb or Mb, where sulfheme derivatives are stable. Furthermore, EPR data suggest that during sulfheme turnover, H_2S can act as a scavenger of H_2O_2 in the presence of LPO without detectable formation of any carbon centered protein radical species,

suggesting that H_2S might be capable to protect the enzyme from radical-mediated damage in the presence of H_2O_2. Sulfheme formation was shown to be slower in the reaction between oxyLPO and H_2S compared to the LPO catalyzed oxidation of sulfide by H_2O_2. Based on the available literature data on heme proteins, we speculate that this might be due to intermediate formation of compound III in the reaction of oxyLPO with sulfide during the process of generating the compound 0 state, which is a proposed central intermediate in the formation of sulfheme derivatives. On the other hand, heme compound 0 can be generated by direct coordination of H_2O_2 to ferric LPO in the presence of H_2O_2.

Keywords

Lactoperoxidase, Hydrogen sulfide, Sulfhemeprotein, Oxo-ferryl intermediate, LPO turnover, Sulfate, Inorganic polysulfides species

1. Introduction

Hydrogen sulfide (H_2S) is produced endogenously in mammalian tissues by four enzymes: cystathionine β-synthase (CBS), cystathionine γ-lyase (CSE), 3-mercaptopyruvate sulfurtransferase (MST), and D-amino acid oxidase (DAO) [1–3]. At low concentrations, H_2S is implied in potential therapeutic effects, such as neuromodulation [4], neuroprotection [5], vasodilation [6], insulin release [7], inflammation [8], angiogenesis [9,10] and cytoprotection [11–13]. H_2S was reported to be predominantly present in almost all examined tissues [14]. It is highly lipophilic and hence could penetrate cells by simple diffusion [15]. However, humans exposure to high concentrations of H_2S or to excessive amounts of particular drugs such as acetanilide, metoclopramide, phenacetin, dapsone, sulfanilamide-containing drugs, can trigger an increase in the physiological concentrations of sulfheme derivatives [16]. Michel et al. [17] showed the formation of an analogous compound upon interaction of oxyMb with H_2S and termed the complex sulfmyoglobin (sulfMb) [17–19]. Both, hemoglobin (Hb) and myoglobin (Mb) in the presence of oxygen (O_2) or hydrogen peroxide (H_2O_2) and H_2S generate sulfhemoglobin (sulfHb) and sulfMb, respectively. High levels of sulfHb and sulfMb alter the protein O_2 transport or storage functionalities, causing a condition known as sulfhemoglobinemia [20]. Apparently, in humans, the threshold between normal and toxic H_2S is equivalent to a relative change in sulfheme concentration from 5 μM to near 100 μM [21].

To understand this phenomena, the chemistry of H_2S has been explored targeting important hemeproteins, like Mb [17–19,22,23], Hb [24], and hemoglobin I (HbI) and mutants from *Lucina pectinata* [21,25–27] as well as catalase [18,28,29], lactoperoxidase (LPO) [30], and myeloperoxidase (MPO) [31]. Radioactive sulfide species demonstrated that a single sulfur atom is incorporated into the heme structure per mole of Mb to form sulfMb [32,33]. The insertion

resulted in a covalent heme modification by the specific incorporation of the sulfur atom across the β-β double bond of heme pyrrole B [27,34]. The sulfheme derivative shows a characteristic optical band around 620 nm and 717 nm, for the ferrous and ferric sulfMb, respectively. The band displacement depends on the type of the sulfheme isomer and, the heme-Fe oxidation and ligation states [19,22,34–37]. The relatively fast formation of sulfMb in the presence of H_2O_2 ($2.5\pm0.1 \times 10^6$ $M^{-1}s^{-1}$) [38] compared to the reaction between just H_2S and myoglobin ($1.6\pm0.3 \times 10^4$ $M^{-1}s^{-1}$) and hemoglobin (3.2×10^3 $M^{-1}s^{-1}$) [23] under aerobic conditions indicates an important role for the peroxide species to increase the reaction rate of sulfheme formation. Additionally, the inverse relationship between an increase in the rate of formation of sulfMb derivatives and the decrease in pH [17,23,38] suggests that H_2S rather than HS^- is the reactive sulfur species in the sulfheme reaction mechanism [21].

Curiously, there is a series of heme proteins that does not form sulfheme [25], for example, HbI from *L. pectinata,* which has Gln in the position 64. However, when glutamine in the 64 position of the protein (Gln64) was site directed mutated to histidine (His64), an optical band at 624 nm characteristic of sulfheme formation was observed. None of the other mutants produce this characteristic sulfheme band, not even the His68 mutant or Arg64. Similarly, resonance Raman shows the formation of satellites bands (1353 cm^{-1} and 1390 cm^{-1}) around the oxidation state marker ν_4, for Mb and the HbIGlnE7His mutant upon reaction with H_2O_2 and H_2S which is not present in the wild type HbI heme protein, indicating the presence of a distorted sulfheme chromophore. Also, these native proteins show two vinyl normal modes at 1620 cm^{-1} and 1626 cm^{-1}, however, upon formation of the sulfMb and sulfHbIGlnE7His mutant, the 1626 cm^{-1} vinyl band is absent. These results support the unique and crucial role that the E7 histidine in the distal site plays in the mechanism of sulfheme formation [21,25]. Given these experimental observations,

the function of the E7 His distal site in the reaction with H_2O_2 and H_2S to form met-aquosulfheme was explored by hybrid quantum mechanical/molecular mechanical methods. The calculations showed the reaction proceeded through the compound II oxo-ferryl intermediate interacting with a sulfide radical (•SH) with the consequent formation of met-aquosulfheme derivatives with a favorable energy drop of 140 kcal/mol [27], which stabilized the product. Under these circumstances, the formation of sulfheme is both kinetically and thermodynamically favorable. Attempts have also been made to understand the reverse reaction of the sulfheme derivatives to the native functional proteins, since apparently significant activation energy may be required to release the bound sulfur from the sulfheme pyrrole ring [18,22,32,39]. However, experiments show that photo-excitation of carboxysulfmyoglobin induced reconversion to MbCO, suggesting that the presence of an excited state may reduce the activation energy needed for the back reaction [22]. Chemically, the reconversion of sulfMb to native Mb has been observed upon reaction of these sulfheme derivatives with H_2O_2, O_2, cyanide (CN^-), sodium dithionite and excess of H_2S, $NaBH_4$, NaN_3, or strong alkaline solutions [18,32,39]. Also radioactive sulfide data demonstrated that sulfMb decomposes to protohemin, with first-order kinetics, to produce sulfate (SO_4^{2-}) as the major sulfide oxidation product [32].

Similar to Mb and Hb, LPO also forms sulfheme [30]. LPO is a mammalian heme peroxidase found in mammary, salivary, lachrymal and bronchial submucosal glands [40,41]. As a member of the innate immune stratagem its primary function is to produce antimicrobial oxidants to protect the host from invading pathogens [40,41]. In its biologically relevant activities LPO uses H_2O_2 to primarily catalyze the oxidation of inorganic thiocyanate (SCN^-) in two-electron oxidation processes to form hypothiocyanate. Alternatively, H_2O_2-mediated oxidation of organic substrates

such as phenols or aromatic amines can be catalyzed by LPO in two consecutive one-electron oxidation processes [42,43].

Structurally, in resting form, the heme group of LPO is in a six-coordinate high-spin aquo ferric state [44]. The distal active site has a histidine 225 and an arginine 327 residue, typical of peroxidases, [45,46] which are important in the formation and stabilization of oxo-ferryl intermediates [47]. Fig. 1A presents that the ferric hydroperoxo intermediate compound 0 (Fe(III)-O-OH Por), the oxo-ferryl intermediates compound I (Fe(IV)=O Por$^{\bullet+}$), and compound II (Fe(IV)-OH Por) are produced from the interaction of H_2O_2 with heme peroxidases by a multistep mechanism [47–50]. At first H_2O_2 binds to oxidize the ferric heme to produce the porphyrin cation radical and a molecule of water. Then a reducing substrate (AH_2) delivers one electron to this derivative to form compound II and a substrate radical (•AH). The enzyme returns to the resting state when compound II is reduced by a second substrate molecule, generating another radical species and a second molecule of water. In the presence of superoxide and excess H_2O_2, LPO forms compound III (ferric-superoxide/ferrous-dioxygen complex) state (Fe(III)-$O_2^{\bullet-}$ Por/Fe(II)-O_2 Por) [49–51]. Fig. 1B shows that a more direct route to compound III is achieved through the reaction between a ferrous heme and O_2. Compound III then can accept a proton and an electron, which leads to the subsequent formation of compound 0 [48].

Regarding the role of H_2S and ferryl intermediaries, it was suggested that LPO compound II interacts with H_2S producing a sulfheme derivative called sulfLPO [30]. The ferrous sulfLPO species has a characteristic band at approximately 638 nm while ferric sulfheme has the transition at 727 nm. In spite of these efforts, there is a need to generate new data that can help to further understand LPO sulfheme development. In this work, we show that: (1) Formation of ferrous sulfLPO and ferric sulfLPO derivatives are directly dependent of the presence of H_2S and

oxidizing agents, like H_2O_2 and O_2; (2) In the presence of oxidizing agents and H_2S, the 638 nm and 727 nm transitions show a continuous increase and decrease in their intensity until all H_2S is consumed, indicating that the turnover of sulfLPO to regenerate the native protein does not lead to any recovery of H_2S, and (3) The turnover of sulfLPO derivatives may lead to oxidized sulfur derivatives such as SO_4^{2-} or polysulfide's. Therefore, the results suggest that H_2S is a non-classical LPO substrate since it reversibly modifies the heme group, and EPR data shows that H_2S scavenges H_2O_2 without detectable formation of a carbon centered radical on the protein moiety globin chain. Surprisingly, horseradish peroxidase (HRP) upon reaction with O_2 or H_2O_2 in the presence of H_2S does not form sulfheme. A similar result is obtained upon the reaction of LPO with hydralazine. Furthermore, LPO sulfheme turnover is slower in the presence of O_2 than with H_2O_2, which together with the observed spectroscopic signatures indicate different sulfheme formation mechanisms in these systems. We propose alternative models to explain these observations.

2. Materials and Methods

All the reagents and proteins were purchased from Sigma-Aldrich unless otherwise indicated. LPO (Sigma type L-2005) was purchased as a lyophilized powder and HRP Type II (Sigma). The concentration of LPO and HRP were determined using the extinction coefficient ε_{412}=114 $mM^{-1}cm^{-1}$ and ε_{403}=102 $mM^{-1}cm^{-1}$. The H_2O_2 was obtained as a 30% solution. The working solutions were prepared using a 0.1 M KH_2PO_4/Na_2HPO_4 buffer. H_2S solutions were prepared daily from Na_2Sx9H_2O in tightly sealed ambar glass bottles. These solutions were diluted in the KH_2PO_4/Na_2HPO_4 buffer containing 1 mM ethylenediaminetetraacetic acid (EDTA). All other chemicals were ACS reagent grade or better.

2.1. UV-vis measurements of LPO reactions with O_2 and H_2O_2 in the presence of H_2S

The interactions of H_2S with LPO were measured with an Agilent 8453 spectrophotometer using sealed quartz cuvettes with septum (1cm path length). The reactions were made titrating 1 µL of the reagents with a gastight syringe into the sample in the cuvette. All the measurements were performed at 25 ^oC and pH 7.0 in 0.1 M KH_2PO_4/Na_2HPO_4 buffer. To evaluate the interactions of native LPO with H_2S in the presence of O_2, H_2S was added to the sample in a gastight syringe. In ferrous LPO, the buffer, Na_2Sx9H_2O, sodium dithionite (DT), and protein solutions were prepared anaerobically by degassing for 30 min and flushing with nitrogen for at least 20 min. To accomplish the reduction of LPO a seven fold excess of DT was added from a freshly prepared anaerobic stock solution. The reaction with H_2S was made when the DT was consumed, monitored by the absorbance decrease at 315 nm, and the LPO remains in the ferrous oxidation state. After the H_2S addition to LPO, the sample was purge for 1 min with O_2 and the associated spectral changes were obtained. The experimental turnover of sulfLPO was followed upon the reaction of LPO with 10.5 µM of H_2O_2 and 375 µM of H_2S. Initially, the formations of the ferryl species were obtained from the addition of three fold excess of H_2O_2 to native LPO. After two minutes, H_2S was added to the reaction. The spectral changes of the formation of 638 nm were observed for periods of 10 sec, 4 min, 6 min and 8 min. The reaction proceeds until the LPO returned to the electronic transition characteristics of the proteins' native state. Then a second aliquot of 21 µM of H_2O_2 was added to the sample leading to a new increase of the 638 nm intensity. The process was repeated several times until all H_2S was used and the reaction products are only related to the classical peroxidative reaction and the 638 nm band was completely absent.

2.2. UV-vis measurements of HRP reactions with H_2S

The interaction with 9.6 µM HRP was investigated by the addition of 29 µM H_2O_2 and the consequently addition 192 µM of H_2S. Initially the formations of the oxo-ferryl species were obtained from the addition of three fold excess of H_2O_2 to native HRP. After three minutes, H_2S was added to the reaction. The spectral changes were recorded at 5 seconds and 10 minutes. The reaction proceeds until the HRP returned to the native state. The interaction of 192 µM of H_2S to 9.6 µM HRP was performed under aerobic conditions. The spectra were taken at 5 minutes and 10 minutes.

2.3. Stopped-flow spectrophotometry of LPO aerobic and anaerobic reaction with H_2S

The interactions of native LPO with H_2S were measured using a π* 180 stopped-flow instrument from Applied Photophysics Inc. (Leatherhead, UK) equipped with a photodiode array detection. All measurements were performed at 25 ^oC and pH 7.0 in 0.1 M KH_2PO_4/Na_2HPO_4 buffer. H_2S interaction to native LPO was performed under but both aerobic and anaerobic conditions. These measurements were made by purging with nitrogen gas for at least 30 min the KH_2PO_4/Na_2HPO_4 buffer (0.1 M), H_2S, and protein solutions. Then 12 µM of native LPO sample and 560 µM H_2S solution were transported to the stopped-flow instrument in gas-tight syringes.

2.4. EPR spectroscopy of LPO reactions with H_2O_2 in the presence of H_2S

Electron paramagnetic resonance (EPR) measurements were carried out on a Varian E-112 spectrometer equipped with a TE_{102} cavity operating at X-band (9 Ghz) frequencies. The sample temperature was held at 77 K using an immersion finger dewar. EPR spectra were recorded using 1 mW microwave power, modulation amplitude 1.00 x 10.00 Gs, 0.5 s time constant and 2000

points. The samples were prepared at pH of 7 in 0.1 M KH_2PO_4/Na_2HPO_4 buffer. The different reactions of H_2S and H_2O_2 with LPO at 300 μM were made in sealed glass bottles and then 200 μL were immediately transferred into quartz EPR tubes (4 mm OD) and frozen in liquid nitrogen. Previously adding the solution, the EPR tube was degassed with N_2.

2.5. Measurement of sulfur derivatives, i.e. sulfate production, upon LPO turnover

The reaction was performed as described in section 2.1, here, after 3 and half hour of the turnover of LPO in the presence of H_2O_2 and H_2S, the sample was centrifuge for 30 thirty minutes in intervals of 10 minutes in a 10 kDa concentrator. The permeate fraction was recover to measure the sulfate production in the reaction following a procedure established in the literature [32]. The 900 μL aliquot was acidified with a conditioning reagent (450 μL) containing concentrated HCl. Barium sulfate was obtained as a precipitate by adding barium chloride to the solution. Then 1 mL of the solution was transferred to a quartz cuvette to measure the optical density at 420 nm. The concentration of sulfate was determined using a calibration curve previously made in a range concentration of 10 ppm – 80 ppm of sulfate with a 1,000 ppm sodium sulfate stock (see e.g. supplemental Fig. S1).

3. Results

3.1. Aerobic and anaerobic interactions of native and ferrous LPO with H_2S

Fig. 2A shows the classic UV-vis spectra of LPO in the native ferric state (dashed-dotted line), with characteristic transitions at 412 nm, 501 nm, 541 nm, 589 nm and 631 nm [49]. Upon addition of 150 μM H_2S under aerobic conditions, the Soret band shifts from 412 nm to 416 nm

and new bands appear at 547 nm, 587 nm, 638 nm and 727 nm (solid line). This first spectrum was recorded at 30 sec, with the subsequent spectra taken at 60 sec, 121 sec, 241 sec and 356 sec, respectively. Arrows indicate the spectral changes associated with the dominant increase in intensity of the 638 nm and 727 nm transitions, corresponding to ferrous sulfLPO and ferric sulfLPO sulfheme species, respectively based on literature data[30]. Interestingly, stopped-flow spectra presented in Fig. 2B (insert) show that under strict anaerobic conditions the addition of 280 μM H_2S to native LPO does not generate the formation of the dominant 638 nm and 727 nm sulfheme derivatives, indicating the need of molecular oxygen to produce these sulfLPO products. To further define the oxygen requirement for the reaction, ferrous LPO was reacted with sulfide with and without subsequent addition of oxygen to the reaction mixture. Fig. 3A shows the spectra of native ferric and ferrous LPO (dashed line) with Soret and Q bands at 412 nm and 501 nm, 541 nm, 589 nm and 631 nm and 444 nm and 561 nm and 593 nm, respectively [50]. The addition of 50 μM H_2S at 5 sec (gray line) and at 1 min (dotted line) to ferrous LPO show no spectral changes. However, subsequent addition of O_2 to this sample generates the species (bold line) dominated by the 638 nm transition. Notice, however, that the 727 nm band is not present in this Fig. 3A spectrum, since it is dominated by the ferrous LPO derivative. Fig. 3B presents a red shift of the Soret band upon the addition of 150 μM H_2S to native ferric LPO under anaerobic conditions and the appearance of two bands at 561 nm and 593 nm. These are characteristic to ferrous LPO indicating sulfide-mediated reduction of ferric LPO to ferrous LPO. Notice, that the spectrum did not show a complete transition of the native ferric LPO to the ferrous state under these conditions. Consistent with this, subsequent addition of O_2 (Fig. 3B inset) results in bands at 416 nm, 547 nm, 587 nm, 638 nm and 727 nm, indicating the formation of both ferric- and ferrous-sulfLPO. Through time, the ferrous and ferric sulfLPO bands decrease in intensity and the protein returns to

the native state. Overall, the data indicate that for LPO the formation of the 638 nm and 727 nm derivative directly depends on the presence of both O_2 and H_2S, leading to the conclusion that under oxidative conditions LPO forms the corresponding sulfLPO derivatives in line with a previous proposal [30].

3.2. Reaction of LPO with H_2O_2 in the presence of H_2S

Fig. 4A presents the characteristic band displacements from native ferric LPO (solid line), with transitions 412 nm, 501 nm, 541 nm, 589 nm and 631 nm to ferryl heme derivative (430 nm, 535 nm and 567 nm), where compound II is accumulated upon reaction of LPO with an excess of H_2O_2 (dashed line) [49]. The addition of 375 μM H_2S to this sample generates both the ferrous and ferric sulfLPO derivative (bold line) with absorbance peaks at 424 nm, 547 nm, 587 nm, 638 nm and 727 nm. The transitions are identical to those present in the reaction, under aerobic conditions, between native LPO and H_2S (Fig. 2A). Here, the 631 nm transition of the LPO native state has very low intensity or is almost absent, while the 638 nm dominates this spectral region. Subsequent spectra, without further addition of H_2S (which regardless remains in excess), at 4 min (dashed dotted line) and 8 min (dotted line) show a shift of the Soret band from 424 nm to 416 nm, the Q bands at 547 nm and 587 nm remain constant and the intensity of the 638 nm band decreases with a concomitant slight increase at 727 nm. Through time the native state transitions appear, indicating that the protein has consumed all available H_2O_2 and returned to the original state, which was observed in the presence of excess H_2S (i.e. representing a mixture of ferrous and ferric LPO derivatives). Upon addition of a second aliquot of 21 μM H_2O_2, without the addition of more H_2S, Fig. 4A shows again the formation of sulfLPO (gray bold line) transitions at 638 nm and 727 nm, which once more decreases with time. This behavior is repeated each time an aliquot of H_2O_2 was

added to the protein-sulfide mixture, for a total period of 1500 sec, until all the H_2S was consumed as indicated by the absence of the ferrous and ferric sulfLPO bands at the longest time point. Overall, the data in Fig. 4A shows that the turnover of the 638 nm and 727 nm species are directly dependent on both H_2O_2 and H_2S. Fig. 4B shows consecutive increase and decrease periods in the 638 band upon addition of H_2O_2 aliquots and subsequent short incubation times, indicating constant turnover of LPO via sulfLPO at excess H_2S. Each new jump is the addition of another aliquot of H_2O_2 to the recovered LPO spectrum in the presence of the remaining H_2S. When all the H_2S has been consumed the remaining absorption spectrum belongs to native LPO. The experiment was reproduced several times using different incubation times, with similar results (see e.g. supplemental Fig. S2). These LPO turnovers indicate that the formation of ferrous and ferric sulfLPO derivatives is a reversible process and does not result in the recovery of H_2S from the sulfheme species, rather induce catalytic oxidation of sulfide.

3.3. Reaction of LPO with H_2O_2 and hydralazine

Comprehensive analyses of the catalytic cycles of MPO with H_2S indicated no sulfheme formation during MPO turnover, but the Compound III state was found to be the central intermediate species in that system with similar UV-vis characteristics to sulfheme species [52]. It was also found that hydralazine oxidation by MPO proceeds via the Compound III state in the absence of sulfide. Compound III of LPO has a completely different spectral signature than the sulfheme of LPO. The Soret band of LPO Compound III is at 423 nm with two intensive bands in the visible range at 550 nm and 584 nm [50,53]. Whereas the sulfheme in LPO shows two intensive bands in the visible range at 638 nm and 727 nm [30]. Therefore, we investigated whether hydralazine oxidation by LPO catalyzed processes would induce similar spectral changes in the

electronic spectra to the sulfheme derivatives of LPO. Fig. 5 shows the interaction of native ferric LPO with hydralazine in the presence of H_2O_2. Ferric LPO interacts with H_2O_2 to generate the oxo-ferryl intermediate species compound II with transitions at 430 nm, 535 nm, 567 nm and 589 nm (dash line). The addition of hydralazine to the system returned the protein to the native state represented by the 412 nm, 501 nm, 541 nm, 589 nm and 631 nm transitions (solid line), without any transient change in absorbance at 638 or 727 nm. This result indicates that hydralazine acts as a substrate and reacts with the oxo-ferryl intermediates by donating electrons to compound II and return LPO to its ferric form. In addition, the absence of the formation of the 638 and 727 nm bands support the notion that these electronic transitions are characteristic of sulfLPO.

3.4. Interactions of Horseradish peroxidase with H_2S

To get further insight into the similarities and differences of peroxidase catalyzed oxidation of sulfide focusing on sulfheme formation, we also investigated the interactions of horseradish peroxidase with sulfide. Fig. 6A presents the typical peaks of metaquo-HRP at 403 nm, 495 nm and 641 nm [54]. The addition of H_2O_2 leads to a mixture of the oxo-ferryl intermediates, compound I and compound II with bands at 407 nm, 527 nm, 552 nm and 646 nm. Contrary to LPO and MPO, upon addition of H_2S to the reaction mixture the majority of the protein returns to the native ferric state, without any indication of sulfHRP formation. In other words, HRP did not show in any moment the classical 638 nm or 620 nm band, which can be attributed to the formation of the sulfheme derivative. Therefore, it is likely that sulfheme formation at the HRP heme is not favorable. Moreover, under anaerobic conditions the addition of H_2S to HRP triggers no spectral changes as indicated in Fig. 6B, suggesting that the protein remains in the native ferric state and the heme may not react with H_2S.

3.5. EPR measurements for the reaction of LPO with H_2O_2 in the presence of H_2S

Fig. 7 shows the spectra of LPO reacting with H_2O_2 in the presence of two different concentrations of H_2S. Fig. 7a shows the EPR spectrum of LPO in buffer solution, while Fig. 7b demonstrates the EPR spectrum, upon the addition of three fold excess of H_2O_2, where a high-spin ferric iron signal and a free radical peak at 2.004 g were observed. The reactions of LPO with H_2O_2 and the subsequent addition of H_2S were carried out at two different concentration ratios: LPO:H_2O_2:H_2S equivalent to 1:3:1 (Fig. 7c) and 1:3:50 (Fig. 7d). At the lower concentration of H_2S (Fig. 7c) the spectrum only shows a high-spin Fe(III) signal and it does not show the free radical peak at 2.004 g. This observation not necessarily means that the radical is not generated; alternatively the radical may have a lifetime which is too short to be trapped in the timescale of sample mixing and freezing. At 50 fold excess of H_2S the spectrum (Fig. 7d) only shows a weak low-spin Fe(III) signal.

The free radical peak with the obtained g value of 2.004 upon addition of H_2O_2 to LPO is characteristic of a carbon centered radical. Previously this radical was suggested to be a tyrosyl radical derived from oxo-ferryl intermediates [55]. The high-spin ferric signal remains transiently stable during LPO cycling in the presence of H_2O_2. The addition of 300 µM of H_2S to the reaction mixture (300 µM LPO and 900 µM H_2O_2) vanishes the amino acids radical peak at 2.004 g. The observed high-spin ferric signal is most likely the result of H_2S consumption by the excess H_2O_2. In Fig. 7d, a low-spin ferric signal at 2.27 g appears in the spectrum following the addition of an excess sulfide (15000 µM) to a similar mixture of LPO and H_2O_2. Based on the observed and reported [56] characteristic UV-vis bands at 727 nm, 416 nm, 547 nm and 587 (Fig. 4A) in a similar reaction mixture this peak can tentatively be assigned to a sulfLPO-Fe(III)-oxygen

complex. In agreement with this assignment, the observed g-value of 2.27 is similar to those reported for oxygenated Mb, HRP and chloroperoxidase species [57]. The relatively low intensity of the signal is in line with formation of a mixture of ferrous (EPR silent) and ferric sulfLPO under these conditions. This ferrous contribution was also observed by UV-vis spectrophotometry with a characteristic band at 638 nm. Moreover, similar to the observations at the lower H_2S concentration (300 µM), the EPR spectra at 15000 µM of H_2S also did not contain any detectable peak in the 2.004 g region. Again, this does not necessarily mean that it is not formed, but it is not detectable on the timescale of the freezing of the sample after the reactants are mixed. Independently, the data shows the impact of H_2S in the observable amino acid radical at 2.004 g of the reaction of LPO and H_2O_2 (Fig. 7b) since upon addition of H_2S the amino acid radical is not observable (Fig. 7c and 7d).

3.6. Products of LPO-sulfLPO turnover

We made an attempt to obtain some insight into the nature of the sulfide oxidation products as a result of LPO-sulfLPO turnover. Motivated by the data which demonstrated that sulfheme decomposes to protohemin, with first-order kinetics to produce SO_4^{2-} as the major product [32], we tried to semi quantitatively investigate sulfate production in the H_2S-H_2O_2-LPO system. Fig. 8A shows an increase in sulfate production as a function of the initial sulfide concentration at 5 µM native LPO and 25 µM H_2O_2 using three different concentration of H_2S: 600 µM (black), 800 µM (dark gray) and 1000 µM (gray), respectively. The experiment was repeated at 50 µM H_2O_2 (Fig. B, insert), where a similar trend was observed, the amount of detected sulfate increases as function of the H_2S concentration. Alternatively polysulfides can also be formed in these systems as in the case of MPO [52], which upon acidification would result in S_8 precipitation and an

increase in turbidity [58–60]. Thus, there is a need for additional experiments to determine the potential presence of sulfane sulfur species in order to better understand the mechanism of LPO-mediated sulfide oxidation.

4. Discussion

The reactions of H_2S with hemeproteins in the presence of O_2 and H_2O_2 have been extensively studied resulting in distinct models to explain sulfheme chemistry [18,19,21,25,27,32,52,61]. Although several mechanistic aspects of sulfheme formation remain unknown, there is sufficient experimental evidence to provide insight into the characteristics of sulfheme generation. For example, the orientation and position of the His residue at the heme active site is crucial for the production of the sulfheme product [25]. Thus, with the exception of a limited group of heme proteins, such as cytochrome *c* oxidase [62], HRP ([18] and this work), MPO [52] and the phosphodiesterase His mutant (Ec DOS-PAS Met95His) [63] (which do not form sulfheme, the distal His seems to be essential for the formation of the heme modification [21,25]. These observations and the tautomeric nature of distal His [64,65] are in agreement with the Fig. 1A and 1B showing the importance of LPO histidine protonation toward the formation of compound 0 and compound III, in the ferryl heme O−O bond cleavage, under two different scenarios dominated by H_2O_2 and O_2, respectively [48].

4.1. Insight into the LPO reactions with H_2S in the presence and absence of O_2

The reaction of native LPO under anaerobic conditions present the reduction of the LPO heme iron by excess of H_2S, as in other met-aquoheme proteins due to the hydrogen bonding environment, and no band at 638 nm or 620 nm are observed. Curiously, both, in native and ferrous

LPO reaction with H_2S in the absence of O_2, the UV-vis spectrum remains unaltered indicating that H_2S does not bind directly to the iron. However in the reaction of native and ferrous LPO with H_2S in the presence of oxygen, generates products with UV-vis peaks at 638 nm and 727 nm which have been assigned previously to the ferrous sulfheme and ferric sulfheme derivative, respectively [30]. Furthermore in Mb and Hb sulfheme derivatives show a 620 nm and 717 nm transition with the same O_2 and H_2S dependence but with a very slow turnover to the native protein [17–19,24,35,39]. In this Q region, the optical spectra of sulfLPO is very similar to sulfMb and sulfHb strongly suggesting that the modification in the heme group is a chlorin type structure in which the sulfur atom is incorporated across the β-β double bond of the pyrrole B [30,61,66]. The data indicate that in the presence of O_2, H_2S modifies directly the LPO heme group producing ferrous sulfLPO and ferric sulfLPO species, while species such as SCN^-, Br^- and Cl^-, do not result in altered UV-vis spectra [67]. Therefore, the observations and the data presented experimentally, in Fig. 2 and Fig, 3 support the discussion that the ferrous sulfLPO and ferric sulfLPO derivatives return slowly to native LPO. Thus, H_2S in the presence of O_2 is a non-classical LPO substrate that forms the sulfheme derivative which then subsequently turns over to generate the native LPO heme. Therefore, H_2S in the presence of O_2 does not lead to an irreversible inhibition of the LPO enzymes, as is the case with other sulfur derivatives such as MMI [68].

4.2. Insights into the LPO reactions with H_2O_2 in the presence of H_2S

Fig. 4A presents the UV-vis spectra of LPO reactions with H_2O_2 in the presence of H_2S and, analogous to the oxygen scenario, the Q region is dominated by the 638 nm transition. Similarly, Fig. 4B, shows the same behavior in the transition upon formation of sulfheme. Regarding this, Fig. 4A demonstrates the changes in the intensity of the 638 nm transition, ferrous

sulfheme LPO, as consumes H_2O_2 in the presence of an H_2S excess. At the end point of the reaction, additional H_2O_2 was added until all of the H_2S was consumed and the classical peroxidative reaction was observed (Fig. 4B). This behavior suggests that the 638 nm species or sulfLPO does not lead to any H_2S generation or transport mechanism, rather, H_2S in LPO acts as a substrate to scavenge excess of H_2O_2 protecting the enzyme from the classical peroxidative reactions. These in vitro results indicates that H_2S can regulate the reactive oxygen species (ROS) produced by the excess of H_2O_2 thus protecting the turnover of LPO. This observation is supported by the data in Fig. 7, which indicates a significant difference between the EPR spectra of LPO plus H_2O_2 in the absence of H_2S (Fig. 7b) and with H_2S added (Figs. 7c and 7d). Under this scenario, LPO EPR results show that during the sulfheme turnover, there is not an observable aromatic amino acids radical formation or that the radical lifetime is too short to allow its trapping upon sample freezing after mixing. Apparently, H_2S can scavenge H_2O_2 without the presence of any carbon center radicals protecting also the LPO system.

Interestingly, HRP, under the same conditions, does not form sulfheme. Fig. 6 shows that H_2S, similar to other heme proteins, inactivates the HPR. However, under identical condition, LPO shows a continuous turnover. Nevertheless, both peroxidases do not bind H_2S to the ferric iron. The distal environments in these peroxidases are very selective to the substrates that bind to the iron. Structurally, Fig. 9 shows both LPO and HRP have a His and Arg in their active site, which are important for their enzymatic activity, but only the former generates sulfheme, while the latter does not [21]. Furthermore, under the same oxidative conditions, H_2S allows LPO to turnover, while HRP does not show the same behavior. This exclusive behavior and the fine tuning of the His, Arg and the heme iron centers generates two completely different scenarios. The crystallographic data in Fig. 9 shows the distances between the His, Arg and the heme iron. In the

case of His is shorter in LPO (4.94 Å), as opposed to HRP (5.99 Å), while Arg case are 7.59 Å and 5.76 Å, respectively, being the former longer that the latter. The data indicate that orientation and position of the His residue at the heme active site are crucial for the synthesis of the sulfheme product. The importance of this His residue is also supported by site-directed mutagenesis in a hemoglobin I, where His 64 replacement with Arg led to the inhibition of sulfheme formation [21,25]. On the other hand the interaction of LPO with H_2O_2 and hydralazine does not generate the 638 nm band and the hydralazine in LPO acts as a classical peroxidase substrate returning the protein to the native ferric state.

4.3. Events in the turnover of sulfLPO-LPO

Early on [30] it was suggested that lactoperoxidase in the ferryl state (compound II) reacts with sulfide to form a typical sulfheme-containing hemeprotein. Despite this mechanism being supported today by several groups in the field of typical sulfheme-containing hemeproteins such as Hb, Mb, and catalase, there is the need to explain why H_2S does not inactivate the enzyme as observed by other sulfur derivatives [17–19,21,24,28,30]. The process of reversion of sulfheme to the native proteins is not new and has been observed in proteins such as Mb, Hb, and catalase under a diversity of oxidizing and reducing agents [18,39,69]. However, it is interesting that under oxidative conditions and H_2S (Figs. 3 and 4), LPO continues its function until all the H_2S is consumed and the classical peroxidative reaction dominates. Thus, the LPO-sulfLPO turnover process does not lead to any H_2S regeneration or transport mechanism.

Curiously, aromatic desulfurization reaction has been studied for many years and literature has been generated on the subject [70–72] indicating for example, that the desulfurization of alkyl and organic aromatic sulfides in the presence of oxidizing agents, like O_2 and H_2O_2, leads to the

production of sulfate [73,74]. In fact, an early work in sulfMb, using radioactive ^{35}S indicated that the decomposition of the isolated sulfheme produces sulfate as the major product, while H_2S, SO_2 and elemental sulfur were ruled out as possible products[32]. Regarding this, Fig. 8 showed an increase in sulfate production after the disappearance of sulfLPO formed upon the interaction of 5 µM native LPO with 25 µM and 50 µM H_2O_2 and three different concentration of H_2S 600 µM (black), 800 µM (dark gray) and 1000 µM (gray), respectively. The results show the same behavior, the amount of detected sulfate increases as function of the H_2S concentration. Overall the results indicate that approximately 20% of the initially added H_2S converts to sulfate. Although it cannot be discerned the direct contributions to the total SO_4^{2-} comes from the reaction H_2O_2 and H_2S or from the turnover of sulfLPO [75]. Furthermore other sulfur species that are also produced [58–60]. Thus, there is a need for additional experiments to determine the products and mechanism of sulfur species generated by the turnover of sulfLPO. Additional turnover reactions which produce oxidized sulfur species could generate polysulfides [12,23,58,76,77]. Thus, the suggestion that desulfurization of the sulfLPO can generate only SO_4^{2-} and native LPO, needs further quantitative studies with more precise techniques other than Ba_2SO_4 precipitation. However, the desulfuration process of heme to generate LPO from sulfLPO, the turnover process is faster in LPO that Mb and Hb suggesting that the positively charged arginine in the heme pocked of LPO facilitates the desulfurization of sulfLPO returning the protein to its native state.

4.4. Formation of sulfheme by H_2S and under different oxidative conditions

The reactions between LPO with H_2S in the presence of O_2 or H_2O_2 show different formation rates to sulfheme. This suggests (Fig. 10) that the rate determining step of sulfheme formation in the presence O_2 is the formation of compound III, while with H_2O_2 it is the formation

of heme compound 0. For example, Fig. 10 B shows the reaction pathway form sulfLPO based on recent DFT/MM potential energy scans method coupled to the CHARMM force field in the doublet, quartet and sextet states indicated that hydrogen transfer from H_2S to Fe(III)-H_2O_2 complex results in homolytic cleavage of the O-O and S-H bond to form •SH, ferryl heme compound II, and a water molecule [27]. Subsequent addition of •SH to pyrrole B carbon of the heme compound II specie leads to a metastable ring-opened episulfide, which become the 3-membered episulfide ring and met-aquo Fe (III). Finally, the 5-membered thiochlorin structure is formed from the 3-membered episulfide ring with very favorable energy drop of 140 kcal/mol [27]. Overall, these results are in agreement with a wide range of experimental NMR data [61]. Fig. 10A shows that intermediates in sulfheme formation can be postulated based on recent work on LPO indicating that compound III (Fe(III)-$O_2^{\bullet-}$ Por) accepts the transfer of an electron and a proton from His 109 (Fig. 1), to form heme compound 0 (Fig. 1B) [48]. Given this observation and taking in consideration the ability of H_2S to undergo homolytic cleavage [27], the route to sulfLPO from native LPO and H_2S in the presence of O_2 is very possible through the compound III intermediate. Here, in Fig 10A, compound III accepts an electron and a proton from H_2S, the substrate, leading to the formation of compound I (*via* Fig. 1B), water and •SH. The downhill reaction, similar to these two radical species, compound I and •SH, leads to the subsequent formation of sulfLPO. Since oxyMb also forms compound III [48,78] and previous studies suggest that the •SH radical is involved in the sulfheme derivative [18,21,25–27], maybe in the case compound III triggers the formation •SH, which interact with the porphyrin ring as the route for the sulfheme formation in the presence of O_2. Apparently, in the mechanism for the sulfheme derivative formation either with O_2 or H_2O_2, the rate limiting step is the generation of compound III or compound 0, respectively.

4.5. Physiological Relevance of LPO and sulfLPO turnover

The *in vivo* significance of the *in vitro* results presented here will require further research regarding: (1) the biological reversibility of LPO and sulfLPO and the role that H_2S may play in scavenging H_2O_2 and preventing the generation carbon center radical in the LPO system; and (2) the possibility of SO_4^{2-} and other sulfur species as possible product of the turnover. The observations that H_2S is required in both of these circumstances and that H_2S is not a product of the reaction are consistent with the physiological functions of LPO and H_2S as anti-inflammatory agents in airways [79]. This can be due to the action of H_2S as a substrate to reverse the LPO inhibition caused by the high levels of H_2O_2 in inflammation sites [80]. The *in vitro* H_2O_2 depletion in the LPO to sulfheme LPO conversion opens a route to explore the *in vivo* prevention of the toxic effects of H_2O_2 in patients with asthma and COPD and the relationship between LPO and CBS and CSE enzymes in the antioxidant nature of H_2S. On the other hand, from the toxic view of H_2S scenarios [76], the primary entrance of H_2S to the body is through the human airway and upon exposure to relatively high concentrations of H_2S, LPO can use sulfLPO turnover as a "sink" for H_2S to protect human body to certain degree from ROS and sulfide toxicity.

Acknowledgements

This work was supported in part by NIH-RISE (Grant R25GM088023) and the National Science Foundation (Grant 0843608 to JLG and CHE-1213550 to GJG). We thank Dr. Syun-Ru Yeh for the stopped-flow instrument use and Ariel Lewis-Ballester for the assistance with it. Also we thank Beatriz Muñoz and Darya Marchany for the assistance.

References

[1] S. Singh, R. Banerjee, PLP-dependent H2S biogenesis, Biochim. Biophys. Acta. 1814 (2011) 1518–1527.

[2] O. Kabil, R. Banerjee, Enzymology of H2S biogenesis, decay and signaling, Antioxid. Redox Signal. 20 (2014) 770–782.

[3] S. Tang, D. Huang, N. An, D. Chen, D. Zhao, A novel pathway for the production of H2S by DAO in ratjejunum, Neurogastroenterol Motil. 28 (2016) 687–692.

[4] K. Abe, H. Kimura, The possible role of hydrogen sulfide as an endogenous neuromodulator., Off. J. Soc. Neurosci. 16 (1996) 1066–1071.

[5] X. Zhang, J.S. Bian, Hydrogen sulfide: A neuromodulator and neuroprotectant in the central nervous system, ACS Chem. Neurosci. 5 (2014) 876–883. doi:10.1021/cn500185g.

[6] M. Bucci, A. Papapetropoulos, V. Vellecco, Z. Zhou, A. Zaid, P. Giannogonas, A. Cantalupo, S. Dhayade, K.P. Karalis, R. Wang, R. Feil, G. Cirino, cGMP-Dependent Protein Kinase Contributes to Hydrogen Sulfide-Stimulated Vasorelaxation, PLoS One. 7 (2012). doi:10.1371/journal.pone.0053319.

[7] G. Tang, L. Zhang, G. Yang, L. Wu, R. Wang, Hydrogen sulfide-induced inhibition of L-type Ca2+ channels and insulin secretion in mouse pancreatic beta cells, Diabetologia. 56 (2013) 533–541. doi:10.1007/s00125-012-2806-8.

[8] J.L. Wallace, J.G.P. Ferraz, M.N. Muscara, Hydrogen sulfide: an endogenous mediator of resolution of inflammation and injury., Antioxid. Redox Signal. 17 (2012) 58–67. doi:10.1089/ars.2011.4351.

[9] A. Papapetropoulos, A. Pyriochou, Z. Altaany, G. Yang, A. Marazioti, Z. Zhou, M.G. Jeschke, L.K. Branski, D.N. Herndon, R. Wang, C. Szabó, Hydrogen sulfide is an endogenous stimulator of angiogenesis., Proc. Natl. Acad. Sci. U. S. A. 106 (2009) 21972–21977. doi:10.1073/pnas.0908047106.

[10] C. Szabó, A. Papapetropoulos, Hydrogen sulphide and angiogenesis: Mechanisms and applications, Br. J. Pharmacol. 164 (2011) 853–865. doi:10.1111/j.1476-5381.2010.01191.x.

[11] V. Yadav, X.-H. Gao, B. Willard, M. Hatzoglou, R. Banerjee, O. Kabil, Hydrogen sulfide modulates eukaryotic translation initiation factor 2? (eIF2?) phosphorylation status in the integrated stress response pathway, J. Biol. Chem. 292 (2017) 13143–13153.

[12] H. Kimura, Hydrogen sulfide and polysulfides as signaling molecules, Proc. Jpn. Acad. Ser. B. Phys. Biol. Sci. 91 (2015) 131–159.

[13] S. Panthi, H.J. Chung, J. Jung, N.Y. Jeong, Physiological importance of hydrogen sulfide: Emerging potent neuroprotector and neuromodulator, Oxid. Med. Cell. Longev. 2016 (2016). doi:10.1155/2016/9049782.

[14] E.A. Wintner, T.L. Deckwerth, W. Langston, A. Bengtsson, D. Leviten, P. Hill, M.A. Insko, R. Dumpit, E. Vandenekart, C.F. Toombs, C. Szabo, A monobromobimane-based assay to measure the pharmacokinetic profile of reactive sulphide species in blood, Br. J. Pharmacol. 160 (2010) 941–957. doi:10.1111/j.1476-5381.2010.00704.x.

[15] J.C. Mathai, A. Missner, P. Kugler, S.M. Saparov, M.L. Zeidel, J.K. Lee, P. Pohl, No facilitator required for membrane transport of hydrogen sulfide, Proc. Natl. Acad. Sci. 106

(2009) 16633–16638. doi:10.1073/pnas.0902952106.

[16] M. Whiteman, S. Le Trionnaire, M. Chopra, B. Fox, J. Whatmore, Emerging role of hydrogen sulfide in health and disease: critical appraisal of biomarkers and pharmacological tools, Clin. Sci. (Lond). 121 (2011) 459–488.

[17] B.Y.H. Michel, A study of sulfhemoglobin, J. Biol. Chem. 126 (1938) 323–348.

[18] P. Nicholls, The formation and properties of sulphmyoglobin and sulphcatalase, Biochem. J. 81 (1961) 374–383.

[19] J.A. Berzofsky, J. Peisach, W.E. Blumberg, Sulfheme Proteins. I. Optical and magnetic properties of sulfmyoglobin and its derivatives, J. Biol. Chem. 246 (1971) 3367–3377.

[20] R. Pietri, E. Román-Morales, J. López-Garriga, Hydrogen sulfide and hemeproteins: knowledge and mysteries, Antioxid. Redox Signal. 15 (2011) 393–404.

[21] B.B. Ríos-González, E.M. Román-Morales, R. Pietri, J. López-Garriga, Hydrogen sulfide activation in hemeproteins: The sulfheme scenario, J. Inorg. Biochem. 133 (2014) 78–86.

[22] J.A. Berzofsky, J. Peisach, J.O. Albem, Sulfheme Proteins III. Carboxysulfmyoglobin: the relation between electron withdrawal from iron and ligand binding, J. Biol. Chem. 247 (1972) 3774–3782.

[23] T. Bostelaar, V. Vitvitsky, J. Kumutima, B.E. Lewis, P.K. Yadav, T.C. Brunold, M. Filipovic, N. Lehnert, T.L. Stemmler, R. Banerjee, Hydrogen sulfide oxidation by myoglobin, J. Am. Chem. Soc. 138 (2016) 8476–8488. doi:10.1021/jacs.6b03456.

[24] R.J. Carrico, W.E. Blumberg, J. Peisach, The reversible binding of oxygen to

sulfhemoglobin, J. Biol. Chem. 253 (1978) 7212–7215.

[25] E. Román-Morales, R. Pietri, B. Ramos-Santana, S.N. Vinogradov, A. Lewis-Ballester, J. López-Garriga, Structural determinants for the formation of sulfhemeprotein complexes, Biochem. Biophys. Res. Commun. 400 (2010) 489–492.

[26] R. Pietri, A. Lewis, R.G. León, G. Casabona, L. Kiger, S.-R. Yeh, S. Fernandez-Alberti, M.C. Marden, C.L. Cadilla, J. López-Garriga, Factors controlling the reactivity of hydrogen sulfide with hemeproteins, Biochemistry. 48 (2009) 4881–4894.

[27] H.D. Arbelo-Lopez, N.A. Simakov, J.C. Smith, J. Lopez-Garriga, T. Wymore, Homolytic cleavage of both heme-bound hydrogen peroxide and hydrogen sulfide leads to the formation of sulfheme, J. Phys. Chem. B. 120 (2016) 7319–7331. doi:10.1021/acs.jpcb.6b02839.

[28] D. Padovani, A. Hessani, F.T. Castillo, G. Liot, M. Andriamihaja, A. Lan, C. Pilati, F. Blachier, S. Sen, E. Galardon, I. Artaud, Sulfheme formation during homocysteine S-oxygenation by catalase in cancers and neurodegenerative diseases, Nat. Commun. 7 (2016) 13386. doi:10.1038/ncomms13386.

[29] K.R. Olson, Y. Gao, E.R. DeLeon, M. Arif, F. Arif, N. Arora, K.D. Straub, Catalase as a sulfide-sulfur oxido-reductase: An ancient (and modern?) regulator of reactive sulfur species (RSS), Redox Biol. 12 (2017) 325–339. doi:10.1016/j.redox.2017.02.021.

[30] S. Nakamura, M. Nakamura, I. Yamazaki, M. Morrison, Reactions of ferryl lactoperoxidase (compound II) with sulfide and sulfhydryl compounds, J. Biol. Chem. 259 (1984) 7080–7085.

[31] Z. Pálinkás, P.G. Furtmüller, A. Nagy, C. Jakopitsch, K.F. Pirker, M. Magierowski, K. Jasnos, J.L. Wallace, C. Obinger, P. Nagy, Interactions of hydrogen sulfide with myeloperoxidase, Br. J. Pharmacol. 172 (2015) 1516–1532.

[32] J.A. Berzofsky, J. Peisach, B.L. Horecker, Sulfheme Proteins IV. The stoichiometry of sulfur incorporation and the isolation of sulfhemin, the prosthetic group of sulfmyoglobin, J. Biol. Chem. 247 (1972) 3783–3791.

[33] S. V Evans, B.P. Sishta, A.G. Mauk, G.D. Brayer, Three-dimensional structure of cyanomet-sulfmyoglobin C., Proc. Natl. Acad. Sci. U. S. A. 91 (1994) 4723–4726.

[34] M.J. Chatfield, G.N. La Mar, R.J. Kauten, Proton NMR characterization of isomeric sulfmyoglobins: preparation, interconversion, reactivity patterns, and structural features, Biochemistry. 26 (1987) 6939–6950.

[35] J.A. Berzofsky, J. Peisach, W.E. Blumberg, Sulfheme Proteins II. The reversible oxygenation of ferrous sulfmyoglobin, J. Biol. Chem. 246 (1971) 7366–7372.

[36] R. Timkovich, M.R. Vavra, Proton NMR spectroscopy of sulfmyoglobin, Biochemistry. 24 (1985) 5189–5196.

[37] L.L. Bondoc, M.H. Chau, M.A. Price, R. Timkovich, Structure of a stable form of sulfheme, Biochemistry. 25 (1986) 8458–8466.

[38] S.H. Libardi, H. Pindstrup, D.R. Cardoso, L.H. Skibsted, Reduction of ferrylmyoglobin by hydrogen sulfide. Kinetics in relation to meat greening, J. Agric. Food Chem. 61 (2013) 2883–2888.

[39] E.A. Johnson, The reversion to haemoglobin of sulphhaemoglobin and its coordination

derivatives, Biochim. Biophys. Acta - Protein Struct. 207 (1970) 30–40.

[40] K.D. Kussendrager, A.C. Van Hooijdonk, Lactoperoxidase: physico-chemical properties, occurrence, mechanism of action and applications, Br. J. Nutr. 84 Suppl 1 (2000) S19–S25.

[41] C. Wijkstrom-Frei, S. El-Chemaly, R. Ali-Rachedi, C. Gerson, M. a Cobas, R. Forteza, M. Salathe, G.E. Conner, Lactoperoxidase and human airway host defense, Am. J. Respir. Cell Mol. Biol. 29 (2003) 206–212.

[42] A.K. Singh, N. Pandey, M. Sinha, P. Kaur, S. Sharma, T.P. Singh, Structural evidence for the order of preference of inorganic substrates in mammalian heme peroxidases: Crystal structure of the complex of lactoperoxidase with four inorganic substrates, SCN -, I -, Br - and Cl -, Int. J. Biochem. Mol. Biol. 2 (2011) 328–339.

[43] S. Sharma, A.K. Singh, S. Kaushik, M. Sinha, R.P. Singh, P. Sharma, H. Sirohi, P. Kaur, T.P. Singh, Lactoperoxidase: structural insights into the function,ligand binding and inhibition, Int. J. Biochem. Mol. Biol. 4 (2013) 108–128.

[44] G. Sievers, Structure of milk lactoperoxidase. A study using circular dichroism and difference absorption spectroscopy, Biochim. Biophys. Acta. 624 (1980) 249–259.

[45] P.G. Furtmuller, M. Zederbauer, W. Jantschko, J. Helm, M. Bogner, C. Jakopitsch, C. Obinger, Active site structure and catalytic mechanisms of human peroxidases, Arch. Biochem. Biophys. 445 (2006) 199–213.

[46] A.K. Singh, N. Singh, S. Sharma, S.B. Singh, P. Kaur, A. Bhushan, A. Srinivasan, T.P. Singh, Crystal structure of lactoperoxidase at 2.4 A resolution, J. Mol. Biol. 376 (2008)

1060–1075.

[47] G. Battistuzzi, M. Bellei, C.A. Bortolotti, M. Sola, Redox properties of heme peroxidases, Arch. Biochem. Biophys. 500 (2010) 21–36.

[48] P.J. Mak, W. Thammawichai, D. Wiedenhoeft, J.R. Kincaid, Resonance Raman spectroscopy reveals pH-dependent active site structural changes of lactoperoxidase compound 0 and its ferryl heme O-O bond cleavage products, J. Am. Chem. Soc. 137 (2015) 349–361.

[49] E. Ghibaudi, E. Laurenti, Unraveling the catalytic mechanism of lactoperoxidase and myeloperoxidase: A reflection on some controversial features, Eur. J. Biochem. 270 (2003) 4403–4412.

[50] W. Jantschko, P.G. Furtmüller, M. Zederbauer, K. Neugschwandtner, C. Jakopitsch, C. Obinger, Reaction of ferrous lactoperoxidase with hydrogen peroxide and dioxygen: An anaerobic stopped-flow study, Arch. Biochem. Biophys. 434 (2005) 51–59.

[51] P.J. Mak, W. Thammawichai, D. Wiedenhoeft, J.R. Kincaid, Resonance Raman spectroscopy reveals ph-dependent active site structural changes of lactoperoxidase compound 0 and its ferryl heme O-O bond cleavage products, J. Am. Chem. Soc. 137 (2015) 349–361.

[52] D. Garai, B.B. Ríos-González, P.G. Furtmuller, J.M. Fukuto, M. Xian, J. López-Garriga, C.C. Obinger, P. Nagy, Mechanisms of myeloperoxidase catalyzed oxidation of H2S by H2O2 or O2 to produce potent protein Cys-polysulfide-inducing species, Free Radic. Biol. Med. 113 (2017) 551–563.

[53] F. Courtin, D. Deme, A. Virion, J.L. Michot, J. Pommier, J. Nunez, The role of lactoperoxidase-H2O2 compounds in the catalysis of thyroglobulin iodination and thyroid hormone synthesis, Eur. J. Biochem. 124 (2005) 603–609.

[54] W.D. Hewson, L.P. Hager, Oxidation of horseradish peroxidase compound II to compound I., J. Biol. Chem. 254 (1979) 3182–3186.

[55] M.L. McCormick, J.P. Gaut, T.S. Lin, B.E. Britigan, G.R. Buettner, J.W. Heinecke, Electron paramagnetic resonance detection of free tyrosyl radical generated by myeloperoxidase, lactoperoxidase, and horseradish peroxidase, J. Biol. Chem. 273 (1998) 32030–32037.

[56] S. Galijasevic, G.M. Saed, M.P. Diamond, H.M. Abu-Soud, High dissociation rate constant of ferrous-dioxy complex linked to the catalase-like activity in lactoperoxidase, J. Biol. Chem. 279 (2004) 39465–39470.

[57] R. Davydov, M. Laryukhin, A. Ledbetter-Rogers, M. Sono, J.H. Dawson, B.M. Hoffman, Electron paramagnetic resonance and electron-nuclear double resonance studies of the reactions of cryogenerated hydroperoxoferric-hemoprotein intermediates, Biochemistry. 53 (2014) 4894–4903. doi:10.1021/bi500296d.

[58] P. Nagy, Mechanistic chemical perspective of hydrogen sulfide signaling, Methods Enzymol. 554 (2015) 3–29. doi:10.1016/bs.mie.2014.11.036.

[59] P. Nagy, C.C. Winterbourn, Rapid reaction of hydrogen sulfide with the neutrophil oxidant hypochlorous acid to generate polysulfides, Chem. Res. Toxicol. 23 (2010) 1541–1543.

[60] R. Greiner, Z. Pálinkás, K. Bäsell, D. Becher, H. Antelmann, P. Nagy, T.P. Dick, Polysulfides link H2S to protein thiol oxidation, Antioxid. Redox Signal. 19 (2013) 1749–1765.

[61] M.J. Chatfield, G.N. La Mar, 1H nuclear magnetic resonance study of the prosthethic group in sulfhemoglobin, Arch. Biochem. Biophys. Biochem Biophys. 295 (1992) 289–296.

[62] C.E. Cooper, G.C. Brown, The inhibition of mitochondrial cytochrome oxidase by the gases carbon monoxide, nitric oxide, hydrogen cyanide and hydrogen sulfide: Chemical mechanism and physiological significance, J. Bioenerg. Biomembr. 40 (2008) 533–539. doi:10.1007/s10863-008-9166-6.

[63] Y. Du, G. Liu, Y. Yan, D. Huang, W. Luo, M. Martinkova, P. Man, T. Shimizu, Conversion of a heme-based oxygen sensor to a heme oxygenase by hydrogen sulfide: effects of mutations in the heme distal side of a heme-based oxygen sensor phosphodiesterase (Ec DOS), Biometals. 26 (2013) 839–852. doi:10.1007/s10534-013-9640-4.

[64] H. Shimahara, T. Yoshida, Y. Shibata, M. Shimizu, Y. Kyogoku, F. Sakiyama, T. Nakazawa, S.I. Tate, S.Y. Ohki, T. Kato, H. Moriyama, K.I. Kishida, Y. Tano, T. Ohkubo, Y. Kobayashi, Tautomerism of histidine 64 associated with proton transfer in catalysis of carbonic anhydrase, J. Biol. Chem. 282 (2007) 9646–9656. doi:10.1074/jbc.M609679200.

[65] S. Li, M. Hong, Protonation, tautomerization, and rotameric structure of histidine: A comprehensive study by magic-angle-spinning solid-state NMR, J. Am. Chem. Soc. 133 (2011) 1534–1544. doi:10.1021/ja108943n.

[66] M.. Chatfield, G.N. La Mar, K.M. Smith, H.K. Leung, R.K. Pandey, Identification of the altered pyrrole in the isomeric sulfmyoglobins: hyperfine shift patterns as indicators of ring saturation in ferric chlorins, Biochemistry. 27 (1988) 1500–1507.

[67] R.P. Ferrari, E.M. Ghibaudi, S. Traversa, E. Laurenti, L. De Gioia, M. Salmona, Spectroscopic and binding studies on the interaction of inorganic anions with lactoperoxidase, J. Inorg. Biochem. 68 (1997) 17–26.

[68] U. Bandyopadhyay, D.K. Bhattacharyya, R. Chatterjee, R.K. Banerjee, Irreversible inactivation of lactoperoxidase by mercaptomethylimidazole through generation of a thiyl radical: its use as a probe to study the active site, Biochem. J. 306 (Pt 3) (1995) 751–757.

[69] A. Tomoda, A. Kakizuka, Y. Yoneyama, Oxidative and reductive reactions of sulphhaemoglobin with various reagents correlated with changes in quaternary structure of the protein, 221 (1984) 587–591.

[70] J. March, Advance Organic Chemistry, Third, Wiley, 1985.

[71] E.I. Stiefel, K. Matsumoto, Transition metal sulfur chemistry, ACS Symposium Series 653, 1996.

[72] E.S. Saltzman, W.J. Cooper, Biogenic sulfur in the environment, ACS Symposium Series 393, 1987.

[73] T. Omori, Y. Saiki, K. Kasuga, T. Kodama, Desulfurization of alkyl and aromatic sulfides and sulfonates by dibenzothiophene-desulfurizing Rhodococcus sp. strain SY1, Biosci. Biotechnol. Biochem. 59 (1995) 1195–1198. doi:10.1271/bbb.59.1195.

[74] R. Javadli, A. de Klerk, Desulfurization of heavy oil, Appl. Petrochemical Res. 1 (2012)

3–19. doi:10.1007/s13203-012-0006-6.

[75] M.R. Hoffmann, Kinetics and mechanism of oxidation of hydrogen sulfide by hydrogen peroxide in acidic solution, Environ. Sci. Technol. 11 (1977) 61–66.

[76] Q. Li, J.R. Lancaster, Chemical foundations of hydrogen sulfide biology, Nitric Oxide - Biol. Chem. 35 (2013) 21–34. doi:10.1016/j.niox.2013.07.001.

[77] V. Vitvitsky, P.K. Yadav, A. Kurthen, R. Banerjee, Sulfide oxidation by a noncanonical pathway in red blood cells generates thiosulfate and polysulfides, J. Biol. Chem. 290 (2015) 8310–8320. doi:10.1074/jbc.M115.639831.

[78] P.J. Mak, J.R. Kincaid, Resonance Raman spectroscopic studies of hydroperoxo derivatives of cobalt-substituted myoglobin, J. Inorg. Biochem. 102 (2008) 1952–1957.

[79] C. Hoi, K. Wu, Review article The role of hydrogen sulphide in lung diseases, Biosci. Horizons. 6 (2013) 1–8.

[80] H. Jenzer, W. Jones, H. Kohler, On the molecular mechanism of lactoperoxidase-catalyzed H2O2 metabolism and irreversible enzyme inactivation, J. Biol. Chem. 261 (1986) 15550–15556.

Figure Legends

Fig. 1. Generation of oxo-ferryl intermediates during peroxidase cycles. (A) Peroxidase cycle through Compound 0. (B) Previously proposed acid catalyzed formation of compound 0 through Compound III [48].

Fig. 2. H_2S interaction with native LPO under aerobic and anaerobic conditions. (A) Spectral changes of the interaction of 3 µM native LPO (-·-·-) with 150 µM H_2S under aerobic conditions. The first spectrum upon addition of H_2S was recorded at 30 sec, with the subsequent spectra taken at 60 s, 121 s, 241 s and 356 s. Arrows indicate direction of the spectral changes. (B, insert) Time resolved stopped-flow spectra of the interaction of 6 µM native LPO with 280 µM H_2S under anaerobic conditions. First spectrum was recorded at 0.81 sec after mixing, with the subsequent spectra taken at 5.6 s, 9.3 s, 21.0 s, 30.0 s, 49.9 s, 69.1 s, 81.1 s, and 100.0 s. respectively.

Fig. 3. Interactions of ferrous (A) and ferric (B) LPO with H_2S under anaerobic conditions and subsequent addition of O_2. (A) Ferrous LPO (- - -) was generated by adding DT to 2.7 µM native LPO (—). The addition of 50 µM H_2S at 5 s (—) and at 1 min (· · ·) show no spectral changes, while subsequent addition of O_2 resulted in sulfLPO formation (▬). (B) Ferrous LPO (—) was partially generated upon the addition of 150 µM H_2S to 2.7 µM native LPO (-·-·-) via sulfide reduction of ferric LPO. The subsequent addition of O_2 generated sulfLPO (▬).

Fig. 4. UV-vis spectral changes indicating sulfLPO formation upon addition of H_2O_2 and H_2S to native LPO. (A) Oxo-ferryl species (compound II) (- - -) were generated by adding 10.5 µM H_2O_2 to 2.1 µM native LPO (—). Addition of 375 µM H_2S to the sample generated sulfLPO with the spectra taken at 10 sec (▬), 4 min (-·-·-), 6 min (· · ·) and 8 min (····). At this last time point another aliquot of 21 µM of H_2O_2 was added, which resulted in an increase of the intensity of the

638 nm band (▬). After a short incubation period, the spectrum recorded at 12 min 30 s (—) show a decrease of the 638 band intensity with time. Arrows indicate direction of the spectral changes. (B) Turnover of LPO via sulfLPO formation. Consecutive increase and decrease in the absorbance at 638 nm upon the addition of H_2O_2 to LPO (bottom) in the presence of H_2S indicate turnover of LPO via intermediate formation of sulfLPO (top). Gray squares indicate time points when aliquots of H_2O_2 was added to the reaction mixture to the recovered (upon incubation) LPO native state.

Fig. 5. Interaction of native LPO with hydralazine in the presence of H_2O_2. Oxo-ferryl species (Compound II) of LPO (- - -) were formed by adding 10.5 µM H_2O_2 to 3.5 µM native LPO (—). Addition of 300 µM hydralazine (▬) return LPO to the native ferric state within the mixing time of our protocol.

Fig. 6. Interaction of ferric HRP with H_2S in the presence and absence of H_2O_2. (A) Reaction of H_2S with HRP oxo-ferryl species. A mixture of compound I and compound II (- - -) were formed by adding 29 µM H_2O_2 to 9.6 µM native HRP (—). No absorbance changes were observed which would have indicated the formation of a sulfheme derivative upon addition of 192 µM H_2S to the sample after 5 s (▬), and 10 min (· · ·) incubation times. (B) Interaction of H_2S with HRP in the absence of added H_2O_2. Spectra were recorded 5 min and 10 min after the addition of 192 µM H_2S to 9.6 µM HRP.

Fig. 7. EPR spectra after the reactions of LPO with H_2O_2 and H_2S. EPR spectra of (a) 300 µM native LPO, (b) 300 µM native LPO reacting with 900 µM H_2O_2, (c) 300 µM native LPO reacting with 900 µM H_2O_2 followed by the addition of 300 µM H_2S, and (d) 300 µM native LPO with 900 µM H_2O_2 and 15000 µM H_2S. The inset shows an enhancement of the signal at the

magnetic field range of 3200 G to 3300 G showing an LPO radical species (most likely a carbon centered amino acids) at 2.004 g.

Fig. 8. Sulfate concentration after sulfLPO formation at different concentrations of H_2O_2 and H_2S. (A) Sulfate concentration of the interaction of 5 µM native LPO with 25 µM H_2O_2 and different concentration of H_2S. (B) Sulfate concentration of the interaction of 5 µM native LPO with 50 µM H_2O_2 and different concentration of H_2S. The different concentrations of H_2S used were 600 µM (black), 800 µM (dark gray) and 1000 µM (gray).

Fig. 9. Distal active site of (A) LPO (PDB:2NQX) and (B)HRP (PDB:1ATJ)

Fig. 10. Proposed mechanism for sulfheme formation and turnover to the native state in the presence of (A) oxygen and (B) hydrogen peroxide.

Fig. 1

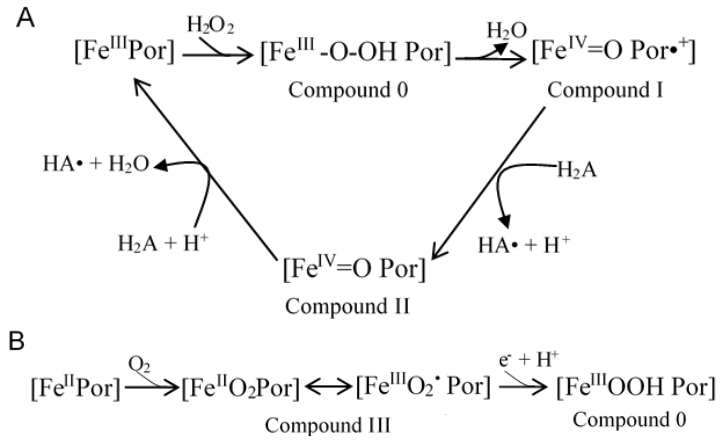
A
[Fe^III Por]
H2O2
[Fe^III -O-OH Por]
Compound 0
H2O
[Fe^IV=O Por•+]
Compound I
HA• + H2O
H2A + H+
[Fe^IV=O Por]
Compound II
H2A
HA• + H+
B
[Fe^II Por]
O2
[Fe^II O2 Por]
[Fe^III O2• Por]
e- + H+
[Fe^III OOH Por]
Compound III
Compound 0

Fig. 2

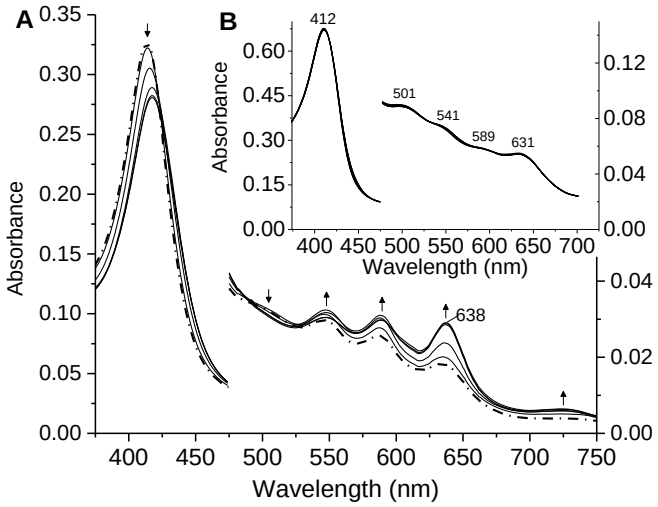

Fig. 3

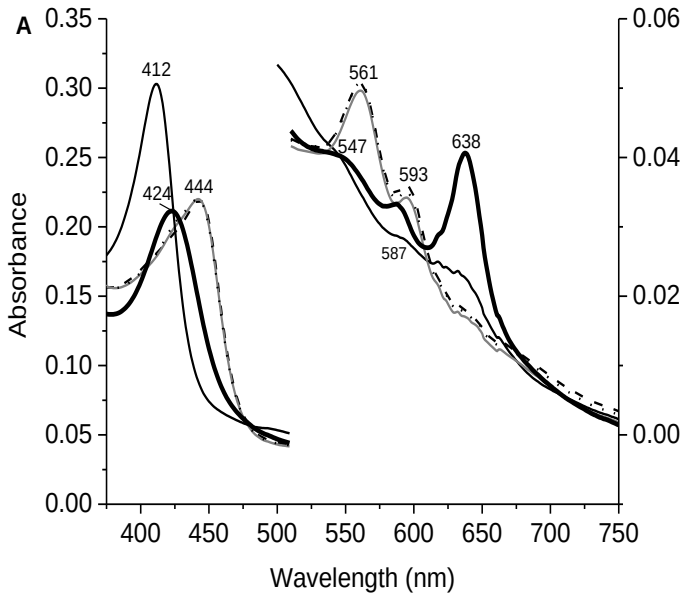
A
Absorbance
Wavelength (nm)
412
424
444
561
547
593
587
638

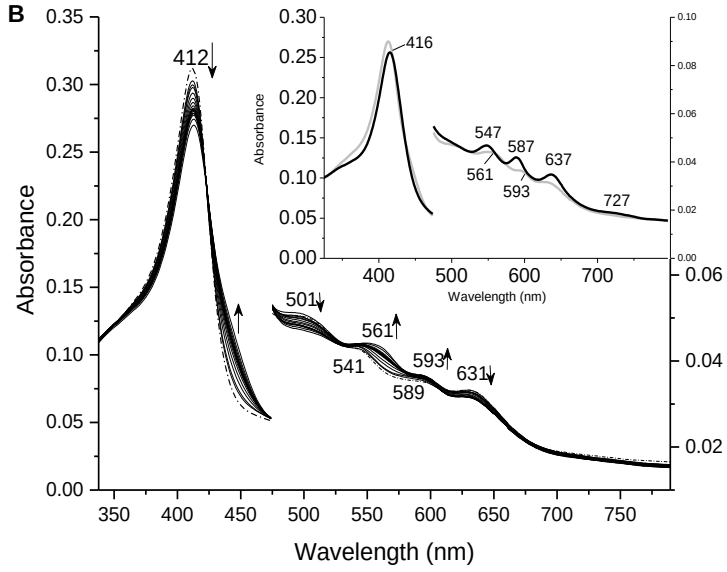
B
Absorbance
Wavelength (nm)
412
416
547
587
561
593
637
727
501
561
541
593
631
589

Fig. 4

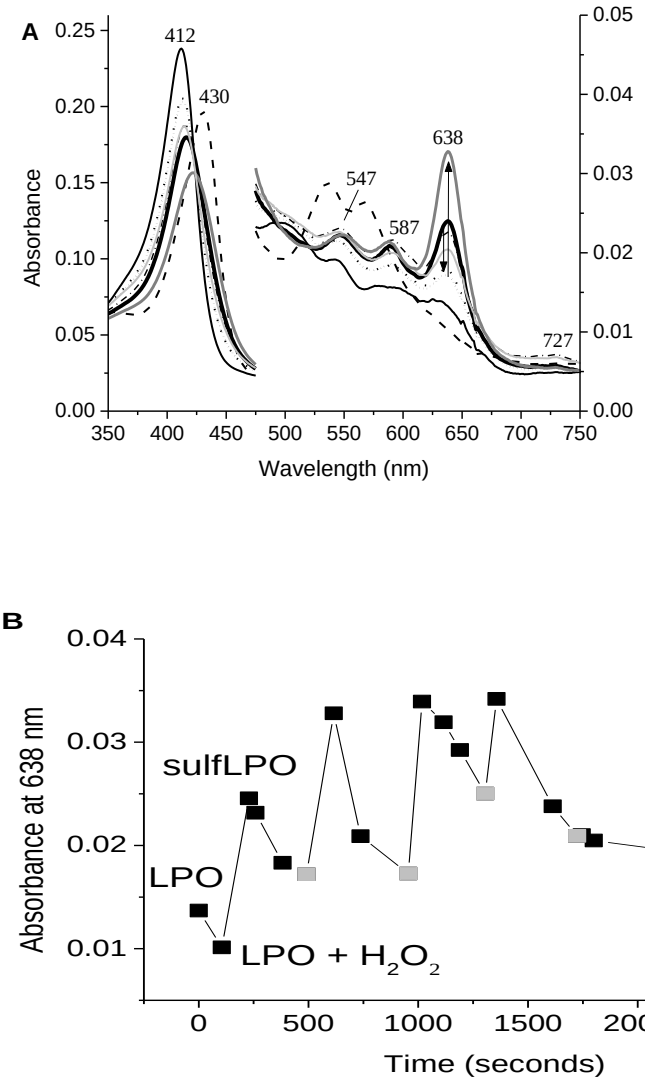
A
412
430
547
587
638
727
Absorbance
Wavelength (nm)
B
sulfLPO
LPO
LPO + H2O2
Absorbance at 638 nm
Time (seconds)

Fig. 5

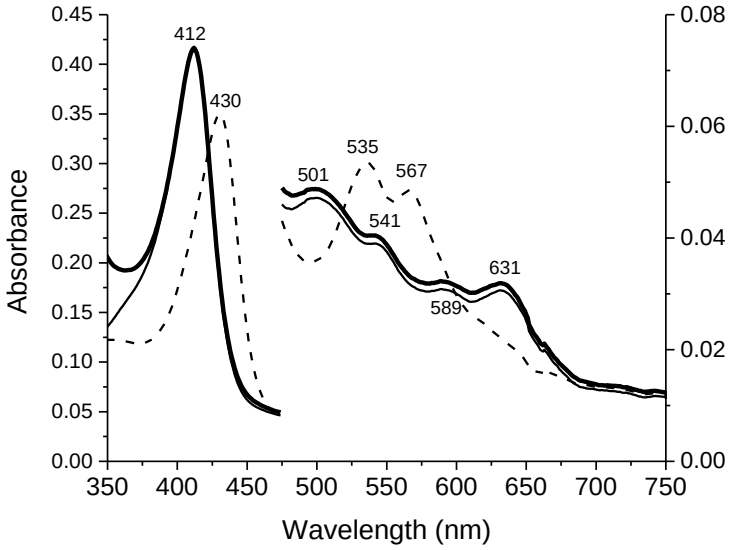
412
430
535
501
567
541
631
589
Absorbance
Wavelength (nm)
0.45
0.40
0.35
0.30
0.25
0.20
0.15
0.10
0.05
0.00
0.08
0.06
0.04
0.02
0.00
350
400
450
500
550
600
650
700
750

Fig. 6

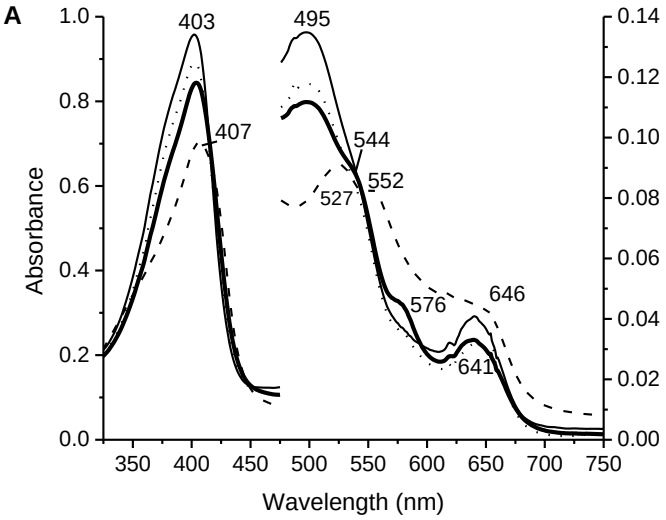
A
403
495
407
544
552
527
576
646
641
Absorbance
Wavelength (nm)

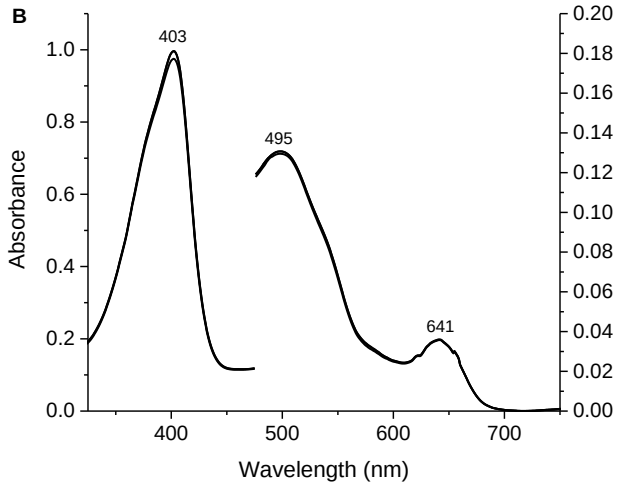
B
403
495
641
Absorbance
Wavelength (nm)

Fig. 7

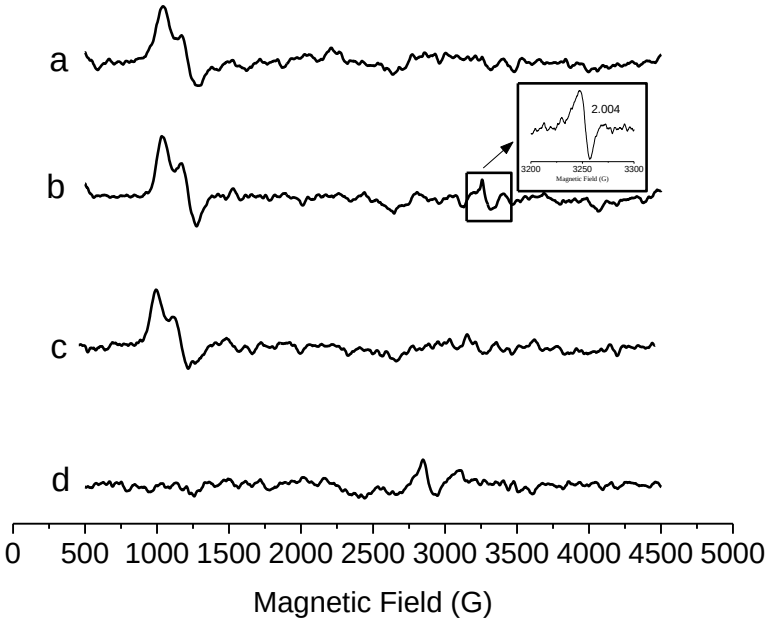
a
b
c
d
2.004
3200
3250
3300
Magnetic Field (G)
0
500
1000
1500
2000
2500
3000
3500
4000
4500
5000
Magnetic Field (G)

Fig. 8

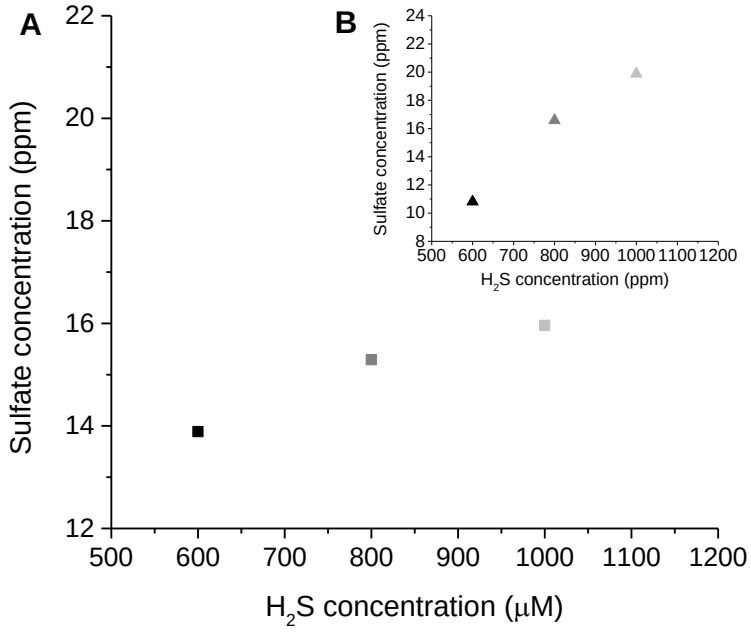
A
B
Sulfate concentration (ppm)
H2S concentration (μM)
Sulfate concentration (ppm)
H2S concentration (ppm)

Fig. 9

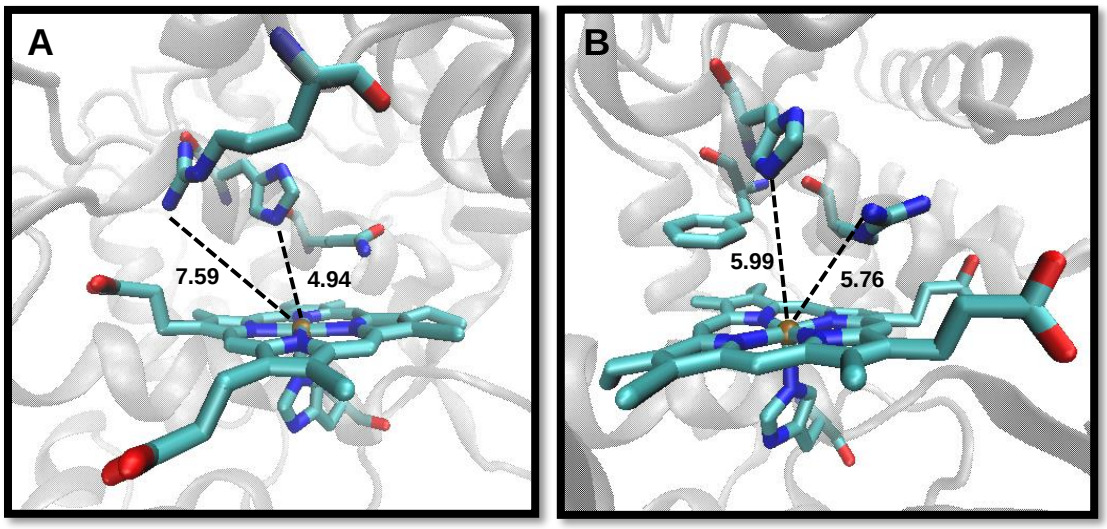

Fig. 10

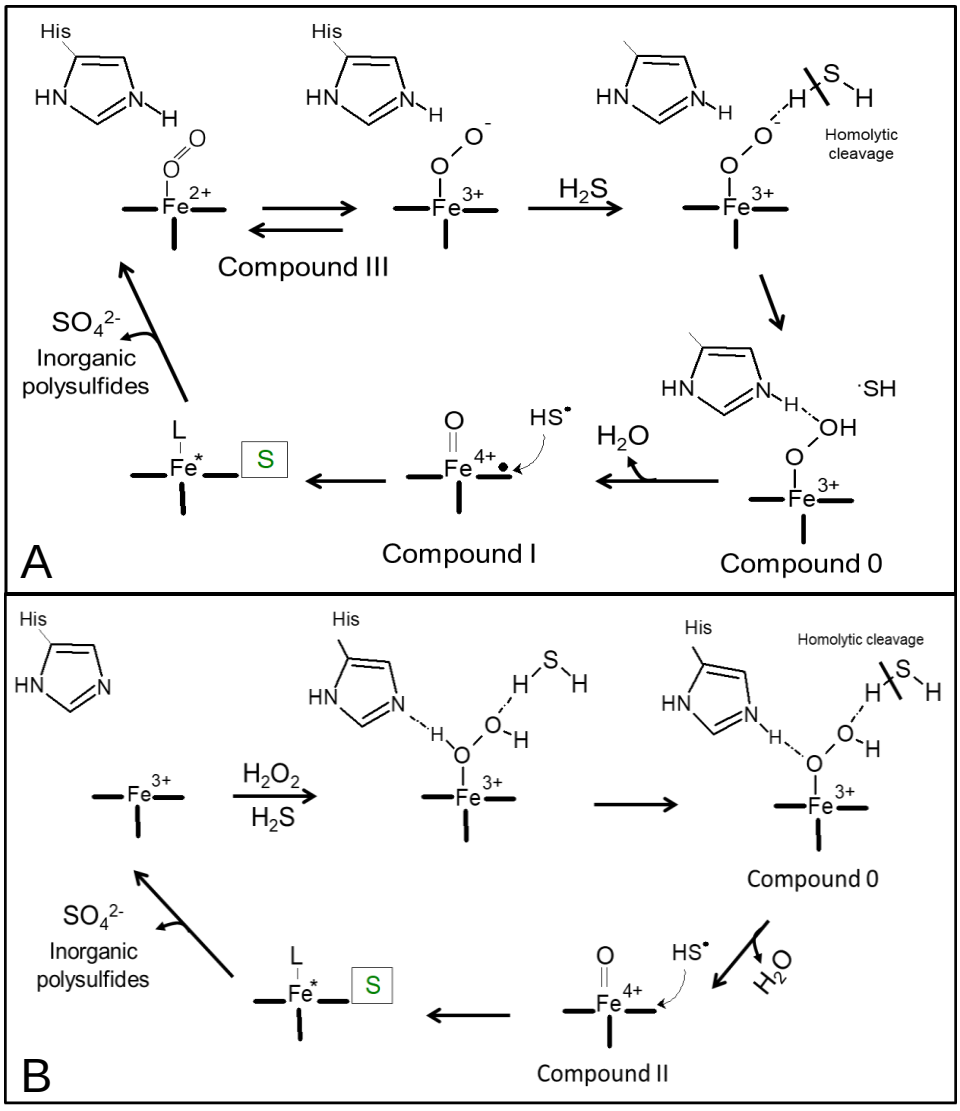
His
Compound III
H_2S
Homolytic cleavage
SO_4^{2-}
Inorganic polysulfides
H_2O
Compound I
Compound 0
A
H_2O_2
H_2S
Compound II
B

Appendix A.

Supplementary Data

Fig. S1

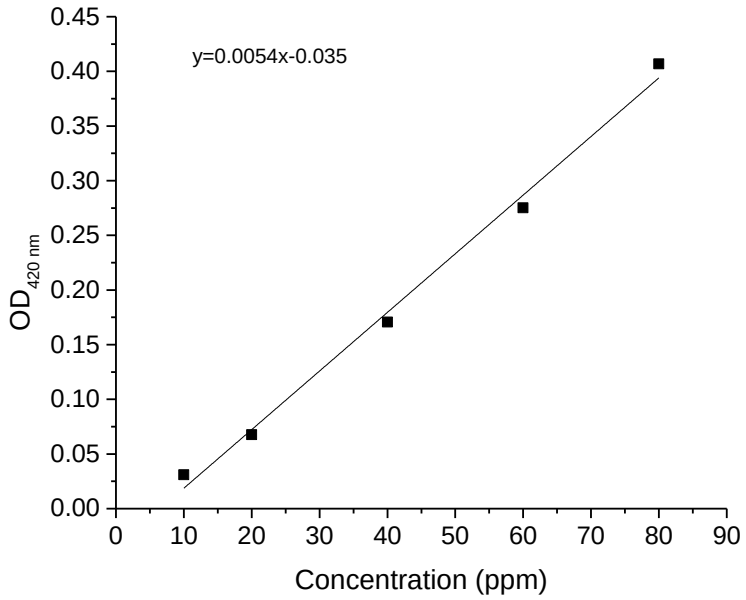

Fig. S1. Calibration curve to determine sulfate concentration. The curve was prepared using a 1,000 ppm sodium sulfate stock.

Fig. S2

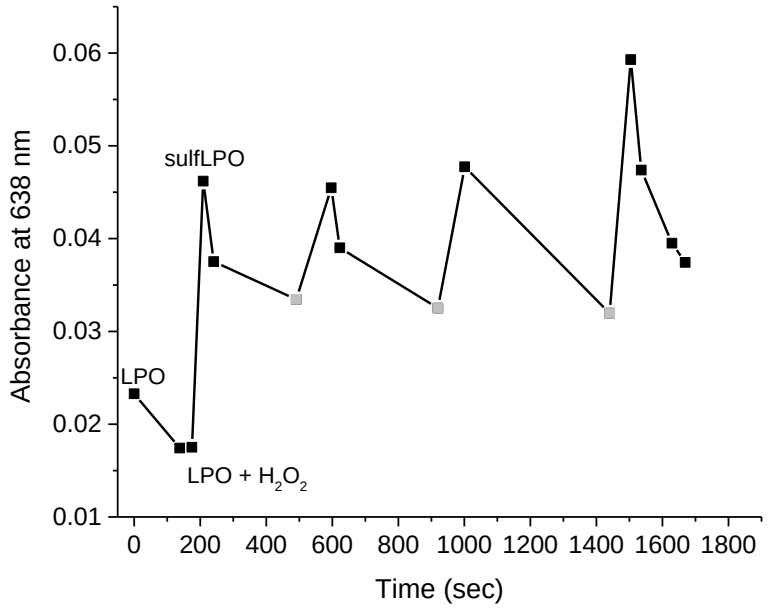

Fig. S2. Turnover of sulflactoperoxidase. Absorbance at 638 nm through time. Starting from LPO (3.5 µM) with the subsequent addition of H_2O_2 (10.5 µM). Then with the addition of H_2S (375uM), the 638 nm band forms. As time passes the 638 nm decreases intensity. Therefore the addition 1µL of H_2O_2 (10.5µM) increases the intensity of the 638 nm band. This turnover continues to happen each time 1uL of H_2O_2 is added.